

(NASA-CR-132875) LAUNCH WINDOW ANALYSIS
OF SATELLITES IN HIGH ECCENTRICITY OR
LARGE CIRCULAR ORBITS Final Report
(Carnegie-Hellon Univ.)

282 P HC \$16.25
272

CSCI 22C G3/30

N70-12478

Unclas
15645

Carnegie-Mellon University
Applied Space Sciences Program

FINAL REPORT
NASA NGR-37-087-001

Launch Window Analysis of Satellites
in High Eccentricity or
Large Circular Orbits

by

Marc L. Renard (Principal Investigator)

S.K. Bhate

R. Sridharan

September 15, 1973

Marc L. Renard
Dr. Marc L. Renard
Associate Prof. of
Applied Space Sciences
and Electrical Engin-
eering

ACKNOWLEDGEMENTS

The authors are very indebted to S.J. Paddack, of the IMP-Projects Office of NASA Goddard Space Flight Center, for many fruitful discussions and for providing us with high accuracy computer orbits and other needed data. Thanks are also due to G. Fried for sending us reference computer results, and to L. Carpenter with whom some aspects of the present work were discussed.

The efficient help of Cheryll M. Conaway in typing and editing this manuscript and many reports and papers, during the course of this grant, is gratefully acknowledged.

TABLE OF CONTENTS

		<u>Page No.</u>
Cover Page		
Acknowledgements		
Table of Contents		
Chapter 1	Purpose of this work	1-1 to 1-2
Chapter 2	Method of Approximate Stability Criteria	2-1 to 2-72
Chapter 3	A Study of Orbits of Large Electricity Quasi-Normal to the Ecliptic	3-1 to 3-42
Chapter 4	A Modified Lidov's Method by Non-Numeric Computation, with Application	4-1 to 4-83
Appendix A-1	Effect of Earth's Oblateness	A1.1 to A1.14
Chapter 5	Singularity-free Methods, Using Regularization, for Circular and Elliptic Orbits	5-1 to 5-44
Appendix A-2	Auxiliary Developments in Singularity-Free Methods	A-2.1 to A-2.5
Chapter 6	Orbital Programs	6-1 to 6-14
Chapter 7	General Conclusions	7-1 to 7-2

CHAPTER 1

Purpose of this Work

Much of what we presently know about "deep space", and the various physical phenomena resulting from the interaction of the earth's magnetic field with the solar wind, has been obtained from experimental evidence gathered by satellites of the EXPLORER series (IMP, for interplanetary monitoring probes).

In order to probe, along the same orbital period of a few days, the near-earth region, the transition region and free interplanetary space, it is convenient to use satellites in geocentric orbits of very large eccentricity, typically in the range of eccentricities $0.9 \lesssim e \lesssim 0.95$. Such orbits present a critical "stability" problem. Their initially low height of perigee is so perturbed by the gravitational effects of the sun and the moon that only a judicious choice of the launch time can guarantee that the satellite orbit will not experience a premature decay in the earth's atmosphere. The determination of these times, or "launch window calculation" had very often be extremely costly proposition if high accuracy numerical integration programs were used. On the other hand, such computation is imperative when the "target dates" are better known. The present work aimed at providing the mission analysts with methods and computing tools for studying the stability and evolution of orbits of large eccentricity. This is the topic of Chapters 2, 3 and 4. Chapters 2 and 3

develop an approach for a lower accuracy, but very fast analysis technique, whereas Chapter 4 resorts to non-numeric computation to obtain a "symbolic theory", applicable to high eccentricity orbits and of average accuracy and computer-time requirements.

Deep space is also investigated by means of satellites in large circular orbits (20 earth's radii, say), which are similarly perturbed by the sun and the moon. Although orbital decay is not a practical problem here, the development of methods of orbital computation, which would be more economical than conventional ones, allow for strong perturbations and be singularity-free, appeared to be a topic of much relevance. Such is the subjects of Chapter 5. Chapter 6 implements the methods of the previous one, and compares them to a straight method of variation of parameters, with time as the independent variable.

It is hoped that the approaches and techniques suggested in this work will be of help to the mission analyst facing the challenge of future space missions.

CHAPTER 2

Method of Approximate Stability Criteria2.1 The Problem

In the pre-launch phase of the mission analysis of satellites in orbits of large eccentricity, there exists a definite need for methods of determination of the orbital stability which would combine EXTREME COMPUTING SPEED with TOLERABLE accuracy on the results.

To be more specific, given a launcher of known capabilities, a launch site, a spacecraft of (roughly) known mass, an orbit of known in-plane geometry (i.e. the initial semi-major axis and eccentricity e), one wishes to "design" an orbit by adjusting, within limits,

- the orbital inclination on the equator (i_α)
- the argument of perigee, referred to the equator (ω_α)
- the time (hour; day; year) of launch (which in turn permits computation of the longitude of nodes, Ω_α , and the time of passage at perigee, T_p)

while satisfying, as explained in more detail in the previous chapter,

- a lifetime constraint
- other constraints of a technical scientific or operational nature (for instance: the angle between the satellite spin axis and the earth-sun line, or solar aspect angle, should be $90^\circ \pm 15^\circ$, say, at injection)

Now it should be remembered that the "lifetime constraint" is relatively imprecise and can often, to some extent, be relaxed. A requirement that the lifetime be "3 years" is not meant to be taken

as a request that the reentry of the satellite into the earth's atmosphere occur at time $t = \text{time of launch} + 1,095.75 \text{ days}$. Therefore, some inaccuracy on the a-priori determination of the lifetime might be tolerable when balanced against the speed and economy with which the prediction can be made.

If a method of extremely high economy is indeed obtained, parametric studies and the "mass production" of launch windows becomes practical. Questions such as this one can be readily answered: "Given this constraint on the solar aspect angle, when in the year 1973 should we launch this satellite so as to fulfill all constraints? What is the penalty paid in lifetime if we make the solar aspect angle condition more stringent? Should we try to modify the ascent phase and obtain a different argument of perigee etc....."

In addition to looking, in this chapter, to a method of appreciably reducing the computing time necessary for obtaining a launch window map, the accent will be put also, as initially proposed^[2-1], on automatizing the graphical presentation of the output in the form most suitable to the users' needs.

2.2 Basic Equations

Let O be the center of the earth, of mass M (Fig. 2.1); $\vec{r} = \vec{Os}$ the geocentric vector to the satellite; m the mass of the satellite (m is infinitesimally small compared to M_\oplus , m_d); m_d , the mass of a disturbing body d , assumed to describe a known Keplerian elliptical orbit about O ; $\vec{r}_{\text{dist}} \equiv \vec{r}_d = \vec{Od}$. Now define the vector from satellite to disturbing

body, $\vec{\rho}$, as (Fig. 2.1)

$$\vec{\rho} \equiv \vec{r}_d - \vec{r} \quad (2.2-1)$$

The following equations hold, if the vectorial pole for the capital R's is the center of mass of the system,

$$\ddot{\vec{R}}_0 = +k^2 m_d \frac{\vec{r}_d}{r_d^3} \quad (2.2-2)$$

$$\ddot{\vec{R}}_d = -k^2 M \frac{\vec{r}_d}{r_d^3} \quad (2.2-3)$$

$$\ddot{\vec{R}} = -k^2 \left(M \frac{\vec{r}}{r^3} - m_d \frac{\vec{\rho}}{\rho^3} \right) \quad (2.2-4)$$

Taking 0 as the origin of vectors, subtracting (2.2-2) from (2.2-3) gives

$$\ddot{\vec{r}}_d + k^2 (m_d + M) \frac{\vec{r}_d}{r_d^3} = 0 \quad (2.2-5)$$

which describes the elliptical motion of d about 0 (with $\mu_{d+M} = k^2 (m_d + M)$).

Subtracting (2.2-2) from (2.2-4) gives

$$\ddot{\vec{r}} + k^2 M \frac{\vec{r}}{r^3} = -k^2 m_d \left(\frac{\vec{r}_d}{r_d^3} - \frac{\vec{\rho}}{\rho^3} \right) \quad (2.2-6)$$

Equation (2.2-6) shows that the elliptical motion of s about 0 (with $\mu = k^2 M$) will be perturbed by the disturbing force due to third-body, m_d ,

$$\vec{F}_{\text{dist}} = -k^2 m_d \left(\frac{\vec{r}_d}{r_d^3} - \frac{\vec{\rho}}{\rho^3} \right) \quad (2.2-7)$$

If more than one body is perturbing the orbit of s, or if other perturbing forces, \vec{F}_{other} , are acting upon s in a frame centered at O and pointing towards fixed directions on the celestial sphere, Equation (2.2-6) should be complemented to read

$$\ddot{\vec{r}} + k^2 M \frac{\vec{r}}{r^3} = \vec{F}_{\text{dist},1} + \vec{F}_{\text{dist},2} + \dots + \vec{F}_{\text{other}} \quad (2.2-8)$$

in which the $\vec{F}_{\text{dist},i}$ ($i = 1, 2, \dots$) have the form given by Eq. (2.2-7).

2.3 Lidov's Theory

2.3.1 System of equations

In 1961, M.L. Lidov made an important contribution to the problem of determining the evolution of satellite orbits under the gravitational perturbations of external bodies^[2-2]. This approach can be summarized as follows. Let a, e, i, ω, Ω be five osculating elements of the satellite orbit; $p = a(1 - e^2)$ is the osculating parameter; v is the true anomaly. Angles such as i, ω, Ω are referred to a plane (such as the equator) invariant in inertial space and passing through O. Along the perturbed orbit, the following relations hold

$$r^2 \left(\frac{dv}{dt} + \frac{d\omega}{dt} + \cos i \frac{d\Omega}{dt} \right) = (\mu p)^{1/2} \quad (2.3-1)$$

or if

$$\gamma = \left[1 + \frac{r^2}{\mu e} F_r \cos v - \frac{r^2}{\mu e} \left(1 + \frac{r}{p} \right) F_t \sin v \right]^{-1} \quad (2.3-2)$$

r, s, n subscripts indicate components along the radius, the positive transverse and the normal direction. $r \frac{dv}{dt}$ and $\sqrt{\mu p}$ are related by

$$r^2 \frac{dv}{dt} = \gamma^{-1} \sqrt{\mu p} \quad (2.3-4)$$

A thorough analysis of the order of magnitude of γ has been made in the course of this grant and is given in [2-3].

The results are slightly different from those put forth by Lidov^[2-2], who argued that, since in the expression (2.3-2) for γ ,

$$F_r, F_v \sim \frac{\mu_d}{r_d^3} r \quad (\text{at most})$$

and if e is close to 1,

$$\gamma = 1 \pm 0 \left[\frac{\mu_d}{\mu} \frac{r^3}{r_d^3} \frac{1}{1 + e \cos v} \right] \approx 1 \pm 0 \left[\frac{\mu_d}{\mu} \frac{a^3}{r_d^3} \frac{1}{1 - e} \right] \quad (2.3-5)$$

In the reasoning, an average of r over M , mean anomaly, must be assumed since $\frac{1}{2\pi} \int_0^{2\pi} r \, dM = a$. If Lidov's estimate, as given in (2.3-5), rather than ours, is taken to assess the departure of γ from unity, one would conclude for example, that if $e = .95$, say, and $\frac{\mu_d}{\mu} \approx \frac{1}{81}$ (moon); then if $\frac{r}{r_\alpha} = \frac{2}{3}$ (up to $\frac{2}{3}$ of earth-moon distance), or $\frac{a}{r_k} \approx \frac{1}{3}$, then

$$\gamma \approx 1 \pm \frac{1}{81} \frac{1}{27} 20 = 1 \pm .0091 \text{ at most}$$

while our estimate (see Ref. [2-3]) would be

$$\gamma \approx 1 \pm .008 \quad \text{at most.}$$

For an extreme eccentricity of 0.95, γ will never depart from 1 by more than 0.8%. Consistent with the accuracy we are striving to obtain (of the order of 1%; Lidov^[2-2] quotes 1-3 per cent^[2-2, p. 720]), and in agreement with Lidov's approximation, the factor γ is taken to be 1 in what follows. With this approximation, planetary equations are written in terms of the five osculating parameters a, i, e, ω, Ω

$$\frac{da}{dt} = 2 \frac{a}{\epsilon} \sqrt{p/\mu} (e F_r \sin v + F_t (1 + e \cos v))$$

$$\frac{de}{dt} = - \frac{r}{ae} \sqrt{p/\mu} F_t + \frac{\epsilon}{2ae} \frac{da}{dt}$$

$$\frac{d\omega}{dt} = \frac{1}{e} \sqrt{p/\mu} [-F_r \cos v + F_t \sin v (1 + \frac{r}{p}) - e \frac{r}{p} F_n \cot i \sin(\omega + v)]$$

$$\frac{d\Omega}{dt} = \frac{r}{\sqrt{\mu p}} \frac{1}{\sin i} F_n \sin(\omega + v)$$

$$\frac{di}{dt} = \frac{r}{\sqrt{\mu p}} F_n \cos(\omega + v)$$

with $\epsilon = 1 - e^2$.

Substituting for dt , from Eq. (2.3-4), in which $\gamma = 1$, and introducing $p = a(1 - e^2)$, the differential system considered by Lidov^[2-2, p. 722] is

$$\frac{dp}{dv} = \frac{2r^3}{\mu} F_t \quad \text{or} \quad \frac{da}{dv} = 2 \frac{r^2 a}{\mu e} (e F_y + F_t)$$

$$\frac{de}{dv} = \frac{r^2}{\mu} (F_r \sin v + (1 + \frac{r}{p}) F_t \cos v + e \frac{r}{p} F_t) = - \frac{r^3}{\mu a e} F_t + \frac{e}{2a e} \frac{da}{dv}$$

$$\begin{aligned} \frac{d\omega}{dv} &= \frac{r^2}{\mu e} (-F_r \cos v + (1 + \frac{r}{p}) F_t \sin v - e \frac{r}{p} \cot i F_n \sin(\omega + v)) \\ &= \frac{r^2}{\mu e} [-F_x + F_t \frac{r}{p} \sin v] - \cos i \frac{d\Omega}{dv} \end{aligned}$$

$$\frac{d\Omega}{dv} = \frac{r^3}{\mu p} \frac{1}{\sin i} F_n \sin(\omega + v)$$

$$\frac{di}{dv} = \frac{r^3}{\mu p} F_n \cos(\omega + v) \quad (2.3-6)$$

2.3.2 Legendre Polynomial (LP) Expansion

The developments proceed to expand \vec{F} , the gravitational disturbing force, i.e. for body d,

$$\begin{aligned} \vec{F} &= \mu_d \left(\frac{\vec{\rho}}{\rho^3} - \frac{\vec{r}_d}{r_d^3} \right) = \mu_d \left(\frac{\vec{r}_d - \vec{r}}{|\vec{r}_d - \vec{r}|^3} - \frac{\vec{r}_d}{r_d^3} \right) = \mu_d \vec{\nabla} \left(\frac{1}{\rho} - \frac{xx_d + yy_d + zz_d}{r_d^3} \right) \\ &= \mu_d \vec{\nabla} \left(\frac{1}{\rho} - \frac{\vec{r} \cdot \vec{r}_d}{r_d^3} \right) \end{aligned}$$

in series of Legendre Polynomials (LP) of argument $\zeta = \cos S_d = \hat{\mathbf{r}} \cdot \hat{\mathbf{r}}_{rd} = \frac{\mathbf{r} \cdot \mathbf{r}_d}{rr_d}$
 Specifically, since $\frac{r}{r_d} < 1$, with assured convergence^[2-4]

$$\begin{aligned} R_{\text{perturbation}} &= \mu_d \left[\frac{1}{\rho} - \frac{rr_d \zeta}{r_d^3} \right] = \\ &= \mu_d \left[(r^2 + r_d^2 - 2rr_d \zeta)^{-1/2} - \frac{rr_d \zeta}{r_d^3} \right] \\ &= \frac{\mu_d}{r_d} \left[\left(1 + \left(\frac{r}{r_d} \right)^2 - 2 \left(\frac{r}{r_d} \right) \zeta \right)^{-1/2} - \frac{r}{r_d} \zeta \right] \end{aligned} \quad (2.3-7)$$

Now, with $\alpha = \frac{r}{r_d}$

$$\begin{aligned} (1 + \alpha^2 - 2\alpha\zeta)^{-1/2} &= 1 - \frac{1}{2}(\alpha^2 - 2\alpha\zeta) + \frac{3}{8}(\alpha^4 - 4\alpha^3\zeta + 4\alpha^2\zeta^2) \\ &= 1 + \alpha \cdot \zeta^2 + \alpha^2 \left(-\frac{1}{2} + \frac{3}{2}\zeta^2 \right) + \dots \\ &= \sum_{k=0}^{\infty} \alpha^k P_k(\zeta) \end{aligned}$$

in which the Legendre Polynomials are

$$P_0(\zeta) = 1$$

$$P_1(\zeta) = \zeta$$

$$P_2(\zeta) = -\frac{1}{2} + \frac{3}{2}\zeta^2 = \frac{1}{2}(3\zeta^2 - 1)$$

$$P_3(\zeta) = -\frac{3}{2}\zeta + \frac{5}{2}\zeta^3 = \frac{1}{2}(5\zeta^3 - 3\zeta)$$

$$P_4(\zeta) = \frac{1}{8}(35\zeta^4 - 30\zeta^2 + 3)$$

$$P_5(\zeta) = \frac{1}{8}(63\zeta^5 - 70\zeta^3 + 15\zeta)$$

.....

Going back to expression (2.3-7)

$$R_{\text{perturbation}} = \frac{\mu_d}{r_d} \left[1 + \sum_{k=2}^{\infty} \left(\frac{r}{r_d} \right)^k P_k(\zeta) \right] \quad (2.3-8)$$

The perturbing force, in turn, is

$$\begin{aligned} \vec{F}_d = \vec{\nabla} R_{\text{perturbation}} &= \frac{\mu_d}{r_d} \sum_{k=2}^{\infty} \left[k \left(\frac{r}{r_d} \right)^{k-1} P_k(\zeta) \hat{\mathbf{l}}_r \right. \\ &\quad \left. + \left(\frac{r}{r_d} \right)^k P_k'(\zeta) \vec{\nabla} \left(\frac{\vec{r}_d \cdot \vec{r}}{r_d r} \right) \right] \end{aligned} \quad (2.3-9)$$

in which $\hat{\mathbf{l}}_r = \frac{\vec{r}}{r}$

$$P_k'(\zeta) = \frac{d}{d\zeta} [P_k(\zeta)]$$

Also

$$\vec{\nabla} \left(\frac{\vec{r}_d \cdot \vec{r}}{r_d r} \right) = \left(\frac{\vec{r}_d}{r_d} \cdot \vec{\nabla} \right) \frac{\vec{r}}{r} + \left(\frac{\vec{r}_d}{r_d} \right) \wedge \text{curl} \frac{\vec{r}}{r}$$

Since $\frac{\vec{r}}{r} = \vec{\nabla}(r)$, the second term vanishes and

$$\begin{aligned} \left(\frac{\vec{r}_d}{r_d} \cdot \vec{\nabla} \right) \frac{\vec{r}}{r} &= \hat{\mathbf{l}}_x \left[\frac{x_d}{r_d} \frac{\partial}{\partial x} \left(\frac{x}{r} \right) + \frac{y_d}{r_d} \frac{\partial}{\partial x} \left(\frac{y}{r} \right) + \frac{z_d}{r_d} \frac{\partial}{\partial x} \left(\frac{z}{r} \right) \right] \\ &\quad + \hat{\mathbf{l}}_y \left[\frac{x_d}{r_d} \frac{\partial}{\partial y} \left(\frac{x}{r} \right) + \frac{y_d}{r_d} \frac{\partial}{\partial y} \left(\frac{y}{r} \right) + \frac{z_d}{r_d} \frac{\partial}{\partial y} \left(\frac{z}{r} \right) \right] \\ &\quad + \hat{\mathbf{l}}_z \left[\frac{x_d}{r_d} \frac{\partial}{\partial z} \left(\frac{x}{r} \right) + \frac{y_d}{r_d} \frac{\partial}{\partial z} \left(\frac{y}{r} \right) + \frac{z_d}{r_d} \frac{\partial}{\partial z} \left(\frac{z}{r} \right) \right] \end{aligned}$$

We have

$$\frac{\partial}{\partial x} \left(\frac{x}{r} \right) = \frac{1}{r} - \frac{x}{r^2} \frac{\partial r}{\partial x}$$

$$\frac{\partial}{\partial x} \left(\frac{y}{r} \right) = - \frac{y}{r^2} \frac{\partial r}{\partial x}$$

$$\frac{\partial}{\partial x} \left(\frac{z}{r} \right) = - \frac{z}{r^2} \frac{\partial r}{\partial x}$$

Gathering terms,

$$\begin{aligned} \left(\frac{\vec{r}}{r_d} \cdot \vec{\nabla} \right) \frac{\vec{r}}{r} &= \frac{x_d \vec{i}_x + y_d \vec{i}_y + z_d \vec{i}_z}{r_d} - \frac{xx_d + yy_d + zz_d}{r_d r^2} \vec{\nabla} r \\ &= \vec{i}_d - \zeta \frac{1}{r} \vec{i}_r \end{aligned}$$

Substituting in (2.3-9), and letting $q \equiv k-1$

$$\vec{F}_d = \frac{\mu_d}{r_d} \sum_{q=1}^{\infty} \left(\frac{r}{r_d} \right)^q [[(q+1)P_{q+1}'(\zeta) - \zeta P_{q+1}'] \vec{i}_r + P_{q+1}'(\zeta) \vec{i}_d]$$

Now, from the recurrence formulae,

$$-P_q' = (q+1)P_q - \zeta P_{q+1}'$$

Finally

$$\vec{F}_d = \frac{\mu_d}{r_d} \sum_{q=1}^{\infty} \left(\frac{r}{r_d} \right)^q [-P_q'(\zeta) \vec{i}_r + P_{q+1}'(\zeta) \vec{i}_d] \tag{2.3-9}$$

The components of \vec{F}_d along axes $(\vec{P}, \vec{Q}, \vec{R})$ are now obtained

$$\vec{P} \cdot \vec{i}_d \stackrel{\text{def}}{=} \epsilon_1 \quad \vec{Q} \cdot \vec{i}_d \stackrel{\text{def}}{=} \epsilon_2 \quad \vec{R} \cdot \vec{i}_d \stackrel{\text{def}}{=} \epsilon_3$$

The director cosines of the unit vector to the satellite, $\hat{\mathbf{I}}_d$, in the satellite system $(\vec{P}, \vec{Q}, \vec{R})$, namely ξ_1, ξ_2, ξ_3 are illustrated on Fig. 2.2.

In the same system, $\hat{\mathbf{I}}_r$ has components $(\cos v, \sin v, 0)$. Also

$$\zeta = \hat{\mathbf{I}}_r \cdot \hat{\mathbf{I}}_d = \xi_1 \cos v + \xi_2 \sin v \quad \text{and let}$$

$$\xi = (\xi_1^2 + \xi_2^2)^{1/2}; \quad \cos v_\xi = \frac{\xi_1}{\xi}; \quad \sin v_\xi = \frac{\xi_2}{\xi}$$

Now, if successive orders in the LP, i.e. $q = 1, 2, \dots$, are considered,

Equation (2.3-4) gives

$$(\vec{F}_d)_1 = \frac{\mu_d}{r_d^2} \left(\frac{r}{r_d}\right) [-P_1'(\zeta) \hat{\mathbf{I}}_r + P_2'(\zeta) \hat{\mathbf{I}}_d]$$

$$(\vec{F}_d)_2 = \frac{\mu_d}{r_d^2} \left(\frac{r}{r_d}\right)^2 [-P_2'(\zeta) \hat{\mathbf{I}}_r + P_3'(\zeta) \hat{\mathbf{I}}_d] \quad (2.3-10)$$

These are the two values of q retained by Lidov. Rewriting these expressions,

with $P_1'(\zeta) = 1$; $P_2'(\zeta) = 3\zeta$; $P_3'(\zeta) = \frac{15}{2} \zeta^2 - \frac{3}{2}$;

$$(\vec{F}_d)_1 = \frac{\mu_d}{r_d^2} \left(\frac{r}{r_d}\right) [-\hat{\mathbf{I}}_r + 3\zeta \hat{\mathbf{I}}_d]$$

$$(\vec{F}_d)_2 = \frac{\mu_d}{r_d^2} \left(\frac{r}{r_d}\right)^2 [-3\zeta \hat{\mathbf{I}}_r + \frac{1}{2}(15\zeta^2 - 3)\hat{\mathbf{I}}_d]$$

which are Lidov's expressions (4), (5) [2-2, p.723]. The computation of the components of $(\vec{F}_d)_1$ and $(\vec{F}_d)_2$ along (r, t, n) are (Fig. 2.2), since

$$\zeta = \frac{\vec{r}_d \cdot \vec{r}}{r_d \cdot r} = \frac{(\vec{r}_{d_0}) \cdot \vec{r}}{r_d \cdot r} = \xi \cos(v - v_\xi),$$

$$(\vec{F}_d)_{1,r} = \frac{\mu_d}{r_d^2} \frac{r}{r_d} [-1 + 3\xi^2 \cos^2(v - v_\xi)]$$

$$(\vec{F}_d)_{1,t} = \frac{\mu_d}{r_d^2} \frac{r}{r_d} [-3\xi^2 \cos(v - v_\xi) \sin(v - v_\xi)]$$

$$(\vec{F}_d)_{1,n} = \frac{\mu_d}{r_d^2} \frac{r}{r_d} [3 \xi \xi_3 \cos(v - v_\xi)] \quad (2.3-11)$$

and similarly for $(\vec{F}_d)_2$ projected along (r, t, n) ,

$$\begin{aligned} (\vec{F}_d)_{2,r} &= \frac{\mu_d}{r_d^2} \left(\frac{r}{r_d}\right)^2 \left[-\frac{9}{2} \xi \cos(v-v_\xi) + \frac{15}{2} \xi^3 \cos^3(v-v_\xi)\right] \\ (\vec{F}_d)_{2,t} &= \frac{\mu_d}{r_d^2} \left(\frac{r}{r_d}\right)^2 \left[-\frac{15}{2} \xi^3 \cos^2(v-v_\xi) \sin(v-v_\xi) + \frac{3}{2} \xi \sin(v-v_\xi)\right] \\ (\vec{F}_d)_{2,n} &= \frac{\mu_d}{r_d^2} \left(\frac{r}{r_d}\right)^2 \left[\frac{15}{2} \xi^2 \xi_3 \cos^2(v-v_\xi) - \frac{3}{2} \xi_3\right] \end{aligned} \quad (2.3-12)$$

At this stage, Lidov introduces the notations:

$$\Delta \equiv \frac{P}{r} = 1 + e \cos v \quad (\text{for the satellite})$$

and

$$\Delta_d \equiv \frac{P_d}{r_d} = 1 + e \cos v_d \quad (\text{for the disturbing body})$$

after which the components of the forces are rewritten:

$$(\vec{F}_d)_{1,r} = 3 \frac{\mu_d}{P_d^2} \frac{P}{P_d} (-\beta_6 + \beta_1 \cos^2 v + 2\beta_3 \sin v \cos v + \beta_2 \sin^2 v) \frac{1}{\Delta}$$

$$(\vec{F}_d)_{1,t} = -3 \frac{\mu_d}{P_d^2} \frac{P}{P_d} [\sin v \cos v (\beta_1 - \beta_2) + (\sin^2 v - \cos^2 v) \beta_3] \frac{1}{\Delta}$$

$$(\vec{F}_d)_{1,n} = 3 \frac{\mu_d}{P_d^2} \frac{P}{P_d} (\beta_5 \cos v + \beta_4 \sin v) \frac{1}{\Delta}$$

$$(\vec{F}_d)_{2,r} = \frac{15}{2} \frac{\mu_d}{P_d^2} \frac{P^2}{P_d^2} \left(-\frac{3}{5} \alpha_1 \cos v - \frac{3}{5} \alpha_2 \sin v + \gamma_1 \cos^3 v\right.$$

$$\left. + 3\gamma_3 \cos^2 v \sin v + 3\gamma_6 \cos v \sin^2 v + \gamma_2 \sin^3 v\right) \frac{1}{\Delta^2}$$

$$\begin{aligned}
(\vec{F}_d)_{2,t} = & \frac{15}{2} \frac{\mu_d}{p_d^2} \frac{p^2}{p_d^2} [-\gamma_3 \cos^3 v (\gamma_1 - 2\gamma_6) \cos^2 v \sin v \\
& - (2\gamma_3 - \gamma_2) \cos v \sin^2 v + \gamma_6 \sin^3 v + \frac{1}{5} \alpha_1 \sin v \\
& - \frac{1}{5} \alpha_2 \cos v] \frac{1}{\Delta^2}
\end{aligned}$$

$$\begin{aligned}
(\vec{F}_d)_{2,n} = & \frac{15}{2} \frac{\mu_d}{p_d^2} \frac{p^2}{p_d^2} (\gamma_4 \cos^2 v + 2\gamma_7 \cos v \sin v + \gamma_5 \sin^2 v \\
& - \frac{\alpha_3}{5}) \frac{1}{\Delta^2} \tag{2.3-13}
\end{aligned}$$

in which

$$\begin{aligned}
\alpha_1 &= \xi_1^4 \Delta_d^4, & \alpha_2 &= \xi_2^4 \Delta_d^4, & \alpha_3 &= \xi_3^4 \Delta_d^4, \\
\beta_1 &= \xi_1^2 \xi_3^3 \Delta_d^3, & \beta_2 &= \xi_2^2 \xi_3^3 \Delta_d^3, & \beta_3 &= \xi_1 \xi_2^3 \Delta_d^3, \\
\beta_4 &= \xi_2 \xi_3^3 \Delta_d^3, & \beta_5 &= \xi_1 \xi_3^3 \Delta_d^3, & \beta_6 &= \Delta_d^3, \\
\gamma_1 &= \xi_1^3 \xi_2^4 \Delta_d^4, & \gamma_2 &= \xi_2^3 \xi_3^4 \Delta_d^4, & \gamma_3 &= \xi_1^2 \xi_2^4 \Delta_d^4, \\
\gamma_4 &= \xi_1^2 \xi_3^4 \Delta_d^4, & \gamma_5 &= \xi_2^2 \xi_3^4 \Delta_d^4, & \gamma_6 &= \xi_2^2 \xi_1^4 \Delta_d^4, \\
\gamma_7 &= \xi_1 \xi_2 \xi_3^4 \Delta_d^4,
\end{aligned}$$

Going back to system (2.3-6), in which $\frac{da}{dv}$ is taken rather than $\frac{dp}{dv}$ in the first equation, and substituting for the forces, their expressions in (2.3-11), (2.3-12) etc., r.h. sides are obtained which depend on the motion of the disturbed body (v) and on the motion of the disturbing body (v_d) through

- powers of $r = \frac{p}{\Delta} = \frac{p}{1 + e \cos v}$
- positive powers of $\sin v$ and $\cos v$
- the greek symbols $\alpha_i, \beta_j, \gamma_k$ etc. of the form

$$\xi_1^a \xi_2^b \xi_3^c \Delta_k^d \quad (2.3-14)$$

in which ξ_1, ξ_2, ξ_3 are the director cosines of the unit vector to the perturbing body in the satellite system ($\vec{P}, \vec{Q}, \vec{R}$).

It is taken for granted that, consistent with the approximation in a first-order theory, the satellite orbital elements a, e, i , etc., are taken as constants in the r.h. side of system (2.3-6) and that the changes in these elements are computed separately, for each disturbing orbit, over one orbit of the satellite and then linearly superposed.

To summarize: suppose that we have a suitable representation for $\xi_1^a, \xi_2^b, \xi_3^c, \Delta_k^d$, given the true anomaly v of the satellite. Then, for any element z for which an equation in system (2.3-6) is written (the set of elements z is denoted z)

After integration of f_{\perp} (with respect to ν) from 0 to 2π , where subscript I is the order of the LP expansion, i.e. I corresponds to forces

$\sim 0[(\frac{r}{r_d})^{1+1}]$, II to forces $\sim 0[(\frac{r}{r_d})^{2+1}]$ etc....., we obtain

$$(\Delta z)_{\text{I}} = \text{change in element } z \text{ due to forces of } \sim 0[(\frac{r}{r_d})^2]$$

and, in total,

$$(\Delta z) = \sum_{j = \text{I, II, III} \dots} (\Delta z)_j \quad (2.3-15)$$

(2.3-15) expresses the change in any orbital element due to the various orders in the LP expansion, i.e. ordering these in columns

$$\begin{array}{l} 1 \quad \left. \begin{array}{l} \downarrow \\ \downarrow \\ \downarrow \\ \vdots \end{array} \right\} \begin{array}{l} (\Delta z)_{\text{I}} \\ (\Delta z)_{\text{II}} \\ (\Delta z)_{\text{III}} \\ \vdots \end{array} \\ \text{LP} \end{array} \quad (2.3-16)$$

2.3.3 Taylor Series expansion

Lidov's theory then further proceeds to expand any of the above referred greek symbols $\alpha_i, \beta_j, \gamma_k$ as

$$\alpha_i = (\alpha_i)_{\text{ref}} + \left(\frac{d\alpha_i}{dt}\right)_{\text{ref}} \Delta t + \left(\frac{d^2\alpha_i}{dt^2}\right)_{\text{ref}} \frac{\Delta t^2}{2!} + \dots \quad (2.3-17)$$

in a Taylor's series about a given point in time, t_{ref} , along the satellite revolution. In Equation (2.3-17), Δt is the difference $t - t_{\text{ref}}$, measuring the time elapsed from t_{ref} . From (2.3-17) and (2.3-14), it follows that

for any $(\Delta z)_{\text{I}}$, $(\Delta z)_{\text{II}}$, ..., any of the rows of (2.3-16) can be further divided as

$$\begin{array}{c}
 \xrightarrow{\hspace{10em}} \text{Taylor Series} \\
 \text{LP} \quad \left\{ \begin{array}{ll}
 (\Delta z)_{1,1} & (\Delta z)_{1,2} \dots \dots \dots \\
 (\Delta z)_{2,1} & (\Delta z)_{2,2} \dots \dots \dots \\
 (\Delta z)_{3,1} & (\Delta z)_{3,2} \dots \dots \dots \\
 \vdots & \vdots
 \end{array} \right. \quad (2.3-18)
 \end{array}$$

thereby providing 2 directions of expansion: the first one (i , first subscript) corresponds to the LP expansion of the forces (term $\sim 0(\frac{r}{r_d})^{i+1}$), and the second one (j , second subscript) to the number of terms, or the order increased by one, retained in the Taylor Series expansion of the quantities $\alpha_i, \beta_j, \gamma_k, \dots$

To appreciate what is involved in the integration of $(\Delta z)_{ij}$, we shall look specifically at the cases:

a) $i = 1, 2, 3, \dots, j = 1$ (FIRST COLUMN IN TABLEAU (2.3-18))

This specifically amounts to assuming that the disturbing body is fixed in space during any one revolution of the satellite. (The disturbing body is "frozen" at an average position) One should expect this approximation to be the better the smaller the ratio of $\frac{r}{r_d}$ (or $\frac{a}{r_d}$), since the α 's, β 's, etc. would indeed be sensibly constant if the period of the satellite was infinitesimally small compared to the period of the disturbing body in its apparent geocentric motion.

The terms to be integrated will involve

$$\begin{matrix} a & b & c & d \\ \xi_1 & \xi_2 & \xi_3 & \Delta_d \end{matrix}$$

appearing as constants: $(\xi_1^a)_{t_{\text{ref}}}$ $(\xi_2^b)_{t_{\text{ref}}}$ $(\xi_3^c)_{t_{\text{ref}}}$ $(1+e_d \cos \nu_d)_{\text{ref}}$,

and Δt does not appear.

- b) $i = 1, 2, 3, \dots, j = 1, 2$ (FIRST AND SECOND COLUMNS IN TABLEAU (2.3-18))

Here it is of course assumed that the α 's, β 's, etc. are sufficiently well described by a straight line tangent to the corresponding curve $\alpha = \alpha(t)$ at $t = t_{\text{ref}}$, (Fig. 2.3). This approximation should hold well if the angular motion of the disturbing body is "slow" compared to that of the disturbed body. For our purpose, such an approximation is amply sufficient for the sun's contribution to the perturbations. The additional terms to be integrated (compared to a)) will involve expressions originating from

$$\begin{matrix} a & b & c & d \\ \xi_1 & \xi_2 & \xi_3 & \Delta_d \end{matrix} \text{ and reading like}$$

$$\sim \Delta t \times [\text{constants computed at } t = t_{\text{ref}}]$$

Similarly, the third column in tableau (2.3-18) accounts for terms in $(\Delta t)^2$ etc...

The assessment of the order of magnitudes of each contribution $(\Delta z)_{ij}$ has been done in detail in [2-3]

2.3.4 Results of Lidov's theory: short-range and long-range

As an example, consider the "11" theory. Namely, only forces of $O\left(\frac{r}{r_d}\right)^2$ are retained in the LP expansion, and furthermore, the perturbing

bodies are fixed at the position they assume at $t = t_{\text{ref}}$. Taking for instance the equation for $\frac{di}{dv}$,

$$\frac{di}{dv} = \frac{r^3}{\mu p} F_n \cos(\omega + \nu)$$

Replacing (F_n) by $(F_n)_1$ as given in (2.3-11),

$$\begin{aligned} \frac{di}{dv} &= 3 \frac{\mu_d}{\mu} \left(\frac{r}{r_d}\right)^3 \frac{r}{p} \xi_3 \cos(\omega + \nu) [\xi_1 \cos \nu + \xi_2 \sin \nu] \\ &= 3 \frac{\mu_d}{\mu} \left(\frac{a}{p_d}\right)^3 \varepsilon^3 \xi_3 \frac{\Delta_d^3}{\Delta^3} \cos(\omega + \nu) [\xi_1 \cos \nu + \xi_2 \sin \nu] \end{aligned}$$

It is apparent that the evaluation of the following definite integrals is required

$$\begin{aligned} \int_0^{2\pi} (\Delta_d^3 \xi_1 \xi_3) \frac{\cos^2 \nu}{\Delta^3} d\nu, \quad \int_0^{2\pi} (\Delta_d^3 \xi_2 \xi_3) \frac{\sin \nu \cos \nu}{\Delta^3} d\nu, \\ \int_0^{2\pi} (\Delta_d^3 \xi_1 \xi_3) \frac{\cos \nu \sin \nu}{\Delta^3} d\nu, \quad \int_0^{2\pi} (\Delta_d^3 \xi_2 \xi_3) \frac{\sin^2 \nu}{\Delta^3} d\nu. \end{aligned}$$

One suspects that as the indices i and j are increased beyond 1, the volume and complexity of the calculation might become prohibitive. Hence, resort was made, in the present project, to non-numeric manipulation on the computer for the development of a modified, extended Lidov's theory. This is treated in Chapter 3.

In his paper^[2-2], Lidov gives for the five elements a, e, i, ω, Ω , the results of the "11", "12" and "21" theories in tableau (2.3-18). Limiting ourselves to the "main" contribution "11", we reproduce Lidov's results (SHORT-RANGE PERTURBATIONS):

$$\Delta_{11}a = 0$$

$$\Delta_{11}e = -15\pi \frac{\mu_d}{\mu} \left(\frac{a}{p_d}\right)^3 \epsilon \epsilon^{1/2} \beta_3$$

$$\begin{aligned} \Delta_{11}\Omega = 15\pi \frac{\mu_d}{\mu} \left(\frac{a}{p_d}\right)^3 \frac{1}{\epsilon^{1/2} \sin i} & \left[\left(1 - \frac{4}{5} \epsilon\right) \beta_5 \sin \omega \right. \\ & \left. + \frac{1}{5} \epsilon \beta_4 \cos \omega \right] \end{aligned}$$

$$\Delta_{11}i = 15\pi \frac{\mu_d}{\mu} \left(\frac{a}{p_d}\right)^3 \frac{1}{\epsilon^{1/2}} \left[\left(1 - \frac{4}{5} \epsilon\right) \beta_5 \cos \omega - \frac{1}{5} \epsilon \beta_4 \sin \omega \right]$$

$$\Delta_{11}\omega = 3\pi \frac{\mu_d}{\mu} \left(\frac{a}{p_d}\right)^3 \epsilon^{1/2} [4\beta_1 - \beta_2 - \beta_6] - \Delta_{11}\Omega \cos i \quad (2.3-19)$$

In the last part of his paper, Lidov investigates the secular changes in the elements of the satellite orbit by integrating the orbit-to-orbit changes, as given by Equation (2.3-19), over the period of the disturbing body. He thereby obtains the following expressions for the secular changes δz in the orbital elements z , per satellite orbital period $\delta\tau_{\text{sat}}$ (LONG-RANGE PERTURBATIONS)

$$\delta_{11}a = 0$$

$$\delta_{11}e = \frac{1}{4} A_d \epsilon \epsilon^{1/2} \sin^2 i \sin 2\omega$$

$$\delta_{11}\Omega = -\frac{1}{2} A_d \frac{\cos i}{\epsilon^{1/2}} [(1 - \epsilon) \sin^2\omega + \frac{1}{5} \epsilon]$$

(2.3-20)

$$\delta_{11}\omega = \frac{1}{2} A_d \frac{1}{\epsilon^{1/2}} [(\cos i - \epsilon) \sin^2\omega + \frac{2}{5} \epsilon]$$

In the above equations, the plane of reference for measuring the angles is the orbital plane of the perturbing body d, and for disturbing body d, A_d is defined here as

$$A_d = 15\pi \frac{\mu_d}{\mu} \left(\frac{a}{p_d}\right)^3 \epsilon_d^{3/2} \quad (2.3-21)$$

Finally, using Equation (2.3-20), Lidov is able to classify the long-range behavior of the perturbed orbits in terms of the two integrals which, besides the trivial one: $a = \text{constant}$, could be determined, namely

$$\begin{aligned} c_1 &= (1 - e^2) \cos^2 i = \epsilon \cos^2 i \\ c_2 &= (1 - \epsilon) \left(\frac{2}{5} - \sin^2 i \sin^2 \omega\right) \end{aligned} \quad (2.3-22)$$

These integrals, which apply to the system of differential equations describing the secular change of the orbital elements due to one perturbing body, in the absence of oblateness, will be used in the approximate stability criteria method which follows.

2.4 The Approximate Stability Criteria Method

2.4.1 Introduction

The approximate stability criteria method was developed under this grant by Renard^[2-5, 2-6]. Its goal is to provide a fast, economical (if less accurate) way of determining the stability of an orbit of large eccentricity and, in final analysis, the quick generation of launch window maps called for in a mission analysis. The method has since been used with success to study the launch windows of several satellites of the IMP (Explorer Series)^[2-7 to 2-9], and is operational at NASA Goddard Space Flight Center.

2.4.2 Some definitions:

- Orbit of large eccentricity: this is defined here as a geocentric orbit having an eccentricity in the approximate range $0.9 \leq e \leq 0.95$, or equivalently a geocentric distance to apogee $R_A \approx 20$ to $40 R_\oplus$ (earth's radius), if an initially low perigee, close to the earth's surface is assumed.
- Stable orbit: rather than being called (as it maybe should) "successful" an orbit is called stable if the height of perigee h_p , remains during the whole spacecraft lifetime, L , larger than some critical value h_p^* , equal to or slightly lower than the initial value h_p^* . h_p^* corresponds to an assumed height of perigee leading to orbital decay in the atmosphere.
- Launch window, launch window map: A launch window is the set of points DL, HL (day of launch, hour of launch) for which stability is realized, and for which a number of technical, scientific or other constraints are met^[2-10 to 2-16]. The boundary of the launch window defines the so-called launch window "map" (Fig. 2.3).

2.4.3 Present method and criteria

2.4.3.1 Evolution of the orbital elements

Fig. 2.4 (a. to f.) illustrates the evolution with time of some characteristic quantities of high eccentricity, stable orbits: the altitude of apogee, the altitude of perigee, the inclination of the equator, the longitude of nodes, the eccentricity and the argument of perigee (Ref. [2-5]). It is noted that for such a stable orbit, and a dense satellite, due to the rapid increase in perigee height, the effects of Earth's oblateness air drag are very limited and affect stability rather indirectly. Thus, in first approximation, they will be neglected in the analysis. Adjustments to the lifetime estimation might have to be made, however, in those special cases where the effect of oblateness plays a more significant role, as is mentioned in Chapter 3.

2.4.3.2 Motivation

A purely numerical determination, on the computer, of the launch window map for a satellite having a required lifetime of at least one year could require an average of 50 to 100 hr. of IBM 7090 per year of possible launch dates. Addressing herself to this problem, M. Moe^[2-17] developed simplified equations which were later solved on the analog computer^[2-18,2-19] at a considerable gain in computational speed and with good agreement between the predicted and exact window contours^[2-10].

It remained tempting, however, to try and define the launch window on the basis of approximate stability criteria which if fulfilled at launch,

would very likely guarantee the whole lifetime. This would result in an economical and fast method on digital computers, more universally available, and allow for better ephemerides of the Moon and the Sun, the orbits of which were taken to be circular in the above mentioned papers. Leroy and Pace^[2-20] had mentioned Lidov's theory (Ref. [2-2]), as a possible way to somewhat restrict the domain to be investigated numerically. With the goal of establishing stability criteria, we found very encouraging that many of the orbital features just described were qualitatively predicted by Lidov's analysis. Of course, the domain of validity of Lidov's results was presumably restricted to lower eccentricities than those retained here. For example in Ref. ([2-2]), Lidov was aiming for an accuracy of 1 to 3% with geocentric orbits of semi-major axis of the order of 30 to 40 x 10³ km. These figures were perhaps too conservative, since analog integration of the similar M. Moe's equations had given good predictions of the launch windows, up to eccentricities of the order of 0.95.

2.4.3.3 Setting up the criteria

For stability, we require that r_p , radius at perigee, not decrease with time, over the satellite lifetime L . Let a , e be the semi-major axis and eccentricity at perigee, respectively, and δz the change in quantity z from one perigee to the subsequent one:

$$\delta r_p = \delta[a(1 - e)] = \delta a \cdot (1 - e) - a \delta e \quad (2.4-1)$$

According to Lidov's "ll" theory (and this is also true for the "kk" theory, $k > 1$, see Chapter 3)

$$\delta a = 0$$

Thus,

$$\delta r_p = - a \delta e$$

Thus, it is required that the orbital eccentricity e have a decreasing trend with time. The constancy of a , as obtained from computer results, is illustrated in Fig. 2-5, for the orbit of Fig. 2-4.

The principle of the present method is to simultaneously require that stability be realized:

- 1) In the long-term (subscript LR, for "long-range"), having characteristic time τ_M (moon) or τ_\odot (sun): CRITERION 1.
- 2) In the short-term (subscript SR, for "short-range"), having characteristic time τ_{sat} , i.e. a few days: CRITERION 2.
- 3) In the intermediate-term, so the "waviness" of the curve of height of perigee vs. time about its trendline is limited (characteristic time $\tau_M/2$ or $\tau_\odot/2$): CRITERIA 3, 4, 5.
- 4) In the very-long term (characteristic time τ_{VLR} , as yet unknown): CRITERION 6.

These various stability criteria are now studied one by one.

LONG-TERM STABILITY

In the long-range, stability should exist for the secular effect of Sun and Moon, i.e. on the average over a period of the perturbing body. As obtained by Lidov (Ref. [2-2]) for one perturbing body "d", and recalled in Equations (2.3-20) above:

$$\delta e_{11} = \frac{1}{4} A_d e \epsilon^{1/2} \sin^2 i_d \sin 2\omega_d \quad (2.4-2)$$

$$A_d = 15\pi \frac{\mu_d}{\mu} \left(\frac{a}{pd}\right)^3 \epsilon_d^{2/3}$$

Note that i_d , ω_d are the inclination of the satellite orbit, and the argument of perigee of the satellite, referred to the orbital plane of perturbing body "d".

For the sun and the moon acting simultaneously, we can therefore state the long-term stability criterion (CRITERION 1)

$$\delta e_{LR} = \frac{1}{4} e \epsilon^{1/2} (A_{\odot} \sin i_{\odot} \sin 2\omega_{\odot} + A_M \sin i_M \sin 2\omega_M) \leq 0 \quad (2.4-3)$$

This will define a long-range stability region, which can easily be plotted in terms of launch hour vs. launch day.

It should be noted that the ratio of the amplitudes A_d , for Moon and Sun, respectively, is

$$\frac{A_M}{A_{\odot}} = \frac{\mu_M}{\mu_{\odot}} \left(\frac{P_{\odot}}{P_M} \right)^3 \left(\frac{\epsilon_M}{\epsilon_{\odot}} \right)^{3/2} = 2.18$$

and is obviously independent of A. As an example, for an orbit having the following characteristics:

$$h_A = 203,632 \text{ km}$$

$$h_P = 192.6 \text{ km}$$

$$e = 0.93932$$

$$\tau_{sat} = 4.1047$$

we obtain

$$\left| \delta h_{p,LR} \right|_{\max} \text{ due to the Sun} = 51.9 \text{ km/revolution}$$

$$\left| \delta h_{p,LR} \right|_{\max} \text{ due to the Moon} = 113.2 \text{ km/revolution}$$

Computer studies of high eccentricity orbits have shown that, starting with a relatively low inclination $0 < i < \frac{\pi}{2}$ on the ecliptic, stable orbits were accompanied by a significant increase in inclination on the plane of the disturbing bodies. It should also be noted here that if only one predominant perturbing body is considered, or at high inclinations on the ecliptic, in which case $i_0 \approx i_M$, the qualitative use of Tisserand's criterion made in [2-11] to account for the eccentricity vs. inclination relationship just appears as a quantitative consequence of Lidov's secular theory to order "11". Indeed,

$$\delta i_{LR} = -\frac{1}{4} A(1 - \epsilon) \frac{1}{\epsilon^{1/2}} \sin i \cos i \sin 2\omega \quad (2.4-4)$$

Dividing (2.4-4) by (2.4-3), and after some manipulation

$$\frac{\delta(\cos i)}{\cos i} = -\frac{\delta\epsilon^{1/2}}{\epsilon^{1/2}}$$

or

$$(1 - e^2)^{1/2} \cos i = \text{constant} \quad (2.4-5)$$

which is one of Lidov's "secular" integrals. Obviously, for stable orbits of $\frac{\pi}{2} < i < \pi$, the inclination will decrease as time increases.

SHORT-TERM STABILITY

As recalled in Equation (2.3-19), Lidov's "11" theory gives for the short-term (subscript SR, for "short-range") change of e due to disturbing body "d", and per satellite revolution:

$$\delta_{11}e = - e\epsilon^{1/2} \frac{A_d}{\epsilon_d^{3/2}} \beta_{3,d} \quad (2.4-6)$$

in which $\beta_{3,d} = \xi_{1,d} \xi_{2,d} \left(\frac{P_d}{r_d}\right)_{\text{ref}}^3$. Fig. 2.2 shows the geometrical significance of β_3 . If the projection of \vec{r}_d on the satellite orbital plane is in the FIRST or THIRD quadrants, then β is > 0 , and from Equation (2.4-6), the orbit is stable in the short-range; if the projection is the SECOND or THIRTH quadrants, the orbit is unstable in the short-range.

Now, for the two disturbing bodies (Sun and Moon), we require short-term stability by stating CRITERION 2:

$$\delta e_{\text{SR}} = - e\epsilon^{1/2} \left[\left(\frac{A_M}{\epsilon_M^{3/2}}\right) \beta_{3,M} + \left(\frac{A_\Theta}{\epsilon_\Theta^{3/2}}\right) \beta_{3,\Theta} \right] \quad (2.4-7)$$

as shown in Fig. 2.7. An alternative form of CRITERION 2 is

$$\left(\frac{\epsilon_\Theta}{\epsilon_M}\right)^{3/2} A \beta_{3,M} + A_\Theta \beta_{3,\Theta} \geq 0 \quad (2.4-8)$$

INTERMEDIATE-TERM STABILITY

Even if the short-term evolution of the eccentricity is favorable initially, $\beta_{3,M}$ will change sign as \vec{l}_M , unit vector to the moon, rotates in inertial space. Therefore, the eccentricity will oscillate, over the lunar month, about an intermediate trendline, which corresponds

to the long-range effect of the Moon and the short-range of the Sun, averaged over τ_M . The slope of this line should be < 0 (Fig. 2-8), which is expressed in CRITERION 3:

$$\delta e_{INT} = \langle \delta e_{SR,\theta} \rangle_{\tau_M} + (\delta e)_{LR,M} < 0 \quad (2.4-9)$$

If the latter condition is fulfilled, it remains to require that the waviness of the eccentricity vs. time curve (or alternatively, h_p vs. t) not be so pronounced that e increases again towards its initial value, at its next maximum (or h_p decreases again towards its initial value, at its next minimum). j designating the index of the perigee passage (the initial perigee has index 1) corresponding to that minimum in h_p , the above requirement is approximately expressed by CRITERION 4 (or 2 + 3 strong).

$$\delta e_j^* = e_j - e_0 = \sum_{k=0}^{j-1} \left[\frac{A_M}{\epsilon_M^{3/2}} \beta_{3,M}^{(k)} + \frac{A_\theta}{\epsilon_\theta^{3/2}} \beta_{3,\theta}^{(k)} \right] \quad 2.4-10$$

It is apparent that criterion 4, which limits the tolerable lunar modulation, encompasses criteria 2 and 3, but these are taken in this order because they are more readily checked than 4. Criterion 4 is then disregarded if 2 or 3 leads to a failure.

Now, the same reasoning is repeated for the solar modulation of the eccentricity vs. time curve (Fig. 2-5). The criterion corresponding here to 3 is $\delta e_{LR} < 0$ (criterion 1), and the one corresponding to criterion 4 is now developed. The upper limit on δe_{LR} on account of the solar modulation about its trendline may be simply approximated, near

the limit of stability; by $\left\{ \frac{2}{\sqrt{2}} \left| \delta e_{\langle SR, \theta \rangle \tau} - \delta e_{LR} \right| \frac{\tau_M}{\tau_{sat}} \right\}$ (amplitude of wave) $\times \frac{1}{9/2\tau_M}$ (time to contact) = $\left| \frac{4}{9\sqrt{3}} (\delta e_{\langle SR, \theta \rangle \tau_M} - \delta e_{LR}) \right|$

CRITERION 5 (or strong) is then stated as

$$(a) \quad \delta e_{LR} < \frac{4}{9\sqrt{3}} (\delta e_{\langle SR, \theta \rangle \tau_M} - \delta e_{LR}) \text{ if } \delta e_{\langle SR, \theta \rangle \tau_M} < \delta e_{LR} \quad (2.4-11)$$

$$(b) \quad \text{taken to be satisfied if } \delta e_{\langle SR, \theta \rangle \tau_M} > \delta e_{LR} \quad (2.4-12)$$

All quantities in (2.4-11) or (2.4-12) have been determined previously.

VERY-LONG-TERM STABILITY (FOR ORBITS WHICH ARE NOT QUASI-NORMAL TO THE ECLIPTIC)

It remains to ensure that the very-long range effect of the motion of the apsidal line of the satellite orbit with respect to the orbital planes of the perturbing bodies will not cause the eccentricity to reach its minimum value before half the expected lifetime has elapsed (Fig. 2.9).

Computational results, for example those of Fig. 2.9 for IMP-C under the solar and lunar influences, suggest that $e_{max} - e$ might be approximated in the region of interest, and when the inclination of the orbit on the ecliptic or the moon's orbital plane is not near 90° (more is said about this in the next section), by a half-sine wave with unknown "very-long-period" τ_{VLR} , in $(0, \tau_{VLR})$. As is shown in Fig. 2-10,

$$e_{max} - e = (e_{max} - e_{min}) \sin \pi \frac{t}{\tau_{VLR}} \quad (2.4-13)$$

Assume that there exist one predominant disturbing body. The non-trivial integrals in Lidov's "11", secular theory are, as given before,

$$c_2 = (1 - e^2)\cos^2 i = \epsilon \cos^2 i$$

$$c_2 = (1 - \epsilon) \left(\frac{2}{5} - \sin^2 i \sin^2 \omega \right) \quad (2.4-14)$$

From these, the extremal values of $\epsilon = 1 - e^2$ can be determined from:

a) if $c_2 > 0$

$$\epsilon_{\max} = 1 - \frac{5}{2} c_2$$

$$\begin{aligned} \epsilon_{\min} = \frac{1}{2} [1 + \frac{5}{3} (c_1 + c_2) - \{ (1 + \frac{5}{3} (c_1 + c_2))^2 \\ - \frac{20}{3} c_1 \}^{1/2}] \end{aligned} \quad (2.4-15)$$

b) if $c_2 < 0$

$\epsilon_{\max}, \epsilon_{\min}$ are roots of the quadratic equation

$$\epsilon^2 - [1 + \frac{5}{3} (c_1 + c_2)] \epsilon + \frac{5}{3} c_1 = 0 \quad (2.4-16)$$

Now, in order to be able to compute c_1, c_2 , for a given initial orbit, we should have a unique plane of reference (orbital plane of the disturbing body), with respect to which angles i and ω of the satellite orbit are measured. For moderate inclinations i on the moon's orbital plane, in view of the small value of the inclination of the moon's orbital plane of the ecliptic ($i_M = 5.145^\circ$), and of the dominant effect of the moon, it can be assumed that the sun approximately describes an orbit coplanar with the moon's orbit (this approximation would break down if $i \approx \frac{\pi}{2}$, and for a perigee located "between" the moon's and the sun's orbital planes^[2-6]).

In this approximation, c_1 and c_2 are computed with values of i, ω referred to the moon's orbital plane. This is the approximation adopted in an early version of the SABAC program, and illustrated in the example of Section 2.5.

For more accuracy, we later decided to use values of c_1 and c_2 which would account for the unequal magnitudes of the amplitudes of the perturbations (" A_d "), for sun and moon, by retaining as values of c_1 and c_2 the weighted averages

$$c_j = \frac{A_M}{A_M + A_\Theta} (c_j)_{\text{Monly}} + \frac{A_\Theta}{A_M + A_\Theta} (c_j)_{\Theta \text{ only}} \quad (j=1,2) \quad (2.4-16)$$

in which $(c_j)_{\text{only}}$ and $(c_j)_{\Theta \text{ only}}$ are computed from (2.4-14) for angles (i_M, ω_M) and $(i_\Theta, \omega_\Theta)$, respectively. This procedure is the one embodied in program SABAC (Version A).

So far, τ_{VLR} is an unknown quantity. If the orbit has been found to be stable in the intermediate range (criterion 3 satisfied), one can use Equation (2.4-13), to define an angle ξ_0 ($0 \leq \xi_0 \leq \frac{\pi}{2}$), where the eccentricity is e_0 .

$$\sin \xi_0 = \frac{e_{\max} - e_0}{e_{\max} - e_{\min}} \quad 0 \leq \xi_0 \leq \frac{\pi}{2}$$

The slope at $\xi = \xi_0$ is estimated to have value $\frac{\delta e_{\text{INT}}}{\tau_{\text{sat}}} (\text{day}^{-1})$ for

τ_{VLR} of the order of one year:

$$\frac{|\delta e_{\text{INT}}|}{\tau_{\text{sat}}} = - \frac{\delta e}{\delta t} = (e_{\max} - e_{\min}) \cdot \cos \xi_0 \cdot \frac{\pi}{\tau_{\text{VLR}}}$$

Normalizing to τ_{sat} , we obtain τ_{VLR} ,

$$\tau_{\text{VLR}} = \pi \tau_{\text{sat}} (e_{\text{max}} - e_{\text{min}}) \cos \xi_0 |\delta e_{\text{INT}}| \quad (2.4-17)$$

The lifetime condition is satisfied if $T^* = \tau_{\text{VLR}} (1 - 2 \frac{\xi_0}{\pi})$ is

larger than L , required lifetime. Thus, CRITERION 6 is stated as follows:

$$\tau_{\text{VLR}} > \frac{L}{1 - 2 \frac{\xi_0}{\pi}} \quad (2.4-18)$$

VERY-LONG RANGE STABILITY (for orbits quasi-normal to the ecliptic)

When the inclination of the orbit on the moon's orbit (or equivalently, on the ecliptic) is in the neighborhood of 90° , the lifetime criterion (6) is modified as follows, for those orbits whose perigee motion, during a significant fraction of the lifetime, occurs between the orbital planes of the two perturbing bodies (Fig. 2.11), for instance under the ecliptic and above the moon's orbital plane.

Since $\pi - \omega$ is then very small, it is no longer valid, even though $i_M \approx i_\odot$, that $\omega_\odot \approx \omega_M$. This explains why the above described criterion leads to predicted lifetimes which are systematically in excess of actual values.

It was found that typically, for an orbit of the IMP-G type ($e_0 = 0.946$; $i_0 \approx 90^\circ$), $\left| \frac{\delta e}{\delta \tau} \right|$ was very small and e would vary over a one-year lifetime between 0.946 and 0.934. Therefore, assuming that the sun describes an orbit in the moon's orbital plane amounts to

neglecting the unfavorable effect of the sun on the (already small) change in eccentricity due to the moon.

The alternative approach taken in the present case (and implemented in digital program SABAC version B) is as follows. A plane $\tilde{\omega}$ is defined, which is obtained by rotating, about the nodal line of the moon in the ecliptic, the plane of the ecliptic towards the moon's orbital plane by an amount $\frac{A_M}{A_M + A_\Theta} i_{M/\Theta}$, where $i_{M/\Theta}$ is the mutual inclination of these two planes (5.145°). For the theoretical justification^[2-6], see the treatment contained in Chapter 3.

Now, let ω_* be the argument of perigee of the satellite orbit, referred to plane $\tilde{\omega}$. The eccentricity will reach a minimum when the perigee will be exactly contained in plane $\tilde{\omega}$, after a time equal to the half-lifetime, $L_*/2$. For confirmation, the reader should refer to Chapter 3. For small $\sin \omega$, in the case of a southwards injection, we write CRITERION 6 (Version B):

$$\frac{L_*}{2} = \frac{\pi - \omega_*}{\left(\frac{\delta\omega_*}{\delta\tau}\right)} > \frac{L}{2} \quad (2.4-18)$$

The time-rate of change of ω_* is computed from $\frac{\delta\omega_*}{\delta\tau} = \left(\frac{\delta\omega}{\delta\tau}\right)_{LR,M} + \left(\frac{\delta\omega}{\delta\tau}\right)_{LR,S} (1+w)$.

In this formula, from Lidov's formula in the long-range

$$\left(\frac{\delta\omega}{\delta\tau}\right)_{LR,d} = A_d [(\cos^2 i_d - \epsilon) \sin^2 \omega_d + \frac{2}{5} \epsilon] \frac{1}{2\epsilon} \quad (2.4-19)$$

Factor $(1+w)$ results from averaging the expression between brackets in $\left(\frac{\delta\omega}{\delta\tau}\right)_{SR}$, due to the sun, i.e., with $e_\Theta \approx 0$,

$$\left(\frac{\delta\omega}{\delta\tau}\right)_{SR,\Theta} \approx \frac{A_\Theta}{5} \epsilon^{1/2} [4\xi_{1,\Theta}^2 - \xi_{2,\Theta}^2 - 1] \quad (2.4-20)$$

The average is taken over half a solar modulation ($\tau_{\odot}/4$), to obtain the linear trend of ω vs. time, and $\xi_{2,S}^2$ can generally be neglected in Equation (2.4-20). More details and examples are given in Chapter 3.

2.5 Examples of Application of the Method of Approximate Stability Criteria

From 1968 to the date of this writing, the approximate criteria approach has been used as a fast, economical tool to generate the launch windows of satellites in orbits of large eccentricity. The present section will deal in some detail with examples of application on satellites: IMP-B, IMP-G, IMP-I, IMP-K and K' (mother-daughter system).

2.5.1 A check of the method: IMP-B launch window

In order to check the effectiveness of the above method, it was decided to try and recover the launch window map for IMP-B, which had been well documented^[2-11].

This launch window map had been established during the preliminary studies on IMP-B and -C. The orbit had the following initial data (at injection):

$$\begin{array}{ll}
 h_p & = 109,952.5 \text{ Nmi} \\
 h_p & = 104 \text{ Nmi} \\
 a & = 108,290.5 \text{ km} \\
 e & = 0.93932277 \\
 i_{\alpha} & = 32.912693 \text{ deg} \\
 \omega_{\alpha} & = 133.659044 \text{ deg}
 \end{array}
 \left. \vphantom{\begin{array}{l} h_p \\ h_p \\ a \\ e \\ i_{\alpha} \\ \omega_{\alpha} \end{array}} \right\} \text{referred to } \alpha \text{ (earth's equator)}$$

Days studied: April 11 to June 15, 1965

Hours studied: 8.00 to 18.00 hr. U.T., time of injection, at perigee

Failure to meet any of the criteria, 1 to 6, led to the rejection of corresponding launch hour on the day considered. The results are compared to those obtained by NASA's numerical integration program ITEM, based on Encke's method (Fig. 2.12). It is seen that the topologically complicated features of the contour separating the "stable" and "unstable" regions are well recovered. The error in predicting "peaks" or "valleys" in the contour is at most of the order of a few tenths of an hour, and much less on the average. The largest discrepancies are recorded at ITEM "marginal" points, i.e. for orbits, otherwise stable, having a height of perigee between 90 and 100 N.mi. for one orbit only, which is of little consequence in practice. This accuracy appears sufficient for the purposes of mission analysis.

It should also be emphasized again that the lifetime condition is far from being the only one to be considered. Constraints of a technological or scientific nature will further reduce the stable region into a much smaller one, acceptable for the mission. In this reduced zone of the maps, a final, accurate study is then made, using elaborate and expensive digital integration methods.

2.5.2 General comments on the economy of the method

It is obviously impossible to accurately pinpoint the savings factor obtained by using one method compared to another, particularly in a time-sharing environment. However, good estimates of the orders of magnitudes can be given, and to the maximum extent possible, the conditions in which comparisons are made will be clearly stated.

As an implementation of the above method, a program called SABAC (for Stability Analysis By Approximate Criteria) was written in FORTRAN 4 to check, on the basis of the above criteria, whether a point on the launch map is stable.

On the UNIVAC 1108 of Carnegie-Mellon University and in OS, it took no more than 0.02 sec per calculation point. This figure should be compared (with, as we said above the "order-of-magnitude" viewpoint) to 7 to 10 min for conventional numerical integration programs run on the same machine, integrating over a one-year lifetime. Hence, an economy factor of the order of 10^4 , with the same amount of information obtained in the determination of the overall launch opportunities.

It is worth mentioning that SABAC includes an analytically defined ephemeris of the Moon, giving the distance with an error smaller than 500 km at maximum. The Sun's ephemeris is read in.

As a last comment, it should be repeated that the method is obviously no substitute for the detailed study, by a numerical integration on a digital computer, of a particular set of launch days and hours, and the corresponding history of the orbital elements over the whole lifetime. But this may now be done only in those finally selected "target" regions of the map, where all conditions of constraint are met.

Program SABAC comprises 2 versions, which differ by the method used to estimate the lifetime. Version A is suitable for orbits which are not quasi-normal to the ecliptic, i.e. it should not be applied to IMP-G. Version B is suitable for orbits nearly normal to the ecliptic, such as the orbit of IMP-G. Both versions are thoroughly documented as part D1

of the volume "Documentation of programs and subroutines" appended to this report. A slightly different version, of the same programs, also exist at NASA, the difference being that a subroutine, SUNEPH, computes the Sun's ephemeris rather than entering the Sun's coordinates as data.

2.5.3 IMP-I launch window

IMP-I (IMP6) was a 636 lb. spin-stabilized spacecraft, with its spin axis nominally perpendicular to the ecliptic plane^[2-9]. It carried a payload of 12 scientific experiments and one engineering experiment. It was launched on March 13, 1971 at 11.15 EST, and inserted into an orbit having the following characteristics

- Orbital period : 4.13 days
- Perigee : 243 km (initial)
- Apogee : 206,258 km (initial)
- Lifetime in orbit: 3.6 years
- Inclination : 28.69 deg.

A preliminary orbit was given to us by GSFC, in late 1969. It had the following parameters

		Revised, 02/70
- Height of Apogee	: 217572.19 km	216676.62 km
- Height of Perigee	: 277.7998 km	240.24 km
- Inclination (equatorial):	28.90053°	28.2996°
- Argument of Perigee:	-53.1456°	-66.2037°
- Longitude of Perigee:	115.91055 (East)	112.67°E
- Latitude of Perigee :	-22.75° (South)	-25.838°S
- Lifetime	: 3 years	3 years

The launch windows of Fig. 2.13-2.14 were obtained.

It is of importance to note here that a NASA GSFC's request, a series of cross-checks were made between NASA's digital integration program (ITEM), SABAC and C-MU's program EOLA. Excellent agreement was found, provided the allowed drop in perigee (73 km) was kept in mind when inputting the data of SABAC. The results are summarized in the following table.

Gross-check of ITEM, SABAC-1A and EOLA

	<u>Day*</u>	<u>TIME*</u>	<u>ITEM</u>	<u>SABAC1-A</u>	<u>EOLA</u>
1)	319	1	Success**	Success	
		2	835 days	777 days	
		18.5	Success	Success	Success
2)	320	19	Success	Success	
		20	Success	Success	
		21	Success	Success	
3)	324	20	Success	Success	
4)	325	19	Failure on 4-th Orbit; perigee ht. = 187 km.	Ripple fail. (Criterion 4)	Perigee history; 240, 267, 168, 327, 189, 142 km.
5)	326	19	Failure on 4-th Orbit; perigee ht. = 134 km.	Ripple fail. (Criterion 4)	Perigee history; 240, 228, 182, 288, 134 km.
6)	328	19	Failure on 1-st Orbit; perigee ht. = 149 km.	Short Range fail (Crit. 2)	Perigee history; 240, 149 km.
		20	Perigee ht. drops to 190 km. in 4 orbits (drop of 29 km. in 1-st orbit).	Short Range fail (Crit. 2)	Drop of 27 km. in 1-st orbit; drops to 200 km. in 4 orbits.
		21	Success	Success	Success
7)	330	19	Failures on 1-st Orbit; perigee ht. = 153 km.	Short Range fail (Crit. 2)	Perigee ht. drops to 148 km. in 1-st orbit.
		21	Perigee ht. drops to 199 km. in 1-st orbit.	Short Range fail (Crit. 2)	Perigee ht. drops to 202 km. in 1-st orbit.
8)	331	21	Perigee ht. drops to 161 km. in 1-st orbit.	Short Range fail (Crit. 2)	Perigee ht. drops to 163 km. in 1-st orbit.

* Day: Day number, 1970 (Reference - Jan. 1 = 0).

Time: U.T. in hrs. at injection (assumed to be at perigee).

**Success: Based on a 3-year lifetime.

	<u>DAY*</u>	<u>TIME*</u>	<u>ITEM</u>	<u>SABAC1-A</u>	<u>EØLA</u>
9)	332	22	Perigee ht. drops to 186 km. in 1-st orbit.	Short Range fail (Crit. 2)	Perigee ht. drops 188 km. in 1-st orbit.
10)	334	24	Perigee ht. drops to 202 km. in 1-st orbit.	Success	

SABAC1-A results reported here permitted a perigee drop of 73 km. (DPLIM = 73 km).

If no perigee drop were permitted, the failure points would remain so, while a few of the "success" points would turn into failure.

EØLA is a digital integration program based on a variation of parameters method with the true anomaly as the independent variable. Earth's oblateness was included in these runs but the atmosphere was not.

B. Kaufman and D.P. Muhonen, at NASA GSFC, carried out a detailed analysis of the IMP-I launch window^[2-9], subject not only to orbital stability constraints but also to other conditions, for instance,

- the spin axis (or centerline)-station vector angle, for any tracking station, should be between 55° and 125° . The reason for this constraint are -8 db and -10 db in the antenna patterns in the regions bounded by centerline-station vector angles of less than about 40° and greater than 135° .
- ecliptic plane apogee-sun angle between 15° and 60° , decreasing with time. This angle is defined as the angle between the Earth Sun line and the projection of the geocentric vector to apogee onto the ecliptic plane. In other words, the projected apogee vector will point to the subsolar point after between 15 and 60 days after injection.

For the fast mapping of the launch window, these authors used the Approximate method of SABAC^[2-5]. Diagrams such as Fig. 2.14 were produced; quoting from [2-9]:

"The rapidity of this program allows one to map out a complete launch window in a single computer run of less than two minutes,

whereas use of numerical integration would require many hours. While this program is approximate and is not intended to be highly accurate, it provides an extremely useful picture of the launch window as a basis for more detailed study. This program was obtained for the IMP project office (p. 2).

On p. 4 of the same report, commenting on the SABAC lifetime contour of Fig. 2.14:

"Various parts of this contour were chosen as test points in the Encke program and it was found that the contour was fairly accurate until approximately March 16, 1971, near 1600 to 1800 hours, where some complex forces apparently are beginning to combine in a manner that SABAC may not consider. As can be seen by the points plotted on the curve, this complex action is most significant around March 26 and appears to be disappearing at about April 10 and therefore is probably a cyclic occurrence related to the Sun. For this reason, if the launch is to occur later than about March 24, extreme care must be used. Several points plotted on Jan. 27 show just how sensitive the lifetime is to injection time where a difference of 1^h 15^m in injection time means the lifetime decreases from more than 3 years to about 4 days! Despite the above-mentioned complexities, Fig. 1 is an excellent starting base for a detailed look at the launch window".

As a final point of interest, in Kaufman and Muhonen's study, a Monte-Carlo procedure to account for the dispersion at injection should be mention here. Fig. 2.15, taken from

[2-9], p. 13, describes the injection covariance matrix. In view of the significant magnitude of the off-diagonal terms, it was thought to be inadequate to only examine $3\text{-}\sigma$ perturbations of the diagonal elements of the covariance matrix. The devised Monte-Carlo procedure generates a set of 350 random state vectors having a normal distribution about the nominal, as defined by the covariance matrix. These 350 random vectors are then converted into the SABAC input coordinates, and using the SABAC program, 350 corresponding launch windows are generated for each launch day considered! (Needless to say, the cost of such a Monte-Carlo study would have been prohibitive if carried out by conventional numerical integration). The launch window lower limit differed by no more than ± 15 minutes from that corresponding to the nominal state vector, and 99% of the upper limits were within 30 minutes of nominal. On that basis, Kaufman and Muhonen could conclude that raising the nominal lower limit by fifteen minutes and lowering the nominal upper limit by 30 minutes should avoid any problems caused by injection state errors.

2.5.4 Mother-daughter mission

A satellite mission on an orbit of large eccentricity, in which a subsidiary satellite ("daughter") will be separated from the main satellite ("mother"), is at present being planned by NASA and ESRO. In the mission analysis of this spacecraft, S.J. Paddack, D.P. Muhonen and G.B. Fried^[2-22] used the approximate criteria method and SABAC to generate a number of launch windows, spanning intervals of several hundred days, for various values of the argument of perigee. Fig. 2.17 is an example reproduced from [2-22].

2.6 Auxiliary Programs

In this section, we shall briefly describe some auxiliary programs developed under this grant and to be used in support of the main program SABAC for the development of launch window maps. They are:

- a program called "ECLIP" (existing in Versions 2, 3) which defines the relevant orbital and injection parameters, for given radius and velocity at injection, given inclinations of the velocity and satellite spin axis vectors on the transverse. It is often desirable that, at a nominal, "ideal" time, the velocity at injection (Version 2) or spin axis at injection (Version 3) be normal to the ecliptic.
- a plotting program for the SABAC output, called "SABPL2" (a slightly modified version was written by G. Fried of NASA GSFC).

2.6.1 Program ECLIP

ECLIP (here, more specifically, ECLIP2) is a program designed to determine, on the basis of given: radius at injection, speed at injection, inclination on the equator, flight path angle (i.e. angle between \vec{V}_{inj} and the transverse vector, in the direction of flight), the following quantities:

- 1) The nominal injection time, on any given day of the year, which guarantees perpendicularity of the velocity vector, \vec{V}_{inj} , to the ecliptic plane (the spin axis is sometimes assumed to be aligned on \vec{V}_{inj}).

- 2) The range of injection time, or "launch opportunity strip", within which the spin axis of the satellite, at injection lies within $\pm 5^\circ$ of the negative normal to the ecliptic (the injection is southwards).
- 3) The solar aspect angle at the boundaries of the above "strip", and at the nominal injection time.

The geometry of the problem is shown in Fig. 2.18.. Let $(X_\epsilon, Y_\epsilon, Z_\epsilon)$ be the geocentric ecliptic system, and $(X_\alpha, Y_\alpha, Z_\alpha)$ the geocentric equatorial system. The coordinate transformations are

$$\begin{pmatrix} X_\epsilon \\ Y_\epsilon \\ Z_\epsilon \end{pmatrix} = \begin{pmatrix} 1 & 0 & 0 \\ 0 & \cos \epsilon & \sin \epsilon \\ 0 & -\sin \epsilon & \cos \epsilon \end{pmatrix} \begin{pmatrix} X_\alpha \\ Y_\alpha \\ Z_\alpha \end{pmatrix}$$

and

$$\begin{pmatrix} X_\alpha \\ Y_\alpha \\ Z_\alpha \end{pmatrix} = \begin{pmatrix} 1 & 0 & 0 \\ 0 & \cos \epsilon & -\sin \epsilon \\ 0 & \sin \epsilon & \cos \epsilon \end{pmatrix} \begin{pmatrix} X_\epsilon \\ Y_\epsilon \\ Z_\epsilon \end{pmatrix}$$

The following vectors and scalars of special importance:

- a) \vec{r}_{inj} , unit vector to the point of injection ($\vec{R}_{inj} = R_{inj} \cdot \vec{r}_{inj}$, radius vector at injection)
- b) \vec{v}_{inj} , unit vector along the velocity at injection ($\vec{V}_{inj} = V_{inj} \cdot \vec{v}_{inj}$, velocity at injection)

- c) \vec{P} , unit to perigee and \vec{Q} unit along the positive semi-latus rectum

The dependence of \vec{P} on \vec{r}_{inj} , \vec{V}_{inj} is recalled here.

$$\vec{R}_{inj} = R_{inj} \cos v_{inj} \vec{P} + R_{inj} \sin v_{inj} \vec{Q}$$

$$\vec{V}_{inj} = \sqrt{\mu/p} [-\sin v_{inj} \vec{P} + (e + \cos v_{inj}) \vec{Q}]$$

Solving for \vec{Q} ,

$$\vec{Q} = \vec{r}_{inj} \frac{1}{\sin v_{inj}} - \frac{\cos v_{inj}}{\sin v_{inj}} \vec{P}$$

Then

$$\vec{V}_{inj} = -\sqrt{\mu/p} \vec{P} \frac{1 + e \cos v_{inj}}{\sin v_{inj}} + \sqrt{\mu/p} \frac{e + \cos v_{inj}}{\sin v_{inj}} \vec{r}_{inj}$$

Finally, with $C = |\vec{r} \wedge \vec{r}'| = \sqrt{\mu p}$

$$\vec{P} = \frac{e + \cos v_{inj}}{1 + e \cos v_{inj}} \vec{r}_{inj} - \frac{\sin v_{inj}}{1 + e \cos v_{inj}} \frac{C}{\mu} \vec{V}_{inj} \quad (2.6-1)$$

- d) γ , flight path angle, is the angle between the velocity vector at injection and the transverse vector, in the direction of flight. γ is taken to be > 0 if the projection of \vec{V}_{inj} on \vec{R}_{inj} is positive, i.e. if injection occurs after perigee.
- e) γ_s , the satellite spin axis angle, is counted from \vec{V}_{inj} into \vec{s} , unit vector along the spin axis (assumed to be in plane $\vec{r}_{inj}, \vec{V}_{inj}$), positive in the direction of positive γ .

It is assumed that the injection is southwards. Of two possible values of Ω_α , longitude on nodes in equatorial plane, the one

to be retained is that which delays most the appearance of long eclipses (more than several hours, near apogee). As will be seen later, this amounts, for posigrade orbits ($i_\alpha \leq \frac{\pi}{2}$) and an injection in the Northern Hemisphere, to requiring that Ω_α (which could be either in the fourth or second quadrant) be in the second quadrant (or $\Omega_\alpha + \pi$, longitude of descending node is in the fourth quadrant)

Numerical injection time

By definition, the nominal injection time is that time t_{inj} , at which the velocity at injection (or vector \vec{v}_{inj}), is aligned on the negative normal to the ecliptic. Thus, $\vec{v}_{inj} = [0 \ 0 \ -1]_\epsilon = [0 \ \sin \epsilon \ -\cos \epsilon]_\alpha$. Evaluating $\vec{r}_{inj} \wedge \vec{v}_{inj}$ in the ϵ -system, if \vec{n} is the unit normal to the orbit,

$$\vec{r}_{inj} \wedge \vec{v}_{inj} = \cos \gamma \vec{n}$$

Thus

$$(\vec{r}_{inj})_\epsilon = [n_{Y_\epsilon} \cos \gamma, -n_{X_\epsilon} \cos \gamma, -\sin \gamma]_\epsilon$$

or

$$\begin{aligned} (\vec{r}_{inj})_\alpha = [n_{Y_\epsilon} \cos \gamma, -n_{X_\epsilon} \cos \gamma \cos \epsilon + \sin \gamma \sin \epsilon, \\ -n_{X_\epsilon} \cos \gamma \sin \epsilon - \sin \gamma \cos \epsilon]_\alpha \end{aligned} \quad (2.6-2)$$

Therefore $(\vec{r}_{inj})_\alpha$ can be determined from γ , once \vec{n} is known. Given i_α , \vec{n} is related to Ω_α through

$$\begin{aligned} (\vec{n}) &= [\sin \Omega_\alpha \sin i_\alpha, -\cos \Omega_\alpha \sin i_\alpha, \cos i_\alpha]_\alpha \\ &= [\sin \Omega_\alpha \sin i_\alpha, -\cos \epsilon \cos \Omega_\alpha \sin i_\alpha + \sin \epsilon \cos i_\alpha, \\ &\quad \cos \epsilon \cos i_\alpha + \sin \epsilon \cos \Omega_\alpha \sin i_\alpha]_\epsilon \end{aligned} \quad (2.6-3)$$

The problem is now simply to find Ω_α such that \vec{v}_{inj} is normal to the ecliptic. Let $(RA)_\epsilon$ be the celestial longitude of the projection of \vec{r}_{inj} on the (X_ϵ, Y_ϵ) plane. Then

$$\begin{aligned}\vec{n} &= [-\sin RA_\epsilon, \cos RA_\epsilon, 0]_\epsilon \\ &= [-\sin RA, \cos \epsilon \cos RA_\epsilon, \sin \epsilon \cos RA_\epsilon]_\alpha\end{aligned}$$

i_α being imposed, if \vec{z}_α is the unit along the Z_α -axis,

$$\vec{n} \cdot \vec{z}_\alpha = \cos i_\alpha = \sin \epsilon \sin RA_\epsilon$$

The quadrant for RA_ϵ (of two possible) being chosen from shadow consideration, as explained above, the angle is determined from

$$\cos RA_\epsilon = \frac{\cos i_\alpha}{\sin \epsilon} \sin RA_\epsilon = \pm \text{sqrt}(1 - \cos^2 RA_\epsilon) \quad (2.6-4)$$

where i_α, ϵ are known.

Now from Equation (2.6-3)

$$\cos \Omega_\alpha = -\frac{n_{Y_\alpha}}{\sin i_\alpha} = -\frac{\cos i_\alpha \cos \epsilon}{\sin i_\alpha \sin \epsilon}$$

and Ω_α is in the same quadrant as RA_ϵ . Note that Ω_α has been obtained from Equation (2.6-4) and (2.6-5) only, and is thus (as well as \vec{n}) independent of γ , flight path angle. The injection time, t_{inj} , is obtained as follows. Let ξ be the angle, measured positively eastwards, between the injection subpoint on the equator, and the orbital descending node (Fig. 2.18). From vectorial equalities, if δ is the injection point,

$$\sin \xi = \frac{\tan \delta}{\tan i_\alpha} \quad \cos \xi = + \text{sqrt}(1 - \sin^2 \xi) \quad (2.6-6)$$

Now let (2.6-6) be computed for the launch point (yielding ξ_1) and the injection point (yielding ξ_2). The Greenwich hour angle at the time of

injection is

$$G_{inj} = G_{00:00 \text{ H.U.T., on day "d"}} + 15.041688*(d*24 + t_{inj}) = G_0 + 15.041688 \text{ (in deg)}$$

$$t_{inj}, \text{ in hours, has to be comprised between 0 and 24.} \quad (2.6-7)$$

Also, if ϕ_L is the longitude of the launch site,

$$G_{inj} = \phi_L + \xi_1 - \xi_2 + \Omega_\alpha + 180 \quad (\text{degrees}) \quad (2.6-8)$$

t_{inj} is computed from

$$t_{inj} = \frac{G_{inj} - G_0}{15.041688} \quad (\text{hours, from 00:00 hrs U.T.})$$

$$15.041688 \text{ (in deg.)}$$

Multiples of 24 are added or subtracted to the numerator so that t_{inj} lies between 0 and 24.

The reduction to perigee, necessary for running data generated by ECLIP in Program SABAC, is embodied in formula (2.6-1), in which, successively,

$$C = R_{inj} V_{inj} \cos \gamma$$

$$e = \text{sqrt}[1 + 2\left(\frac{C}{\mu}\right)^2 * \left(\frac{1}{2} V_{inj}^2 - \frac{\mu}{R_{inj}}\right)]$$

$$p = \frac{e^2}{\mu}$$

$$a = \frac{p}{1 - e^2}$$

$$\tau_{sat} = 2 \frac{a^{3/2}}{\sqrt{\mu}}$$

$$h_A = a(1 + e) - R_{\oplus}$$

$$h_P = a(1 - e) - R_{\oplus}$$

$$\cos v_{inj} = \left(\frac{C^2}{\mu} - R_{inj} \right) / (e R_{inj}) \text{ and } \sin v_{inj} = (\text{Sign } \gamma) \sqrt{1 - \cos^2 v_{inj}}$$

\vec{P} , from (2.6-1), is equal to $[X_P, Y_P, Z_P]$ in the α -system.

Z_P , longitude of perigee, is given by: $\sin \delta_P = Z_P$;

$$\cos \delta_P = \sqrt{1 - Z_P^2}$$

$$\cos E_{inj} = e + (R_{inj} \cos v_{inj})/a ; \sin E_{inj} = \sqrt{1 - \cos^2 E_{inj}}$$

$$T_{injection \text{ to perigee}} = \frac{a^{3/2}}{\sqrt{\mu}} (e \sin E_{inj} - E_{inj})$$

(This quantity is positive for injection before perigee or $\gamma < 0$;

negative for injection after perigee or $\gamma > 0$)

Finally, if the unit along the nodal line is $\vec{i}_{\Omega} = \frac{1}{\sin i_{\alpha}} [\vec{Z}_{\alpha} \wedge \vec{n}_{\alpha}]$, then ω_{α} , argument of perigee, is obtained from $\cos \omega_{\alpha} = \vec{i}_{\Omega} \cdot \vec{P}$; $\sin \omega_{\alpha} = \vec{n}_{\alpha} \cdot [\vec{i}_{\Omega} \wedge \vec{P}]$.

Launch Opportunity "Strip"

The launch opportunity strip is obtained by setting limits on the angular departure between the satellite spin axis vector, \vec{s} , and the negative normal to the ecliptic. Now, assume that the nominal injection time has been determined as above. δ , latitude of injection, being fixed, at time t (t_{inj}^* is supposed to be the nominal injection time), we have

$$\vec{r}_{inj,t} = [\cos \delta \cos RA_{\alpha,t}, \cos \delta \sin RA_{\alpha,t}, \sin \delta]$$

$$\vec{n}_t = [\sin i_\alpha \sin \Omega_{\alpha,t}, -\sin i_\alpha \cos \Omega_{\alpha,t}, \cos i_\alpha]$$

$$\Omega_{\alpha,t} = (\Omega_\alpha)_{t_{inj}^*} + 15.041688(t - t_{inj}^*)$$

$$RA_{\alpha,t} = (RA)_{\alpha,t_{inj}^*} + 15.041688(t - t_{inj}^*)$$

The unit vector along the spin axis of the satellite is given by

$$\vec{S} = \cos(\gamma + \gamma_s) \vec{n}_t \wedge \vec{r}_{inj,t} + \sin(\gamma + \gamma_s) \vec{r}_{inj,t}$$

The (spin-axis, negative normal to the ecliptic) angle σ , is given by

$$\sin \sigma = |\vec{S} \wedge \vec{Z}_e| \quad (0 \leq \sigma \leq 90^\circ) \quad (2.6-9)$$

and the solar aspect angle β , given the Earth-Sun vector \vec{I}_{E-S} at t , by

$$\sin \beta = |\vec{I}_{E-S} \wedge \vec{S}| \quad (2.6-10)$$

An example of result of these calculations is shown in Fig. 2.18.

A Fortran V computer program, called ECLIP, has been written at C-MU and is described in documentation D-2. It determines, for given R_{inj} , V_{inj} , i_α , γ , γ_s , the nominal injection time, the launch opportunity strip, the values of angles σ and β . It has also been used by S.J. Paddack in the mission analysis of IMP-G^[2-8].

Modified version (ECLIP3)

In this version, the nominal injection point is defined on the basis of the satellite spin axis vector \vec{S} (defined by γ_s) being normal to the ecliptic. Formula (2.6-2) still holds, with γ_s replacing γ . Obviously, the latitude and longitude of injection will depend on γ_s . The time of

injection, computed as above, only corresponds to the time when the orbital plane (of fixed i_α) contains the normal to the ecliptic; it is thus γ_s - and γ - independent. For instance, if we chose $\gamma_s = -\gamma$, \vec{s} is along the transverse and the injection occurs in the ecliptic. With that equality, the launch window strip can be determined without any need to restructure program ECLIP.

2.6.2 Program SABPL2

SABPL2 is a plotting program documented in D-3, accepting the punched output from SABAC 1 or SABAC 2. It plots the launch window and launch opportunity "strip" as defined above. The strip is horizontal (if output is from SABAC) or oblique (if output is from SABAC 2, with the "strip" defined by ECLIP)

REFERENCES - Chapter 2

- [2-1] Renard, M.L.: "Launch Window Analysis of High Eccentricity Orbits", Proposal #1 to NASA, Applied Space Sciences Program, Carnegie-Mellon University, December 1967.
- [2-2] Lidov, M.L.: "The Evolution of Artificial Satellites of Planets Under the Action of Gravitational Perturbations of External Bodies", Planet. Space Science, 9, pp. 719-759, 1962.
- [2-3] Sridharan, R: "Evolution of the Orbital Elements in Geocentric Orbits of High Eccentricity by Non-Numeric Computation". Ph.D. Thesis, Applied Space Sciences Program, December 1972.
- [2-4] Brouwer, D. and Clemence, G.M.: Methods of Celestial Mechanics, Ac. Press, 1961.
- [2-5] Renard, M.L.: "Approximate Stability Criteria for Highly Eccentric Orbits About the Earth". Presented at 19th Congress of the International Federation, New York, Oct. 1968. Proc. of 19th Int. Astronautical Congress, 2, Astrodynamics and Astrionics, pp. 13-25, 1970.
- [2-6] Renard, M.L.: "Practical Stability of High Eccentricity Orbits Quasi-Normal to the Ecliptic", Presented at AIAA Astrodynamics Conf., Princeton, August 1969. JSR. 7(10) pp.1208-1214, 1970.
- [2-7] Renard, M.L. and Sridharan, R.: "Launch Window of a Highly Eccentric Satellite in an Orbit Normal to the Ecliptic: IMP-G", 9th Semi-Annual Astrodynamics Conf., NASA GSFC, April 1969.
- [2-8] Paddack, S.J.: "IMP-G Orbit and Launch Time", GSFC Doc. No. X-724-69-252, June 1969.
- [2-9] Kaufmann, B., and Muhonen, D.P.: "IMP-I Launch Window Analysis", GSFC Doc. No. X-551-71-5, January 1971.
- [2-10] Montgomery, H.E. and Paddack, S.J.: "S-49 Launch Window and Orbit", GSFC Doc. No. X-640-63-119, July 1963.
- [2-11] Paddack, S.J. and Shute, B.E.: "IMP-C Orbit and Launch Time Analysis", GSFC Doc. No. X-633-65-40, 1965.
- [2-12] Shute, B.E.: "Prelaunch Analysis of High Eccentricity Orbits", NASA Tech. Note D-2530, December 1964.
- [2-13] Shute, B.E. and Chiville, J.: "The Lunar-Solar Effect on the Orbital Lifetimes of Artificial Satellites with Highly Eccentric Orbits", Planet. Sp. Sc., 14(4), pp. 361-369.
- [2-14] Renard, M.L.: "HEOS-A Orbit", ESRO Internal Doc. DSP/65, ESRO, June 1965.

- [2-15] Göllnitz, H. and Renard M.L.: "Orbital restraints on the release of a body along a highly eccentric orbit", Max-Planck-Institute, Report for Extraterrestrial Physics, Report 28/66, Oct. 1966.
- [2-16] Göllnitz, H. and Renard, M.L.: "Release Windows for the Ejection of a body along a Highly Eccentric Orbit", *Astronautics Acta*, 14(1), pp. 23-46, Nov. 1968.
- [2-17] Moe, M.M.: "Solar-Lunar Perturbations of the Orbit of an Earth Satellite", *ARS JI.*, 30(5), pp. 485-487, May 1960.
- [2-18] Praguski, W., Stricker, J. and Miessner, W.: "Launch Window Study and Analog Orbit Stability Program", Report ER-13634, Martin-Marietta Corporation, October 1964.
- [2-19] Stricker, J., and Miessner, W.: "Launch Window Program", *Simulation* 31, 7(3), pp. 134-141, 1966.
- [2-20] Leroy, M. and Paçé, V., SEREB, Private communication (1966).
- [2-21] An. "IMP 6 First Year Report", GSFC Document, March 1972.
- [2-22] Paddack, S.J., Muhonen, D.P., Fried, G.B.: "Orbit Considerations for the Mother-Daughter Mission", Goddard Space Flight Center, Inf. Memo, June 1972.

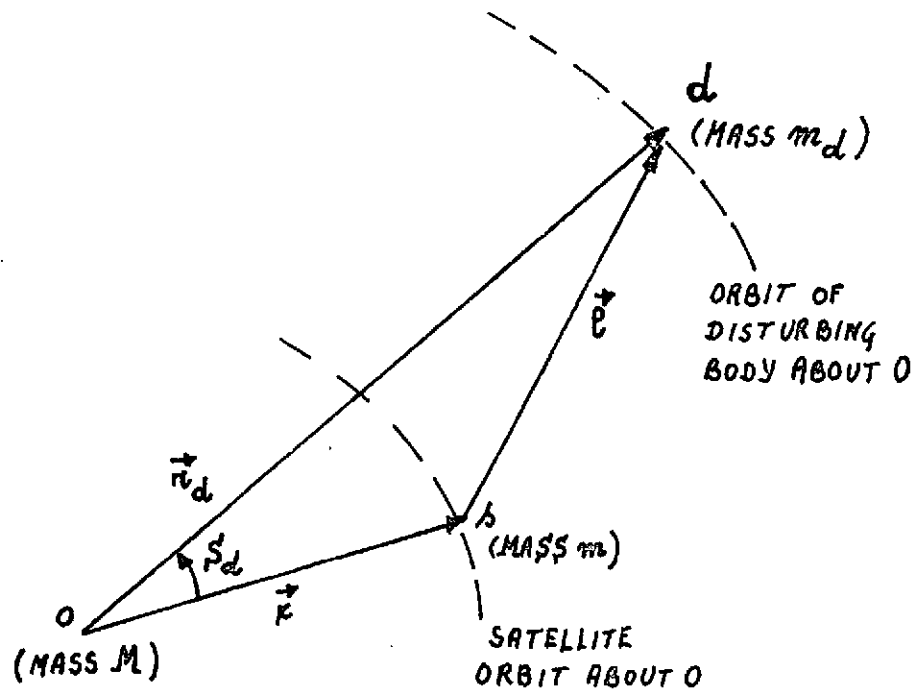


FIG. 2-1. GEOMETRY AND NOTATIONS.

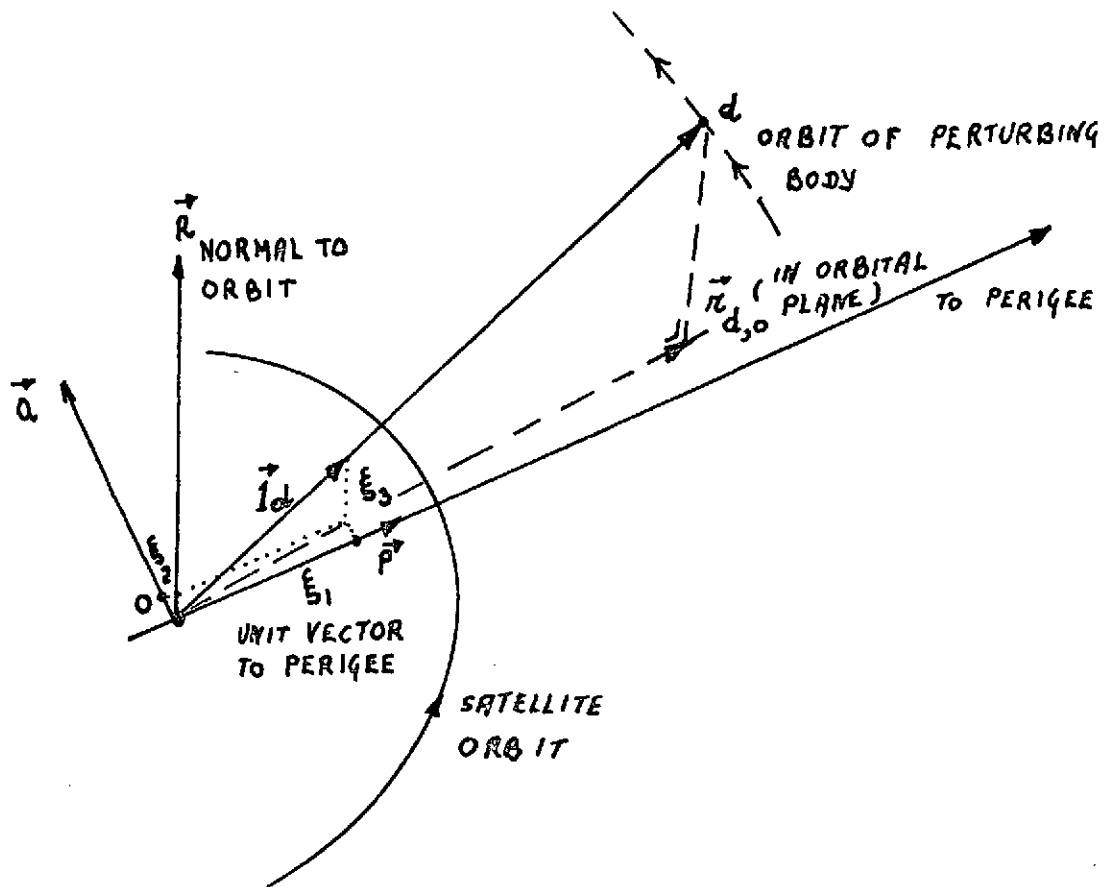


FIG. 2-2. DIRECTOR COSINES OF UNIT VECTOR TO PERTURBING BODY

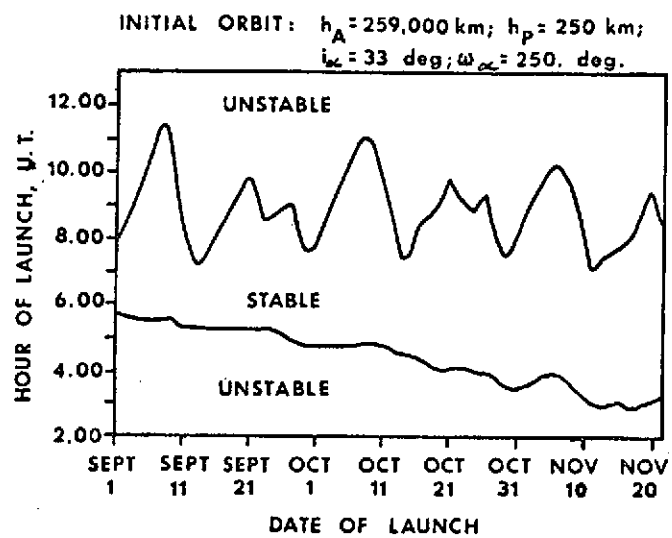


FIG. 2-3. EXAMPLE OF LAUNCH WINDOW MAP

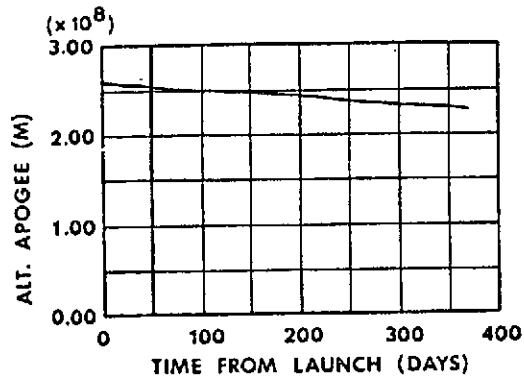


FIG. 2a

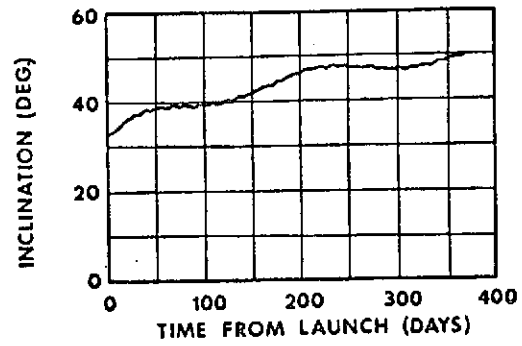


FIG. 2c

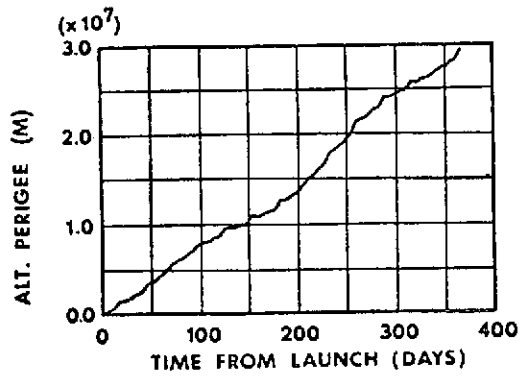


FIG. 2b

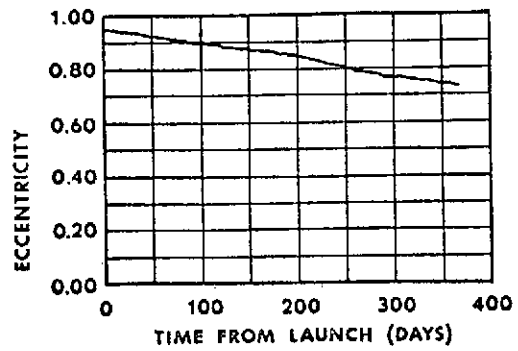


FIG. 2d

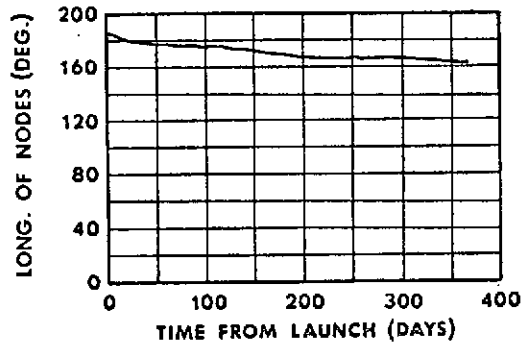


FIG. 2e

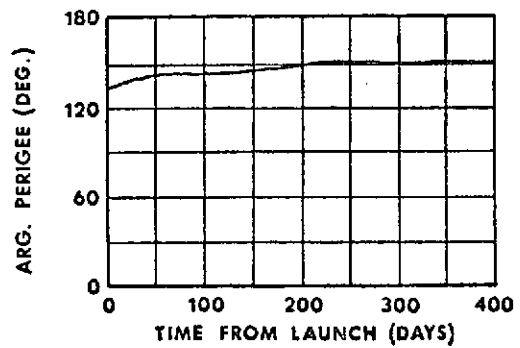


FIG. 2f

FIG. 2-4. VARIATION OF ORBITAL PARAMETERS WITH TIME

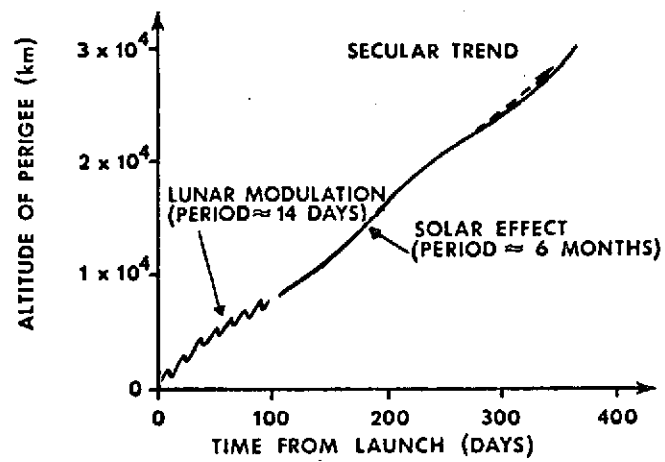


FIG. 2-5. Short-term and long-term effects on altitude of perigee.

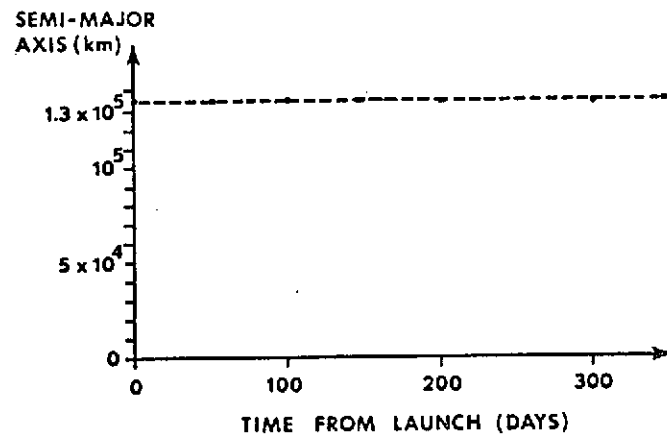


FIG. 2-6. CONSTANCY OF SEMI-MAJOR AXIS.
(ORBIT OF FIG. 2-4)

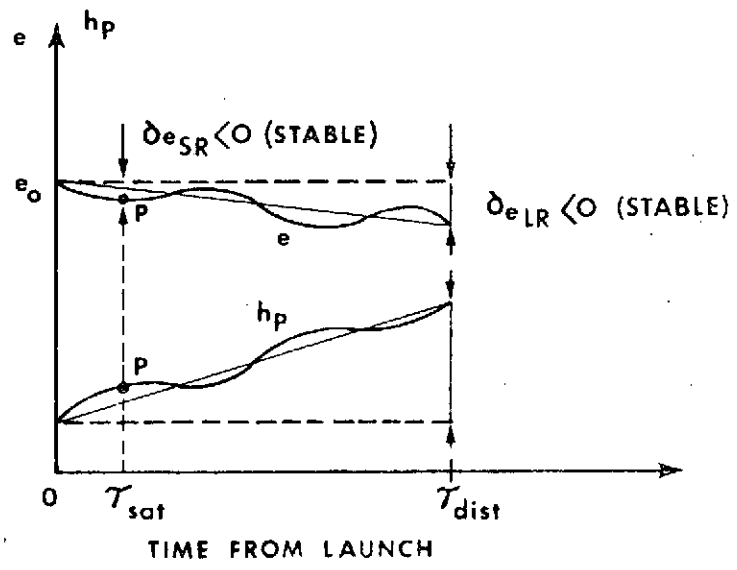


FIG. 2-7. SHORT-TERM AND LONG-TERM CHANGES OF e AND h_p .

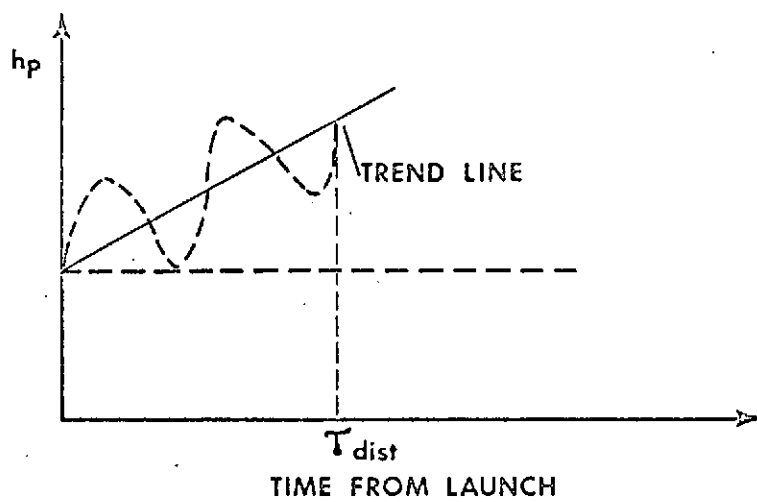


FIG. 2-8. LIMIT ON AMPLITUDE OF MODULATION

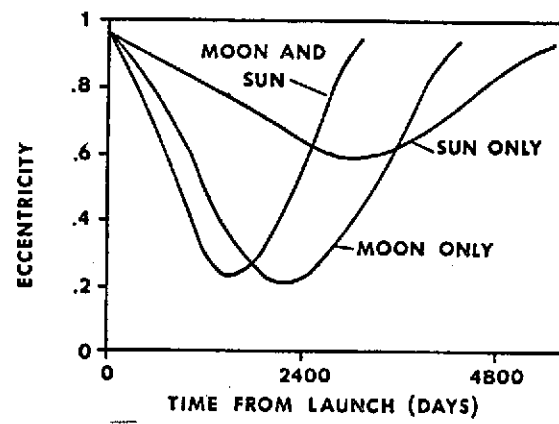


FIG. 2-9. VERY-LONG-TERM EVOLUTION OF THE ECCENTRICITY.
(After B. Shute [2-12]).

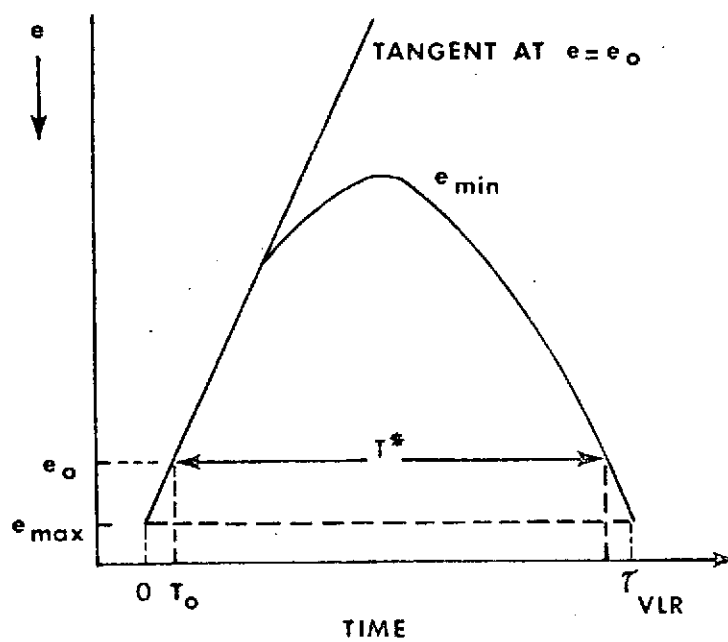


FIG. 2-10. VERY-LONG RANGE STABILITY FROM e -CURVE.

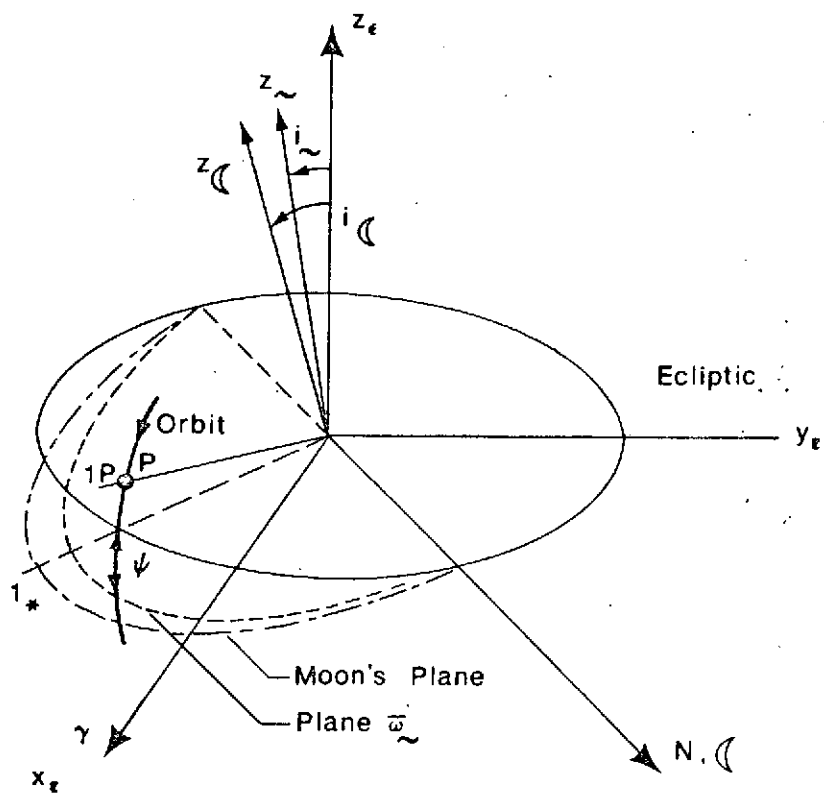


FIG:2-11. Geometry of Plane $\tilde{\omega}$

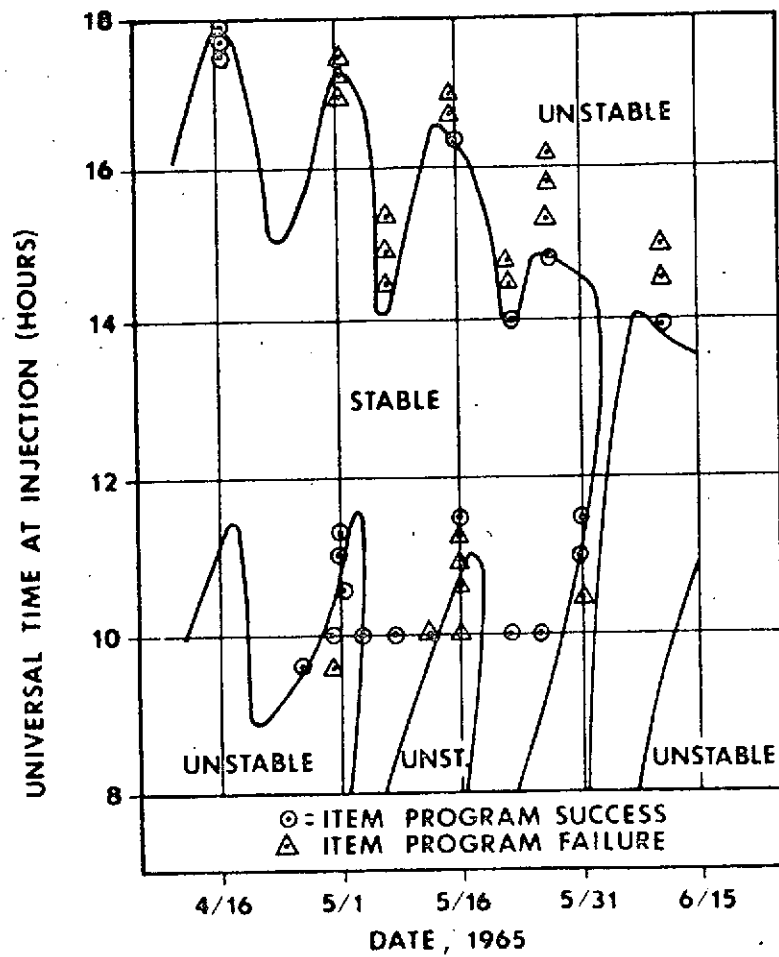
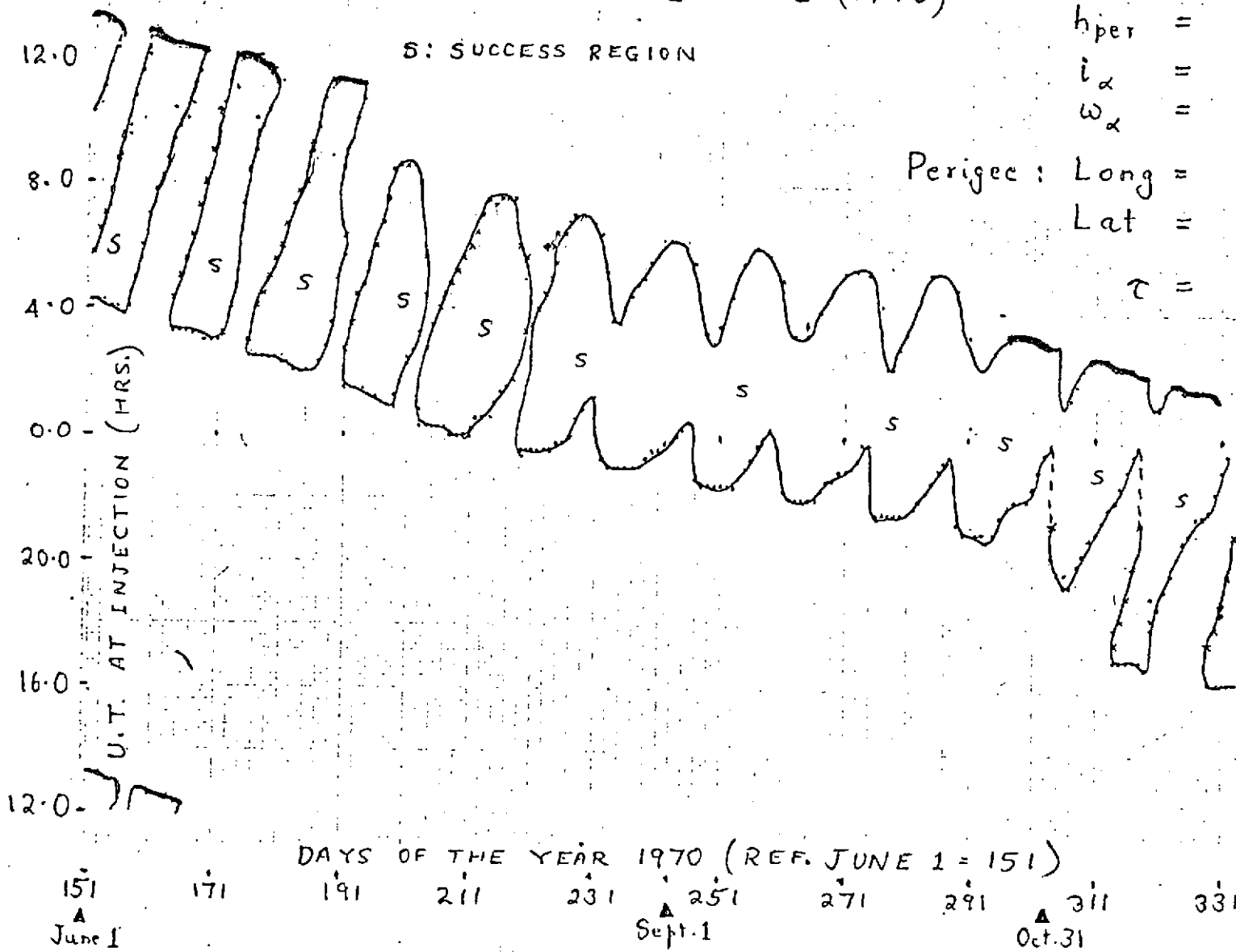


FIG.2-12. COMPARISON OF RESULTS FROM NUMERICAL INTEGRATION AND THIS THEORY.

LAUNCH WINDOW FOR IMP-I (1970)

S: SUCCESS REGION



DATA:

$$h_{apo} = 217,572.190 \text{ M.}$$

$$h_{per} = 277,800. \text{ M.}$$

$$i_{\alpha} = 28.9 \text{ deg.}$$

$$\omega_{\alpha} = -53.14 \text{ deg.}$$

Perigee: Long = 115.91 deg. E.

Lat = 22.75 deg. S.

$$\tau = 4.51 \text{ days}$$

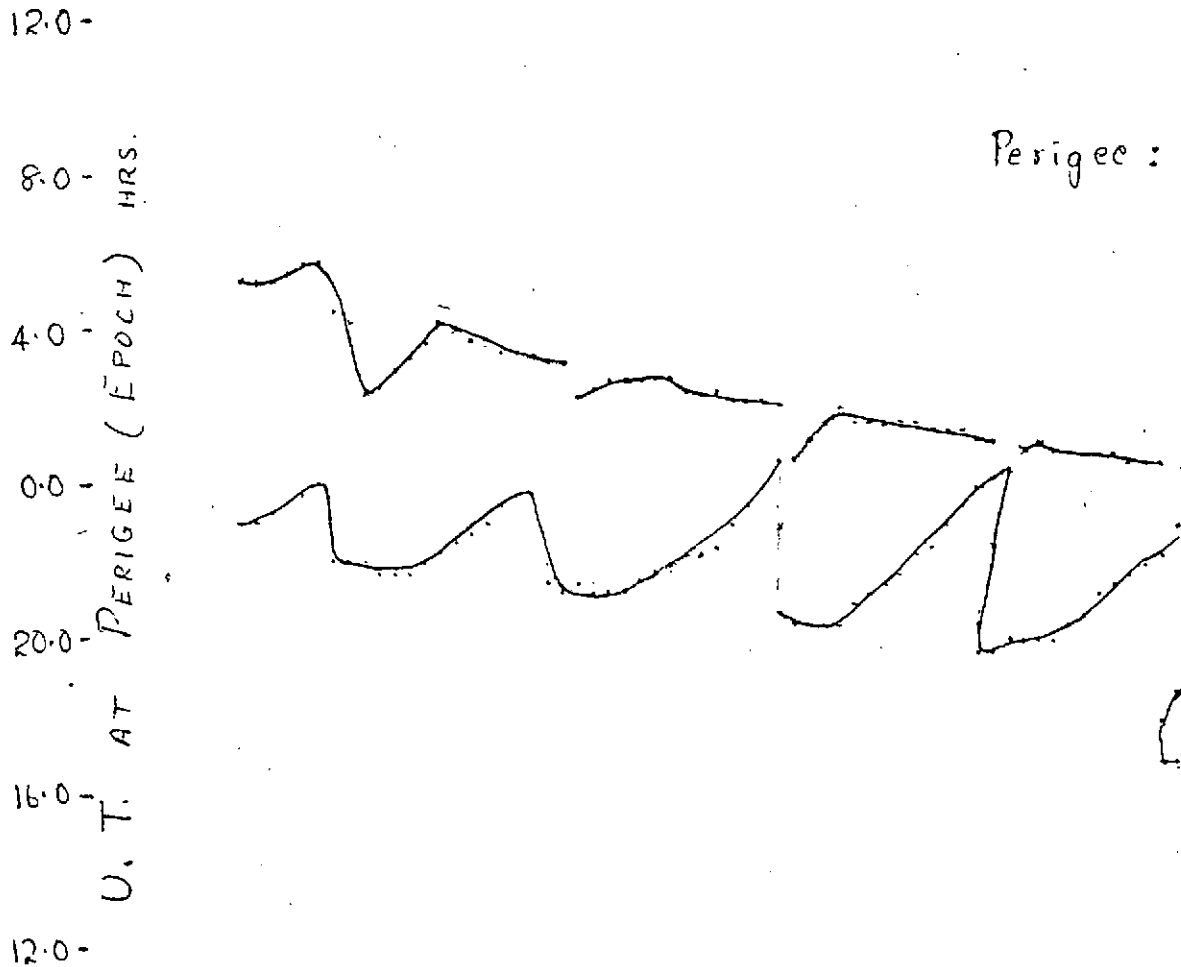
FIG.2-13. LAUNCH WINDOW
IMP-I(Orbit 1)

March 1970

LAUNCH WINDOW FOR IMP-I.

$h_{apo} = 216,676.62 \text{ Km}$
 $h_{per} = 240.24 \text{ Km}$
 $i_{\alpha} = 28.2996^{\circ}$
 $\omega_{\alpha} = -66.2037^{\circ}$

Perigee: Long. = $112.67^{\circ} \text{ E.}$
 Lat. = $25.838^{\circ} \text{ S.}$



271

DAY NO. (YEAR 1970) Nov. 10
 291
 Prepared Launch Date: Nov. 17
 311
 Nov 20
 331

REF: JAN. 1 = 0

FIG. 2-14 LAUNCH WINDOW FOR IMP-I (Orbit 2)

INJECTION STATE VECTOR

1. ALTITUDE, ABOVE MEAN EQUATOR (km)	231.35075	
2. VELOCITY (km/sec)	10.806989	
3. FLIGHT PATH ANGLE (deg.)	0.	
4. FLIGHT PATH AZIMUTH (deg.)	73.5944	
5. LATITUDE (deg.)	-23.966	(SOUTH)
6. LONGITUDE (deg.)	111.449	(EAST)

COVARIANCE MATRIX

①	②	③	④	⑤	⑥
319.475	-.301558	-1.89925	3.06964	-1.85248	-7.01463
	.000314949	.00168757	-.00303874	.00174996	.00661598
		.0536598	-.0191042	.0116318	.0393667
			.0982999	-.0183223	-.0649491
				.0111156	.0392638
					.159351

FIG. 2-16. COVARIANCE TABLE, IMP-I ORBIT
(FROM REF. [2-9])

MOTHER/DAUGHTER MISSION OMEGA = 0 7/77-2/78

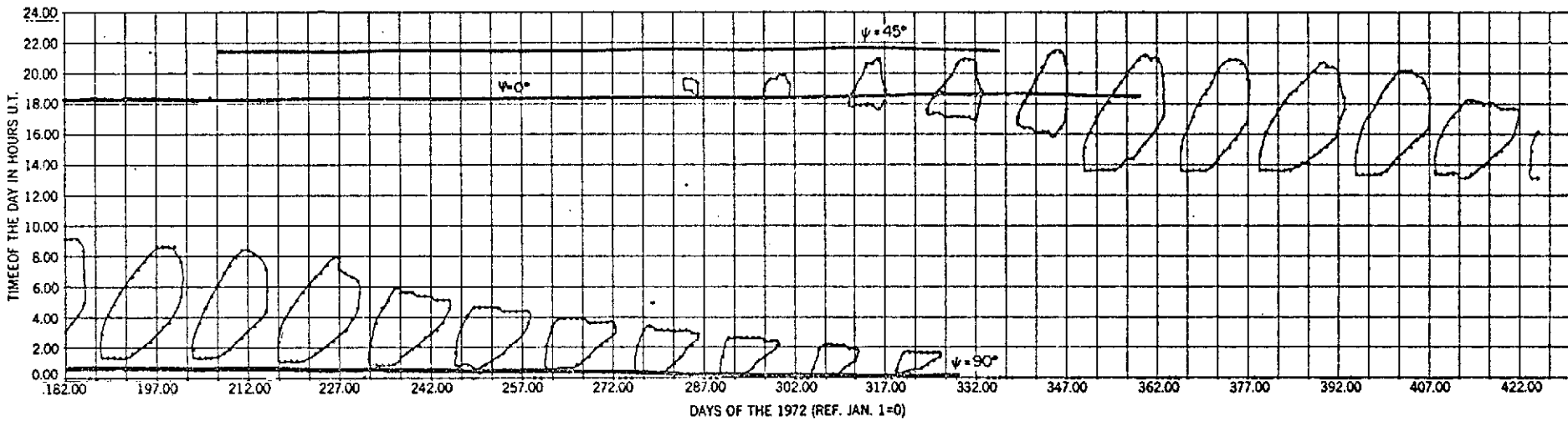


FIG. 2-17. LAUNCH WINDOW OF MOTHER-DAUGHTER MISSION (From Ref. [2.22]),

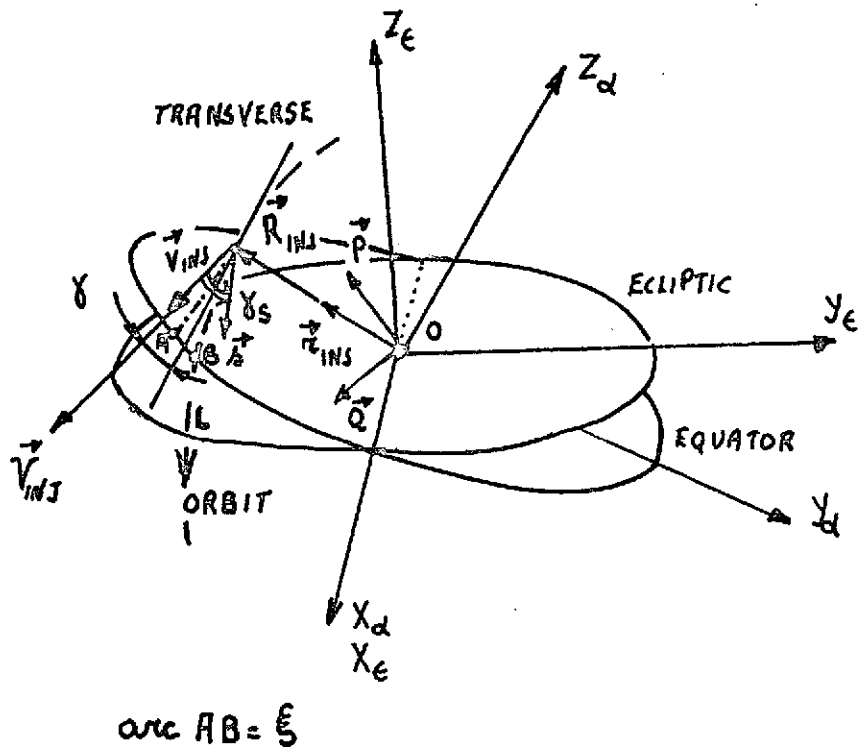


FIG. 2-18. GEOMETRY AT INJECTION.

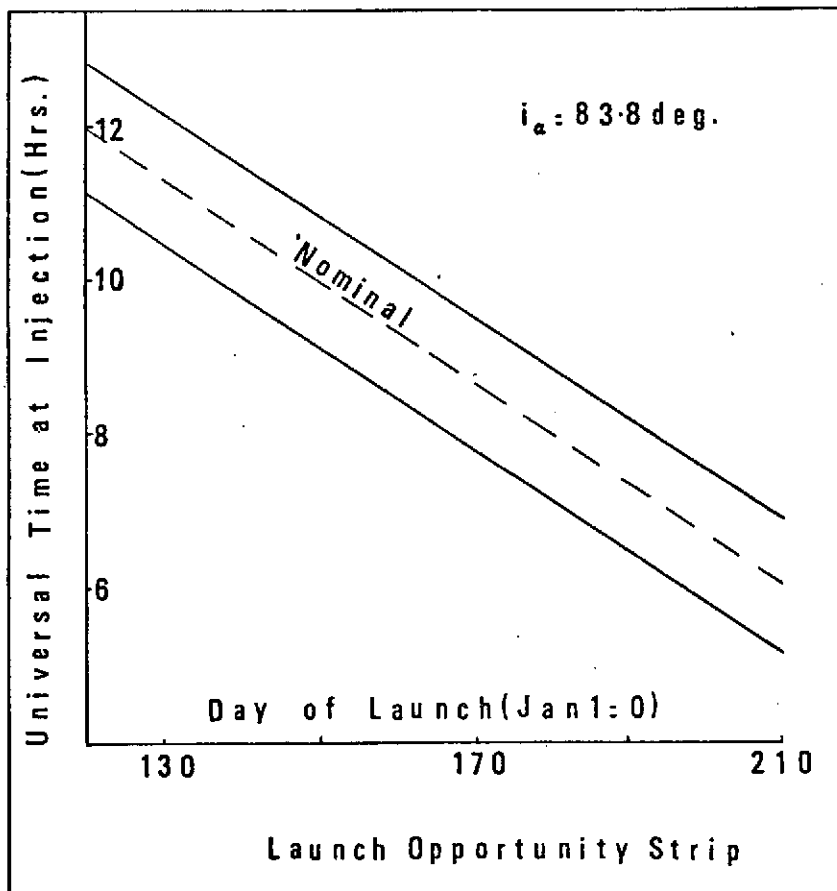


FIG. 2-19. LAUNCH WINDOW "STRIP".

CHAPTER 3

A Study of Orbits of Large Eccentricity Quasi-Normal
to the Ecliptic

3.1 Introduction

Relatively early in the present study (1968-1970), it appeared of interest to initiate a study of the "practical" stability (in the sense specified in Chapter 2) of high eccentricity orbits having an inclination on the ecliptic close to 90° . This was to be the case for satellite IMP-G, which was launched in June 1969. A very detailed description of the results has appeared elsewhere^{[3-1],[3-2]}.

A thorough study of IMP-G orbit and launch time was carried out at NASA GSFC by S.J. Paddack^[3-3], who used as computing technique ITEM and a Perturbation Routine for final, accurate results by numerical integration on a computer, and our program SABAC, based on the approximate criteria approach, for the fast generation of global launch windows. ECLIP, written at C-MU, was also used to define the launch opportunity strip, defining a nominal time, and an interval on both sides of this nominal time, in which the alignment of the satellite spin axis on the normal to the ecliptic is closely realized.

As is schematized on Fig. 3.1, taken from Ref.[3-3], it is clear that if, to simplify the reasoning, we assume that the velocity at injection is very nearly coincident with the satellite spin axis and is normal to the ecliptic, the resulting orbit will be inclined by $i_e = 90^\circ$ on the

plane of the ecliptic. The corresponding inclination on the equator i_α , for a southwards injection, will be comprised between 90° (if $\Omega_\epsilon = \Omega_\alpha = +90^\circ$) and $66.55^\circ = 90^\circ - \epsilon$ (if $\Omega_\epsilon = \Omega_\alpha = +180^\circ$). The fourth and first quadrants for $\Omega_\epsilon, \Omega_\alpha$ would correspond to retrograde orbits, and the third one might lead to prolonged times in eclipse, near apogee, for up to 9 hours^[3-3]: therefore, these three quadrants are not to be considered, and we shall assume from now on that $90^\circ \leq \Omega_\epsilon$ or $\Omega_\alpha \leq 180^\circ$.

In the following, the approximate criteria shall be used consistently; the lifetime criterion is described in Section 2-4.

3.2 Study of the Stability of Orbits Nearly Normal to the Ecliptic^[3-1].

3.2.1 Simplified model: planar case.

As an approximation, we shall first consider, that in view of the smallness of the inclination of the moon's orbital plane on the ecliptic ($I_M = 5.145^\circ$), those two planes are approximately coincident. With the notations of Chapter 2, let i_d be the inclination of the satellite orbit on the orbital plane of perturbing body "d". As said above, we have approximately (Fig. 3.2)

$$i_M \simeq i_S \simeq 90^\circ$$

Long-Range and Very Long-Range Stability

As explained in Chapter 2, we shall use Lidov's "11", secular theory. With the above simplification, we can define " A_d " as the sum $A_M + A_S$ (Note again that A_M/A_S is independent of a , and equal to 2.18).

The changes in the orbital elements due to the sun and the moon, per satellite orbit, are (angles, referred to the ecliptic, are not subscripted)

$$\delta a = \delta i = \delta \Omega = 0 \quad (3.2-1)$$

$$\delta e = e \epsilon^{1/2} (A_M + A_S) \frac{\sin 2\omega}{4} \quad (3.2-2)$$

$$\delta \omega = \frac{A_M + A_S}{20} \zeta \quad (3.2-3)$$

$$\zeta = (5 \cos 2\omega - 1) \left(1 - \frac{c_2''}{5 \cos 2\omega - 1} \right) \quad (3.2-4)$$

$$c_2'' = (1 - \epsilon_0) (5 \cos 2\omega_0 - 1)$$

Subscript "0" refers to initial values.

To this approximation, orbits initially normal to the ecliptic will remain so for all time and will have a constant longitude of nodes. Now consider Lidov's constants, c_1 and c_2 , which are integrals of the "11", secular differential equations of motion:

$$\begin{aligned} c_1 &= \cos^2 i = \epsilon_0 \cos^2 i_0 = 0 \\ c_2 &= (1 - \epsilon) \left(\frac{2}{5} - \sin^2 \omega \right) = (1 - \epsilon_0) \left(\frac{2}{5} - \sin^2 \omega_0 \right) = \frac{c_2''}{10} \end{aligned} \quad (3.2-5)$$

Any of the orbits will be represented by point $(c_2, 0)$ on segment AC of the c_2 axis of Lidov's (c_1, c_2) diagram (Fig. 3.3). From Equations (3.2-1) to (3.2-4), the evolutions of ω and e are described by Lidov's discussion^[3-4], in which A_d is replaced by $A_M + A_S$.

$$\text{Let } \omega_1^* = \frac{1}{2} \arccos\left(\frac{1}{5}\right) = 39.23^\circ, \omega_2^* = \pi - \omega_1^*, \omega_3^* = \pi + \omega_1^*, \omega_4^* = 2\pi - \omega_1^*.$$

Then, considering that $\delta e = -A(1 - \epsilon) \epsilon^{1/2} \frac{\sin 2\omega}{2}$,

- a) $\omega_4^* < \omega < \omega_1^*$ (Region 1, Fig. 3.4) or $\omega_2^* < \omega < \omega_3^*$ (Region 3, Fig. 3-4)

If initially, $\omega_0 < 0$ ($\omega_0 < \pi$), e decreases until ω reaches $0(\pi)$.

The minimum for e is given by

$$e_{\min}^2 = \frac{1}{4}e_0^2(5 \cos 2\omega_0 - 1) \quad (3.2-6)$$

Thereafter, e increases and reaches e_{\max} at $\omega_{e,\max}$. With R_{\oplus} , earth's radius, and h_p^* , critical height of perigee, it is obtained

from

$$1 - e_{\max}^2 = 1 - \left[1 - \frac{R_{\oplus} + h_p^*}{a}\right]^2 \quad (3.2-7)$$

$$5 \cos 2\omega_{e,\max} - 1 = (1 - \epsilon_0)(5 \cos 2\omega_0 - 1) \frac{1}{e_{\max}^2} \quad (3.2-8)$$

and $\omega_{e,\max}$ is in the same region as ω_0 . If initially, $\omega_0 > 0$ ($\omega_0 > \pi$), there is never a decrease in eccentricity. From the viewpoint of long-range stability (Criterion 1 of approximate criteria method), sub-regions 1a, 3a are acceptable.

- b) $\omega_1^* > \omega > \omega_2^*$ (Region 2, Fig. 3.4) or $\omega_3^* < \omega < \omega_4^*$ (Region 4, Fig. 3.4)

Here ω decreases. If initially, $\omega_0 > \frac{\pi}{2}$ ($\omega > \frac{3\pi}{2}$), e decreases

until $\omega = \frac{\pi}{2}$ ($3\pi/2$). The minimum for e is

$$e_{\min}^2 = \frac{1}{6}e_0^2(1 - 5 \cos 2\omega_0) \quad (3.2-9)$$

Thereafter, e increases up to the value given by Equation (3.2-7).

If initially $\omega_0 < \frac{\pi}{2}$ ($\omega_0 < 3\pi/2$), the eccentricity is always increasing. Thus, from the viewpoint of long-range-stability, region 2b, and 4b, are acceptable.

By reason of symmetry, and since, as was mentioned earlier, our interest here lies in orbits with southwards injection, the analysis will be restricted, without loss of generality, to the second and third quadrants of the orbital plane (Fig. 3.2). On Fig. 3.4, point "B" corresponds to $\omega = \omega_2^*$ and appears as an unstable point, whereas point "D", for which $\omega = \omega_3^*$, appears as a stable point. Only 2b and 3a are acceptable for long-range stability in these two quadrants.

If very-long-range stability is now considered, an assessment of the orbital lifetime can be made here, provided it is fairly large compared to the periods of the perturbing bodies (in practice, the required lifetime equals many orbital periods of the moon, but only one or a few orbital periods of the sun.) This so-called "long-range" (LR) lifetime reads, in satellite periods,

Region 2b ($\pi/2 < \omega_0 < \omega_2^*$)

$$\left(\frac{L}{2}\right)_{LR} = \frac{20}{A} \int_{\omega_0}^{\pi/2} \zeta^{-1} d\omega \quad (3.2-10)$$

Region 3a ($\omega_2^* < \omega_0 < \pi$)

$$\left(\frac{L}{2}\right)_{LR} = \frac{20}{A} \int_{\omega_0}^{\pi} \zeta^{-1} d\omega \quad (3.2-11)$$

in which ζ is given by Equation (3.2-4). As an example, L_{LR} is given, in days, as a function of ω , for an orbit of $e_0 = 0.945991$, $a = 124,283$ km, $\tau_{sat} = 5.0468$ days (Region 3a., neighborhood of the ecliptic) (Fig. 3.5).

If the orbit originates at $\omega = \omega_2^* \pm \eta$ (η small and positive angle) evolution $B_- \rightarrow A$ will lead to a larger L_{LR} than evolution $B_+ \rightarrow C$:

if X is the point having argument $\pi - 2\omega_1^* = 101.54^\circ$, the time spent along $B \rightarrow X$ is the same as that along $B \rightarrow C$. Thus

$$t_{B \rightarrow A} = t_{B \rightarrow X} + t_{X \rightarrow A} > t_{B \rightarrow C}$$

In conclusion, larger lifetimes will be possible in region 2b, the larger the closer the argument of perigee is to ω_2^* . In region 3a, for maximum L_{LR} , ω should be made equal to $\omega_2^* + 0$. The upper limit for L_{LR} in this region is infinite since $L_{LR} \rightarrow \infty$ when $\omega \rightarrow \omega_2^*$.

SHORT-RANGE AND INTERMEDIATE-RANGE STABILITY

The short-range behavior of the eccentricity, which determines the short-range stability, is described by Equation (2.4-7)

$$\delta e_{SR} = -e\epsilon^{1/2} \left[\frac{A_M}{\epsilon_M^{3/2}} \beta_{3,M} + \frac{A_S}{\epsilon_S^{3/2}} \beta_{3,S} \right] \quad (3.2-12)$$

From Fig. 3-1, it is apparent that if ω were 180° , as is the case for an injection, at perigee, in the ecliptic plane, $\xi_{2,d}$ would vanish and initially, the short-term stability would be neutral (Criterion 2).

Due to the short-range increase of ω , as given by

$$(\delta\omega)_{\omega_0=\pi} = \frac{3}{5}\epsilon^{1/2} \left[\left(\frac{A_M}{\epsilon_M^{3/2}} \right) \left(\frac{P_M}{r_M} \right)^3 + \left(\frac{A_S}{\epsilon_M^{3/2}} \right) \left(\frac{P_S}{r_S} \right)^3 \right] > 0 \quad (3.2-13)$$

there is, however, intermediate-term instability (Criterion 4) since $\xi_{2,d}$ will become < 0 at the next orbit. Thus, in the quadrants considered, for short-term stability it is required that the perigee be above the ecliptic plane

$$\frac{\pi}{2} < \omega < \pi \quad (3.2-14)$$

which also ensures LR stability (Criterion 1)

$$\delta e_{LR} = \frac{1}{4} e \epsilon^{1/2} A \sin 2\omega < 0 \quad (3.2-15)$$

For intermediate-term stability, a margin (of the order of a few degrees) should be provided, so that the perigee is sufficiently above the plane of the disturbing bodies. In order to obtain actual lifetimes which are as long as possible, one could possibly select those launch days in the year leading to a slope, on the e vs. time from launch curve, and over a time of the order of $\tau_s/4$, which is as small as possible. For fixed e_0 , $i_d = \frac{\pi}{2}$, ω_0 and thus fixed values of Lidov's constants c_1 and c_2 , $(\delta e_{LR})_M$ is fixed. One requires to make $\langle \delta e_{SR,S} \rangle \tau_s/4$ as small as possible. As an example, for a celestial longitude of the radius vector at injection RA_ϵ , in the fourth quadrant (Fig. 3.6), the best launch day of the year will be that for which the unit vector to the sun is along axis $3_p = 3_*$ normal to the orbit, on the average over $\tau_s/4$ (half a solar modulation.) An example is treated in Section 3.3.

Conclusions from simplified model

In summary, to the approximation of the simplified model, and with an analysis restricted, without loss of generality, to the second and third quadrants of the orbital plane, it is concluded that

- a) the highest realizable value, in region 3a. of Fig. 3.4, for the long-range assessed lifetime is defined by Equation (3.2-11),

where ω_0 is the minimum feasible ω .

- b) short-term and long-term stability are strictly realized for ω in the second quadrant, whereas intermediate-term stability requires that ω differ from π (or $\pi/2$) by a negative (positive) margin, in practice a few degrees for a lifetime of one year.
- c) it is possible to define a best day in the year leading to maximum actual lifetime for given e_0, ω and inclination on the equator.

3.2.2 Effect of the inclination of the moon's orbit on the ecliptic

We still assume that the satellite orbital plane is normal to the ecliptic, $RA_{\epsilon, P}$ is defined as the celestial longitude of perigee (Fig. 2-11) If P is sensibly in the plane of the ecliptic, and above the moon's plane, let $\Omega_{\epsilon, M}$ be the longitude of nodes of the moon's orbital plane, referred to the ecliptic. Thus

$$\Omega_{\epsilon, M} - \pi < RA_{\epsilon, P} < \Omega_{\epsilon, M}$$

Stability is assured in the long-range, since $(\delta e)_{LR, S} = 0$ and $(\delta e)_{LR, M} < 0$. The locus of southernmost (northernmost) admissible perigee points on the unit sphere is obtained by writing

$$(\delta e)_{LR} \approx (1 - \epsilon)\epsilon^{1/2} (A_M \psi_M + A_S \psi_S) = 0 \quad (3.2-16)$$

with $\psi_d = \pi - \omega_d$. It is approximately the arc of great circle having normal Z_0 inclined by

$$\tilde{i} = \frac{A_M}{A_M + A_S} I_M \quad (3.2-17)$$

on the normal to the ecliptic, Z_ϵ , in plane (Z_ϵ, Z_M) . In the long-range, therefore, I_M may be accounted for by rotating the ecliptic by \tilde{i} about the

nodal line of the moon. This new plane of reference, called $\bar{\omega}_.$, then replaces the ecliptic.

As an example, for a nominal injection at perigee and in the ecliptic (fourth quadrant), Fig. 2.11 shows that an inclination on the equator $i_\alpha = 90^\circ$ should maximize the long-range assessed lifetime if $\Omega_{\epsilon, M} = 0^\circ$ (which is in the case in early spring 1969), in a range for i_α

$$\frac{\pi}{2} - \epsilon < i_\alpha < \frac{\pi}{2}$$

An example is treated in Section 3.3.

In the short-range, were the sun alone, condition

$$\frac{\pi}{2} < \omega < \pi$$

would still hold, i.e. stability in the short-range would be realized when the perigee is in the second quadrant of the orbit. If the injection occurs at perigee, in the ecliptic plane, the short-term effect due to the sun alone is zero; the moon critically determines short-range stability. If the projection on the ecliptic of the vector to perigee, \vec{OP} , in Fig. 2.11, is normal to the moon's nodal line in the ecliptic, \vec{ON}_M , the moon is certainly favorable or neutral if

$$\xi_{1, M} \xi_{2, M} > 0$$

and cannot be satisfied throughout the lunar month.

In the intermediate-range, the margin on ω , to which we referred above, should not be construed with reference to plane $\bar{\omega}_.$. The condition on the best day of launch still holds approximately, to $O(L_M^2)$.

3.2.3 Effect of a small departure of the orbital inclination from normal to the ecliptic

Earlier, we defined a "nominal" orbit as one normal to the ecliptic, and it is desirable to qualify the effects of a slight departure, Δi_ϵ , from being normal to the ecliptic. Such a departure will be caused, for example, by the Earth's rotation for a launch slightly earlier or later than nominal.

Lidov's formulae, in the "11", secular theory^[3-4], written up to $O(\Delta i_\epsilon)$, yield

$$\delta \epsilon_{LR} = -\frac{1}{2} A(1 - \epsilon) \epsilon^{1/2} \frac{\sin 2\omega}{2} \quad (3.2-17)$$

For long-range stability, it is required that $\delta \epsilon_{LR} > 0$, or $\sin 2\omega < 0$.

To the same approximation,

$$\delta \omega_{LR} = \frac{1}{2} A \epsilon^{1/2} \left[\frac{2}{5} - \sin^2 \omega \right] \quad (3.2-18)$$

Therefore, the developments of the two previous sections concerning long-range stability apply.

In the long-range, the orbital inclination varies according to

$$\delta i_{LR} = -\frac{1}{4} A(1 - \epsilon) \sin 2\omega \frac{\Delta i_\epsilon}{4\epsilon^{1/2}} \quad (3.2-19)$$

and i will increase (decrease) for $\Delta i_\epsilon > 0$ or $i < \frac{\pi}{2}$ ($\Delta i_\epsilon < 0$ or $i > \frac{\pi}{2}$)

and tend to $\frac{\pi}{2}$ for stable orbits.

The rotation of the line of nodes will be of order Δi_ϵ ,

$$\delta \Omega_{LR} = -\frac{1}{2} A \Delta i_\epsilon \left[(1 - \epsilon) \sin^2 \omega + \frac{\epsilon}{5} \right] \frac{1}{\epsilon^{1/2}} \quad (3.2-20)$$

Developments relating to short- and intermediate-term stability involve geometrical conditions in the orbital plane, and still apply to $O(\Delta i_\epsilon)$.

3.2.4 A Priori Prediction of Orbital Lifetime

It has been seen in Section 2.4.3.3 that, in order to assess the orbital lifetime, T_* , and compare it to the required lifetime, L , one possible method consists in computing Lidov's constants $c_{1,d}$ and $c_{2,d}$, for the sun and the moon, and to weigh them with amplitudes A_M and A_S to obtain resultant c_1 and c_2 . It has also been mentioned that for orbits nearly normal to the ecliptic, $i_M \cong i_S \cong 90^\circ$, the approximation $\omega_M \cong \omega_S$ might not hold at all if, say, $\pi - \omega_d$ is a small angle (injection southwards, near the ecliptic). In particular, in the equation

$$\delta e_{LR,d} = A_d e \varepsilon^{1/2} \sin^2 i_d \sin 2\omega_d$$

$\sin 2\omega_d$ might be of different sign for the sun and for the moon.

Therefore, it appeared necessary, for satellites spending a significant fraction of their lifetime "between" the orbital planes of these two perturbing bodies, to come up with a better method of estimating the orbital lifetime T_* . Typically, when the unfavorable influence of the sun ($\delta e > 0$) on the evolution of the eccentricity, as would be the case if c_1, c_2 were with reference to the moon's orbital plane only, it was found^(3.2-1) that the inaccuracy in some parts of the contour of the map (determined by the lifetime criterion) was of the order of 0.3h, a large error in the case of IMP-G.

The alternative method adopted in this case has been briefly described in Section 2.4.3.3, but will be repeated here. Plane $\bar{\omega}_d$, as defined above, is the reference plane used to compute the argument of perigee of

of the satellite ω_{\sim} (Fig. 2.11). Now, half of the orbital lifetime, $T_*/2$, will correspond to the time needed for the perigee point to reach plane $\bar{\omega}_{\sim}$. The time-rate of change of ω_{\sim} is computed in equation

$$\frac{\delta\omega_{\sim}}{\delta\tau} = \left(\frac{\delta\omega_{\sim}}{\delta\tau}\right)_{LR,M} + \left(\frac{\delta\omega_{\sim}}{\delta\tau}\right)_{LR,S} (1 + w)$$

as being due to the long-range effect of the moon and, in order to capture the linear trend of ω_{\sim} vs. time, the average of the short-range effect of the sun $\left(\frac{\delta\omega}{\delta\tau}\right)_{SR,S}$ taken over half a solar modulation cycle, $\tau_S/4$ (see Fig. 2.5). As an example, it is interesting to note, in Fig. 3.7, where ω_{α} vs. time has been obtained from numerical integration program EOLA, that the crossing of plane $\bar{\omega}_{\sim}$ (as marked by the arrow) quite accurately corresponds to the topping off of the height of perigee.

To be more specific, we consider the "11", short-term theory, as embodied in Equations (2.3-14). Per orbit of the satellite, $\delta\tau_{sat}$, if e_S is neglected ($a_{\delta} \cong p_S$) and $i_S \cong \frac{\pi}{2}$, for body "S",

$$\frac{\delta\omega_{\sim}}{\delta\tau_{sat}} = \frac{A_S}{5} \varepsilon^{1/2} (4\xi_{1,S}^2 - \xi_{2,S}^2 - 1)$$

In the vicinity of the ecliptic, $\xi_{2,S}^2$ can be neglected. Now

$$\xi_{1,S}^2 \cong \cos^2(RA_S - RA_P)$$

in which RA_P is the celestial longitude of the perigee. Let $\phi = RA_S - RA_P$.

$$\begin{aligned}
\left\langle \frac{\delta\omega_{\sim}}{\delta\tau_{\text{sat}}} \right\rangle \tau_S/4 &\approx \frac{1}{5} A_S \epsilon^{1/2} \left\langle 4 \frac{1 + \cos 2\phi}{2} - 1 \right\rangle \tau_S/4 \\
&= \frac{1}{5} A_S \epsilon^{1/2} + \frac{1}{5} A_S \epsilon^{1/2} \times \left(-\frac{4}{\pi} \sin 2\psi_{\text{inj}} \right) \\
&= \left(\frac{\delta\omega_{\sim}}{\delta\tau_{\text{sat}}} \right)_{\text{LR,S}} + \left(\frac{\delta\omega_{\sim}}{\delta\tau_{\text{sat}}} \right)_{\text{LR,S}}^w
\end{aligned}$$

in which

$$w = -\frac{4}{\pi} \sin 2\phi_{\text{inj}}$$

For an injection in the neighborhood of the ecliptic, and given i_α , a "best" day is one which minimizes $\frac{\delta\omega_{\sim}}{\delta\tau}$, or for which

$$(RA_S - RA_P)_{\text{INJ}} = \phi_{\text{inj}} = \frac{5\pi}{4} \pm k \frac{\pi}{2} \quad (k \text{ positive integer or zero}).$$

An example is given in the Section 3.3. In the same section, Table 3.3-I also shows the good agreement obtained, by this procedure, between the predicted lifetimes, the latter being obtained from numerical integration programs (EOLA or NASA's ITEM).

3.2.5 Effect of the Earth's oblateness on the orbital lifetime

In the course of the present study and the subsequent application to IMP-G, it was found that orbital lifetimes can be significantly enhanced by the effect of the equatorial bulge (J_{20} term in the Earth's potential), by up to 20% in some cases under study. It is recalled that so far the Earth's potential had been considered spherical in the analysis. As is well known, due to J_{20} , there will be no secular changes of the satellite semi-major axis, inclination or eccentricity. The line of apsides (in the

orbital plane) and the line of nodes (in the plane of the equator) will rotate at rates proportional to $4-5 \sin^2 i_\alpha$ and $\cos i_\alpha$, respectively. Since all i_α considered here are higher than critical, $(\delta\omega_\alpha/\delta\tau)_{obl}$ is < 0 , and in the range investigated, its magnitude is maximum when $i_\alpha = 90^\circ$.

The same "beneficial" effect of oblateness on the stability of high eccentricity orbits of natural satellites is mentioned in examples given by J. Kovalevsky^[3-4] and Lidov^[3-5].

Typically, the kind of orbits studied here have perigees which rise very little (10^3 to 2×10^3 km) over the whole orbital lifetime. This is in contrast with the more frequent occurrence described for example by Shute^[3-6].

3.2.6 Conclusions of the study

The conclusions and practical implications of the above study, when applied (without loss of generality) to a satellite launched southwards, into an orbit quasi-normal to the ecliptic, with a perigee in region 3a of Fig. 3.4, are as follows:

- a) High celestial latitudes of the perigee are required for the stability in all ranges. They will be the more favorable the closer the argument of perigee referred to $\bar{\omega}_\alpha$ is to $\pi - \frac{1}{2} \arccos(\frac{1}{5})$. In particular, a positive flight path angle (i.e. injection after perigee) will be beneficial, within limits allowed on the drop in perigee height as compared to injection height, and mandatory if the injection is to take place in the close vicinity of the ecliptic.

- b) For a nominal launch, at perigee and in the ecliptic, and fixed eccentricity e and inclination i_α , it is possible to define a best day in the year giving the longest lifetime.
- c) The most suitable inclination on the equator, for a nominal launch, is that corresponding to an orbital ascending node at $+\frac{\pi}{2}$ from the moon's node.
- d) If the nodal line of the moon is sensibly aligned on the vernal line (the case in early spring 1969), the angular height of perigee above $\bar{\omega}_\alpha$ is $\pi - \omega_{\epsilon,P} + \psi$ (Fig. 2.11). Therefore, if $i_\alpha < 90^\circ$, advantage can be taken of the Earth's rotation to increase this angle, and consequently the lifetime, by launching earlier than the nominal time.

These conclusions were used with profit in the mission analysis of a high eccentricity satellite in an orbit nearly normal to the ecliptic, IMP-G^[3-2]. This study is described hereunder.

3.3 Application to an Actual Satellite: IMP-G

3.3.1 IMP-G orbital data

The abovementioned study of IMP-G orbit and launch time, carried out by S.J. Paddack^[3-3], should be referred to for more specific details and mission analysis studies. Our motivation here was to use the results of Section 3.2 and apply them to satellite IMP-G, in order to possibly predict the qualitative and quantitative effects of the launch parameters on the orbital evolution, and more specifically the orbital lifetime (required to be larger than 1 year, even for the 3σ velocity dispersion orbit).

A description of a typical orbit follows:

IMP-G

$$h_A = 235,463 \text{ km}$$

$$h_p = 343 \text{ km}$$

$$e = 0.946$$

$$\tau_{\text{sat}} = 5.05 \text{ days}$$

γ (flight path angle = angle $(\vec{I}_{V_{\text{inj}}}, \vec{I}_{\text{transverse}})$, positive if

$$\vec{I}_{V_{\text{inj}}} \cdot \vec{I}_{r_{\text{inj}}} > 0): -2^\circ \text{ to } +2^\circ.$$

γ_s (satellite centerline angle: angle $(\vec{I}_{\text{spin axis}}, \vec{I}_{V_{\text{inj}}})$): -2° to $+2^\circ$.

i_e (inclination of orbit on ecliptic): about 90° , at nominal time

Injection in 4th quadrant of ecliptic

The above list calls for a few comments: IMP-G is spin-stabilized, without active attitude control. It was desirable that the spin axis vector \vec{I}_s , aligned within a few degrees on the velocity vector at injection \vec{V}_{inj} , be normal to the plane of the ecliptic, within a narrow tolerance $\Delta\zeta = \pm 5^\circ$. Injection is made very close to perigee (within a few degrees). Hence, the resulting orbit will be very nearly normal to the ecliptic. For example, if $\gamma = \gamma_s = \Delta\zeta = 0^\circ$, i.e. for an injection at perigee with velocity and spin axis vectors exactly aligned on the negative normal to the ecliptic, $-Z_e$, the perigee at the so called nominal time will be in the ecliptic, at celestial longitude $RA_{e,\text{inj}}$ depending on the inclination on the equator, i_α (Fig. 3.8). For obvious reasons, posigrade orbits are preferred ($i_\alpha \leq 90^\circ$),

and to avoid long periods in the earth's shadow at the outset of the mission, only injection in the fourth quadrant of the ecliptic are to be considered:

$$-90^\circ \leq RA_{\epsilon, inj} \leq 0^\circ$$

The constraint on the alignment of the satellite centerline on $-Z_\epsilon$ limits the launch opportunity to a "strip" of width equal to about 1.7 hour, symmetric about the line of nominal launches (Fig. 3.9). As illustrated in Fig. 3.10, the degrees of freedom in choosing a "suitable" orbit, with a special emphasis put on achieving larger lifetimes, are

- a) hour of launch, HL, inside the strip, on a given day
- b) day of launch, DL
- c) inclination on the equator, i_α
- d) flight path angle at injection, γ
- e) satellite centerline-velocity vector angle, γ_s

The conclusions of Section 3.2.3.6 will now be used in a systematic investigation of the effect of these parameters on the orbital evolution.

3.3.2 Parametric study of IMP-G

3.3.2.1 Launch opportunity strip

Above described ECLIP program was used to define the launch opportunity strip based on a specified maximum angle $\Delta\zeta$ between the spin axis and the normal to the ecliptic. This strip defines a range of permissible injection within the specified tolerance. The "backbone" of this strip is the time of nominal injection times, at which the spin axis and the normal to the ecliptic are exactly aligned (Fig. 3.9). This can correspond to a

nominal injection, i.e. in the ecliptic plane. The misalignment γ_s between the velocity vector at injection and the spin axis, should then be compensated for by an equal and opposite flight path angle, γ (Fig. 3.10).

3.3.2.2 Launch window

The stability analysis of the orbits derived from program ECLIP was carried out by means of program SABAC.

a) Influence of the flight path at injection, γ

To an increase in the magnitude of γ for constant R_{inj} , V_{inj} , there corresponds a drop in the height of perigee equal to about 4 km/deg, of change in γ , in the range $|\gamma| \leq 2^\circ$. The rate increases with increasing γ .

All things being equal, a positive flight path angle (injection "after" perigee) causes a high initial angle of perigee above plane $\bar{\omega}$, consequently a larger lifetime. This leads to an improvement in the "quality" of the launch window, as measured by the area covered by the "success" region within the launch opportunity strip. Fig. 3-11 to 3.12 graphically portray this for the IMP-G satellite.

b) Influence of launch time on a given day

It is apparent for Fig. 3.10 to 3.12 that the launch window seems to be more favorable at times earlier than that of the nominal injection. Fig. 3-13, which is a plot of the predicted lifetime as a function of the time of day, also indicates the same effect. As was mentioned in Section 3.2, in early spring 1969,

the nodal line of the Moon is very sensibly aligned on the positive vernal line, axis X_ϵ (in Fig. 2.11). The angular height of perigee, approximately equal to $\pi - \omega_{\epsilon, P} + \psi$, is increased, for given i_α , when the injection occurs earlier than at the nominal time, due to the rotation of the Earth in inertial space. It is also clear that if $i_\alpha = 90^\circ$ and for this position of the Moon's nodal line, the lifetime will top off at nominal injection time, a fact illustrated by Fig. 3.13.

c) Improvement of the lifetime with the satellite centerline misalignment angle, γ_s

Figure 3.14 illustrates that the lifetime increases with ω_\sim , argument of perigee relative to plane $\bar{\omega}_\sim$. The figure is a plot for a nominal injection of IMP-G, and $i_\alpha = 90^\circ$, the high values of ω_\sim being attained by the use of a negative γ_s and a compensating, positive γ .

d) Influence of the launch day

For an injection in the close vicinity of the ecliptic, a "best day" for given i_α is one for which $(RA_\epsilon - RA_{\epsilon, P}) = \phi$, at injection, is $\frac{5\pi}{4}$, since $\frac{\delta\omega_\sim}{\delta\tau}$ is minimized. This is shown by Fig. 3.15, for $i_\alpha = 83.8^\circ$ (nominal injection of IMP-G^[3-3]).

e) Influence of the inclination on the equator, i_α

In the period spring-summer 1969, the celestial longitude of nodes of the Moon is close to 0° (within 5° over March-July 1969).

Hence ω , and the lifetime, increase with inclination in the interval $66.55^\circ \leq i_\alpha \leq 90^\circ$. For nominal injection conditions, and $\omega = 0$, the lifetime is plotted vs. inclination i_α in Fig. 3.16.

f) + 3 σ orbits

Due to the dispersion on the actual values of the velocity at injection, it is important that the launch window also be determined for extreme cases, such as a 3 σ error on the velocity at injection. The probability of having more than a 3 σ error on the injection conditions is only 0.26%. The following list summarizes the 1 σ (1 standard deviation) with the Delta launch vehicle, as taken from Ref. [3-3].

1- σ Vehicle Errors

Latitude	$\pm 0.4337^\circ$
Longitude	$\pm 0.2335^\circ$
Altitude	± 15.426 km
Speed	± 0.010998 km/sec
Azimuth flight path angle	$\pm 0.6526^\circ$
Elevation flight path angle	$\pm 0.5208^\circ$
Spin axis azimuth angle	$\pm 2.0435^\circ$
Spin axis elevation angle	$\pm 1.6827^\circ$

The 3 σ dispersion limits on the velocity at injection were studied for the IMP-G launch window, and are illustrated in Fig. 3.17. It is seen that until day 160, approximately, the 3 σ window is

totally closed, and that around the middle of the year (from day 180 to 210), the window is favorable, even in the $+3\sigma$ dispersion case.

3.3.2.3 Comparison with numerical integration programs

In more detail than Fig. 3.7, Figures 3.18 and 3.19 show the evolution of some orbital parameters for a sample IMP-G orbit, as obtained from digital integration program EOLA. The simultaneous topping off of ω and of the height of perigee have already been mentioned, and this provides an experimental justification to the procedure adopted to assess the orbital lifetime.

Comparative lifetime values for IMP-G, as obtained from SABAC, Version B, on one hand, and from NASA's ITEM (Encke's method) and EOLA (Variation of parameters) are tabulated in Table 3.3-I.

DAY 1969	Inj. hour U.T.	γ deg.	γ_s deg.	Life days		Int. prog. ^a
				pred.	act.	
06/01	9.488	1.5	-1.3	413	410	VP
06/01	9.988	1.5	-1.3	340	370	VP
06/14	9.321	-1.28	-1.3	425	404	VP
					397	EM
05/01	11.363	1.5	0	362	389	VP
05/01	12.263	1.5	0	319	348	VP
05/08	10.097	1.5	0	FAIL ^b	364	VP
05/08	10.297	1.5	0	355	369	VP

^aVP: Method of variation of parameters; EM: Encke's method

^bAt T + 0.1h:350

Table 3.3-I Comparison of predicted and actual lifetimes

As the table shows, the average error between the predicted and actual lifetime values is of the order of 5%, and on the pessimistic side. Case 4 is a case in point. It corresponds to the evolution portrayed in Figures 3.18 and 3.19. The predicted lifetime was 362 days and actual one 389 days. Case 7, on the other hand, illustrates an inaccuracy in the definition of the lifetime boundary. However, the lifetime predicted for the next point on the same launch day (for a step of 0.1 hour) is in good agreement with the actual value.

3.3.3 Implications for IMP-G orbit

On the basis of the above study, recommendations could be made regarding the choice of an orbit having a long lifetime, ample launch opportunities and still fulfilling a set of additional constraints. The finally selected orbit would have to consider, of course, the capabilities and limitations of the launch vehicle. Of particular interest here, is the combination of a positive flight path angle with a negative "spin axis centerline-velocity vector" angle. The latter combination will enhance stability throughout the launch opportunity "strip" and/or permit injection at more moderate southern geographic latitudes.

3.3.4 Conclusions

In this example, it has been shown that the method of approximate stability criteria could be used with profit in a parametric study of the influence of various orbital elements on orbital lifetimes and the launch window map. The analysis resulted in practical recommendations which can be assessed within the perspective of the global mission.

REFERENCES-Chapter 3

- [3-1] Renard, M.L.: "Practical Stability of High Eccentricity Orbits Quasi-Normal to the Ecliptic", Presented at AIAA Astrodynamics Conf., Princeton, August 1969. JSR. 7(10) pp.1208-1214, 1970.
- [3-2] Renard, M.L. and Sridharan, R.: "Launch Window of a Highly Eccentric Satellite in an Orbit Normal to the Ecliptic: IMP-G", 9th Semi-Annual Astrodynamics Conf., NASA GSFC, April 1969.
- [3-3] Paddack, S.J.: "IMP-G Orbit and Launch Time", GSFC Doc. No. X-724-69-252, June 1969.
- [3-4] Kovalevsky, J. "Sur la théorie du mouvement d'un satellite à fortes inclinaison et excentricité" Reprint, Int. Astr. Union, Symposium # 25, 1966
- [3-5] Lidov, M.L.: "The Evolution of Artificial Satellites of Planets Under the Action of Gravitational Perturbations of External Bodies", Planet. Space Science, 9, pp. 719-759, 1962.
- [3-6] Shute, B.E.: "Prelaunch Analysis of High Eccentricity Orbits", NASA Tech. Note D-2530, December 1964.

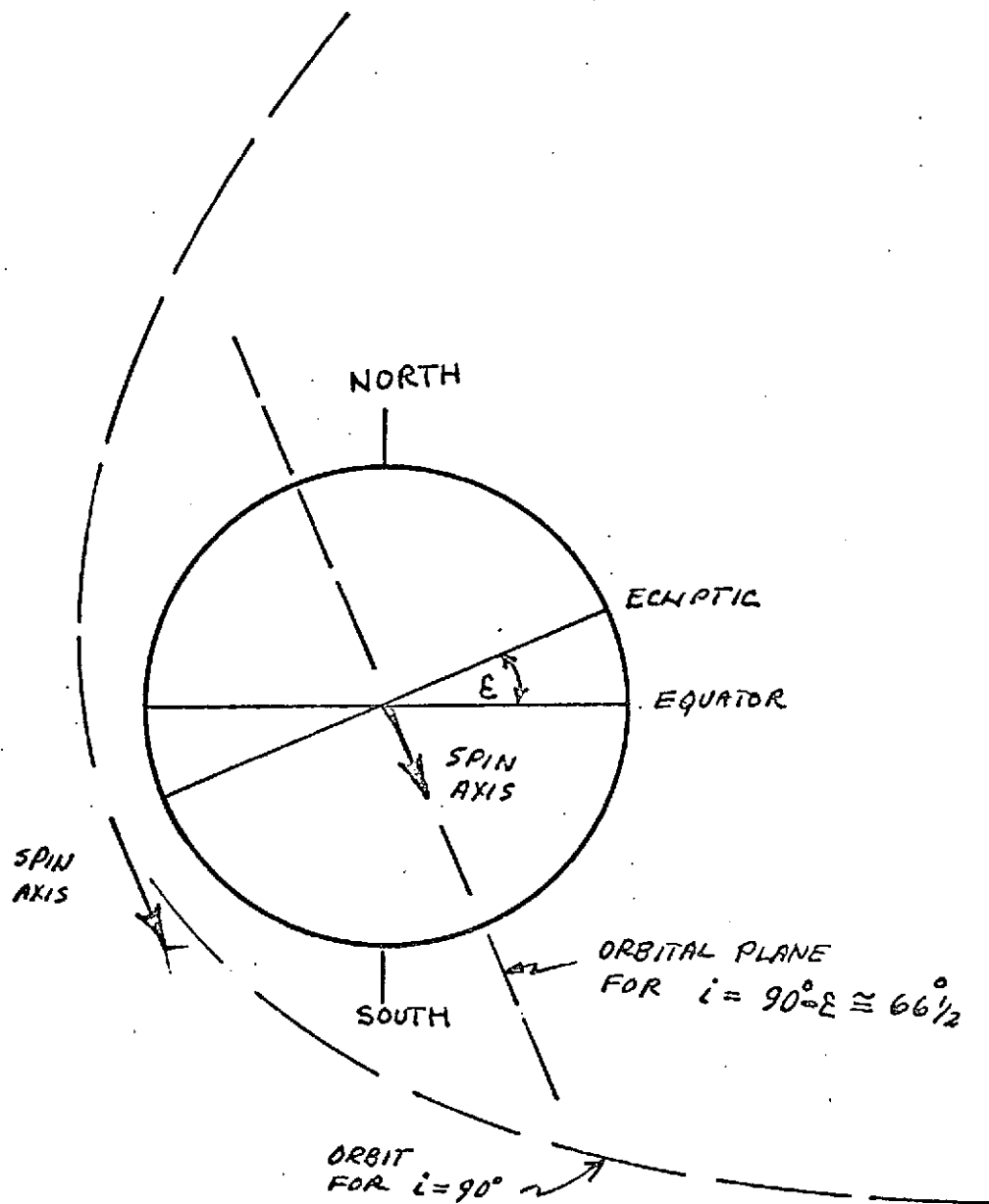


FIG. 3-1. Orbit-spin axis relation. (From Ref. 3-3)

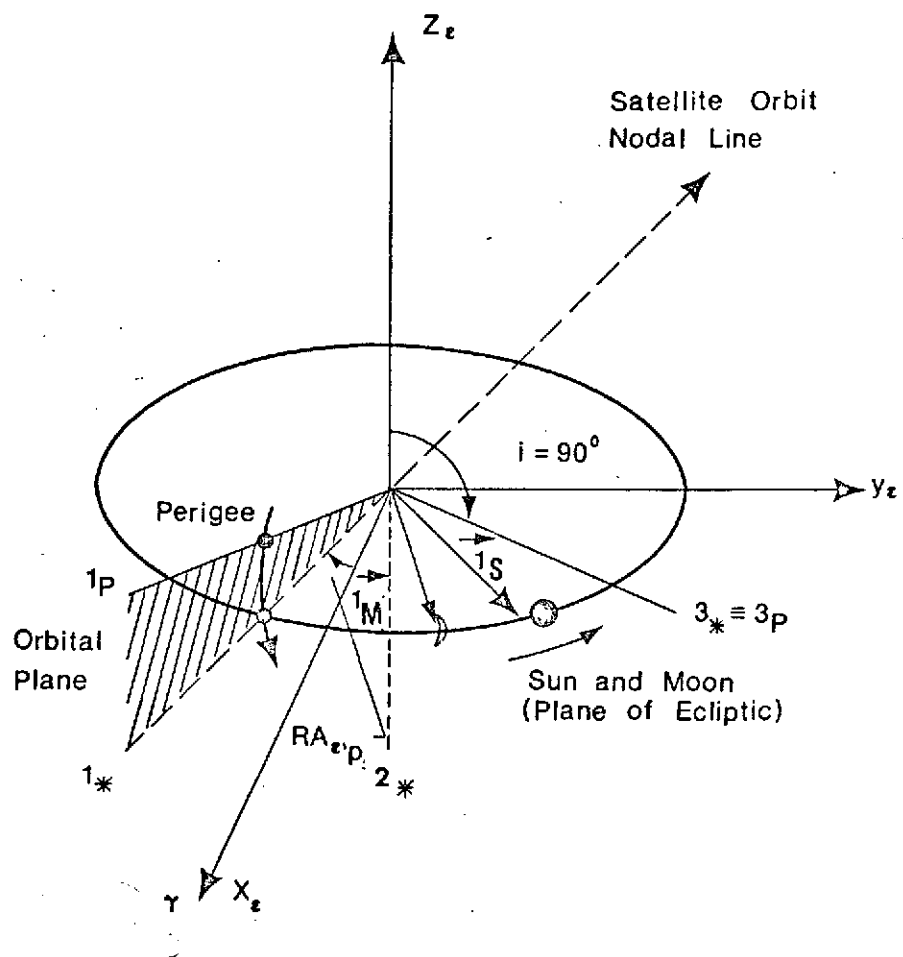


FIG.3-2. GEOMETRY OF SIMPLIFIED PROBLEM.

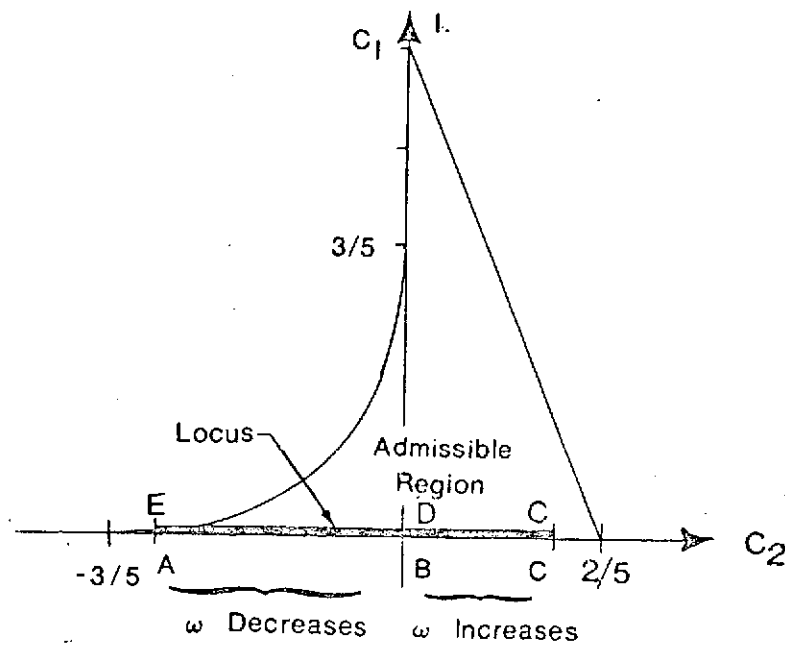
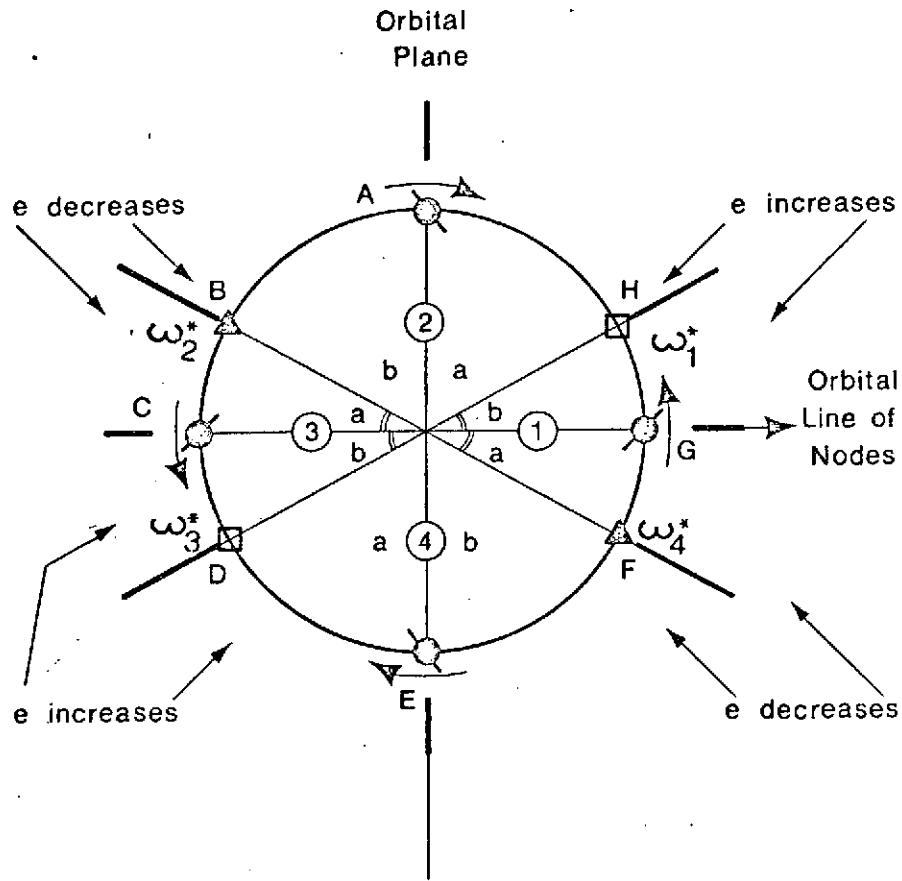


FIG.3-3. LIDOV'S diagram (c_1, c_2)



↗ Evolution of ω for Increasing Time

□ Stable Point

▲ Unstable Point

⊙ Minimum of Eccentricity $e_{\min}^2 = \frac{e_0^2 (5 \cos 2\omega_0 - 1)}{4}$

⊙ Minimum of Eccentricity $e_{\min}^2 = \frac{e_0^2 (1 - 5 \cos 2\omega_0)}{6}$

FIG. 3-4. EVOLUTION OF ARGUMENT OF PERIGEE AND ECCENTRICITY WITH TIME.

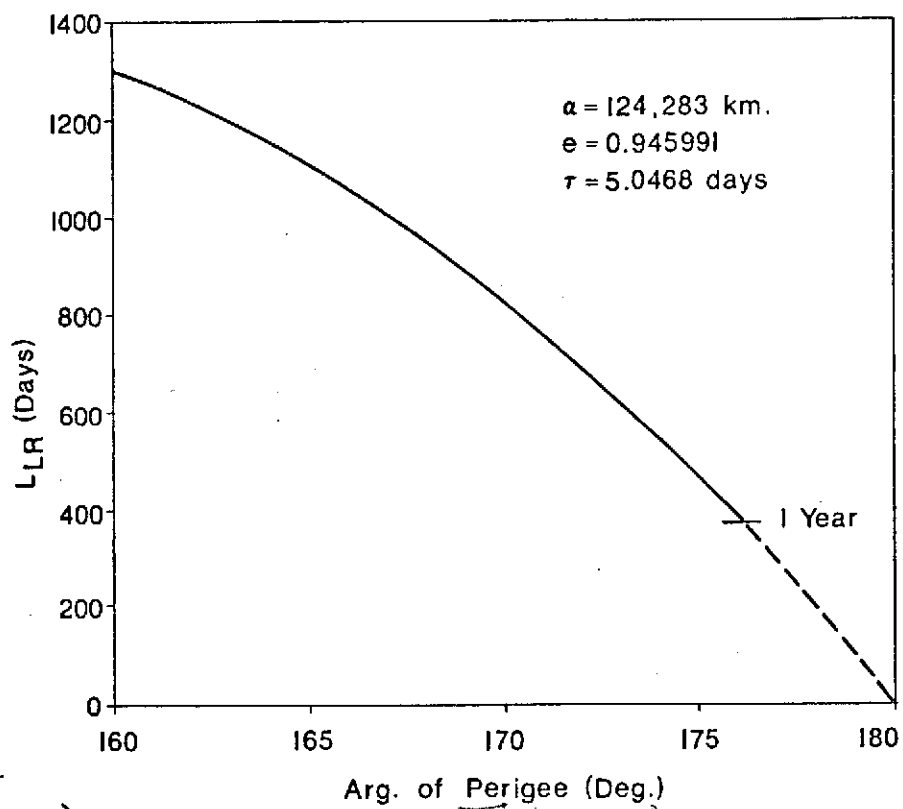


FIG. 3-5. LONG-RANGE LIFETIME VS. ARGUMENT OF PERIGEE AT INJECTION.

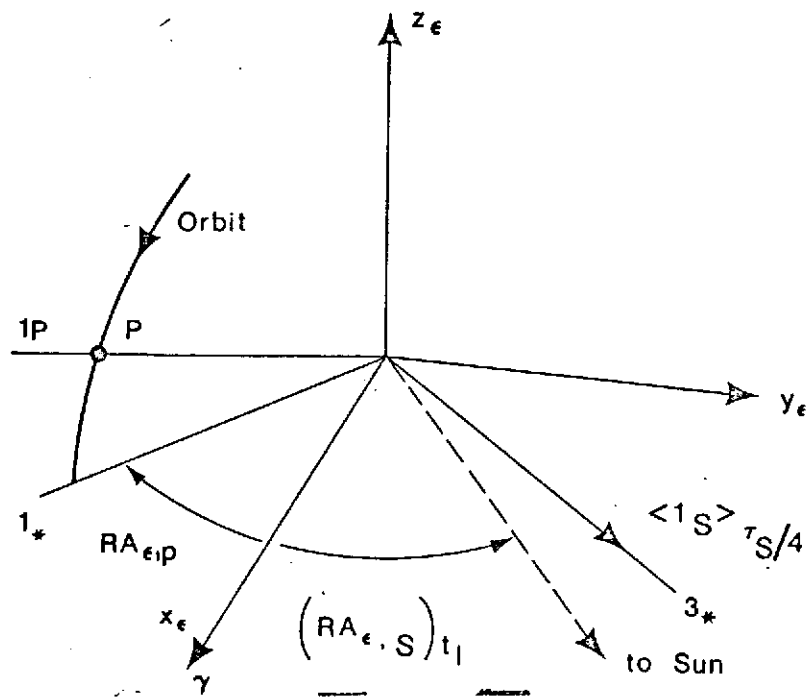


FIG. 3-6. GEOMETRY OF "BEST" LAUNCH DAY.

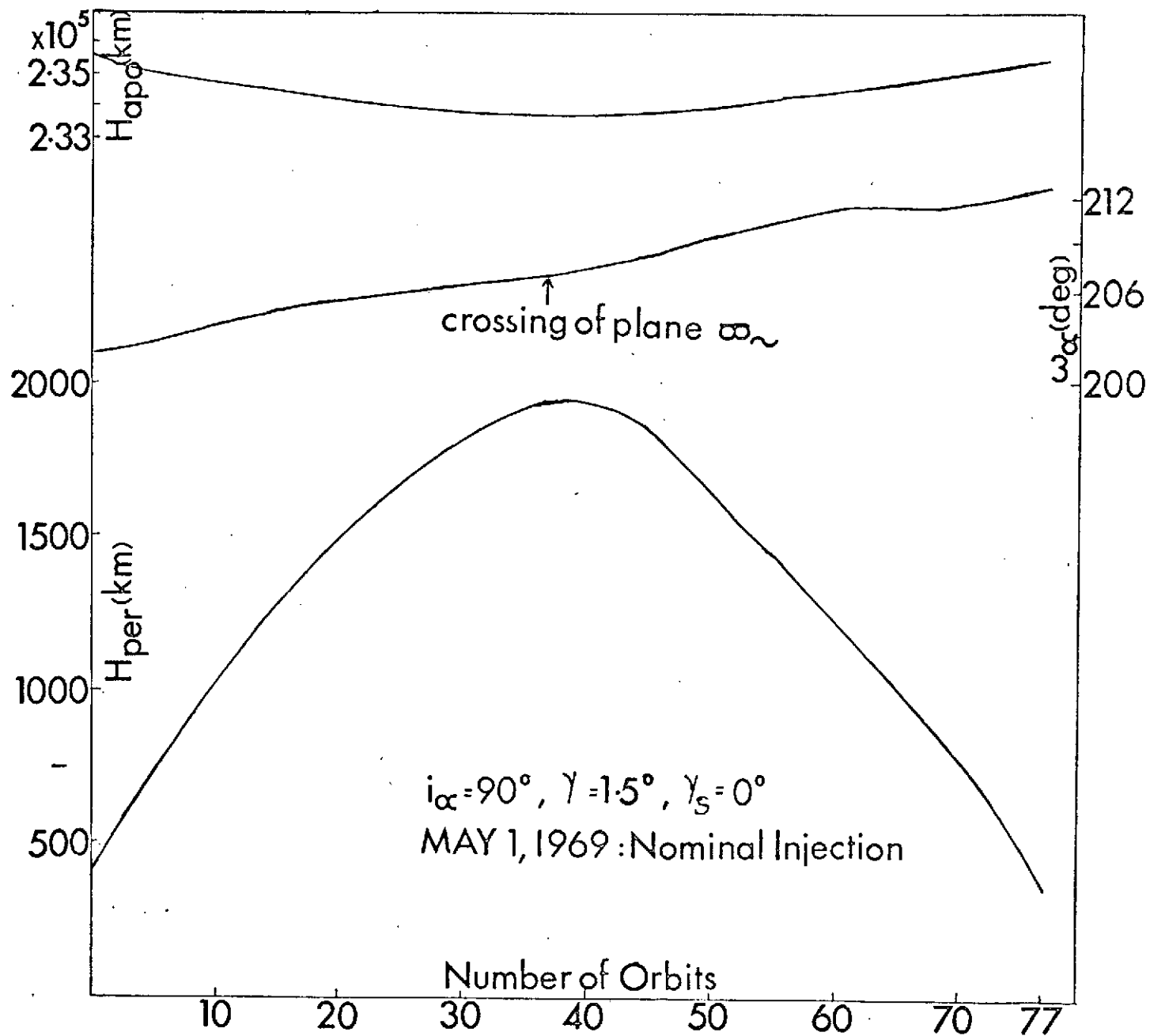
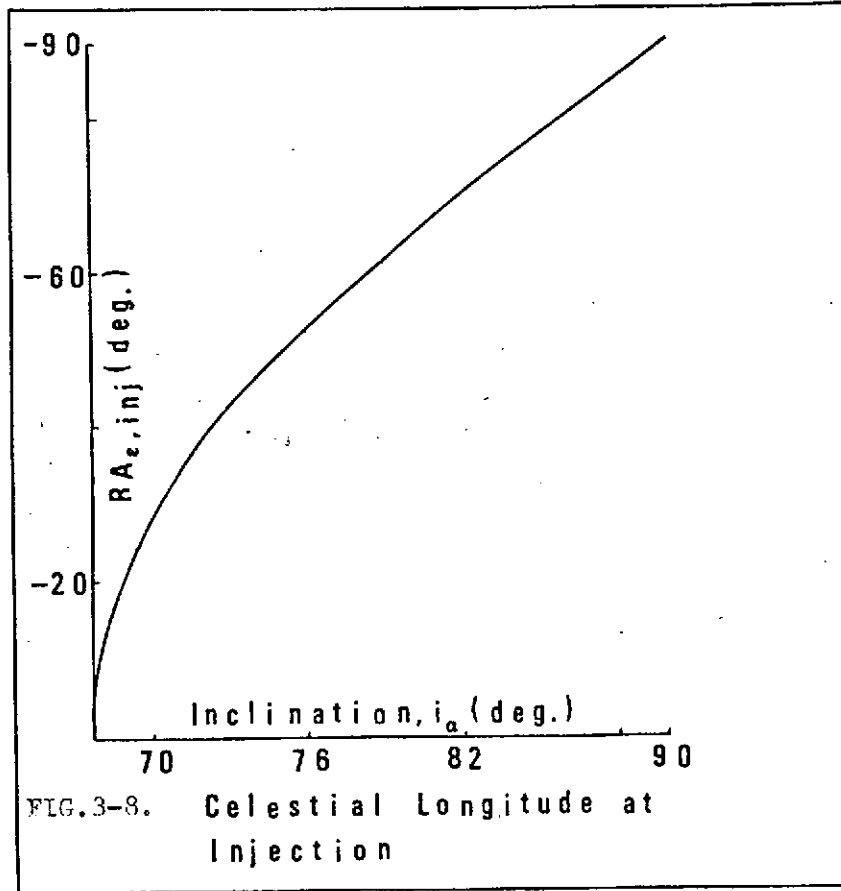
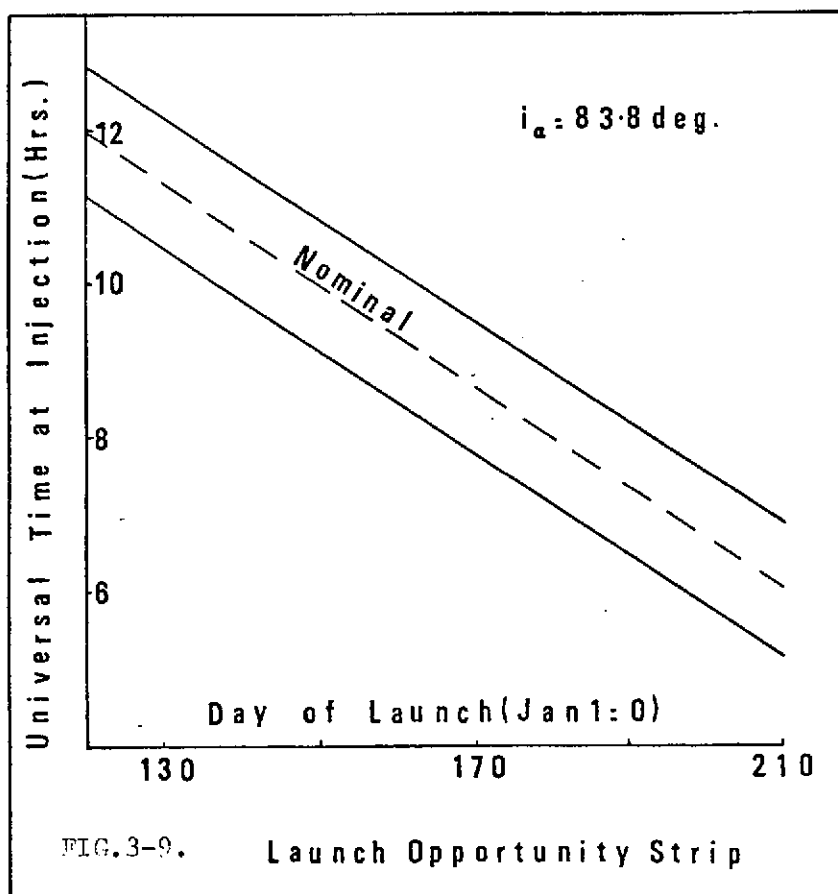


FIG. 3-7. ORBITAL ELEMENTS VS. TIME, FROM NUMERICAL INTEGRATION.





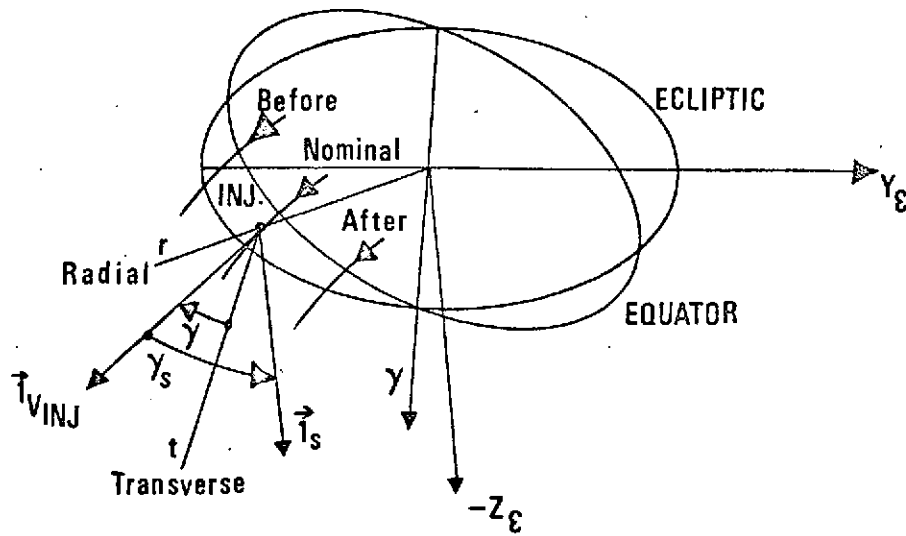


FIG. 3-10. DEGREES OF FREEDOM.

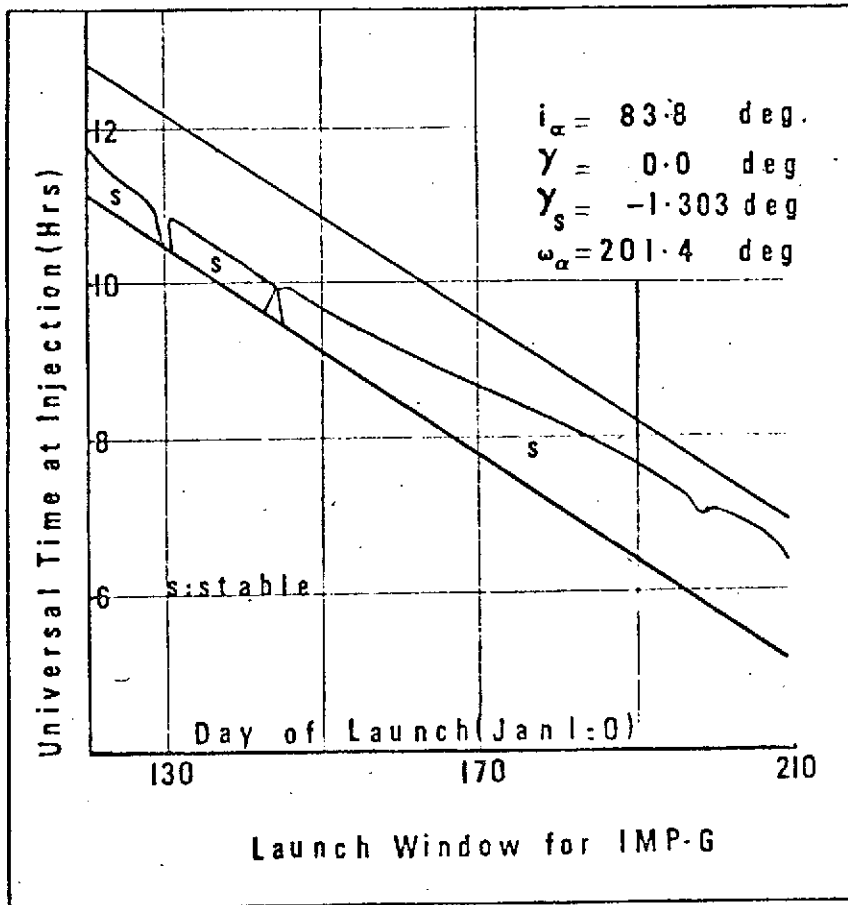


FIG.3-11. Effect of Flight Path Angle

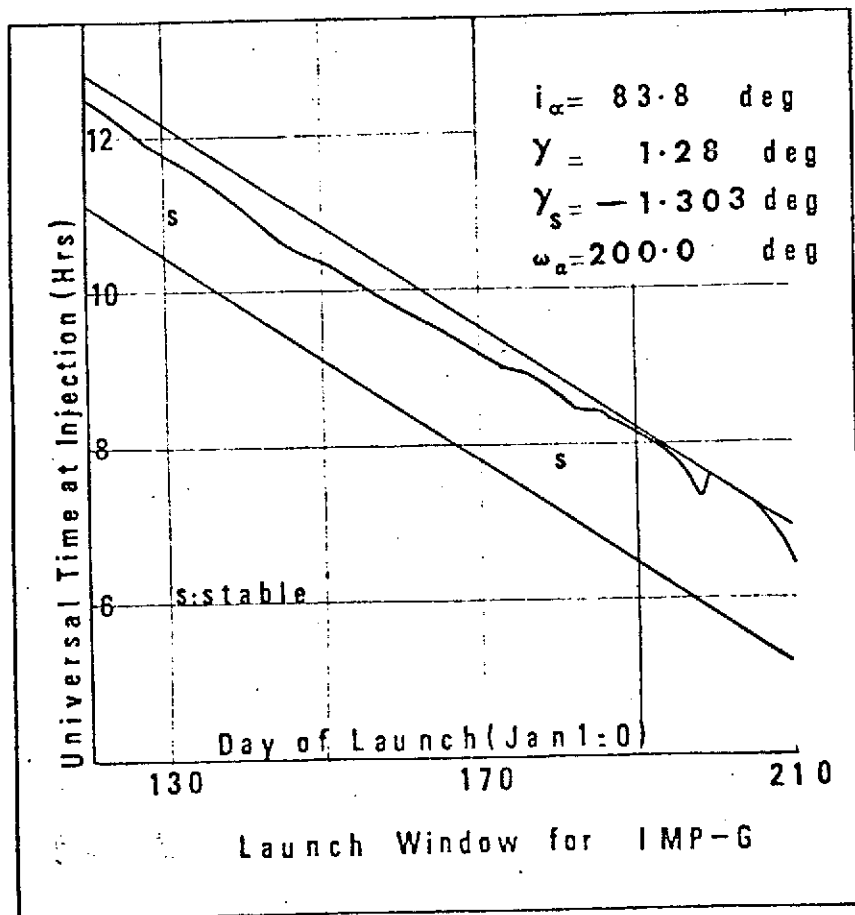
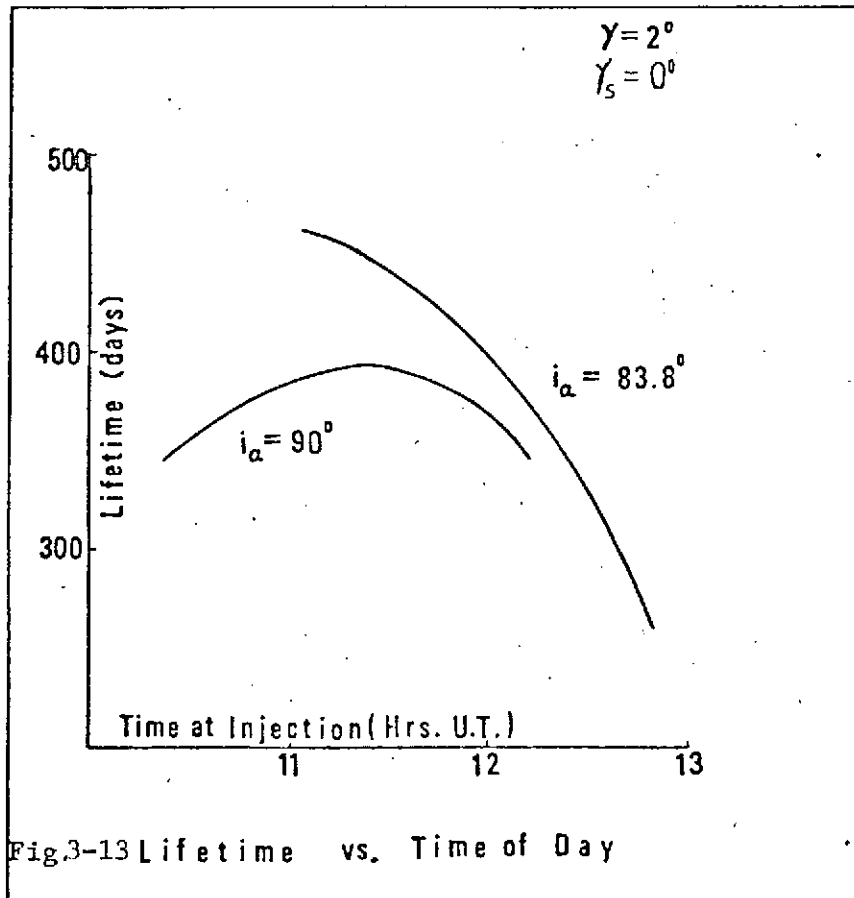
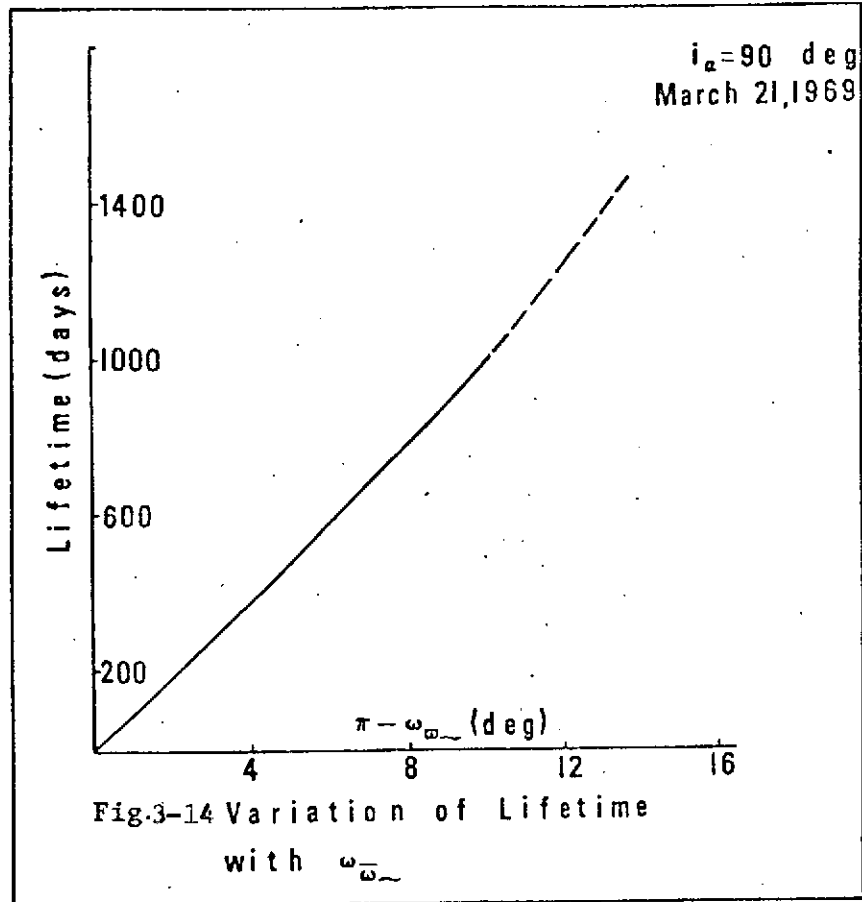
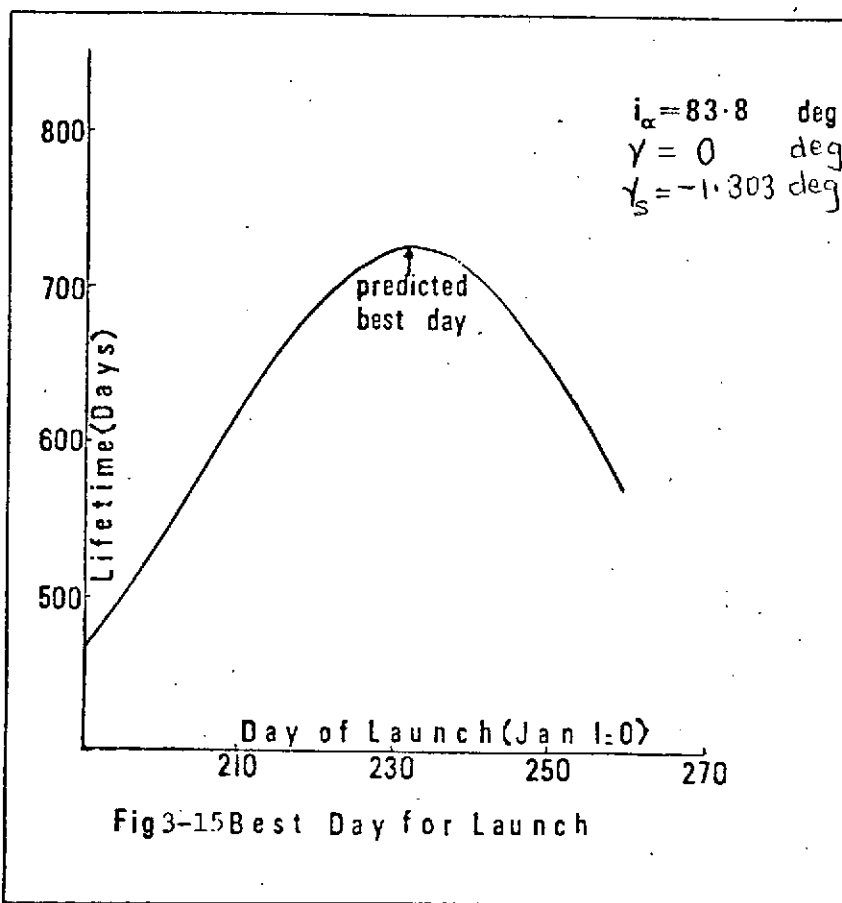
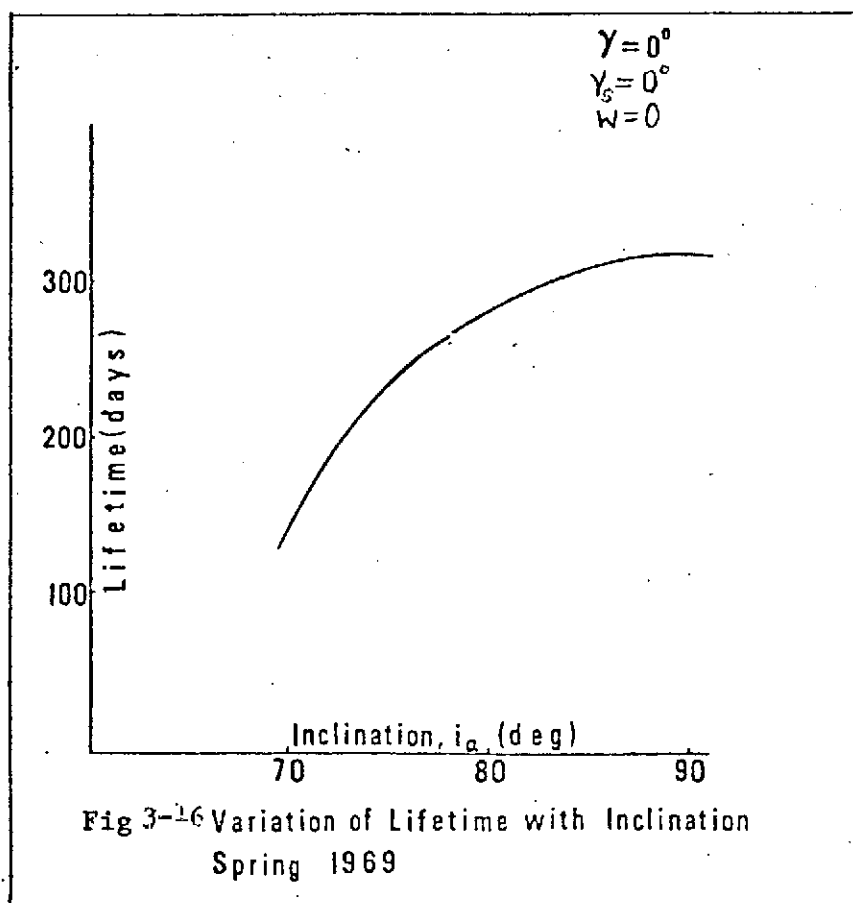


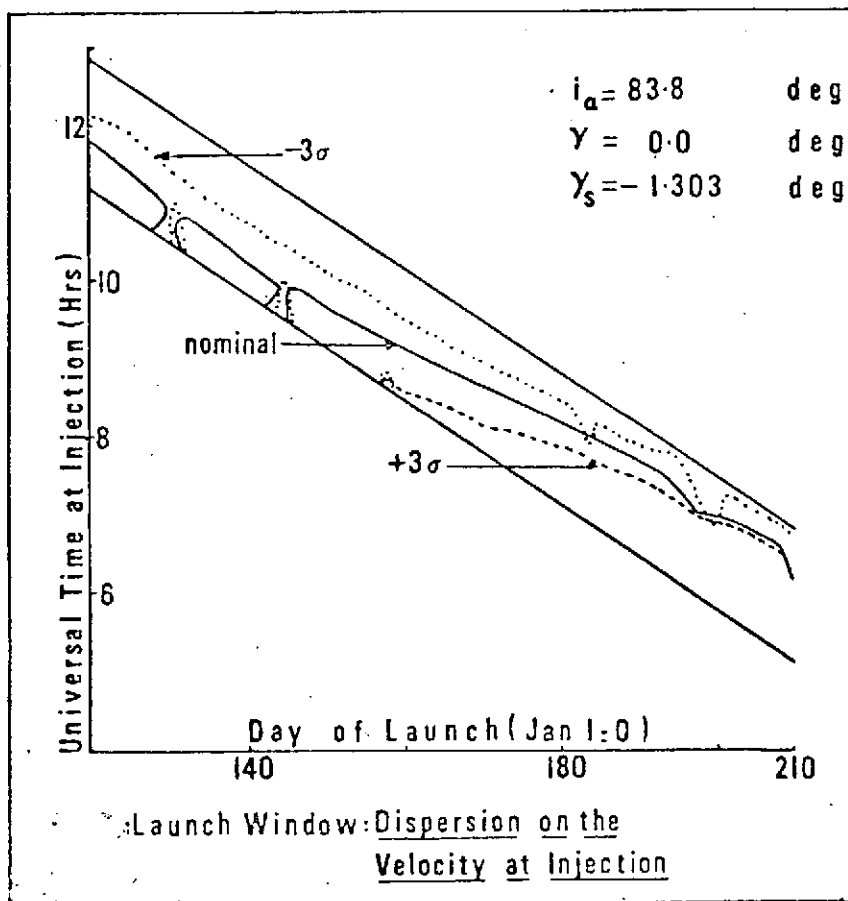
FIG. 3-12: Effect of Flight Path Angle











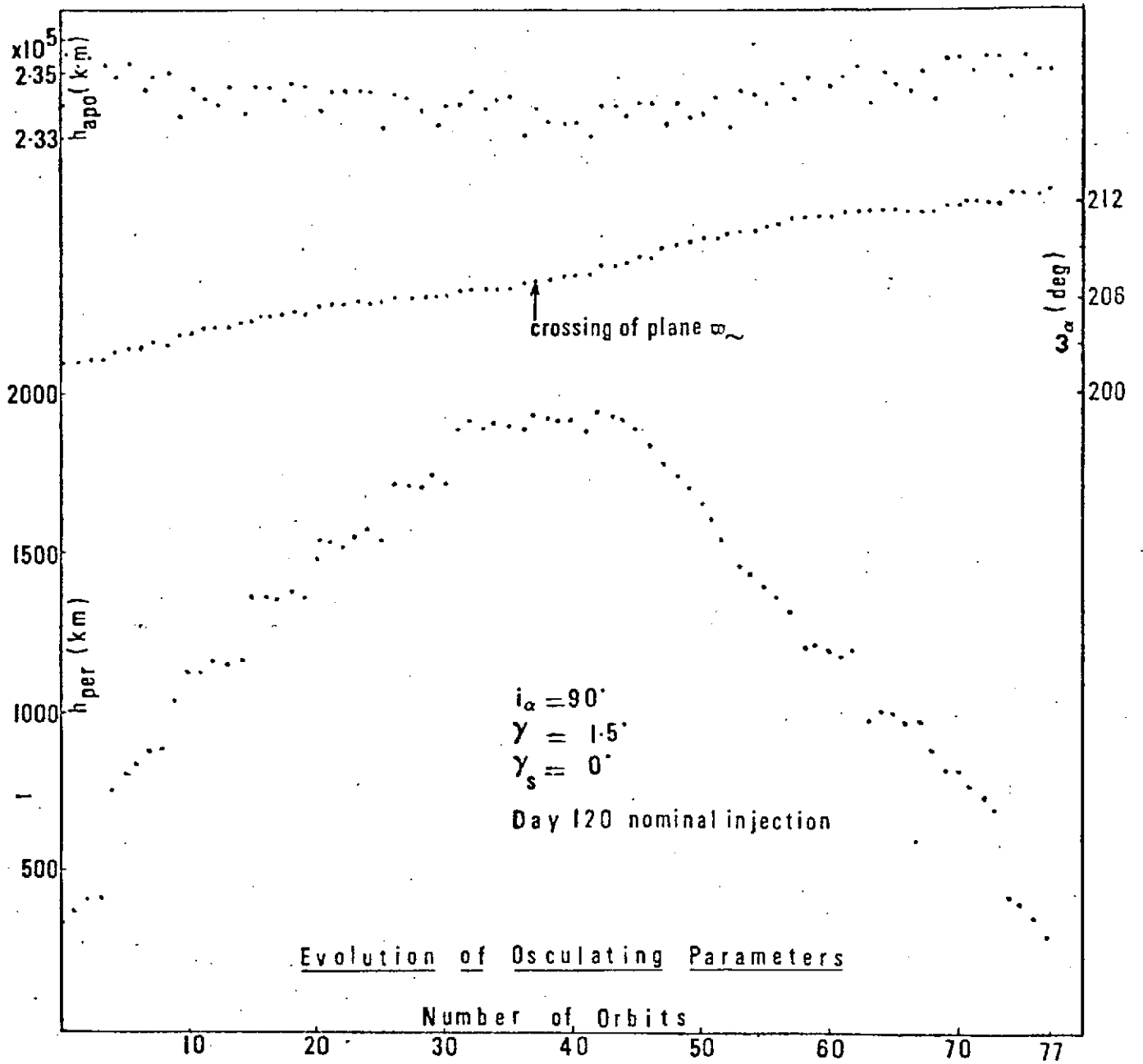


FIG.3-18.

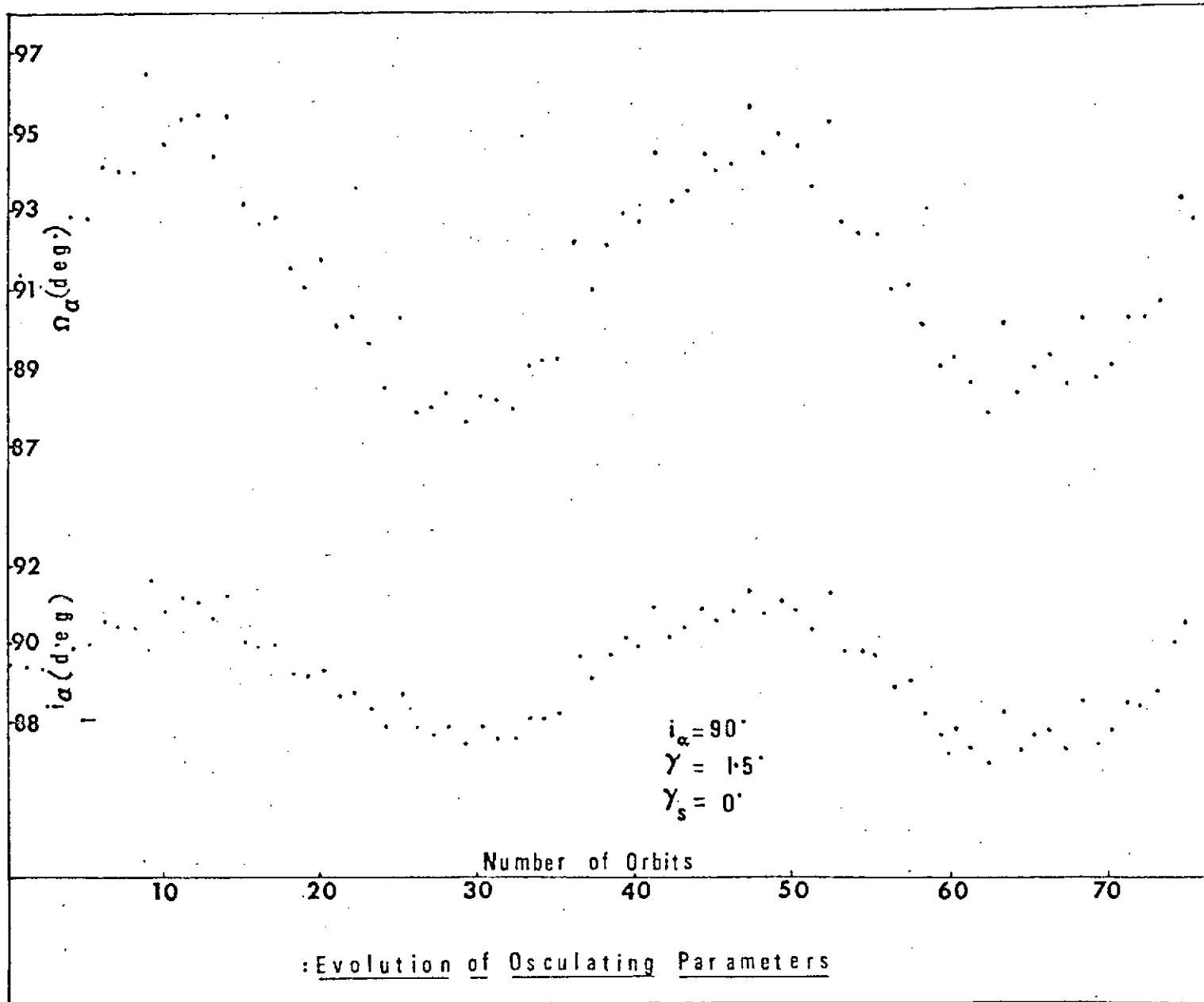


FIG. 3-19

CHAPTER 4

A Modified Lidov's Method by Non-Numeric Computation, with Applications

In this chapter we shall deal with the application of non-numeric computation to the theory of geocentric orbits of large eccentricity. The developments constitute a modification and an extension of Lidov's theory^[4-1]; a modification because it recognizes that Lidov only introduces and studies five orbital elements, whereas rigorously six of them should appear; an extension, because the developments are pushed to higher order than the "11", "21", and "12" terms of Lidov, thanks to the labor-saving and error-free features of non-numeric computation. Finally, the effect of oblateness is considered and numerical examples are given to illustrate the degree of accuracy and the marked economy in computer time obtained by using the present approach. The main lines of the developments add a few specific examples are given here. For much more detailed information, the reader should refer to the Ph.D. thesis^[4-2] written by one of the authors of this report (R. Sridharan), as the Principal Investigator's (Marc L. Renard) advisee.

4.1 Motivation

It is well realized by any mission analyst that repetitive, high-accuracy calculations amounting in one way or another to direct, numerical integration of the orbit, can be a very expensive proposition in terms of effort and computer time. Figures of the order of 10 to 15 min per

launch "point" (day in the year, hour in the day) of the launch window are quite realistic if a modified Encke's method is used on a large IBM system (7094 or 360 series). The awareness of this problem led to the development and use of a method of lower, but sufficient, accuracy, and of very high computational economy, which has been described in Chapter 2.

Between these ends of the spectrum, at the inception of the present study, there seemed to be a real need for a theory of intermediate complexity which basically

- would be less costly than digital integration, by a factor of 10 to 100.
- would include a sixth element, thereby resulting in an improvement of the prediction of the "time flow" along the orbit
- would be adequate for eccentricities up to 0.95
- could be implemented on a digital computer, for the repetitive calculations called for in mission analysis.

4.2 Main Features of the Approach

There are two main features in the approach: an extension of Lidov's theory so as to include a sixth osculating element, and the use of symbolic manipulation on the computer. These two points are now discussed in more detail.

4.2.1 Extension of Lidov's theory

Lidov's theory^[4-1] has been described at length in Chapter 2. It is recalled that the equations of motion which are retained are five in

number. They describe the time-rate of changes of elements, a , e , i , ω , Ω as equal to expressions in the right-hand side, in which the small perturbing forces due to a third body appear as factors. But any sixth element, such as T_* , the time of perigee at the epoch (perigee), in Kepler's equation of time

$$E - e \sin E = n(t - T_*)$$

is conspicuously absent from Lidov's theory. Furthermore, the "11", "21", "31" terms given by Lidov for five elements do not suffice to obtain high accuracy in the case of high eccentricity orbits ($0.9 \leq e \leq 0.95$).

Roth^[4-33] developed more such terms by hand computation, but did not go far enough in the Legendre Polynomial (LP) expansion of the force, as will be shown later. Furthermore, his choice of the sixth element is apparently inconsistent, as will be shown in a later discussion.

The goal will thus be to obtain a "theory" describing the perigee-to-perigee variations of the orbital elements. The developments will be rendered more accurate both by the inclusion of a sixth osculating element, which will result in a more accurate timing of the occurrence of perigees and in a better computation of lifetimes; and by carrying the LP and Taylor series of the perturbing forces to the order deemed necessary from estimates of accuracy.

Alternate, relevant approaches and methods are examined by Sridharan in a literature survey^[4-2], and include contributions by Kozai^[4-3] Musen^[4-4 to 4-6], Smith^[4-7], Fisher and Murphy^[4-8], Fisher^[4-9] and Cook and Scott^[4-10].

4.2.2 Symbolic manipulation (non-numeric computation) on the computer

A rough assessment of the algebra and "bookkeeping" involved in proceeding to develop a modified Lidov's theory along the lines described in Chapter 2, rapidly points up the need for mechanizing the work through the use of SYMBOLIC COMPUTATION. As a result of using this technique, in a special-purpose program, the extension of the theory to any order would be carried out automatically on the computer. The process flow would be as follows:

I INPUT: Coded differential equation, "order" desired etc...



II

Processor: implements the algorithm, reorders terms etc.



III OUTPUT: Theory, expressed as a set of formulae, to order specified

Parts I, II, III will be examined in detail hereunder. At this stage, however, the advantages of symbolic manipulation could already be described as follows:

- Automatic development of the theory to any order
- Mechanization of substitution, transformation, etc. to automatically condense, simplify, compare formulae
- Saving of analyst's time and effort
- No errors in algebra, given a pre-tested "correct" program and a "good" computer. The latter are not minor reservations, of course,

but given a sufficient volume of computation, any analyst is bound to make errors, in spite of the fact that most of his time might have been spent in rechecking algebraic expressions.

It is apparent in the literature that with the availability of computers came a vivid interest in automating the development of analytical theories. Considerable effort^[4-11 to 4-34] has been invested in building special purposes programs and using existing languages for literal computations in perturbation theories for the moon, planets and satellites.

Thorough surveys of existing systems and problems being studied were made by Davis^[4-11] and Jefferys^[4-12].

Poisson Series, of the form

$$\phi(\vec{x}, \vec{y}) = \sum [\vec{P}_j \cos(\vec{j}_T \vec{y}) + \vec{Q}_j \sin(\vec{j}_T \vec{y})]$$

in which

\vec{x} is a n-vector of polynomial variables

\vec{y} is a m-vector of trigonometric variables

\vec{j} is a n-vector of integers

\vec{P}_j, \vec{Q}_j are polynomials in the polynomial variables having,

possibly, negative exponents also.

have been the object of numerous special purpose programs^[4-13 to 4-26], which aim at economically and efficiently performing the following manipulations^[4-11]

- creation and annihilation of series
- parsing
- differentiation and integration
- substitution

- numerical evaluation

Among many contribution, we could mention Barton's^[4-14] expansion of the lunar disturbing function to the tenth order in the LP expansion and his attempt^[4-16] to develop Delaunay's canonical transformation for the elimination of periodic terms, which ran into severe space problems on the computer. This "space" constraint, and the enormous amounts of Central Processing Unit (CPU) time needed for list processing are the two major difficulties encountered in symbolic computation. Eckert and Eckert^[4-15] used an IBM 620 and a Symbolic Programming System to obtain a lunar theory of increased precision.

Deprit^[4-25] developed an analytical theory of the moon based on Lie transforms^[4-32], using a set of processors developed for series manipulation^[4-22]. Deprit and Rom^[4-20] also used Lie transforms and series processors to develop the analytical solution of the main problem in Satellite Theory (all gravitational harmonics are zero except J_2).

Carpenter^[4-27] developed a program for automatic computation of general planetary perturbations to first order, using Hansen's theory. Seidelmann^[4-28] modified Hansen's method by using an iterative process instead of a Taylor series.

To conclude, it can be said that the adoption of techniques or procedures to economize on time and space results in a restriction of the class of problems that can be handled and conflicts with characteristics of portability and readability of the programs. The more complex and more specialized the system, the more dependent it becomes on specific hardware configurations.

4.3 The Choice of Elements

It is recalled that Lidov's original theory^[4-1] was developed in terms of the true anomaly, ψ , as the independent variable. Yet only five elements appear in the differential equations expressing the rates of change of the parameters with true anomaly, namely a , e , i , ω , Ω (angles are referred to some plane of reference, not necessarily the orbital plane of a disturbing body, but so that Ω is defined). An element is missing: it could plausibly be T_* (time of perigee at perigee) or M_* (mean anomaly at epoch). The inclination of this element in the present theory which thus modifies Lidov's theory, will be shown to be critical in timing the occurrence of perigee in the orbit, as opposed to geometrically defining the trajectory.

In the present study, M_* , mean anomaly at epoch, was chosen as the sixth element. In Appendix A-1, the derivation of the differential equation for M_* is given, with the procedure for computing the elapsed time from M_* .

Since Lidov, in his work, only used five elements, it implicitly amounted to assuming that the unperturbed period of the satellite adequately represented the flow of time along the orbit. M. Moe^[4-29] made a similar assumption, which is also present in the analog application of her work^[4-30]. In Musen's work on long-perturbations^[4-4 to 4-6], where mean anomaly is used as the independent variable, or on short-period perturbations^[4-31 to 4-32], in which the eccentric anomaly is used, the perturbations of a sixth element were considered.

Roth^[4-33 to 4-34], in his attempted extension of Lidov's study, used time t as the sixth variable. The equation for $\frac{dt}{dv}$ was arrived at by extending and truncating the equation relating t to v . From equation

$$\frac{dv}{dt} = \frac{\sqrt{\mu p}}{r^2} \left[1 + \frac{r^2}{\mu e} F_r \cos v - \frac{r^2}{\mu e} \left(1 + \frac{r}{p} \right) F_t \sin v \right]$$

or

$$\begin{aligned} \frac{dt}{dv} &= \frac{r^2}{\sqrt{\mu p}} \left[1 + \frac{r^2}{\mu e} F_e \cos v - \frac{r^2}{\mu e} \left(1 + \frac{r}{p} \right) F_t \sin v \right]^{-1} \\ &= \frac{r^2}{\sqrt{\mu p}} \left[1 - \frac{r^2}{\mu e} F_r \cos v + \frac{r^2}{\mu e} \left(1 + \frac{r}{p} \right) F_t \sin v \right] + O(\epsilon_*^2) \end{aligned} \quad (4.3-1)$$

if the forces are of $O(\epsilon_*)$. Neglecting terms of $O(\epsilon_*^2)$, the equation for the perturbations of time is arrived at by considering the first term in the above bracket to be the 2-body expression (which it is not), or that

$$\left(\frac{dt}{dv} \right)_{\text{pert}} - \left(\frac{d\Delta t}{dv} \right)_{2b} = \left(\frac{r^2}{\sqrt{\mu p}} \right)_{2b} \left[- \frac{r^2}{\mu e} F_r \cos v + \frac{r^2}{\mu e} \left(1 + \frac{r}{p} \right) F_t \sin v \right] \quad (4.3-2)$$

In our opinion, there is a basic flaw in this approach. In the first five equations as in Lidov and in our work, $\dot{\gamma}$ has been set to unity, whereas in the sixth equation, $\dot{\gamma}$ has been expanded in order to generate an equation for time t . This equation is linear in the forces, and thus allows superposition. But nowhere does the feature of double integration appear, which normally accompanies this element in any perturbation theory. To quote Kovalevsky^[4-35]

"....We must therefore carry out a double integration of the equation giving the semi-major axis before being able to obtain the mean anomaly. This is an important general result. Whatever method is used, no problem of perturbed trajectory can be solved in celestial mechanics without carrying out a double integration at some stage....."

In the light of this comment, we can recall that \underline{t} is not an osculating element. Thus in the perturbed motion, the first term in the bracket of Equation (4.3-1), which is an "instantaneous analog" to the mean motion will be perturbed as compared to its value in the unperturbed case, the perturbation being of order ϵ and noted $O_1(\epsilon)$. Thus

$$\frac{dt}{dv} = O(1) + O_1(\epsilon_*) + O_2(\epsilon_*)$$

where $O_2(\epsilon)$ corresponds to the two last terms in the bracket of Equation (4.3-1). This yields

$$\begin{aligned} \Delta t &= \int_0^{2\pi} \frac{d}{dv} (\Delta t) dv \\ &= [O(1) + O_I^*(\epsilon_*) + O_{II}(\epsilon)] \end{aligned}$$

and $O_I(\epsilon_*)$ results from the perturbation of $\frac{r^2}{\sqrt{\mu a}}$. Thus, to be consistent, perturbation of the mean motion should be included, which in turn will lead to introducing into the sixth equation a term involving $a + \frac{da}{dv}$ before integrating with respect to v over $(0, 2\pi)$. As Equation (4.3-1) illustrates, this Roth has failed to include.

This problem does not arise with osculating element M_* (mean anomaly at epoch) adopted in the present study. We have, as in Appendix A-1 ,

$$\frac{dM_*}{dv} = - \frac{2r^3}{\mu a \epsilon^{1/2}} F_r + \frac{3}{2} \frac{nt}{a} \frac{da}{dv} - \epsilon^{1/2} \left(\cos i \frac{d\Omega}{dv} + \frac{d\omega}{dv} \right)$$

It is seen that the unperturbed mean motion does not appear alone, and that the term linear in time accounts for the double integration.

In Appendix A-1 , the sixth quantity used by Roth has been evaluated for the J_{20} term of the earth's oblateness. The result has been compared against a digital integration program (EOLA-TP) run for a high eccentricity orbit with J_{20} perturbations only. Fig. A .1 shows this comparison for the time of passage at perigee using either Roth's sixth element or M_* , or EOLA-TP. Table 4-1 also gives the data from which Fig. 4.1 is plotted. It is seen that Roth's elements predict negligible change in the apsidal period, which is not true. Using M_* gives a close approximation to the digital integration. Incidentally, Roth's work does not at all consider the sometimes significant effects of oblateness in orbits of high eccentricity.

4.4 Number of Terms ' Δz_{ij} ' to be Retained

With the same notation as in Chapter 2, let Δz_{ij} designate a change in osculating element z over an orbit of the satellite (more precisely, over

an interval $(0, 2\pi)$ in the true anomaly v). The first subscript, \underline{i} , is the "order" of the Legendre Polynomial term considered, in the LP expansion of the perturbing force \vec{F}_d . The second one, \underline{j} , is decreased by one, the order of the derivative retained, for the term studied, in the Taylor's series expansion of products such as $\xi_1^a \xi_2^b \xi_3^c \Delta^d$ about the position that the disturbing body assumes at the reference time, t_{ref} .

One remembers that in Chapter 2, expression γ

$$\gamma = \left[1 + \frac{r^2}{\mu e} F_r \cos v - \frac{r^2}{\mu e} \left(1 + \frac{r}{p} \right) F_t \sin v \right]^{-1}$$

such that

$$\frac{dt}{dv} = \gamma \frac{r^2}{\sqrt{\mu p}}$$

never differs from 1 by more than 0.8%, at maximum, in the worst possible case, for $e = 0.95$. It was therefore taken to be 1. Barring other considerations, the approximation on γ should set a lower bound on the terms to be generated.

Ref. [2-3] as said above, gives estimates of "maximum" amplitudes^[4-2] for the (Δz) . To recapitulate the formulae

a) along the LP expansion,

$$|(\Delta z)_{q+1}| \leq \left(\frac{a}{pk} \right) \frac{q+2}{q+1} \frac{2q+5}{q+3} |(\Delta z)_q|$$

with q the order of the force term being considered.

b) along the Taylor Series expansion

$$|(\Delta z)_{j+1}| \leq \frac{1}{j!} \left(\frac{\pi n_k}{n} \right)^j |(\Delta z)_1|$$

where j is the order of the derivative retained in the term being considered.

On the basis of these estimates, tables of relative "maximum" amplitudes of such terms were drawn up: Table 4-2 lists three such examples, for various "large" eccentricities, with the moon as perturbing body. Table 4-3 contains an example for the sun. Needless to say, we should expect that for the moon, it will be required to much higher values of "i" and "j" in the case of orbits of large eccentricities, than might be the case for the sun as the perturbing body. An answer as to how many terms ought to be retained in a specific case is of great interest. Previous work did not focus on the question: Roth^[4-33] did not set up a precise estimate, and Lidov examined the "11", "12" and "21" terms for five elements only. Table 4-2 shows that for orbits of $e > 0.92$, the number of terms needed, if the approximation of γ were regarded as the criterion would be very high (beyond $q = 5$ in Δz_{qj}) for the moon as perturbing body. Now, despite the use of symbolic computation, the required computer time and memory space are very high for high orders of the theory, as will be discussed later. In all cases tabulated in Table 4-2, it is seen that, for the moon as perturbing body,

$$\Delta_{51} \approx 0.12(\Delta_{11} + \Delta_{21} + \Delta_{31} + \Delta_{41})$$

$$\Delta_{61} \approx 0.09(\Delta_{11} + \Delta_{21} + \Delta_{31} + \Delta_{41} + \Delta_{51})$$

1 being the (normalized) magnitude of the "11" contribution to Δz_{total} . As a tentative cut-off point, the value 0.1 was adopted for the factor multiplying the parentheses in the above expression, and the theory

developed includes terms

$$\Delta_{11}, \Delta_{12}, \Delta_{13}, \Delta_{21}, \Delta_{22}, \Delta_{31}, \Delta_{41}, \text{ and } \Delta_{51}$$

In the section where the results of the developments are checked against high-precision numerical integration, it will be seen that this order of the theory is indeed adequate in practice for orbits of $e < 0.95$.

To conclude this question, we might remark that the relative effects of Sun and Moon, in the "qth" force term can be listed, as in Table 4-4. Let, from Ref. [4-2] ,

$$\left| \vec{F}_q \right|_{\max} \leq \frac{\mu}{r_d^2} \left(\frac{r}{r_d} \right)^q (q+1)$$

In a perturbation equation, that for $\frac{d\Omega}{dv}$ example, this gives

$$\frac{d\Omega}{dv} \sim \frac{\mu_d}{\mu} \frac{r}{p \sin i} (q+1) \left(\frac{r}{r_d} \right)^{q+2} \sin(\omega + v)$$

and the relative effects of sun and moon are measured by the ratio

$$\left| \frac{(\Delta\Omega)_S}{(\Delta\Omega)_M} \right| \sim \frac{\mu_S}{\mu_m} \left(\frac{r_M}{r_S} \right)^{q+2}$$

In this estimate, sun and moon have been assumed to describe coplanar orbits. The ratio is listed in Table 4-4 for low values of q. The same estimate would apply to the other osculating elements.

4.5 The Effect of Earth's Oblateness

The effects of earth's oblateness on orbits of large eccentricity have been found to be quite significant on natural satellites^[4-36] or artificial satellites, such as IMP-G^[4-37 to 4-38]. In the present study,

only J_{20} will be retained, since other harmonics are of order 10^{-3} or less compared to it. Its secular effect, obtained by integrating the corresponding perturbation equation with respect to v , will be superimposed on the effects of the sun and the moon. It is well known that there are no secular variations in elements a , e , or i due to J_{20} . The secular variations in Ω, ω and M_* due to J_{20} are evaluated in 4.10.

4.6 Symbolic Integration System

In the present section, a field of integrals is defined which are to be computed in order to obtain closed form expressions for the changes of the elements, over one orbital period of the unperturbed orbit. The recursive relations involved in the calculation are obtained. An estimate is made of the "explosive" growth in the number of terms to be calculated for the " Δz_{ij} " contribution. The results of this study stress the definite need to resort to symbolic computation for error-free algebra and for bypassing the formidable task of hand computation. The elements involved in the choice of a particular programming language are discussed. The system is described in its various parts. Finally, the relevant programs and space and time estimates are given.

4.6.1 Field of integrals

It has been seen in Chapter 2 that the integral form '(I.F.)' to be dealt with needs

$$(I.F.)_{s,u,v,q} \stackrel{\text{def}}{=} \int_0^{2\pi} (\Delta t)^s \frac{\sin^u v \cos^v v}{(1+e \cos v)^q} dv \quad (4.6-1)$$

in which

s, u, v, q are non-negative integers

$$q \geq 1 ;$$

$$q > u + v \quad (4.6-2)$$

Integrating (4.6-1) implies a series of recursive operations in a finite field of expressions (A 'field' is defined here as a set of expressions closed under integration, such as polynomials in several variables, polynomials in sine and cosine of an angle, etc.). Basic form (4.6-1) will in the process of computation evoke only linear combinations of numbers of the set. The element members of the field of expressions are not separately tabulated, but the recursion relations hereunder are defining each and every one of them.

4.6.2 Notations

Let $\Delta \equiv 1 + e \cos v$

$$L_{u,v,q} \equiv \frac{\sin^u v \cos^v v}{\Delta^q}$$

$$H_{u,q} \equiv \frac{\sin^u v}{\Delta^q} = L_{u,0,q}$$

$$I_{v,q} \equiv \frac{\cos^v v}{\Delta^q} = L_{0,v,q}$$

$$J_{v,q} \equiv \frac{\sin v \cos^v v}{\Delta^q} = L_{1,v,q}$$

$$K_{u,q} \equiv \frac{\sin^u v \cos v}{\Delta^q} = L_{u,1,q}$$

$$M_q \equiv \frac{1}{\Delta^q} = L_{0,0,q}$$

$$S_1 \equiv \int M_1 dv = \frac{2}{\epsilon^{1/2}} \arctan\left[\frac{(1-e)}{\epsilon^{1/2}} \tan \frac{v}{2}\right]$$

and

$$S_1 \Big|_0^{2\pi} = \frac{2\pi}{\epsilon^{1/2}}$$

$$\text{Let } S_m \equiv \int M_2 S_{m-1} dv$$

$$R_1 \equiv \int M_2 dv$$

(4.6-3)

$$C_1 \equiv \sqrt{\frac{\mu}{p^3}} = \frac{n}{\epsilon^{3/2}}$$

Note that

$$\frac{d}{dv} (\Delta t) = \frac{r^2}{\sqrt{\mu p}} = \frac{M_2}{C_1} \quad (4.6-4)$$

Δt is the time measured from some fixed reference time, t_{ref} , and should be considered as one variable, in contrast with the notation ' Δ ' defined above, or Δ in Δz_{ij} , designating the change of element z in the "ij" theory.

4.6.3 A set of vanishing definite integrals (I.F.)_{s,u,v,q}

The reference time, t_{ref} , is chosen as that corresponding to the occurrence of apogee along the unperturbed orbit^[4-1]. Hence, Δt is an odd function of v about $v=\pi$,

$$-\frac{\pi}{2} \leq \Delta t \leq \frac{\pi}{2}$$

and

$$(\Delta t)_v = -(\Delta t)_{2\pi-v}$$

It is readily apparent that the integrand of (4.6-1) is odd or even about $\pi = v$, depending on the sum of the exponents of (Δt) and $\sin v$, $(s+u)$. Thus

$$(\text{IF})_{s,u,v,q} = \int_0^{2\pi} (\Delta t)^s \frac{\sin^u v \cos^v v}{(1+e \cos v)^q} dv = \begin{cases} 0 & \text{if } (s+u) \text{ is odd} \\ \neq 0 & \text{if } (s+u) \text{ is even} \end{cases} \quad (4.6-5)$$

and the corresponding sets of (IF)'s can be ignored in what follows.

4.6-4 Recursive relations for $s = 0$

Let $s=0$ in $(\text{IF})_{s,u,v,q}$. The case $s \neq 0$ will be treated in 4.6.5. In all recursive relations, the goal is to monotonically decrease the value of the integer value of q ($q \geq 1$). Since q has to be larger than $u+v$, non-negative integers, u and v will also have to decrease to 0 or 1. After applying the relevant recursion forms the final results obtained is a lengthy primitive expression, evaluated by substitution of the limits 2π and 0 for v .

4.6.4.1 Integral of $L_{u,v,q}$

Using integration by parts, and the fact that

$$\int \frac{\sin v}{\Delta^q} dv = \frac{1}{(q-1)e} \frac{1}{\Delta^{q-1}} \quad (4.6-6)$$

it is easy to obtain

$$\int L_{u,v,q} dv = \frac{1}{(q-1)e} L_{u-1,v,q-1} - \frac{u-1}{(q-1)e} \int L_{u-2,v+1,q-1} dv \\ + \frac{v}{(q-1)e} \int L_{u,v-1,q-1} dv \quad (4.6-7)$$

with $q > 1$.

4.6.4.2 Integral of $K_{u,q}$

By integration by parts, and using (4.6-6) and $\cos^2 v = 1 - \sin^2 v$,

we get

$$\int K_{u,q} dv = \frac{1}{(q-1)e} K_{u-1,q-1} + \frac{1}{(q-1)e} \int H_{u,q-1} dv - \frac{u-1}{(q-1)e} \int H_{u-2,q-1} dv \quad (4.6-8)$$

with $q > 1$.

4.6.4.3 Integral of $H_{u,q}$

Using

$$\cos v = \frac{1}{e}(\Delta-1) \quad (4.6-9)$$

we obtain

$$\int H_{u,q} dv = \frac{1}{(q-1)e} \frac{\sin^{u-1}}{\Delta^{q-1}} - \frac{u-1}{(q-1)e} \int K_{u-2,q-1} dv \quad (4.6-10)$$

or

$$\int H_{u,q} dv = \frac{1}{(q-1)e} H_{u-1,q-1} - \frac{u-1}{(q-1)e^2} \int H_{u-2,q-2} dv \\ + \frac{u-1}{(q-1)e^2} \int H_{u-2,q-1} dv \quad (4.6-11)$$

4.6.4.4 Integral of $I_{v,q}$

This computation requires the value of $\int I_{v-1,q-1} dv$, i.e.

$$\begin{aligned} \int I_{v-1,q-1} dv &= \int \frac{\cos^{v-1} v}{\Delta^{q-1}} dv \\ &= \frac{\sin v \cos^{v-2} v}{\Delta^{q-1}} + (v-2) \int \frac{\cos^{v-3} v \sin^2 v}{\Delta^{q-1}} dv \\ &\quad - (q-1)e \int \frac{\sin^2 v \cos^{v-2} v}{\Delta^q} dv \end{aligned}$$

Solving for $\int I_{v,q} dv$, using $\cos^2 v = 1 - \sin^2 v$

$$\begin{aligned} \int I_{v,q} dv &= -\frac{1}{(q-1)e} J_{v-2,q-1} + \frac{(v-1)}{(q-1)e} \int I_{v-1,q-1} dv \\ &\quad + \int I_{v-2,q} dv - \frac{(v-2)}{(q-1)e} \int I_{v-3,q-1} dv \end{aligned} \quad (4.6-12)$$

valid for $v > 2$, $q > 2$.

For $v = 1$

$$\int I_{1,q} dv = \frac{1}{e} \int M_{q-1} dv - \frac{1}{e} \int M_q dv \quad (4.6-13)$$

4.6.4.5 Integral of $J_{v,q}$

$$\int J_{v,q} dv = \frac{1}{(q-1)e} I_{v,q-1} + \frac{v}{(q-1)e} \int J_{v-1,q-1} dv \quad (4.6-14)$$

with $q > 1$

4.6.4.6 Integral of M_q

$$\begin{aligned}
\int M_q dv &= \int \frac{dv}{\Delta^q} \\
&= \int \frac{\sin^2 v}{\Delta^q} dv + \int \frac{\cos^2 v}{\Delta^q} dv \\
&= \frac{1}{(q-1)e} \frac{\sin v}{\Delta^{q-1}} - \frac{1}{(q-1)e} \int \frac{\cos v}{\Delta^{q-1}} dv
\end{aligned}$$

$$\frac{1}{e^2} \left[\int \frac{dv}{\Delta^{q-2}} - 2 \int \frac{dv}{\Delta^{q-1}} + \int \frac{dv}{\Delta^q} \right] \quad (4.6-15)$$

wherein the identity

$$\cos^2 v = \frac{1}{e^2} (\Delta^2 - 2\Delta + 1)$$

has been used. Using (4.6-13) in the expression for $\int M_q dv$, $\epsilon = 1-e^2$, and rearranging,

$$\begin{aligned}
\int M_q dv &= -\frac{e}{(q-1)\epsilon} H_{1,q-1} + \frac{2q-3}{(q-1)} \int M_{q-1} dv + \frac{2q-3}{(q-1)\epsilon} \int M_{q-1} dv \\
&\quad - \frac{q-2}{(q-1)\epsilon} \int M_{q-2} dv \quad (4.6-16)
\end{aligned}$$

valid for $q > 1$.

For $q=1$, we defined

$$\int M_1 dv \equiv S_1 \quad (4.6-17)$$

Also, from (4.6-16), written for $q = 2$

$$R_1 = \int M_2 dv = -\frac{e}{\epsilon} H_{1,1} + \frac{S_1}{\epsilon} \quad (4.6-18)$$

4.6.5 Recursive relations for $s > 0$.

The recursive relations for the integration of $(IF)_{s,u,v,q} =$

$$\int (\Delta t)^s L_{u,v,q} dv = \Delta t^s \int L_{u,v,q} dv - \frac{s}{C_1} \int \Delta t^{s-1} M_2 [\int L_{u,v,q} dv] dv$$

From the formulae of the previous section,

$$\int L_{u,v,q} dv = a_0 S_1 + \sum_m a_m \cdot (\text{function of type H,I,J,K or L}) \quad (4.6-19)$$

with the a_i 's ($i = 0,1,2,\dots$) being constant. Thus, in (4.6-19), we are reduced to integrating known forms, plus a term of the form

$$\int (\Delta t)^s M_2 S_m dv = (\Delta t)^s S_{m+1} - \frac{s}{C_1} \int (\Delta t)^{s-1} M_2 S_{m+1} dv$$

4.6.5.1 Evaluation of S_m

$$\begin{aligned} S_m &= \int S_{m-1} M_2 dv \\ &= S_{m-1} [\int M_2 dv] - \int M_2 S_{m-2} [\int M_2 dv] dv \end{aligned}$$

But $R_1 \equiv \int M_2 dv$, $dR_1 = M_2 dv$. Thus

$$\begin{aligned} S_m &= S_{m-1} R_1 - \int S_{m-2} M_2 R_1 dv \\ &= S_{m-1} R_1 - S_{m-2} \frac{R_1^2}{2!} + \int S_{m-3} M_2 \frac{R_1^2}{2!} dv \end{aligned}$$

Finally

$$S_m = \sum_{\alpha=1}^{m-1} (-1)^{\alpha-1} S_{m-1} \frac{R_1^\alpha}{\alpha!} + \frac{(-1)^{m-1}}{(m-1)!} \int M_1 R_1^{m-1} dv \quad (4.6-20)$$

Let

$$\mathcal{T}_m \equiv \int M_1 R_1^{m-1} dv \quad (4.6-21)$$

Thus, since

$$R_1 = -\frac{e}{\epsilon} H_{1,1} + \frac{S_1}{\epsilon}$$

we get

$$\mathcal{T}_m = \int M_1 \left(-\frac{e}{\epsilon} H_{1,1} + \frac{S_1}{\epsilon} \right)^{m-1} dv$$

The integrand is expanded by the binomial formula. For the complete evaluation of \mathcal{T}_m , the following relations are also needed:

$$\int H_{u,v} S_1^q H_{u,v} dv - q \int S_1^{q-1} M_1 \left[\int H_{u,v} dv \right] dv \quad (4.6-22)$$

and

$$\int S_1^q M_1 dv = \frac{S_1^{q+1}}{q+1} \quad (4.6-23)$$

This completes the set of recursive formulae

4.6.6 Closure and character of the field of expressions.

The field of expressions is closed under integration under the conditions specified in Equation (4.6-2). Ref. 4-2 shows that it was necessary to use "mixed" axes for the components of the forces in the differential equations of motion, namely $(\vec{r}, \vec{t}, \vec{u})$: radial, transverse and normal directions, and $(\vec{P}, \vec{Q}, \vec{R})$: to perigee, normal to perigee

in the orbital plane, and normal to the orbital plane.

It is also evident from the reduction formulae and associated definitions, that the field of expressions is essentially not polynomial or trigonometric, neither is it "poly-trig". Transcendentals such as $\arctan(a_1 \tan a_2)$ are involved, and the field, though finite, is rather general in character.

4.6.7 Explosion of terms

The "explosion" of the number of terms under integration is briefly reviewed in this section, and given in much more detail in Ref. [4-2]. As an example, for the first few orders ($q = 1$ to 5) of the LP expansion, and for each variational equation, we have the following number of terms generated, as a minimum:

$$q = 1 \quad T_1 = \text{number (1)} \geq 2$$

$$q = 2 \quad T_2 = \text{number (2)} \geq 15$$

$$q = 3 \quad T_3 = \text{number (3)} \geq 18$$

$$q = 4 \quad T_4 = \text{number (4)} \geq 60$$

$$q = 5 \quad T_5 = \text{number (5)} \geq 70$$

following, roughly, a law $\sim 2^{2[\text{largest integer in } \frac{q}{2}]} + 2$

Further, in the Taylor's series expansion of the perturbing body motion, the next stage is to multiply each of these terms by $\frac{1}{\Delta}$ and integrate. Each of the above terms again produces at least

T_q terms of its own; thus

$$T_{\text{total}} \geq (T_q)^2$$

Therefore, both along the LP expansion ($q > 1$) and the Taylor Series expansion ($s > 0$), the process "blows up": a large number of terms are produced which have to be cataloged and collated during integration. As has been pointed earlier, a very significant amount of the analyst's time is spent in gathering and checking the results. In the approach based on machine symbolic computation, once the program has been checked against known results, the theory can be extended to any order automatically, subject to time and memory limitations. More important, the recitude of the results is assured, without extensive rechecking.

4.7 The Choice of a Language

Due to the abovementioned "general" character of the field of expressions, we are prevented from using a prepackaged symbolic integration program for the generation of the theory. A special system for integration within said field was written^[4-2], in a suitable programming language. The latter was chosen on the following considerations:

- the language should "match" the character of the field
- the program at hand uses a large amount of normal,
- the language should be capable of numerical work
- it should be generally available, for portability

Additional factors were: compact representation of elements and functions; dynamic allocation of storage (space saving; growth of

expression not always predictable); recursion, garbage collection features; compact storage of lists in a canonical form (to recognize common or identical sub-expressions); facilities for rational arithmetic (accuracy, recognition of identities).

Among the languages examined for the task, were ASSEMBLER, FORTRAN, ALGOL, PL/1, SAC, FORMULA ALGOL, LISP and FORMAC. FORMAC^[4-'39] was retained here for the following reasons:

- it satisfied most of the above requirements
- it is a general purpose algebraic manipulation language
- it has built-in simplification and substitution procedures through a canonical form of storage of expressions
- it is embedded in PL/1, making the arithmetic, control, recursion and dynamic features of PL-1 readily available.
- PL/1 string storage is used for lists not being processes, thereby counteracting the storage expenses of FORMAC (double word at each node in a list)
- space allocation can be controlled by an intelligent use of a list-erasing instruction
- the program is readable; it performs algebraic operations as easily as arithmetic ones
- it is widely available at most IBM scientific computer installations

4.8 Overview of Theory Generator

Fig. 4-1 shows the main parts of the Theory Generator used to generate the extended, modified Lidov's theory contained in what follows.

Equation Generator: it accepts as input the order of the LP expansion of the force term (i.e. the highest value taken on by i) and delivers as output the variational equations for all six elements considered here, with the force components internally generated.

Preprocessor: this minor routine scans the output of the Equation Generator and collects terms which have an identical "operative" part. The symbolic integration is performed on the equation

$$C_1(\Delta t)^S f(v)$$

with $f(v)$ containing $\sin v$, $\cos v$ and Δ terms, and C_1 (not necessarily numerical) a coefficient, and preprocessing assures that only the "operative" part $(\Delta t)^S f(v)$ is operated upon only once, with the C_1 's as coefficients.

Symbolic Integrator: this "core" program accepts as input the variational equations, and the order of the Taylor Series expansion. The equations (to the order specified) are integrated, and the integrals are evaluated between the limits 0 and 2π in v , true anomaly

Simplifier: accepts the "new" output of the Symbolic Integrator, processes it through a series of substitutions and simplifications,

collects terms and generates, in an internally specified format, the final theory.

The design of the package is such that each program is a "block", written in FORMAC, independent of the other blocks, with communication between blocks, or to the user, effected through punched cards or files in punched card format stored in mass memory. Printouts of the input, and printouts or storage of the outputs at each stage facilitate the checking of the flow of information.

The final output will be the "theory", as a file or a set of punched cards. In order to render the theory usable for the user's numerical calculations, a small amount of further processing was required, more specifically:

- the replacement of integer fractions by their decimal equivalents;
- the definition of "user's variables" to replace common sub-expressions appearing in the variation formulae for more than one element, which will improve the speed of numerical calculation using the theory.

The formulae obtained on the final result of the theory were then incorporated in a PL/1 program, VØLER, described in Section 4.11.

As regards storage requirements for expressions, they are inherently high, since each operator, operated and associated pointer occupies one or two words of storage. Formula manipulation systems and user programs are also very cumbersome. Thus, in order to

successfully execute any large program, it is of importance that space-conserving and -releasing techniques be used whenever possible. In FORMAC, this is made possible by the commands

- SAVE, which stores unneeded expressions on disk;
- ATOMIZE, which erases a list and releases the corresponding space

Furthermore, the compact string storage feature of PL/1 has been used to a considerable extent to economically store lists not in immediate use. ATOMIZE has also been used profusely, but SAVE has not been used desirably, as it is too expensive in time. Instead, at every stage, as soon as an output is generated, it is stored on to a file, or punched out, and the space is released by erasing the list. In the trade-off between time and working storage, a penalty has often to be paid in time, due to the memory space limitations of most digital computer systems. This might take the form of integrating again a previously integrated "operative part" of which the result had to be outputted in a previous run, or of allowing the package to be segmented, with the user interacting with the system between blocks. The attached risk of error is decreased, however, by visual checks against user-or system-created errors.

4.9 Details on Theory Generator

Each of the above parts is now briefly analyzed.

4.9.1 Equation Generator: Program FREQN

Fig. 4-2 gives a flow chart of the program, and Ref. [4-2] contains a complete listing; given the recursion formulae, the Legendre

polynomials are generated up to one order higher than the required "q". Their derivatives are computed using the DERIV function of FORMAC, and some common symbolic coefficients are generated in the order shown in the last box of the flow chart.

As soon as it is generated, each differential equation is expanded. Each rate of variation of an element z with v , $\frac{dz}{dv}$ will be a series of terms $\sum_i c_i f_i(v)$, where as described before the c_i are coefficients and the $f_i(v)$ are "operative parts". Each separate such term is punched out or stored on file.

Along with the whole FORMAC system and service routines, the program requires:

- 107 k bytes of memory on an IBM 360
- for PORDER, 4 (or "q" = 4), a CPU time of 7.5 minutes (CMU IBM 360/67 TSS)

4.9.2 Preprocessor program COLLECT

The function of COLLECT, as mentioned above, is to gather terms having identical operative parts. This is carried out separately for each differential equation, in order to save time by avoiding repeated integration of identical operative parts. A listing is given in Ref. [4-2].

4.9.3 Symbolic Integrator

This "block" implements the recursive procedures of Section 4.6, with the appropriate control, parsing and evaluation routines. A flow chart of this block is given in Fig. 4-3.

I/O ROUTINE: Procedure INPUT 1

Data : - order "j" of Taylor's series expansion desired
 - output of FREQN, for given q, one term at a time

Function: the term is passed to the supervisor for integration

Output: the final integrated output is printed and punched out, or stored on file

SUPERVISOR: Procedure HIGHORD

Input : term furnished by I/O routine

- Function:
- a) examines the terms to be integrated
 - b) if it has no operative part, it is returned to the I/O as a "constant"
 - c) if it has an operative part, the latter is isolated; the Taylor index j , is updated if necessary; a call is issued to the Pattern Recognizer
 - d) after completing the integration, it calls on the Evaluator
 - e) it also monitors integration that might be needed during the evaluation process

Output: result of completely evaluated result is passed back to the I/O routine.

PATTERN RECOGNIZER: Procedure SICODEL, with its internal procedure PATTERN.

Function: The term is examined to see if the relation of Equation (4.6-5) is satisfied. If so, the integral is set to zero and sent back to the supervisor. If not, the exponents of "sin v ", "cos v ", " Δ " are determined, and the appropriate integration procedure is used.

Procedures for the integration:

- DELDEL: for integrating $\int M_q dv = \int L_{o,o,q} dv$
- DELCOS: for integrating $\int L_{v,q} dv = \int L_{o,v,q} dv$
- DELSIN: for integrating $\int H_{u,q} dv = \int L_{u,o,q} dv$
- DELSICO: for the integration of the general term $\int L_{u,v,q} dv$

Note that in Fig. 4.3, the diodes indicate direction of calls.

For instance, DELSIN can call on DELDEL, DELCOS or itself, but not on DELSICO.

EVALUATOR: Procedure EVALUAT

Function: its primary function is to substitute the limits 0 and 2π on v , in the integrated result. Further integrals, of type S_m , which might have to be evaluated, are obtained by calling internal routine SVALU, which may issue a call to TVALU. It also determines

the derivative of the perturbing body terms $\xi_1^a \xi_2^b \xi_3^c \Lambda_k^d$.

The TVALU procedure integrates terms like

$$\tau_m = \int R_1^{m-1} M_1 dv$$

in which expression (4.6-18) is substituted for R_1 . The expression is carried out. Control is passed back to the Evaluator for substitution of the limits.

As can be seen, the Symbolic Integrator is fairly complex. In terms of time for integration, it is very much effected by the "explosion" of terms to be processed, specially along the Taylor Series Expansion dimension, j . As an illustration

- Space occupied in core, including FORMAC and series routines: 161 K bytes.

- Time for $\Delta_{11}M_*$ = 1.5 minutes

$\Delta_{13}M_*$ = 28 minutes

$\Delta_{21}M_*$ = 9.5 minutes

$\Delta_{22}M_*$ = 40 minutes

$\Delta_{31}M_*$ = 25 minutes

$\Delta_{51}M_*$ = 4.5 hours

This integration is by far the most time-consuming because of the presence of term $t \frac{da}{dv}$, which necessitates going to one order higher in $(\Delta t)^S$ than specified by the input data "j" (order of Taylor Series expansion).

- Time for Δ_{12}^{ω} = 3 minutes

Δ_{13}^{ω} = 11 minutes

Δ_{22}^e = 8 minutes

Δ_{31}^e = 10 minutes

Δ_{41}^e = 28 minutes

Δ_{51}^e = 1.5 hours

The above estimates are made on a TSS environment, and are not actual CPU time (the system overhead may be as high as 50% under peak load).

SIMPLIFIER: Procedure SIMPF6

Function: to compress the result and print it out in "usable" form. The set of simplifications is based on visual examination of the integrated output. It mainly consists of substitution and removal of common factors. The final result is collected according to the coefficients dependent on the perturbing bodies. Consequently, an extremely compact form of the final theory results, as compared to their volume prior to the SIMPLIFIER. A listing of SIMPLF6 is given in Ref. [4-2] .

Output: a set of punched cards (or file) containing the theory for each element, for each pair (ij). As mentioned earlier in Section 4.8, two later subsequent steps geared to efficient numerical computations are the decimalization of fractions, and the labeling of common sub-expressions.

Space requirements: about 100 K bytes, including FORMAC and service routines.

Time requirements: they are quite significant. For example,

$$\Delta_{13}\omega = 5 \text{ minutes}$$

$$\Delta_{22}\omega = 12 \text{ minutes}$$

$$\begin{aligned}\Delta_{31}\omega &= 2 \text{ minutes} \\ \Delta_{41}\omega &= 2.5 \text{ minutes} \\ \Delta_{51}\omega &= 3.5 \text{ minutes}\end{aligned}$$

4.9.4 Example

An example, going from raw data to final output, is given in Ref. [4-2]. Times taken at each stage are also tabulated.

4.10 Results of the Theory: perturbations formulae

4.10.1 The formulae

In this section, all six osculating elements a , e , i , ω , Ω , M_* are tabulated for the following orders "ij" (Δ_{ij} is the "ij" change of element z).

$$\begin{array}{lll}\Delta_{11} & \Delta_{12} & \Delta_{13} \\ \Delta_{21} & \Delta_{22} & \\ \Delta_{31} & & \\ \Delta_{41} & & \\ \Delta_{51} & & \end{array}$$

An important point to mention here is that the formulae were checked against those of Lidov^[4-1], for the first five elements and orders "11", "12" and "21"; and against those obtained by hand by Roth^[4-33]; for the first five elements and orders "11", "12", "13", "21", "22" and "31". (The sixth quantity he used as a variable is discussed in Section 4.3). The agreement was complete, which gives us the highest degree of confidence of the recitude of formulae produced by our theory generator.

For completeness, the secular perturbations of Ω , ω and M_* due to the J_{20} term are also reproduced.

Notice that, in the formulae, names have been given to some common sub-expressions. They may be repeated and should be strictly associated with their definitions within the scope of the "ij" order in which they appear at any moment.

Formulae Δ_{11z}

LP expansion = 1st order ($(\frac{r}{r_k})$ term)

Taylor expansion = 1st order ("constant" term)

Let

$$\phi = \Delta_k^3, \quad \delta = \frac{\mu_k}{\mu} \left(\frac{a}{p_k}\right)^3,$$

$$\beta_1 = \xi_1^2 \phi, \quad \beta_2 = \xi_2^2 \phi, \quad \beta_3 = \xi_1 \xi_2 \phi,$$

$$\beta_4 = \xi_2 \xi_3 \phi, \quad \beta_5 = \xi_1 \xi_3 \phi, \quad \beta_6 = \phi,$$

$$\epsilon = 1 - e^2,$$

T = time at epoch (perigee), τ = period of satellite

n = mean motion of satellite

$$\Delta_{11a} = 0$$

$$\Delta_{11e} = -15\pi \delta e \epsilon^{1/2} \beta_3$$

$$\Delta_{11i}^* = 3\pi \frac{\delta}{\epsilon^{1/2}} [(5-4\epsilon)\beta_5 \cos \omega - \epsilon\beta_4 \sin \omega]$$

$$\Delta_{11\Omega} = 3\pi \frac{\delta}{\epsilon^{1/2} (\sin i)} [(5-4\epsilon)\beta_5 \sin \omega + \epsilon\beta_4 \cos \omega]$$

$$\Delta_{11\omega} = 3\pi \delta \epsilon^{1/2} (4\beta_1 - \beta_2 - \beta_6) - (\cos i)\Delta_{11\Omega}$$

$$\Delta_{11M_*} = \frac{3\pi}{2a} (\Delta_{11a}) - \epsilon^{1/2} (\Delta_{11\Omega}(\cos i) + \Delta_{11\omega}) \\ + \frac{\pi}{2} \delta [(8 + 12e + 15e^2)\beta_6] \quad \text{-(cont'd on next page)}$$

*The coefficient δ of Δ_{11i} is incorrectly printed as (a/p_k) instead of $(a/p_k)^3$ in Lidov's paper^(1.19).

$$-3(1+12e+22e^2)\beta_1$$

$$-21\epsilon\beta_2]$$

$$\Delta_{11}T = -(\Delta_{11}M_*)/n$$

Formulae $\Delta_{12}Z$

LP expansion = 1st order ($(\frac{r}{r_k})$ term)

Taylor expansion = 2nd order ((Δt) term)

Let

$$\delta = \frac{\mu_k}{\mu} \left(\frac{a}{P_k}\right)^3, \quad n_k = \text{mean motion of perturbing body,}$$

e_k = eccentricity of perturbing body

θ_k = true anomaly of perturbing body in its orbit,

$\dot{\theta}_k = \frac{d\theta_k}{dt}$ = angular speed of perturbing body in its orbit,

$$\xi_{1p} = \frac{d\xi_1}{d\theta_k}, \quad \xi_{2p} = \frac{d\xi_2}{d\theta_k}, \quad \xi_{3p} = \frac{d\xi_3}{d\theta_k}$$

$$\phi = \Delta_k^3, \quad \phi_p = \frac{d\phi}{d\theta_k} = -3\Delta_k^2 e_k (\sin \theta_k)$$

$$\beta_1 = (2\xi_1\xi_{1p}\phi + \xi_1^2\phi_p)\dot{\theta}_k$$

$$\beta_2 = (2\xi_2\xi_{2p}\phi + \xi_2^2\phi_p)\dot{\theta}_k$$

$$\beta_3 = [(\xi_1 \xi_{2p} + \xi_{1p} \xi_2) \phi + \xi_1 \xi_2 \phi_p] \dot{\theta}_k$$

$$\beta_4 = [(\xi_2 \xi_{3p} + \xi_{2p} \xi_3) \phi + \xi_2 \xi_3 \phi_p] \dot{\theta}_k$$

$$\beta_5 = [(\xi_1 \xi_{3p} + \xi_{1p} \xi_3) \phi + \xi_1 \xi_3 \phi_p] \dot{\theta}_k$$

$$\beta_6 = \phi_p \dot{\theta}_k$$

$$\Delta_{12a} = -\frac{3}{2} \delta \text{ at} [e(e+4) (\beta_2 - \frac{\beta_6}{3}) \\ + (2e^2 + 4e - 1) (\beta_1 - \beta_2)]$$

$$\Delta_{12e} = -3\delta \epsilon \tau [\frac{1}{4}(e+4) (\beta_2 - \frac{\beta_6}{3}) \\ + (\frac{e}{8} - \frac{1}{3}) (\beta_1 - \beta_2)]$$

$$\Delta_{12i} = \frac{9}{8} \delta \tau [e^2 + \frac{32}{9} e - \frac{2}{3}] (\beta_4 \cos \omega - \beta_5 \sin \omega)$$

$$\Delta_{12\Omega} = \frac{9}{8} \delta \frac{\tau}{\sin i} [e^2 + \frac{32}{9} e - \frac{2}{3}] (\beta_5 \cos \omega + \beta_4 \sin \omega)$$

$$\Delta_{12\omega} = -3 \delta \frac{\tau}{e} (\frac{9}{8} e^3 + \frac{8}{3} e^2 - e - \frac{4}{3}) \beta_3$$

$$-\Delta_{12\Omega}(\cos i)$$

$$\Delta_{12M_*} = \frac{3}{2} \frac{\pi}{a} (\Delta_{12a}) - \epsilon^{1/2} (\Delta_{12\Omega}(\cos i) + \Delta_{12\omega}) \\ + \delta \epsilon^{1/2} \tau (\frac{15}{2} - 40e - \frac{45}{4} e^2) \beta_3$$

$$\Delta_{12T} = -(\Delta_{12M_*})/n$$

Formulae Δ_{13Z}

LP expansion = 1st order ($(\frac{r}{r_k})$ term)

Taylor expansion = 3rd order ($(\Delta t)^2$ term)

Let

$$\delta = \frac{\mu_k}{\mu} \left(\frac{a}{p_k}\right)^3$$

$$\ddot{\theta}_k = \frac{d^2 \theta_k}{dt^2} = \text{angular acceleration of perturbing body in its orbit.}$$

$$\dot{\theta}_k = \frac{d\theta_k}{dt} = \text{angular speed of perturbing body in its orbit}$$

$$\xi_{1p} = \frac{d\xi_1}{d\theta_k}, \quad \xi_{2p} = \frac{d\xi_2}{d\theta_k}, \quad \xi_{3p} = \frac{d\xi_3}{d\theta_k}$$

$$\phi = \Delta_k^3$$

$$\phi_p = \frac{d\phi}{d\theta_k} = -3\Delta_k^2 e_k \sin \theta_k$$

$$\phi_{pp} = \frac{d^2 \phi}{d\theta_k^2} = 6\Delta_k^2 e_k \sin^2 \theta_k - 3\Delta_k^2 e_k \cos \theta_k$$

$$\beta_1 = [2\phi(\xi_{1p}^2 - \xi_1^2) + 4\xi_1\xi_{1p}\phi_p + \xi_1^2\phi_{pp}] \dot{\theta}_k^2$$

$$+ (2\xi_1\xi_{1p}\phi + \xi_1^2\phi_p) \ddot{\theta}_k$$

$$\beta_2 = [2\phi(\xi_{2p}^2 - \xi_2^2) + 4\xi_2\xi_{2p}\phi_p + \xi_2^2\phi_{pp}] \dot{\theta}_k^2$$

$$+ (2\xi_2\xi_{2p}\phi + \xi_2^2\phi_p) \ddot{\theta}_k$$

$$\beta_3 = [2\phi(\xi_{1p}\xi_{2p} - \xi_1\xi_2) + 2\phi_p(\xi_1\xi_{2p} + \xi_{1p}\xi_2)$$

$$+ \xi_1\xi_2\phi_{pp}] \dot{\theta}_k^2 + [(\xi_1\xi_{2p} + \xi_{1p}\xi_2)\phi + \xi_1\xi_2\phi_p] \ddot{\theta}_k$$

$$\beta_4 = [2\phi(\xi_{2p}\xi_{3p} - \xi_2\xi_3) + 2\phi_p(\xi_2\xi_{3p} + \xi_{2p}\xi_3)$$

$$+ \xi_2\xi_3\phi_{pp}] \dot{\theta}_k^2 + [(\xi_2\xi_{3p} + \xi_{2p}\xi_3)\phi + \xi_2\xi_3\phi_p] \ddot{\theta}_k$$

$$\beta_5 = [2\phi(\xi_{1p}\xi_{3p} - \xi_1\xi_3) + 2\phi_p(\xi_1\xi_{3p} + \xi_{1p}\xi_3)$$

$$+ \xi_1\xi_3\phi_{pp}] \dot{\theta}_k^2 + [(\xi_1\xi_{3p} + \xi_{1p}\xi_3)\phi + \xi_1\xi_3\phi_p] \ddot{\theta}_k$$

$$\beta_6 = \phi_{pp} \dot{\theta}_k^2 + \phi_p \ddot{\theta}_k$$

$$\Delta_{13a} = \delta \frac{a}{\epsilon} \frac{\tau^2}{1/2 \pi} \beta_3 \left(-4e - \frac{15}{8} e^2 + 4e^3 + \frac{9}{8} e^4 + \frac{3}{4} \right)$$

$$\Delta_{13e} = \frac{\epsilon}{2ae} (\Delta_{13a}) + \frac{\delta}{2} \frac{\tau^2}{\pi} \frac{\epsilon^{1/2}}{e} \left[\frac{26}{3} e - \frac{5}{4} \pi^2 e^2 + \frac{27}{16} e^2 - \frac{10}{3} e^3 - \frac{21}{32} e^4 - \frac{3}{4} \right] \beta_3$$

$$\text{Let } C = \frac{\beta_5}{\epsilon^{1/2}} \left(-\frac{22}{3} e + \left(\pi^2 - \frac{33}{32} \right) e^2 + 2e^3 + \frac{3}{8} e^4 + \frac{\pi^2}{4} + \frac{3}{8} \right)$$

$$D = \beta_4 \epsilon^{1/2} \left(\frac{4}{3} e + \frac{9}{32} e^2 + \frac{\pi^2}{4} - \frac{3}{8} \right)$$

$$\text{Then, } \Delta_{13\Omega} = \frac{1}{2} \frac{\tau^2}{(\sin i)} \frac{\delta}{\pi} [C \sin \omega + D \cos \omega]$$

$$\Delta_{13i} = \frac{1}{2} \frac{\tau^2}{\pi} \delta [C \cos \omega - D \sin \omega]$$

$$\Delta_{13\omega} = -(\Delta_{13\Omega}) \cos i$$

$$+ \frac{\delta}{2} \frac{\tau^2}{\pi} \frac{\epsilon^{1/2}}{e} \left[\beta_1 \left(-\frac{33}{32} e + \pi^2 e + 3e^2 + \frac{3}{4} e^3 - \frac{11}{3} \right) \right.$$

$$+ \beta_2 \left(-\frac{\pi^2}{4} e + \frac{21}{32} e - 2e^2 - \frac{9}{16} e^3 + \frac{2}{3} \right)$$

$$\left. + \beta_6 \left(-\frac{\pi^2}{4} e + \frac{e}{8} - \frac{e^2}{3} - \frac{e^3}{16} + 1 \right) \right]$$

$$\begin{aligned}
\Delta_{13}M_* &= \frac{3}{2} \frac{\pi}{a} (\Delta_{13}a) - \epsilon^{1/2} (\Delta_{13}\Omega(\cos i) + \Delta_{13}\omega) \\
&+ \frac{\delta}{2} \frac{r^2}{\pi} \left[\epsilon\beta_2 \left(\frac{39}{16} - \frac{13}{8} \pi^2 - \frac{26}{3} e - \frac{117}{64} e^2 \right) \right. \\
&+ \beta_6 \left\{ \frac{\pi^2}{3} + e \left(\frac{3}{2} \pi^2 - 13 \right) \right. \\
&+ \left. e^2 \left(\frac{7}{8} \pi^2 - \frac{13}{16} \right) + \frac{13}{9} e^3 + \frac{13}{64} e^4 \right\} \\
&+ \beta_1 \left\{ \frac{5}{8} \pi^2 - \frac{39}{16} + e \left(\frac{143}{3} - \frac{9}{2} \pi^2 \right) \right. \\
&+ \left. e^2 \left(\frac{429}{64} - \frac{17}{4} \pi^2 \right) - 13e^3 - \frac{39}{16} e^4 \right\}]
\end{aligned}$$

$$\Delta_{13}T = -(\Delta_{13}M_*)/n$$

Formulae $\Delta_{21}Z$

LP expansion = 2nd order $\left(\left(\frac{r}{r_k} \right)^2 \text{ term} \right)$

Taylor expansion = 1st order ("constant" term)

$$\delta = \frac{\mu_k}{\mu} \left(\frac{a}{P_k} \right)^4, \quad \phi = \Delta_k^4$$

$$\alpha_1 = \xi_1 \phi, \quad \alpha_2 = \xi_2 \phi, \quad \alpha_3 = \xi_3 \phi,$$

$$\gamma_1 = \xi_1^3 \phi, \quad \gamma_2 = \xi_2^3 \phi, \quad \gamma_3 = \xi_1^2 \xi_2 \phi,$$

$$\gamma_4 = \xi_1^2 \xi_3 \phi, \quad \gamma_5 = \xi_2^2 \xi_3 \phi, \quad \gamma_6 = \xi_2 \xi_1^2 \phi,$$

$$\gamma_7 = \xi_1 \xi_2 \xi_3 \phi,$$

$$\Delta_{21a} = 0$$

$$\Delta_{21e} = \frac{75}{8} \pi \delta \epsilon^{1/2} [(7-6\epsilon)\gamma_3 + \epsilon\gamma_2 - (7-3\epsilon)\frac{\alpha_2}{5}]$$

Letting, for brevity,

$$C = [(7-4\epsilon)\gamma_4 + \epsilon\gamma_5 - (7-3\epsilon)\frac{\alpha_3}{5}]$$

$$D = 2\epsilon\gamma_7$$

we write,

$$\Delta_{21\Omega} = -\frac{75}{8} \pi \delta \frac{e}{\epsilon^{1/2}} \frac{1}{(\sin i)} [C \sin \omega + D \cos \omega]$$

$$\Delta_{21i} = -\frac{75}{8} \pi \delta \frac{e}{\epsilon^{1/2}} [C \cos \omega - D \sin \omega]$$

$$\Delta_{21\omega}^* = -\frac{75}{2} \pi \delta \frac{\epsilon^{1/2}}{e} [(\frac{5}{4} - \epsilon)\gamma_1 - (\frac{1}{2} - \frac{3\epsilon}{4})\gamma_6 - \frac{\alpha_1}{20}(13-9\epsilon)] - \Delta_{21\Omega}(\cos i)$$

$$\begin{aligned} \Delta_{21M_*} &= \frac{3}{2} \frac{\pi}{a} (\Delta_{21a}) - \epsilon^{1/2} (\Delta_{21\Omega}(\cos i) + \Delta_{21\omega}) \\ &+ \frac{15}{8} \pi \delta [45\epsilon\gamma_6 + (8+21\epsilon+24\epsilon^2+52\epsilon^3)\gamma_1 \\ &- \frac{3}{5} \alpha_1(8+36\epsilon+24\epsilon^2+37\epsilon^3)] \end{aligned}$$

$$\Delta_{21T} \doteq -(\Delta_{21M_*})/n$$

*The term underlined is misprinted as γ_4 in Lidov's paper

Formulae Δ_{22z}

$$\text{LP expansion} = 2\text{nd order } \left(\left(\frac{r}{r_k} \right)^2 \text{ term} \right)$$

$$\text{Taylor expansion} = 2\text{nd order } ((\Delta t) \text{ term})$$

Let

$$\delta = \frac{\mu_k}{\mu} \left(\frac{a}{p_k} \right)^4, \quad \phi = \Delta_k^4, \quad \phi_p = -4\Delta_k^3 e_k (\sin \theta_k)$$

$$\xi_{lp} = \frac{d\xi_1}{d\theta_k}, \quad \xi_{2p} = \frac{d\xi_2}{d\theta_k}, \quad \xi_{3p} = \frac{d\xi_3}{d\theta_k}$$

$$\dot{\theta}_k = \frac{d\theta_k}{dt} = \text{angular speed of perturbing body in its orbit,}$$

$$\alpha_1 = (\xi_{1p} \phi + \xi_1 \phi_p) \dot{\theta}_k$$

$$\alpha_2 = (\xi_{2p} \phi + \xi_2 \phi_p) \dot{\theta}_k$$

$$\alpha_3 = (\xi_{3p} \phi + \xi_3 \phi_p) \dot{\theta}_k$$

$$\gamma_1 = (3\xi_1^2 \xi_{1p} \phi + \xi_1^3 \phi_p) \dot{\theta}_k$$

$$\gamma_2 = (3\xi_2^2 \xi_{2p} \phi + \xi_2^3 \phi_p) \dot{\theta}_k$$

$$\gamma_3 = (2\xi_1 \xi_{1p} \xi_{2p} \phi + \xi_1^2 \xi_{2p} \phi + \xi_1^2 \xi_2 \phi_p) \dot{\theta}_k$$

$$\gamma_4 = (2\xi_1 \xi_{1p} \xi_{3p} \phi + \xi_1^2 \xi_{3p} \phi + \xi_1^2 \xi_3 \phi_p) \dot{\theta}_k$$

$$\gamma_5 = (2\xi_2 \xi_{2p} \xi_{3p} \phi + \xi_2^2 \xi_{3p} \phi + \xi_2^2 \xi_3 \phi_p) \dot{\theta}_k$$

$$\gamma_6 = (2\xi_2 \xi_{2p} \xi_{1p} \phi + \xi_2^2 \xi_{1p} \phi + \xi_2^2 \xi_1 \phi_p) \dot{\theta}_k$$

$$\gamma_7 = [(\xi_{1p} \xi_{2p} \xi_{3p} + \xi_1 \xi_{2p} \xi_{3p} + \xi_1 \xi_2 \xi_{3p}) \phi$$

$$+ \xi_1 \xi_2 \xi_3 \phi_p] \dot{\theta}_k$$

$$\Delta_{22a} = 2\tau\delta a \left[\frac{75}{16} e \epsilon \gamma_6 - \frac{\alpha_1}{8} (12 - 6e + 36e^2 + \frac{21}{2} e^3) \right. \\ \left. + \frac{5}{8} \gamma_1 (4 - \frac{9}{2} e + 12e^2 + 6e^3) \right]$$

$$\Delta_{22e} = \tau\delta \frac{\epsilon}{e} \left[(30e + \frac{615}{64} e^2 - \frac{645}{64}) e \gamma_6 \right. \\ \left. + \alpha_1 (-\frac{3}{8} e + \frac{3}{2} e^2 + \frac{21}{64} e^3 + \frac{3}{2}) \right. \\ \left. + \gamma_1 (\frac{255}{64} e - \frac{25}{2} e^2 - \frac{15}{4} e^3 - \frac{5}{2}) \right] \\ + \frac{\epsilon}{2ae} (\Delta_{22a})$$

Letting

$$C = (\frac{255}{32} e - 25e^2 - \frac{15}{2} e^3 - 5) \gamma_7$$

$$D = [\alpha_3 (-\frac{3}{8} e + \frac{3}{2} e^2 + \frac{21}{64} e^3 + \frac{3}{2}) \\ + \gamma_4 (\frac{255}{64} e - \frac{25}{2} e^2 - \frac{15}{4} e^3 - \frac{5}{2}) \\ + \gamma_5 (-5 - \frac{135}{64} e) \epsilon]$$

we have

$$\Delta_{22\Omega} = \frac{\tau\delta}{(\sin i)} [C \sin \omega + D \cos \omega]$$

$$\Delta_{22i} = \tau\delta [C \cos \omega - D \sin \omega]$$

$$\begin{aligned} \Delta_{22}\omega &= \tau \frac{\delta}{e} \left[\alpha_2 \left(-\frac{3}{8} + \frac{3}{2} e + \frac{111}{64} e^2 - \frac{9}{2} e^3 - \frac{21}{16} e^4 \right) \right. \\ &\quad + \gamma_3 \left(\frac{255}{64} - \frac{45}{2} e - \frac{615}{32} e^2 + \frac{75}{2} e^3 + 15e^4 \right) \\ &\quad + \frac{5}{64} \gamma_2 (-9 + 64e + 36e^2) \epsilon] \\ &\quad - \Delta_{22}\Omega(\cos i) \end{aligned}$$

$$\begin{aligned} \Delta_{22}M_* &= \frac{3}{2} \frac{\pi}{a} (\Delta_{22}a) - \epsilon^{1/2} (\Delta_{22}\Omega(\cos i) + \Delta_{22}\omega) \\ &\quad + \delta \tau \epsilon^{1/2} \left[\gamma_2 \epsilon \left(20 + \frac{135}{16} e \right) \right. \\ &\quad \quad + \frac{15}{8} \gamma_3 \left(16 - \frac{51}{2} e + 80e^2 + 24e^3 \right) \\ &\quad \quad \left. + 9 \alpha_2 \left(-2 + \frac{e}{2} - 2e^2 - \frac{7}{16} e^3 \right) \right] \end{aligned}$$

$$\Delta_{22}T = - \Delta_{22}M_*/n$$

Formulae Δ_{31Z}

$$\text{LP expansion} = 3\text{rd order} \left(\left(\frac{r}{r_k} \right)^3 \text{ term} \right)$$

$$\text{Taylor expansion} = 1\text{st order ("constant" term)}$$

Let

$$\delta = \frac{\mu_k}{\mu} \left(\frac{a}{p_k} \right)^5, \quad \phi = \Delta_k^5$$

$$\begin{aligned}
\alpha_1 &= \xi_1^2 \phi, & \alpha_2 &= \xi_2^2 \phi, & \alpha_3 &= \xi_1 \xi_2 \phi, \\
\alpha_4 &= \xi_2 \xi_3 \phi, & \alpha_5 &= \xi_1 \xi_3 \phi, & \alpha_6 &= \phi, \\
\beta_1 &= \xi_1^4 \phi, & \beta_2 &= \xi_1^3 \xi_2 \phi, & \beta_3 &= \xi_1^2 \xi_2^2 \phi, \\
\beta_4 &= \xi_1 \xi_2^3 \phi, & \beta_5 &= \xi_2^4 \phi, & & \\
\gamma_1 &= \xi_1^3 \xi_3 \phi, & \gamma_2 &= \xi_1^2 \xi_2 \xi_3 \phi, & & \\
\gamma_3 &= \xi_1 \xi_2^2 \xi_3 \phi, & \gamma_4 &= \xi_2^3 \xi_3 \phi, & &
\end{aligned}$$

$$\Delta_{31a} = 0$$

$$\begin{aligned}
\Delta_{31e} &= \frac{105}{8} \delta \pi \epsilon^{1/2} e [3\alpha_3(2 + e^2) \\
&\quad - 7\beta_2(2e^2 + 1) - 7\epsilon\beta_4]
\end{aligned}$$

Letting

$$\begin{aligned}
C &= [(630e^2 + 105) \frac{\gamma_3}{8} - (\frac{615}{8} e^2 + \frac{135}{4} e^4 + \frac{15}{2}) \frac{\alpha_5}{\epsilon} \\
&\quad + (\frac{315}{2} e^2 + 105 e^4 + \frac{105}{8}) \frac{\gamma_1}{\epsilon}]
\end{aligned}$$

$$\begin{aligned}
D &= [-(\frac{45}{8} e^2 + \frac{15}{2}) \alpha_4 + (630e^2 + 105) \frac{\gamma_2}{8} \\
&\quad + \frac{105}{8} \epsilon \gamma_4]
\end{aligned}$$

Then,

$$\Delta_{31\Omega} = \delta \pi \frac{\epsilon^{1/2}}{(\sin i)} [C \sin \omega + D \cos \omega]$$

$$\Delta_{31i} = \delta \pi \epsilon^{1/2} [C \cos \omega - D \sin \omega]$$

$$\begin{aligned}
\Delta_{31}\omega &= -\Delta_{31}\Omega(\cos i) \\
&+ \pi\delta\epsilon^{1/2} \left[\frac{525}{8} \epsilon\beta_3 - \frac{735}{8} e^2\beta_3 - (540e^2 + 615)\frac{\alpha_1}{8} \right. \\
&\quad + (105e^2 + \frac{315}{4})\beta_1 \\
&\quad + \frac{15}{8}(6e^2 + 1)\alpha_2 - \frac{105}{8} \epsilon\beta_5 \\
&\quad \left. + (\frac{45}{8} e^2 + \frac{15}{2})\alpha_6 \right]
\end{aligned}$$

$$\begin{aligned}
\Delta_{31}M_* &= \frac{3}{2} \frac{\pi}{a} (\Delta_{31}a) - \epsilon^{1/2} (\Delta_{31}\Omega(\cos i) + \Delta_{31}\omega) \\
&+ \delta\pi \left[-\frac{105}{8} \beta_1 \left(\frac{3}{4} + 8e + 21e^2 + 8e^3 + 20e^4 \right) \right. \\
&\quad - \frac{3}{4} \alpha_6 (8 + 12e + 37e^2 + 12e^3 + \frac{141}{8} e^4) \\
&\quad - \frac{1155}{32} \epsilon^2\beta_5 + \frac{165}{16} \alpha_2 (4 + 3e^2)\epsilon + \frac{15}{8} \alpha_1 (10 + 48e(1+e^2)) \\
&\quad \left. + \frac{307}{2} e^2 + 87e^4 \right] - \frac{1155}{16} \beta_3 (1 + 5e^2 - 6e^4)
\end{aligned}$$

$$\Delta_{31}T = -(\Delta_{31}M_*)/n$$

Formulae $\Delta_{41}Z$

$$\text{LP expansion} = 4\text{th order } \left(\left(\frac{r}{r_k} \right)^4 \text{ term} \right)$$

$$\text{Taylor expansion} = 1\text{st order ("constant" term)}$$

Let

$$\delta = \frac{\mu_k}{\mu} \left(\frac{a}{p_k} \right)^6, \quad \phi = \Delta_k^6,$$

For economy of notations, only the following symbols will be explicitly defined:

$$\begin{aligned}\alpha_1 &= \xi_1^2, & \alpha_2 &= \xi_1^4, & \alpha_3 &= \xi_1^6, \\ \beta_1 &= \xi_2^2, & \beta_2 &= \xi_2^4, & \beta_3 &= \xi_2^6, \\ \gamma_1 &= \xi_1 \xi_2,\end{aligned}$$

Note that these symbols are not identical to, or consistent with those used for Δ_{11} , Δ_{21} , Δ_{31} ; that ϕ appears as a factor in the products and that ξ_1 , ξ_2 , ξ_3 , also appear explicitly.

$$\begin{aligned}\Delta_{41a} &= 0 \\ \Delta_{41e} &= \pi \delta \epsilon^{1/2} \phi \left[-\frac{735}{32} \alpha_1 \xi_2 (2 + 23e^2 + 8e^4) \right. \\ &\quad + \frac{2205}{64} \alpha_2 \xi_2 (1 + 16e^2 + 16e^4) \\ &\quad + \frac{105}{64} \xi_2 (8 + 20e^2 + 5e^4) \\ &\quad + \frac{2205}{32} \alpha_1 \beta_1 \xi_2 (1 + 8e^2) \epsilon \\ &\quad - \frac{735}{32} \beta_1 \xi_2 (2 + e^2) \epsilon \\ &\quad \left. + \frac{2205}{64} \epsilon^2 \beta_2 \xi_2 \right]\end{aligned}$$

Letting

$$\begin{aligned}c &= \frac{1}{32} \left[-\frac{105}{2} (8 + 20e^2 + 5e^4) \frac{e}{\epsilon} \right. \\ &\quad + 2205 (2 + 7e^2 + 2e^4) \frac{e}{\epsilon} \alpha_1 \\ &\quad \left. - 6615 (1 + 2e^2) e \alpha_1 \beta_1 \right]\end{aligned}$$

(cont'd.)

$$- \frac{2205}{2} (5 + 20e^2 + 8e^4) \frac{e}{\epsilon} \alpha_2$$

$$- \frac{2205}{2} \epsilon \epsilon \beta_2 + 735(2 + e^2) e \beta_1]$$

$$D = \frac{1}{16} [735(2 + e^2) e \gamma_1 - 2205 \epsilon \epsilon \gamma_1 \beta_1 - 2205(1 + 2e^2) e \gamma_1 \alpha_1]$$

we have

$$\Delta_{41}\Omega = \frac{\delta \pi \epsilon^{1/2}}{(\sin i)} \xi_3 \phi [C \sin \omega + D \cos \omega]$$

$$\Delta_{41}i = \delta \pi \epsilon^{1/2} \xi_3 \phi [C \cos \omega - D \sin \omega]$$

$$\Delta_{41}\omega = \frac{\pi \delta}{32e} \epsilon^{1/2} \phi [-735(-2 + 3e^2 + 5e^4) \xi_1 \beta_1$$

$$+ \frac{2205}{2} (-1 + 5e^2) \epsilon \xi_1 \beta_2$$

$$- \frac{105}{2} (8 + 60e^2 + 25e^4) \xi_1$$

$$- 2205(1 + 3e^2 - 10e^4) \xi_1 \alpha_1 \beta_1$$

$$+ 735 (2 + 21e^2 + 10e^4) \xi_1 \alpha_1$$

$$- \frac{2205}{2} (1 + 12e^2 + 8e^4) \xi_1 \alpha_2] - (\cos i) \Delta_{41}\Omega$$

$$\Delta_{41}M_* = \frac{3}{2} \frac{\pi}{a} (\Delta_{41}a) - \epsilon^{1/2} (\Delta_{41}\Omega (\cos i) + \Delta_{41}\omega)$$

$$+ \pi \delta \phi [- \frac{9555}{32} (2 + e^2) \epsilon \epsilon \xi_1 \beta_1$$

$$+ \frac{63}{32} (64 + \frac{335}{2} e + 320e^2 - \frac{95}{2} e^3) \epsilon \xi_1 \beta_2$$

(cont'd.)

$$\begin{aligned}
& + \frac{15}{16}(12 + 122e + 120e^2 + 335e^3 + 60e^4 + \frac{407}{4} e^5)\xi_1 \\
& - 63(3 - \frac{545}{32}e + 15e^2 - 20e^3)\epsilon\xi_1\alpha_1\beta_1 \\
& - \frac{105}{32}(16 + 102e + 160e^2 + 477e^3 + 80e^4 + 166e^5)\xi_1\alpha_1 \\
& + \frac{315}{64}(43e + 96e^2 + 268e^3 + 48e^4 + 136e^5 + \frac{48}{5})\xi_1\alpha_2 \\
& + (-\frac{3}{8}e - \frac{4}{15}e^2 - \frac{e^3}{8} - \frac{4}{3})(\frac{945}{2}\xi_1\beta_2 - \frac{2835}{4}\xi_1\alpha_1\beta_1)\epsilon \\
& + (\frac{5}{8}e + \frac{16}{15})(\frac{945}{2}\xi_1\beta_2 - \frac{2835}{4}\xi_1\alpha_1\beta_1)\epsilon^2]
\end{aligned}$$

$$\Delta_{41}T = -(\Delta_{41}M_x)/n$$

Formulae for $\Delta_{51}z$

$$\text{LP expansion} = 5\text{th order } (\frac{r}{r_k})^5 \text{ term}$$

$$\text{Taylor expansion} = 1\text{st order ("constant" term)}$$

With the same notation as for Δ_{41} , let

$$\delta = \frac{\mu_k}{\mu} \left(\frac{a}{p_k}\right)^7, \quad \phi = \Delta_k^7$$

$$\alpha_1 = \xi_1^2, \quad \alpha_2 = \xi_1^4, \quad \alpha_3 = \xi_1^6$$

$$\beta_1 = \xi_2^2, \quad \beta_2 = \xi_2^4, \quad \beta_3 = \xi_2^6$$

$$\gamma_1 = \xi_1\xi_2,$$

$$\Delta_{51a} = 0$$

$$\begin{aligned} \Delta_{51e} &= \delta\pi\epsilon\epsilon^{3/2} \phi \left[-\frac{31185}{64} \epsilon \gamma_1 \beta_2 \right. \\ &\quad - 315 \left(\frac{5}{4} e^2 + \frac{15}{64} e^4 + \frac{3}{4} \right) \frac{\gamma_1}{\epsilon} \\ &\quad + 945 \left(\frac{95}{32} e^2 + \frac{3}{4} e^4 + \frac{3}{4} \right) \frac{\gamma_1 \alpha_1}{\epsilon} \\ &\quad - 2079 \left(\frac{5}{4} e^2 + \frac{3}{4} e^4 + \frac{15}{64} \right) \frac{\gamma_1 \alpha_2}{\epsilon} \\ &\quad + 2835 \left(\frac{3e^2}{32} + \frac{1}{4} \right) \gamma_1 \beta_1 \\ &\quad \left. - 10395 \left(\frac{e^2}{4} + \frac{3}{32} \right) \gamma_1 \alpha_1 \beta_1 \right] + \frac{\epsilon}{2ae} (\Delta_{51a}) \end{aligned}$$

Letting

$$\begin{aligned} C &= \left[\frac{3465}{8} (e^2 + \frac{1}{8}) \epsilon \xi_1 \beta_2 \right. \\ &\quad + \frac{105}{8} \left(\frac{39}{2} e^2 + \frac{225}{8} e^4 + 5e^6 + 1 \right) \frac{\xi_1}{\epsilon} \\ &\quad - \frac{945}{4} \left(\frac{23}{8} e^2 + e^4 + \frac{1}{4} \right) \xi_1 \beta_1 \\ &\quad - \frac{945}{32} (45e^2 + 80e^4 + 16e^6 + 2) \xi_1 \frac{\alpha_1}{\epsilon} \\ &\quad + \frac{3465}{4} (2e^2 + 2e^4 + \frac{1}{8}) \xi_1 \alpha_1 \beta_1 \\ &\quad \left. + \frac{693}{64} (120e^2 + 240e^4 + 64e^6 + 5) \xi_1 \frac{\alpha_2}{\epsilon} \right] \end{aligned}$$

$$D = \left[-\frac{945}{32} (2 + e^2) \epsilon \xi_2 \beta_1 + \frac{3465}{64} \xi_2 \beta_2 \epsilon^2 \right] \quad (Cc)$$

$$\begin{aligned}
& + \frac{105}{64} (20e^2 + 5e^4 + 8)\xi_2 \\
& + \frac{3465}{4} (e^2 + \frac{1}{8})\epsilon\xi_2\alpha_1\beta_1 \\
& - \frac{945}{4} (\frac{23}{8}e^2 + e^4 + \frac{1}{4})\xi_2\alpha_1 \\
& + \frac{3465}{8} (2e^2 + 2e^4 + \frac{1}{8})\xi_2\alpha_2]
\end{aligned}$$

we have

$$\Delta_{51}\Omega = \delta\pi \frac{\epsilon^{1/2}}{(\sin i)} \xi_3\phi [C \sin \omega + D \cos \omega]$$

$$\Delta_{51}i = \delta\pi\epsilon^{1/2} \xi_3\phi [C \cos \omega - D \sin \omega]$$

$$\begin{aligned}
\Delta_{51}\omega = & \epsilon^{1/2} \delta\pi\phi \left[\frac{10395}{32} (1 - 4e^2)\alpha_1\beta_2\epsilon \right. \\
& + \frac{2835}{64} (e^2 + 1)\beta_2\epsilon \\
& + \frac{2835}{32} (10e^2 + 8e^4 - 7)\alpha_1\beta_1 \\
& + \frac{315}{32} (75e^2 + 20e^4 + 26)\alpha_1 \\
& + \frac{10395}{64} (-16e^4 + 5)\alpha_2\beta_1 \\
& - \frac{945}{64} (160e^2 + 48e^4 + 45)\alpha_2 \\
& + \frac{693}{8} (20e^2 + 8e^4 + 5)\alpha_3 \\
& - \frac{315}{64} (10e^2 + 5e^4 - 4)\beta_1 \\
& + \frac{15}{8} \left(-\frac{35}{2}e^2 - \frac{35}{8}e^4 - 7 \right) \\
& \left. - \frac{3465}{64} \epsilon^2\beta_3 \right] \\
& - (\cos i) \Delta_{51}\Omega
\end{aligned}$$

$$\begin{aligned}
\Delta_{51}M_* &= \frac{3}{2} \frac{\pi}{a} (\Delta_{51}a) - \epsilon^{1/2} (\Delta_{51}\Omega(\cos i) + \Delta_{51}\omega) \\
&+ \delta\pi\phi \left[-\frac{1575}{128} (20e^2 + 5e^4 + 8)\epsilon\beta_1 \right. \\
&+ \frac{14175}{64} (23e^2 + 8e^4 + 2)\epsilon\alpha_1\beta_1 \\
&- \frac{51975}{128} (16e^2 + 16e^4 + 1)\epsilon\alpha_2\beta_1 \\
&+ \frac{14175}{128} (2 + e^2)\epsilon^2\beta_2 - \frac{17325}{128} \epsilon^3\beta_3 \\
&+ \left(\frac{45}{4} e + \frac{1125}{16} e^2 + \frac{75}{2} e^3 + \frac{6075}{64} e^4 + \frac{45}{4} e^5 \right. \\
&\quad \left. + \frac{2385}{128} e^6 + \frac{15}{2} \right) \\
&- \frac{315}{32} (24e + 135e^2 + 80e^3 + \frac{885}{4} e^4 \\
&\quad + 24e^5 + 46e^6 + 6)\alpha_1 \\
&+ \frac{945}{4} \left(3e + \frac{435}{32} e^2 + 10e^3 + 30e^4 + 3e^5 + 7e^6 + \frac{7}{16} \right) \alpha_2 \\
&- \frac{693}{16} \left(12e + 45e^2 + 40e^3 + 120e^4 + 12e^5 + 38e^6 + \frac{9}{8} \right) \alpha_3 \\
&- \frac{51975}{128} (8e^2 + 1)\epsilon^2\alpha_1\beta_2]
\end{aligned}$$

$$\Delta_{51}T = - (\Delta_{51}M_*)/n$$

Formulae Δz due to Oblateness

The only term in the oblateness potential considered in the following formulae is J_2 .

$$\text{Let } K = J_2 \left(\frac{R}{p} \right)^2$$

where R = equatorial radius of earth

p = parameter of satellite orbit

= ae

$$\begin{aligned}\Delta\Omega &= -3K\pi(\cos i) \\ \Delta\omega &= 6K\pi\left(1 - \frac{5}{4}\sin^2 i\right) \\ \Delta M_* &= 3K\frac{\pi}{E}(1+e)^3(1-3\sin^2 i \sin^2 \omega) \\ \Delta T &= -(\Delta M_*)/n\end{aligned}$$

4.10.2 Auxiliary formulae relating to the perturbing body

It was explained earlier that all terms which depend on the position of perturbing body "d" are calculated at a time, t_{ref} , corresponding to the occurrence of apogee along the unperturbed orbit.

Keplerian orbits are adopted as models for the sun and the moon. At any time, the orbital elements are calculated using the mean elements at epoch 1900 Jan 0.5 and their secular variation^[4-40]. The mean anomaly of the perturbing body is similarly calculated. θ_k° , which is here the true anomaly of the perturbing body in its orbit, is computed using the formulae of elliptic expansions^[4-41]. $\dot{\theta}_k^\circ$, angular velocity, and $\ddot{\theta}_k^\circ$, angular acceleration, respectively, are calculated by taking the time derivatives of θ_k in terms of the mean anomaly, the mean motion of the perturbing body being known. The coordinates of the perturbing body in its orbit are also calculated using relevant formulae^[4-41] for $\frac{r_k}{a_k} \cos \theta_k$ and $\frac{r_k}{a_k} \sin \theta_k$.

Let $[T_r]$ be the transformation matrix from the $(\vec{P}_k, \vec{Q}_k, \vec{I}_{n_k})$ system to the $(\vec{P}, \vec{Q}, \vec{I}_n)$ system of the satellite. $[T_r]$ is independent of θ_k . If ξ_1, ξ_2, ξ_3 are the derived director cosines of the unit to the perturbing body in the $(\vec{P}, \vec{Q}, \vec{I}_n)$ system, then

$$\begin{pmatrix} \xi_1 \\ \xi_2 \\ \xi_3 \end{pmatrix} = [T_r] \begin{pmatrix} \cos \theta_k \\ \sin \theta_k \\ 0 \end{pmatrix}$$

and if, as in 4.10.1, $\xi_{ip} = \frac{d\xi_i}{d\theta_k}$ ($i = 1, 2, 3$),

$$\begin{pmatrix} \xi_1 \\ \xi_2 \\ \xi_3 \end{pmatrix} = [T_r] \begin{pmatrix} -\sin \theta_k \\ \cos \theta_k \\ 0 \end{pmatrix}$$

Similarly, with $\xi_{ipp} = \frac{d}{d\theta_k} [\xi_{ip}]$, ($i=1, 2, 3$),

$$\xi_{1pp} = -\xi_1$$

$$\xi_{2pp} = -\xi_2$$

$$\xi_{3pp} = -\xi_3$$

In other words, second and higher order derivatives of ξ_1, ξ_2, ξ_3 , with respect to θ_k can be written in terms of ξ_1, ξ_2, ξ_3 or $\xi_{1p}, \xi_{2p}, \xi_{3p}$.

4.10.3 Some comments

It is readily apparent that at higher orders of the LP expansion, the formulae became increasingly longer and more complex. The formulae might be condensed a little by recognizing common subexpressions in a hand translation of the formulae. The chances of error, however, might in final analysis far outweigh the improvement in computer time.

With regard to the perturbations in oblateness, note that they depend on factor K :

$$\Delta\omega, \Delta\Omega \sim K=J_2 \frac{R^2}{p} \sim \frac{1}{\epsilon^2}$$

and

$$\Delta M_* \sim \frac{K}{\epsilon} \sim \frac{1}{\epsilon^3}$$

In orbits of large eccentricity, ϵ is of the order of 0.1, and changes quite significantly overtime. Thus oblateness perturbations are quite sensitive to inaccuracies; the next section will illustrate this problem of small divisor.

Finally, as long as any one plane, say the equator, has been used as the same reference throughout, the perturbations on the angles, as well as those on a and e , which are due to the sun, the moon or the oblateness, respectively, can be summed up directly.

4.11 Numerical Verification of the Theory

The "closed form" theory describing the changes in the orbital elements, z , to orders "11", "12", "13", "21", "22", which has been obtained by non-numeric computation, is expressed by the formulae of Section 4.10 and is implemented in program VØLER, was checked by comparing its predictions to those of high accuracy numerical integration programs (NASA's ITEM and C-MU EOLA-T). The present section discusses those verifications and analyses the significant gains realized in computer time and the level of accuracy achieved.

4.11.1 Program VØLER

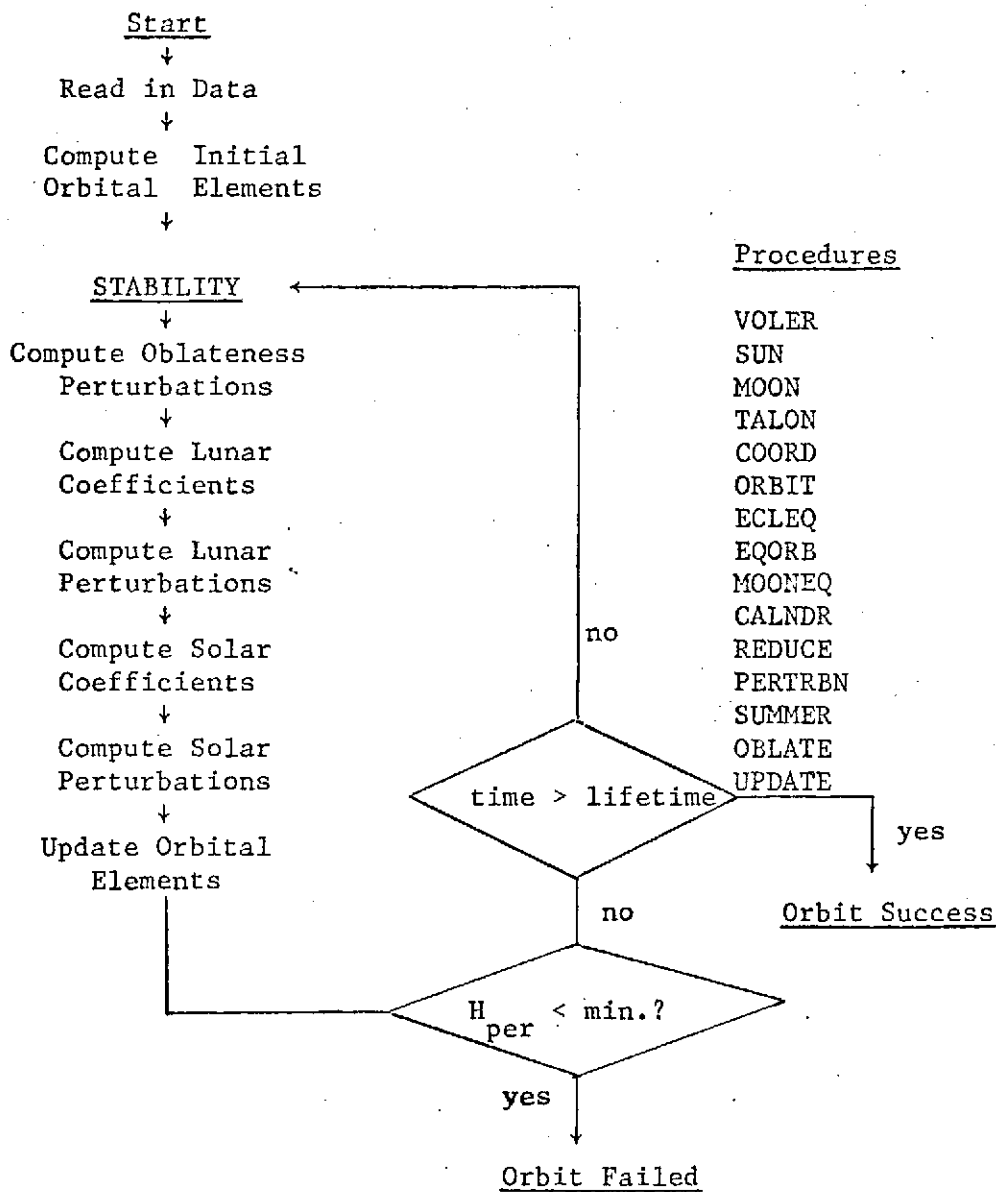
A program called VØLER (for eVolution of Orbital eLements in high Eccentricity oRbits) has been written in PL/1, which uses the theory of Section 4.10 to predict the evolution of orbits of satellites perturbed by the gravitational effects of the sun, the moon and the earth's oblateness. A flow chart follows, which lists the names of all procedures in the program. A brief description of these is given hereunder.

VØLER.

Procedure VØLER is the main calling procedure. It initializes structures and arrays, reads in data and calls all the major procedures. Input and output are controlled by this procedure.

SUN.

Procedure SUN computes the position of the sun at any given time. The model used is based on the mean elements of the sun at epoch 1900 Jan. 0.5 and their secular variation. The procedure calculates the position of the sun in the equatorial system of the earth; and then computes the array ξ of the projections of the unit vector to the sun on the orbital axes of the satellite. The array ξ_p , being the deriva-



Flow Chart of Program VOLER

tives of the array ξ with respect to the true anomaly of the sun in its orbit, is also computed.

MOON.

Procedure MOON performs the same functions as procedure SUN but for the moon. The arrays ξ and ξ_p , for the moon, are also computed. The model for the moon is again based on epoch data at 1900 Jan. 0.5 and the mean secular variation of the elements.

TALON.

Procedure TALON computes the longitude of nodes of the satellite orbit, given the geocentric, equatorial latitude and longitude of the perigee, the direction of launch (north or south), the time, and the sidereal time at Greenwich at 0.0 Hrs. U.T. on Jan. 1 of the year of launch. The direction of launch, along with the latitude indicates whether the satellite is approaching or leaving the ascending node, i.e., the intersection of the positive nodal line with the orbital plane. It is always assumed that the satellite is injected into orbit at perigee (or that reduction to perigee has been effected elsewhere).

COORD.

Procedure COORD is called by procedures SUN and MOON. It computes the coordinates of the perturbing body in its orbit, given its mean anomaly and eccentricity, using formulae of elliptic expansions.

ORBIT.

Procedure ORBIT computes the components of the \vec{P} , \vec{Q} and \vec{i}_n axes

of the orbit of the satellite in the geocentric equatorial system.

ECLEQ, EQORB, MOONEQ.

Procedures ECLEQ, EQORB and MOONEQ transform co-ordinates from one reference system to another. ECLEQ transforms from ecliptic to equatorial; EQORB from equatorial to satellite orbital axes; MOONEQ from the moon's plane to the equatorial system.

CALNDR.

Procedure CALNDR converts the time, day and month of launch to an equivalent number of days since the beginning of the year of launch. This procedure is also called when a satellite orbit decays; it then calculates the day, month and year of the collapse of the satellite given its lifetime.

REDUCE.

Procedure REDUCE normalizes angles to a value between 0° and 360° .

PERTRBN.

Procedure PERTRBN is the major procedure which contains all the theoretical results, obtained as formulae and presented in Chapter 4. It calculates the perturbations of the osculating elements of the orbit over one orbital period.

SUMMER.

Procedure SUMMER is called by PERTRBN and merely sums up all the perturbations of various orders.

OBLATE.

Procedure OBLATE computes the secular oblateness perturbations due to the J_{20} term on the satellite orbit, using the formulae in Chapter 4.

UPDATE.

Procedure UPDATE updates the orbital elements by adding the total perturbations to their initial values.

The time requirements are: about 0.6 sec of CPU time (IBM 360/67, TSS, version 8.1) to compute over one orbital period. Thus the computing time is inversely proportional to the orbital period. As an example

<u>Orbital Period</u>	<u>CPU time/year of orbit</u>
2.5 days	90 sec
4.0 days	55 sec
5.0 days	43 sec
6.0 days	37 sec

The above range corresponds to $0.92 < e < 0.95$, with a low initial perigee ($h_p \approx 200$ km.).

This should be compared to the time taken for the digital integration of the equations of motion over one orbital period by ITEM, EOLA-T... Typically, for the higher eccentricities, the CPU time might be of the order of 10 to 20 minutes per year of orbital evolution. Therefore, in a rough sense (since comparisons ought to be made

on the same computer, using the same input/output procedures etc.), the savings factor of VOLER is in the range of 10 to 60, the high factor applying to larger eccentricity cases. This, obviously, is obtained at a cost in accuracy, but this cost is often perfectly tolerable for many purposes in mission analysis.

In the following, a few significant examples are described. For a more exhaustive treatment, the reader should refer to [4-2].

4.11.2 Type of orbits studied in the examples

Two major parameters characterize the examples studied

- 1) Eccentricity: we consider "large" eccentricities defined here by

$$0.9 \lesssim e \lesssim 0.955$$

Note that, in the "11" Lidov's theory, it is shown that

$$\Delta_{11} \sim \left(\frac{a}{P_k}\right)^3 e \epsilon^{1/2}$$

and if we compute the ratios

$$(\Delta e)_{e=0.945} / (\Delta e)_{0.92} = 2.9$$

Therefore, it is seen that the perturbation increases by a factor of about 3, even over the "small" range considered.

- 2) Inclination: both planetary-type orbits, i.e. having small inclination on the orbits of the perturbing body, and orbits quasi-normal to the ecliptic (such as for IMP-G) will be considered, with data considered by NASA for specific satellites, and in one case post-flight data of an actual satellite.

- 2) EOLA-T. It is a numerical integration program, developed at C-MU under this grant, using a method of variation of parameters (conventional osculating elements), with time as the independent variable. Its detailed features are given in Chapter 6. Again, for the purposes of the comparison, EOLA-T was run only with the sun, the moon and oblateness (the latter only where indicated).

4.11.4 Some examples treated

A. High inclination orbit (IMP-G type orbit)

These are described best by the tables below comparing the results of VOLER with those of a high accuracy numerical integration, which can be characterized as follows

1A: "medium high" eccentricity ~ 0.93 with OBLATENESS

1B: "medium high" eccentricity ~ 0.93 without OBLATENESS

The agreement appears very good, with errors of the order of 2 days/year (0.55%) on the timing of perigee, 0.04%/year on the eccentricity.

TABLEInitial Orbital Data: IMP-G - Example 1

	<u>1A</u>	<u>1B</u>
H-Per*:	405.62	402.78
a :	95,804.57	94,940.95
e :	0.929191	0.928577
i :	86.8665	86.8659
Ω :	105.8008	105.8045
ω :	-160.0022	-159.9953
t_{inj} : Year	1969	1969
Month,Day	June 24	June 24
Hour (UT)	17.96431	17.96448

* In all tables in this chapter, the following abbreviations are used:

- N : Orbit number
- t : Time since injection (days)
- R-Per: Distance to perigee (Km)
- H-Per: Height of perigee (Km)
- a : Semi-major axis (Km)
- e : Eccentricity
- i : Inclination (deg)
- Ω : Longitude of nodes (deg)
- ω : Argument of perigee (deg)
- t_{inj} : Time at injection into orbit at perigee

TABLEComparison of Numerical Results (IMP-G - Example 1A)

	Theory	N.I.*	Theory	N.I.
N	53	53	107	107
t	179.28	178.69	362.70	360.77
R-Per	8,128	8,123	9,447	9,430
H-Per	1,750	1,745	3,069	3,052
a	95,746	95,412	95,690	95,132
e	0.91511	0.91486	0.90128	0.90087
i	86.55	86.41	86.51	86.46
Ω	105.23	105.11	104.87	104.83
ω	200.04	200.04	201.57	201.47

No lifetime figures available

*N.I.: Numerical Integration (Program ITEM)

TABLEComparison of Numerical Results (IMP-G - Example 1B)

	<u>Theory</u>	<u>N.I.*</u>	<u>Theory</u>	<u>N.I.</u>
N	53	53	107	107
t	178.66	178.69	360.66	360.78
R-Per	7,745	7,763	7,970	7,968
H-Per	1,367	1,385	1,592	1,590
a	94,908	94,927	94,831	94,844
e	0.91840	0.91822	0.91596	0.91599
i	86.47	86.46	86.90	86.78
Ω	105.79	105.78	106.14	106.06
ω	202.98	203.05	206.42	206.59

*N.I.: Numerical Integration (Program ITEM)

B. Low Inclination orbits

The orbital inclination on the orbital planes of the perturbing bodies is relatively low. Considering, as one example among many listed in Ref. [4-2], a "very high" eccentricity orbit such as that of IMP-I ($e_0 = 0.943$).

The comparison between the results of this theory, through VOLER, and of a numerical integration are given graphically (Fig. 4-4 to 4-7) and also in the table hereunder. It is seen that an accumulating error is present, which however does not grow to be very large at the end of one year: about 1% in the timing of perigee and in the distance of perigee due to the inaccuracy in a and $1-e^2$. Yet, the errors are not unduly large, and the overall trend is sufficiently well captured at a savings in computer time of the order of about 50.

TABLEInitial Orbital Data: IMP-I - Example

H-Per	236.28
a	115,067.60
e	0.9425169
i.	28.7763
Ω	216.0352
ω	302.3777
t_{inj}	
Year.....	1971
Month,Day.....	March 13
Hour (UT).....	16.00

TABLEComparison of Numerical Results (IMP-I - Example)

	<u>Theory</u>	<u>N.I.*</u>	<u>Theory</u>	<u>N.I.</u>
N	40	40	80	80
t	179.24	177.83	359.13	355.7
R-Per	14,535	14,256	22,858	23,116
H-Per	8,157	7,878	16,480	16,738
a	115,103	114,186	115,047	114,240
e	0.87372	0.87515	0.80131	0.79765
i	37.54	38.81	44.34	43.36
Ω	193.18	193.13	184.78	186.48
ω	324.4	324.38	334.53	332.70

* N.I.: Numerical Integration (Program ITEM)

4.12 Conclusions

The present chapter demonstrates the power of non-numeric computation to generate a closed-form theory (from perigee to perigee) for high eccentricity orbits. An extended, modified Lidov's theory has been developed and implemented in a numerical program VOLER, which simply evaluates the values taken by the symbolic expressions obtained after one satellite revolution. This method seems to be ideally suited for calculations in a mission analysis, where requirements for extremely high accuracy might be treated for the low computer time and ease of use of the present approach.

- [4-1] Lidov, M.L.: "The Evolution of Artificial Satellites of Planets under the Action of Gravitational Perturbations of External Bodies", Planet. Space Science, 9, pp. 719-759, 1962.
- [4-2] Sridharan, P., "Evolution of the Orbital Elements in Geocentric Orbits of High Eccentricity by Non-Numeric Computation," Ph.D. Thesis, Applied Space Sciences Program, Carnegie-Mellon University, December 1972.
- [4-3] Kozai, Y.: "On the Effects of the Sun and the Moon upon the Motion of a Close-Earth Satellite", Smithsonian Astrophysical Observatory Research in Space Science, Special Report No. 22, March 1959.
- [4-4] Musen, P.: "On the Long-Period Lunisolar Effect in the Motion of the Artificial Satellite", Jl. of Geophys. Res., 66(6), June 1961, pp. 1659-1665.
- [4-5] Musen, P.: "A Discussion of Halphen's Method for the Secular Perturbations and its Application to the Determination of Long-Range Effects in the Motions of Celestial Bodies , Part 1", NASA Tech. Rept. R-176, 1963.
- [4-6] Musen, P.: "On the Long-Period Lunar and Solar Effects on the Motion of an Artificial Satellite, 2", Jl. of Geophys. Res., 66(9), pp. 2797-2805, Sept. 1961.
- [4-7] Smith, A.S.: "A Discussion of Halphen's Method for the Secular Perturbations and its Application to the Determination of Long Range Effects in the Motions of Celestial Bodies , Part 2", NASA Tech. Rept. R-194, June 1964.
- [4-8] Fisher, D. and Murphy, J.P.: "Short-Period Lunar and Solar Perturbations for Artificial Satellites", NASA TM X-55683 (also X-547-66-493), October 1966.
- [4-9] Fisher, D.: "The Lunar and Solar Perturbations in the Motion of an Artificial Satellite due to the Fourth Degree Legendre Polynomial", NASA TM X-55864 (also X-547-67-201), April 1967.
- [4-10] Cook, G.E., and Scott, D.W.: "Lifetimes of Satellites in Large-Eccentricity Orbits", Planet. Space Sci., 15, pp. 1549-1556, 1967.

- [4-11] Davis, M.S.: "Programming Systems for Analytical Developments on Computers", *Astron. Jl.*, 73(3), pp. 195-202, April 1968.
- [4-12] Jeffreys, W.H.: "Automated Algebraic Manipulation in Celestial Mechanics", in *Proc. of the Second Symposium on Symbolic and Algebraic Manipulation*, Ed.: S.R. Petrick, ACM Special Interest Group on Symbolic and Algebraic Manipulation (SIGSAM), 1971, pp. 328-331.
- [4-13] Herget, P. and Musen, P.: "The Calculation of Literal Expansions", *Astron. Jl.*, 64, pp. 11-20, 1959.
- [4-14] Barton, D.: "Lunar Disturbing Function", *Astron. Jl.*, 71(6), pp. 438-442, 1966.
- [4-15] Eckert, W.J. and Eckert, D.A.: "The Literal Solution of the Main Problem of the Lunar Theory", *Astron. Jl.*, 72(10), pp. 1299-1308, 1967.
- [4-16] Barton, D.: "On Literal Developments of the Lunar Theory with the aid of a Computer", *Astron. Jl.*, 72(10), pp. 1281-1287, 1967.
- [4-17] Kovalevsky, J.: "Review of Some Methods of Programming of Literal Developments in Celestial Mechanics", *Astron. Jl.*, 73(3), pp. 203-209, 1968.
- [4-18] Chapront, J. and Mangeney-Ghertzman, L.: "Applications of Literal Series to the Main Problem of Lunar Theory" *Astron. Jl.* 73(3) pp. 214-216, 1968.
- [4-19] Jeffreys, W.H.: "A Fortran-Based List Processor for Poisson Series", *Cel. Mech.*, 2(4), 474-480, 1970.
- [4-20] Deprit, A. and Rom, A.: "The Main Problem of Artificial Satellite Theory for Small and Medium Eccentricities", *Celestial Mech.*, 2(2), 166-206, 1970.
- [4-21] Broucke, R.: "How to Assemble a Keplerian Processor", *Cel. Mech.*, 2(1), pp. 9-20, 1970.
- [4-22] Rom, A.: "Mechanized Algebraic Operations (MAO)", *Cel. Mech.*, 1(3/4), 301-319, 1969.
- [4-23] Broucke, R. and Garthwaite, K.: "A Programming System for Analytical Series Expansions on a Computer", *Cel. Mech.*, 1(2), pp. 271-289, 1969.

- [4-24] Deprit, A., Henrard, J. and Rom, A.: "Analytical Lunar Ephemeris: Brouwer's Suggestion", *Astron. Jl.*, 75(6), pp. 747-750; 1970.
- [4-25] Deprit, A., Henrard, J. and Rom, A.: "Lunar Ephemeris: Delaunay's Theory Revisited", *Science*, 168(3939), pp. 1569-1570, June 1970.
- [4-26] Deprit, A and Rom, A.: "Lindstedt's Series on a Computer", *Astron. Jl.*, 73(3), pp. 210-213, 1968.
- [4-27] Carpenter, L.: "Computation of General Planetary Perturbations, Part I", NASA Tech. Note D-1898, 1963.
- [4-28] Seidelmann, P.K.: "An Iterative Method of General Perturbations Programmed for a Computer", *Cel. Mech.*, 2(2), pp. 134-146, 1970.
- [4-29] Moe, M.M.: "Solar-Lunar Perturbations of the Orbit of an Earth Satellite", *ARS Jl.*, 30(5), pp. 485-487, May 1960.
- [4-30] Stricker, J., and Miessner, W.: "Launch Window Program", *Simulation Jl.*, 7(3), pp. 134-141, 1966.
- [4-31] Musen, P.: "A Modified Hansen's Theory as applied to the Motion of Artificial Satellites", NASA Tech. Rept. D-492, 1960.
- [4-32] Musen, P., Bailie, A., and Upton, E: "Development of the Lunar and Solar Perturbations in the Motion of an Artificial Satellite", NASA Tech. Rept. D-494, Jan. 1961.
- [4-33] Roth, E.A.: "Luni-Solar Perturbations of a Highly Eccentric Orbit Satellite", ESRO Scientific Rept. SR-9 (ESOC), ESRO, April 1968.
- [4-34] Roth, E.A.: "Launch Window Study for the Highly Eccentric Orbit Satellite HEOS-1", *Celestial Mechanics*, 2, pp. 369-381, 1970.
- [4-35] Kovalevsky, J.: "Introduction to Celestial Mechanics", Springer-Verlag New York, Inc., 1967, p. 42.
- [4-36] Kovalevsky, J., "Sur la Théorie du Mouvement d'un satellite à Fortes Inclinaison et Excentricité", Reprint, International Astronomical Union, Symposium No. 25, 1966.
- [4-37] Renard, M.L.: "Practical Stability of High Eccentricity Orbits Quasi-Normal to the Ecliptic", *JSR*, 7(10), pp. 1208-1214, 1970.

- [4-38] Renard, M.L., and Sridharan, R.: "Launch Window of a Highly Eccentric Satellite in an Orbit Normal to the Ecliptic: IMP-G", Presented at the 9th Semi-Annual Astrodynamics Conference, Goddard Space Flight Center, April 1969.
- [4-39] Tobey, R., Baker, J., Crews, R., Marks, P., Victor, K.: "PL/I-FORMAC Interpreter, User's Reference Manual", IBM Type 3 Program, Oct. 1967.
- [4-40] Nautical Almanac Offices of the U.K. and U.S.A.: "Explanatory Supplement to the Astronomical Ephemeris and the American Ephemeris and Nautical Almanac", pp. 98-111.
- [4-41] Moulton, F.R.: "An Introduction to Celestial Mechanics", Dover Publications Inc., Second Revised Edition (1970), pp. 171-172.

TABLE 4.1

Comparison of Roth's Sixth "Element", Our Sixth
Element and Numerical Integration

Initial Orbital Period of Satellite = 5.04680 days

Orbit No.	Time at Perigee (in days) by		
	Roth's Sixth "Element"	Our Sixth "Element"	EOLAT
1	5.0468	4.9621	4.9629
5	25.2339	24.8073	24.8148
10	50.4677	49.6068	49.6294
15	75.7015	74.3987	74.4442
20	100.9354	99.1831	99.2599
30	151.4029	148.7276	148.8918
40	201.8705	198.2434	198.5261
50	252.3382	247.7310	248.1615

CM

TABLE 4-2

Orders of Magnitude of Terms: LP and Taylor Expansion

"Extremely high" eccentricity

$e = 0.95$, $a/p_k = 0.342$ for the moon, $(\pi n/n_k) = 0.588$
for the moon

Δ_{qj}	j =		
	1	2	3
q = 1	1.0*	0.6	0.17
2	0.9	0.54	0.15
3	0.74	0.44	0.12
4	0.58	0.35	
5	0.44		
6	0.32		

TABLE 4-3Orders of Magnitudes of Terms: For the Sun

$$e = 0.95, a/p_k = 0.88 \times 10^{-3} \text{ for the sun, } (\pi n)/n_k = 0.05$$

Δ_{qj}		
j = 1 2		
i = 1	1.0	0.05
2	2.3×10^{-3}	

TABLE 4-4Ratio of Perturbations Due to the Sun and the Moon

$$\mu_{\text{sun}}/\mu_{\text{moon}} = \frac{\mu_s}{\mu} \frac{\mu}{\mu_m} = 3 \times 10^5 \times 81$$

$$= 2.43 \times 10^7$$

$$r_{\text{moon}}/r_{\text{sun}} = 3.844 \times 10^5 / (1.5 \times 10^8)$$

$$= 2.56 \times 10^{-3}$$

Let R_q = ratio of the effects of sun and moon for the
q-th LP force component

$$\text{Then, } R_1 = 2.43 \times 10^7 \times (2.56)^3 \times 10^{-9}$$

$$\approx \underline{0.39}$$

$$R_2 = 2.43 \times 10^7 \times (2.56)^4 \times 10^{-12}$$

$$\approx 0.001 \text{ etc.}$$

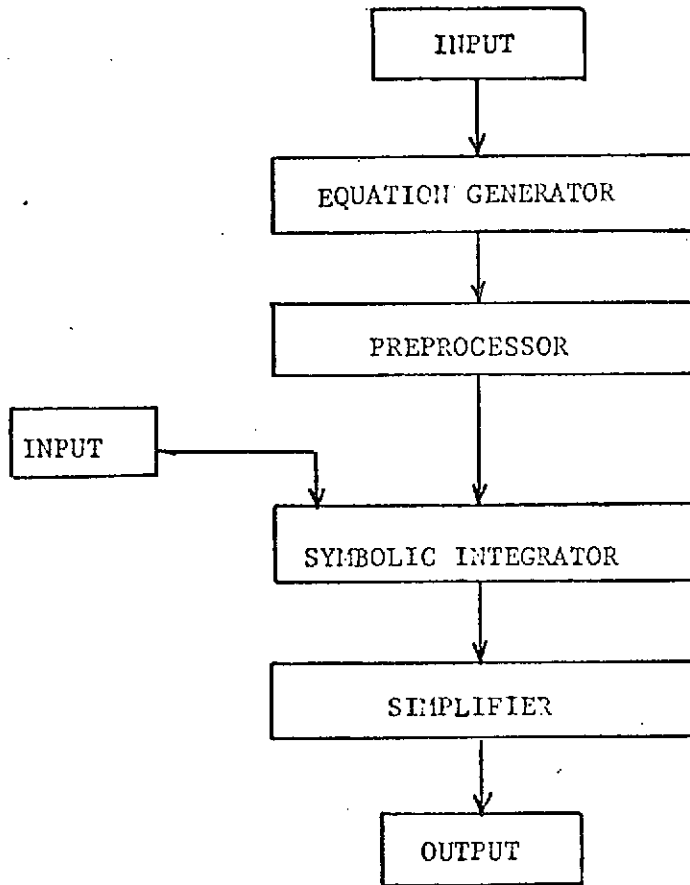


FIG. 4-1 OVERVIEW OF THE THEORY GENERATOR

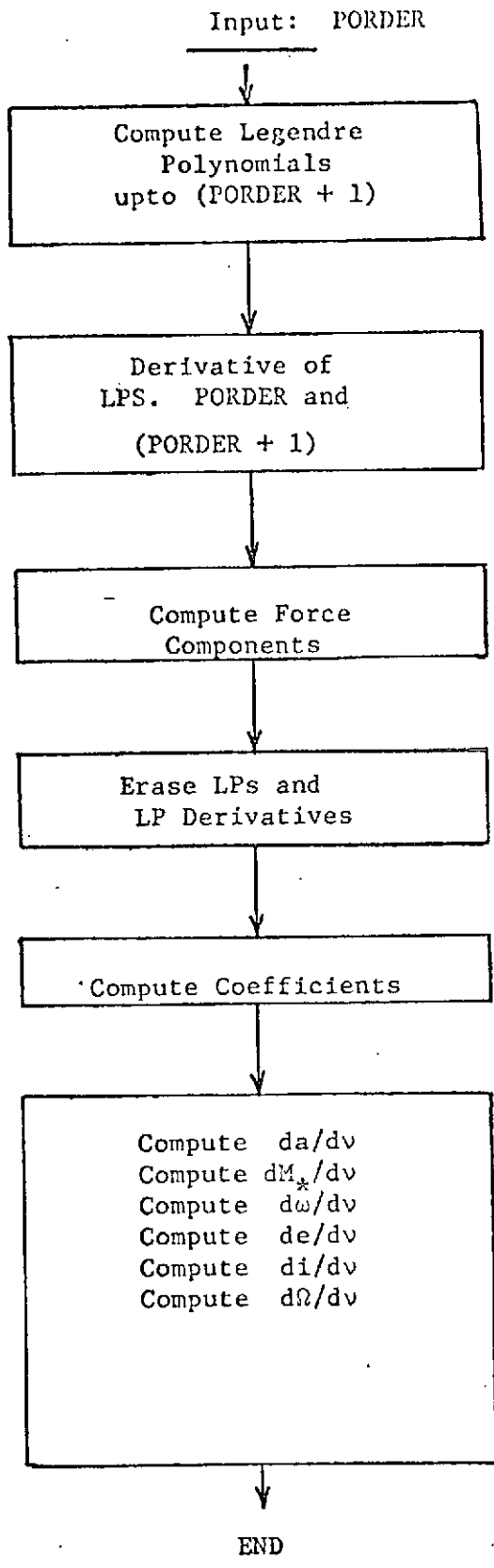


FIG. 4-2. FLOW CHART OF PROGRAM FREQN

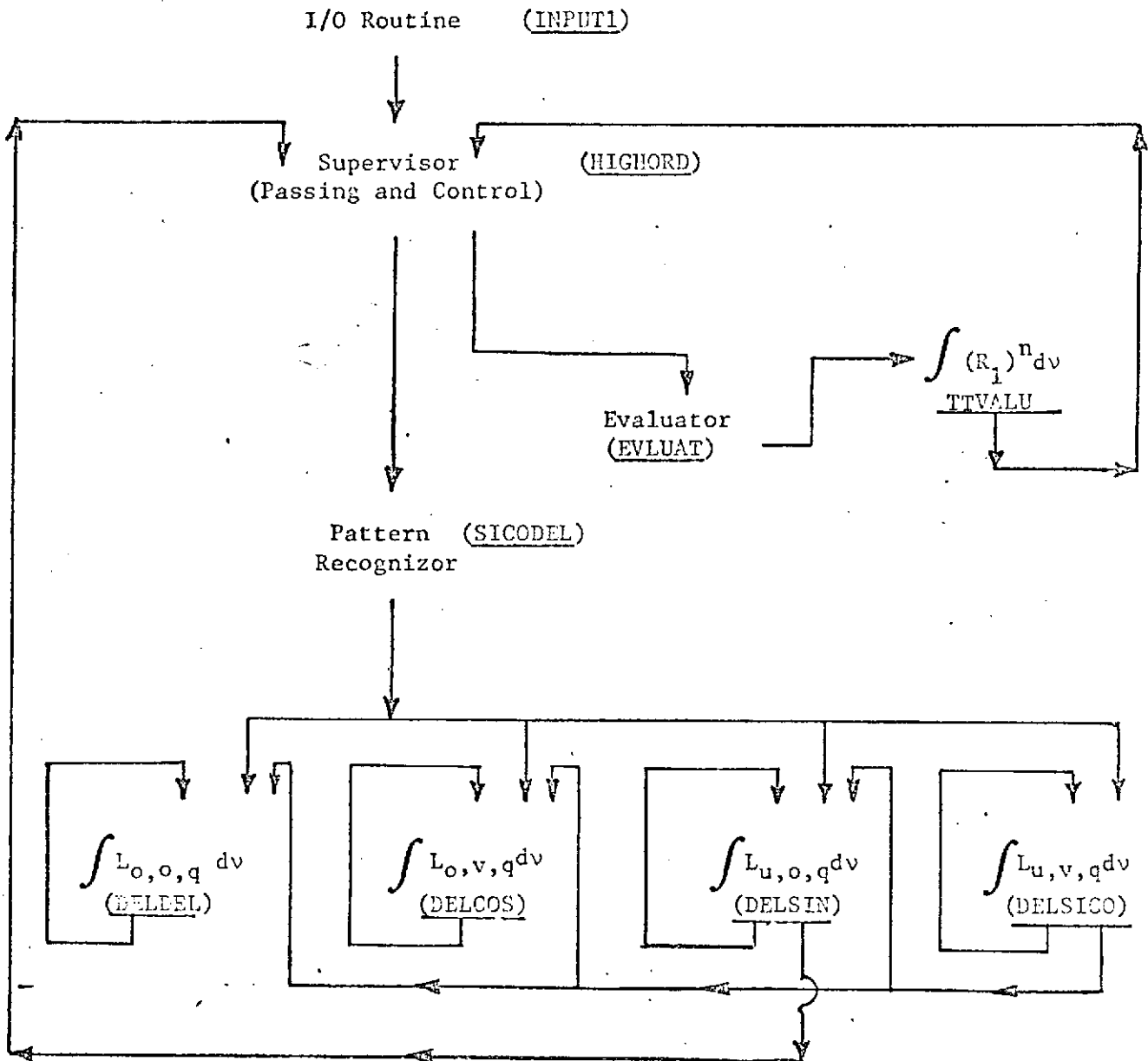


FIG. 4-3. FLOW CHART OF SYMBOLIC INTEGRATOR
 (ARROWS INDICATE DIRECTION OF
 PERMISSIBLE CALLS BETWEEN PROCEDURES.)

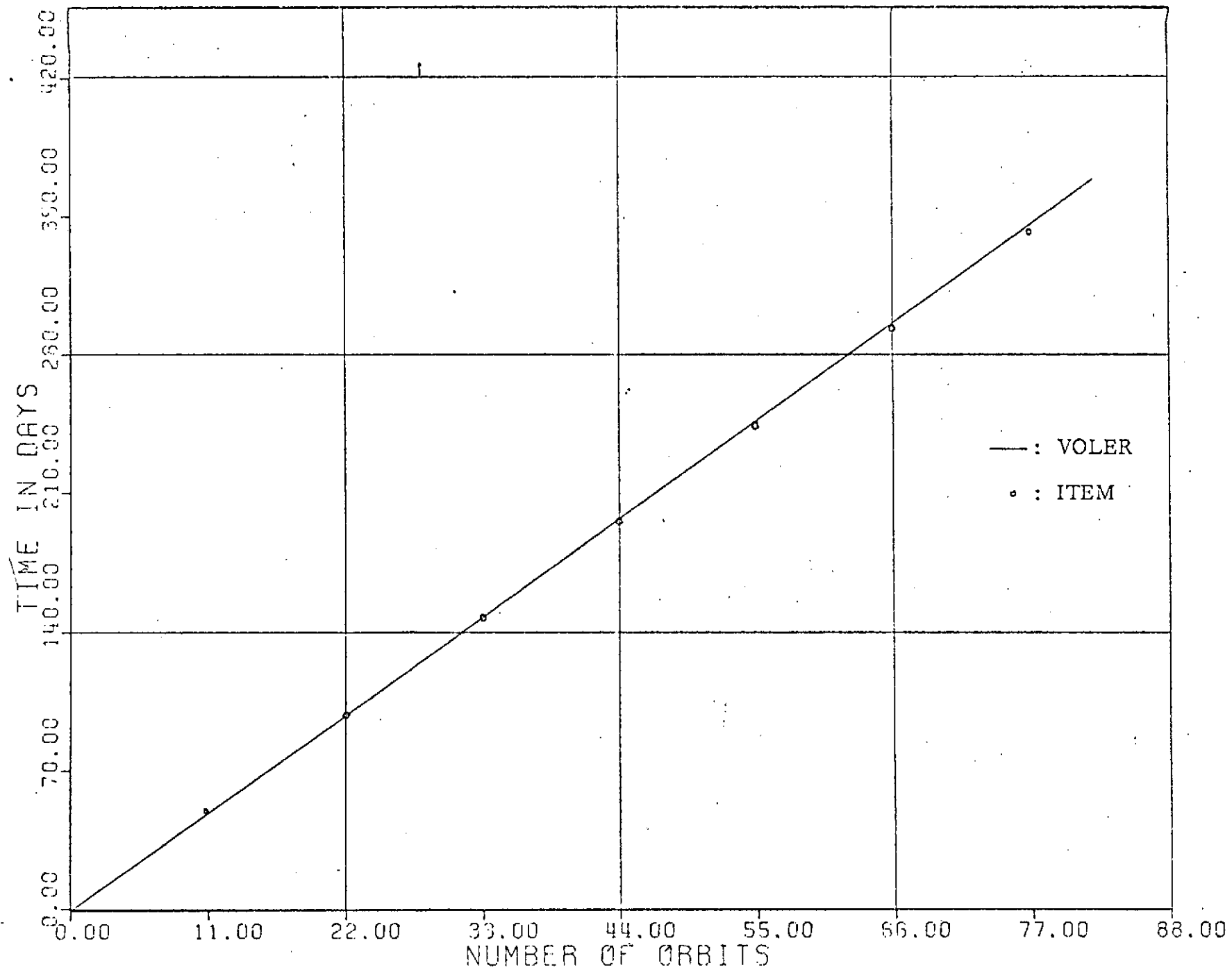


Figure 4-4. Evolution of Elements: IMP-I Example
Time at perigee vs. number of orbits

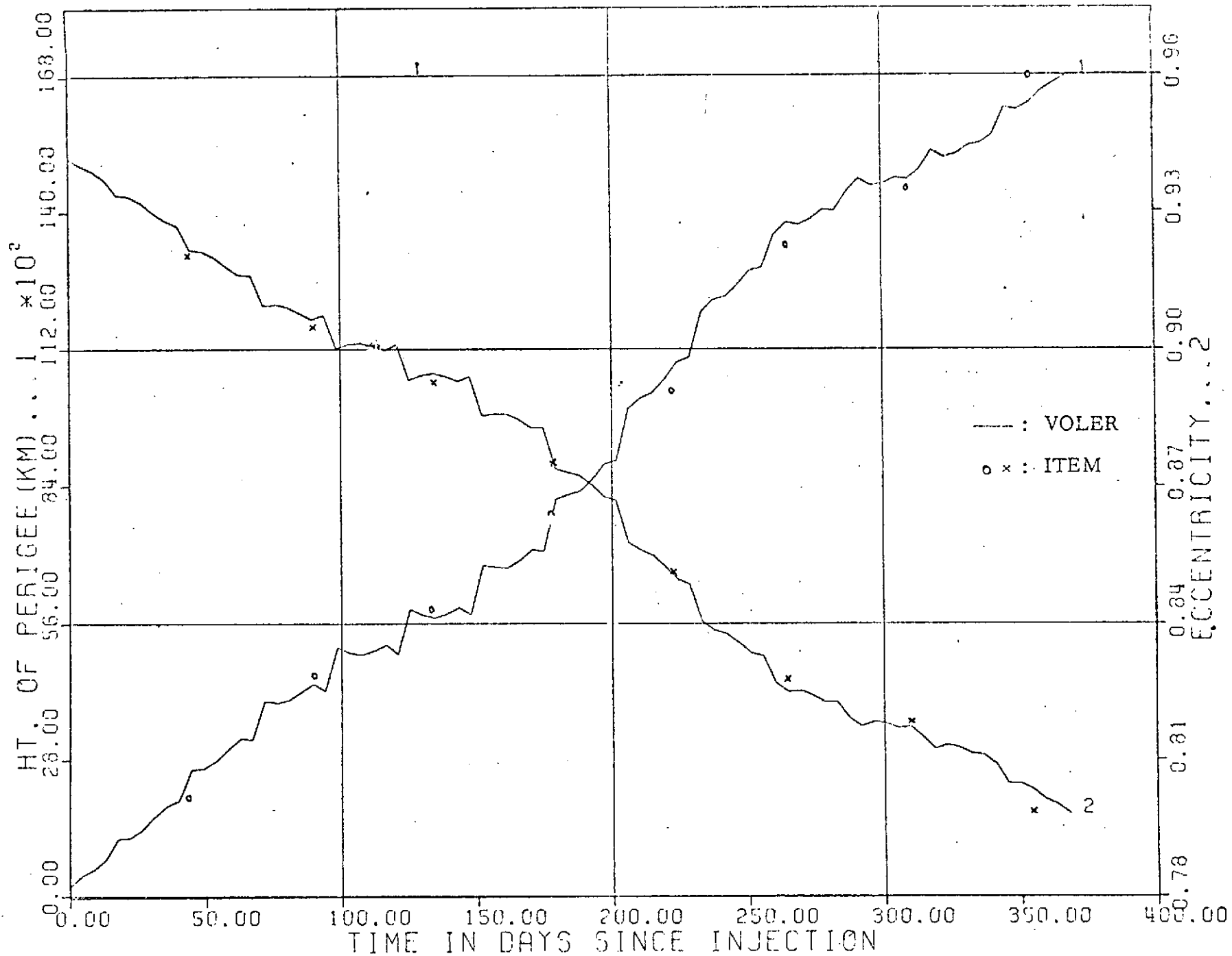


Figure 4.5. Evolution of Elements; IMP-I Example

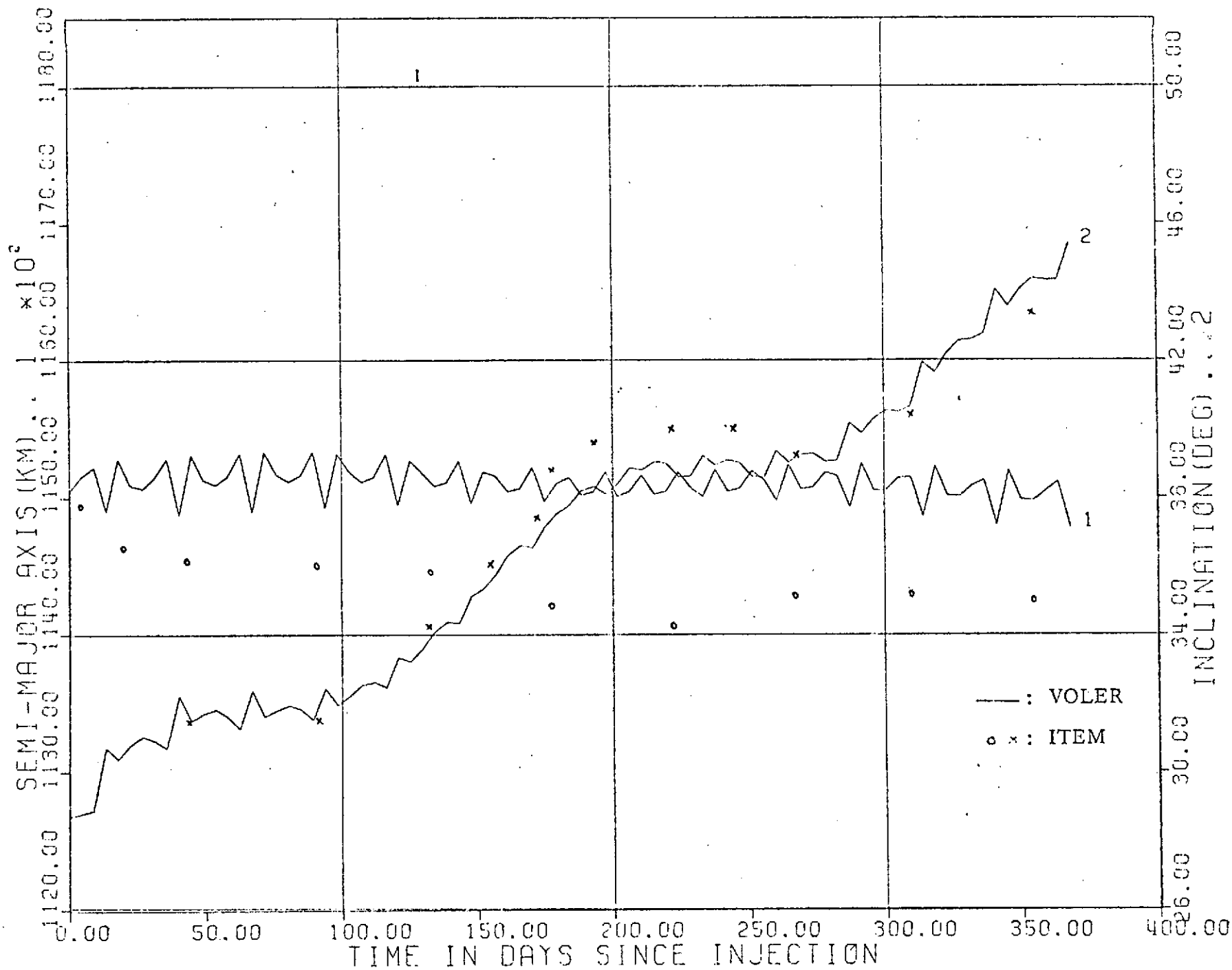


Figure 4.6. Evolution of Elements: IMP-I Example \

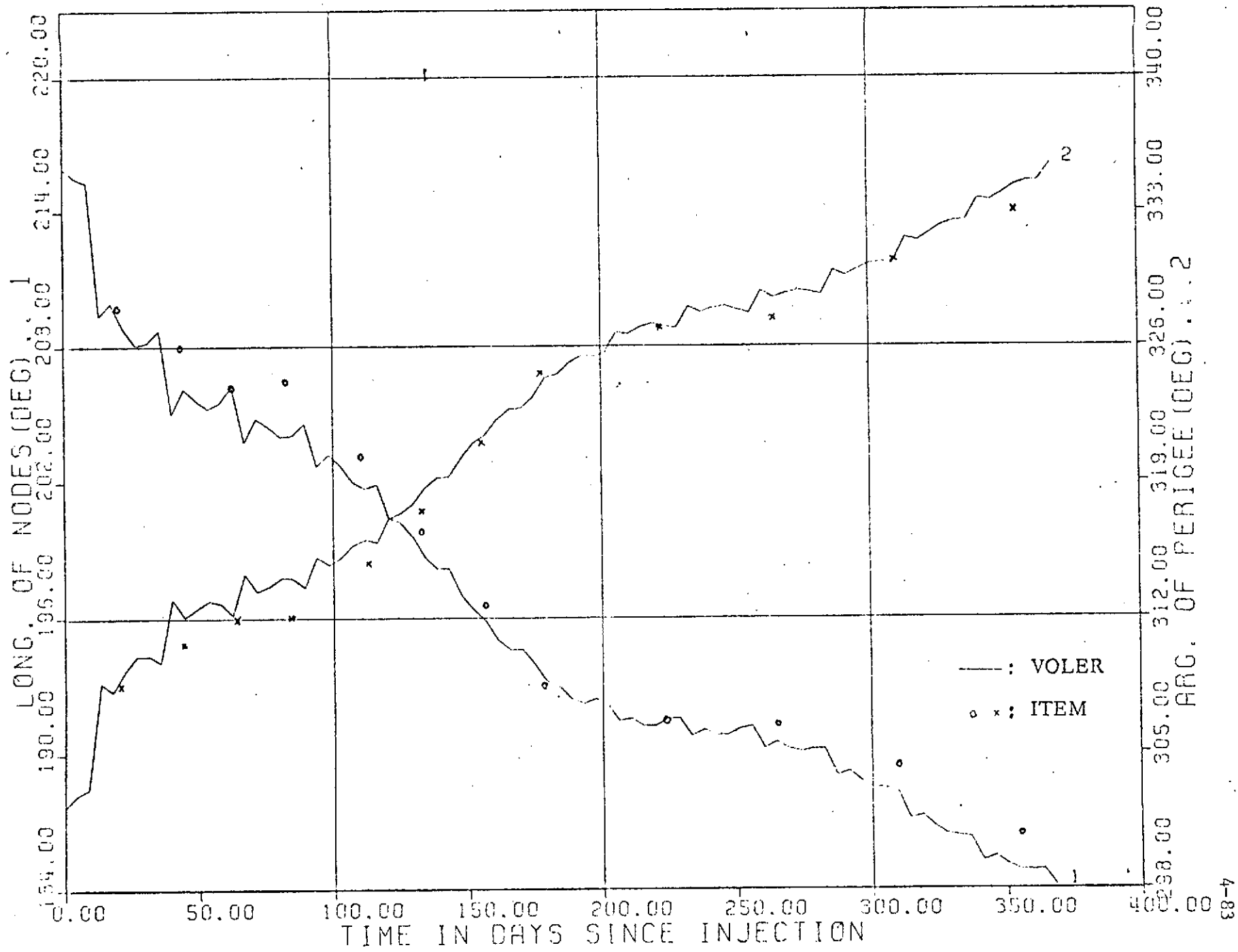


Figure 4.7. Evolution of Elements: IMP-I Example

APPENDIX A.1Effects of Earth's Oblateness

A satellite, in an orbit of high eccentricity, spends a considerable portion of its orbital revolution quite far away from the earth (on the apogee side of the orbit). Nevertheless, the effects of the oblateness of the earth are significant. The secular effects of the principal term, J_{20} , was the sole term considered. Note that J_{30} and subsequent terms are at least of order 10^{-3} compared to J_{20} .

It is well known that there are no secular variations due to J_{20} , over an unperturbed orbital period of the satellite, in the semi-major axis, eccentricity and inclination. The variations in the longitude of nodes and the argument of perigee are found in many books on celestial mechanics. The variation for the last element M_* , however, is not given elsewhere in the form presented here, to the author's knowledge. The integration of this element is dealt with in detail.

Oblateness: Potential and Force

For a spheroid (symmetry with respect to polar axis),
the potential is given as

$$U = \frac{\mu}{r} \left[1 - \sum_{m=2}^{\infty} J_m \left(\frac{R_e}{r} \right)^m P_m(\sin \delta) \right] \quad (\text{A.1.1})$$

where

r = distance from the center of mass of the earth
to the satellite

J_m = numerical coefficients

R_e = radius of the earth

$P_m(\sin \delta)$ = m -th Legendre Polynomial in the argument ($\sin \delta$)

δ = latitude of the satellite

and μ = gravitational constant of the earth.

The values of the first few constants J_m

are:

$$J_2 = 1082.86 \pm 0.1 \times 10^{-6}$$

$$J_3 = -2.45 \pm 0.07 \times 10^{-6}$$

$$J_4 = -1.03 \pm 0.2 \times 10^{-6}$$

Consider the m -th term

$$U_m = - \frac{K_m}{r^{m+1}} P_m(\sin \delta) \quad (\text{A.1.2})$$

where $K_m = \mu J_m R_e^m$

Then, the force due to this term is

$$\begin{aligned}\vec{F}_m &= \vec{\nabla} U_m \\ &= -K \frac{P_m}{r^{m+1}} \vec{\nabla} \left(\frac{1}{r^{m+1}} \right) - \frac{K_m}{r^{m+1}} \vec{\nabla} (P_m)\end{aligned}\quad (\text{A.1.3})$$

$$\vec{\nabla} \left(\frac{1}{r^{m+1}} \right) = - \frac{(m+1)}{r^{m+2}} \vec{1}_r \quad (\text{A.1.4})$$

where $\vec{1}_r$ is the unit vector directed to the satellite.

$$\vec{\nabla} (P_m) = \sum \vec{x}_i \frac{\partial}{\partial x_i} P_m,$$

where \vec{x}_i = unit vectors of the earth reference system (referred to, elsewhere, as $\vec{x}_\alpha, \vec{y}_\alpha, \vec{z}_\alpha$)

$$\therefore (P_m) = \sum x_i P'_m \frac{\partial}{\partial x_i} (\sin \delta) \quad (\text{A.1.5})$$

where $P'_m(z) = \frac{d}{dz} P_m(z)$

Note that

$$\sin \delta = (\vec{1}_r \cdot \vec{x}_3)$$

Carrying out the algebra, Eq. (A.8.5) reduces to

$$P_m = -P'_m \frac{\sin \delta}{r} \vec{1}_r + P'_m \frac{\vec{x}_3}{r} \quad (\text{A.1.6})$$

Now,

$$\vec{x}_3 = (\vec{x}_3 \cdot \vec{1}_r) \vec{1}_r + (\vec{x}_3 \cdot \vec{1}_t) \vec{1}_t + (\vec{x}_3 \cdot \vec{1}_n) \vec{1}_n \quad (\text{A.1.7})$$

where $(\vec{1}_r, \vec{1}_t, \vec{1}_n)$ are the instantaneous orbital axes and the parentheses indicate dot products.

Also, from orbital geometry,

$$\begin{aligned} (\vec{x}_3 \vec{i}_r) &= \sin \delta = \sin i \sin (\omega+\nu) \\ (\vec{x}_3 \vec{i}_t) &= \sin i \cos (\omega+\nu) \\ (\vec{x}_3 \vec{i}_n) &= \cos i \end{aligned} \quad (\text{A.1.8})$$

Substituting Eqs. (A.1.7) and (A.1.8) in Eq. (A.8.6) and simplifying,

$$\vec{\nabla} P_m = \frac{P_m}{r} [\sin i \cos (\omega+\nu) \vec{i}_t + \cos i \vec{i}_n] \quad (\text{A.1.9})$$

Substituting Eqs. (A.1.4) and (A.1.9) in Eq. (A.1.3),

$$\begin{aligned} \vec{F}_m &= \vec{\nabla} U_m \\ &= \frac{K_m}{r^{m+2}} [(m+1) P_m \vec{i}_r - P_m' (\sin i \cos (\omega+\nu) \vec{i}_t + \cos i \vec{i}_n)] \end{aligned} \quad (\text{A.1.10})$$

where the argument of the LP, P_m and P_m' , is $\sin \delta$. The prime denotes differentiation of P_m with respect to the argument.

The components of \vec{F}_m along the instantaneous orbital axes can be determined by taking the appropriate dot products. Thus,

$$\begin{aligned} F_1 &= (\vec{F}_m \vec{i}_r) = \frac{K_m (m+1)}{p^{m+2}} \Delta^{m+2} P_m \\ F_2 &= (\vec{F}_m \vec{i}_t) = -\frac{K_m}{p^{m+2}} \Delta^{m+2} P_m' \sin i \cos (\omega+\nu) \\ F_3 &= (\vec{F}_m \vec{i}_n) = -\frac{K_m}{p^{m+2}} \Delta^{m+2} P_m' \cos i \end{aligned} \quad (\text{A.1.11})$$

where $\Delta = (1 + e \cos v)$

and $r = p/\Delta$

Secular Variation in Ω

$$\frac{d\Omega}{dv} = \frac{r^3}{\mu a e (\sin i)} F_3 \sin(\omega+v) \quad (\text{A.1.12})$$

Substituting from Eq. (A.1.11) for $m=2$, and integrating with respect to v between the limits 0 and 2π ,

$$(\Delta\Omega)_{ob} = -\frac{3K_2}{\mu p} \pi \cos i$$

Letting
$$K = \frac{K_2}{\mu p^2} = J_2 \left(\frac{R_e}{P}\right)^2 \quad (\text{A.1.13})$$

$$(\Delta\Omega)_{ob} = -3K \pi (\cos i) \quad (\text{A.1.14})$$

Secular Variation in ω

$$\frac{d\omega}{dv} = \frac{r^2}{\mu e} [-F_x + F_2 \frac{r}{p} \sin v] - (\cos i) \frac{d\Omega}{dv} \quad (\text{A.1.15})$$

Note that

$$F_x = F_1 \cos v - F_2 \sin v$$

Substituting from Eq. (A.1.11) for $n=2$, and integrating with respect to v between the limits 0 and 2π ,

$$(\Delta\omega)_{ob} = -\frac{K_2\pi}{4\mu p^2} (18 \sin^2 i - 12) - (\cos i)(\Delta\Omega)$$

Substituting for $\Delta\Omega$ from Eq. (A.1.13) and for K_2 from Eq. (A.1.14), and simplifying

$$(\Delta\omega)_{ob} = 6K\pi \left(1 - \frac{5}{4} \sin^2 i\right) \quad (A.1.16)$$

Secular Variation in M_*

$$\frac{dM_*}{dv} = \frac{-2r^3}{\mu a \epsilon^{1/2}} F_1 + \frac{3}{2} \frac{nt}{a} \frac{da}{dv} - \epsilon^{1/2} \left(\cos i \frac{d\Omega}{dv} + \frac{d\omega}{dv} \right)$$

where n = mean motion of satellite

$$\text{and} \quad \frac{da}{dv} = \frac{2r^2}{\mu \epsilon} (\epsilon F_y + F_2) \quad (A.1.17)$$

This integration will be looked at term-by-term.

Substituting from Eq. (A.1.11) for $n=2$,

$$\begin{aligned} \text{Term (1)} &= -\frac{2r^3}{\mu a \epsilon^{1/2}} F_1 = -\frac{2r^3}{\mu a \epsilon^{1/2}} \frac{3K_2}{p^4} \Delta^4 P_2 \\ &= -6K\epsilon^{1/2} P_2 \Delta \\ &= -3K\epsilon^{1/2} \Delta (3\sin^2 i \sin^2(\omega+\nu) - 1) \end{aligned}$$

for $P_2 = P_2(\sin \delta)$ and $\sin \delta = \sin i \sin(\omega+\nu)$

Thus, on integration,

$$\begin{aligned} \text{Term (1)} &= -3K\epsilon^{1/2} \int_0^{2\pi} \Delta \left(\frac{3}{2} \sin^2 i - 1 \right. \\ &\quad \left. - \frac{3}{2} \sin^2 i \cdot \cos 2(\omega + \nu) \right) d\nu \\ &= -6K\epsilon^{1/2} \pi \left(\frac{3}{2} \sin^2 i - 1 \right) \end{aligned} \quad (\text{A.1.18})$$

Next,

$$\begin{aligned} \text{Term (2)} &= \frac{3}{2} \frac{n\tau}{a} \frac{da}{d\nu} \\ &= \frac{3}{2} \frac{n\tau}{2a} \frac{da}{d\nu} + \frac{3}{2} \frac{n(\Delta t)}{a} \frac{da}{d\nu} \end{aligned} \quad (\text{A.1.19})$$

where t = time measured from perigee
 $= \frac{\tau}{2} + (\Delta t)$
 τ = period of satellite
 and (Δt) = time measured from apogee

Since the secular variation in a is zero, the first term on the right-hand side of Eq. (A.1.19) drops out on integration.

$$\begin{aligned} \text{Term (2)} &= 3n(\Delta t) \frac{r^2}{\mu\epsilon} (eF_y + F_2) \\ &= \frac{3np^2}{\mu\epsilon} \frac{(\Delta t)}{\Delta^2} (eF_1 \sin \nu + F_2 \Delta) \end{aligned} \quad (\text{A.1.20})$$

as $F_y = F_1 \sin \nu + F_2 \cos \nu$

$$\begin{aligned} \text{Term (2)} &= \frac{9nK}{\epsilon} (\Delta t) \left[\frac{e}{2} (3 \sin^2 i \sin^2(\omega + \nu) - 1) \Delta^2 \sin \nu \right. \\ &\quad \left. - \frac{\Delta^3}{2} \sin^2 i \sin 2(\omega + \nu) \right] \quad (\text{A.1.21}) \end{aligned}$$

Integration of Eq. (A.1.21) will be written out in detail.

The generic form would be

$$\int (\Delta t) f(\nu) d\nu = (\Delta t) \int f(\nu) d\nu - \frac{1}{C_1} \int \frac{d\nu}{\Delta^2} (\int f(\nu) d\nu)$$

where

$$\frac{d}{d\nu} (\Delta t) = \frac{P^{3/2}}{\sqrt{U}} \frac{1}{\Delta^2} = \frac{1}{C_1} \frac{1}{\Delta^2} \quad (\text{A.1.22})$$

Thus, (the limits, 0 and 2π , are not marked for convenience)

$$\begin{aligned} & - \frac{e}{2} \int (\Delta t) \Delta^2 \sin \nu d\nu \\ &= - \frac{e}{2} \left[- \left(\frac{(\Delta t) \Delta^3}{3e} \right) + \frac{1}{3e C_1} \int \Delta d\nu \right] \\ &= \frac{\tau}{6} (1 + e)^3 - \frac{2\pi}{6 C_1} \quad (\text{A.1.23}) \end{aligned}$$

$$\begin{aligned} & \frac{3e}{2} \sin^2 i \sin^2 \omega \int (\Delta t) \Delta^2 \sin \nu \cos^2 \nu d\nu \\ &= \frac{3e}{2} \sin^2 i \frac{\sin^2 \omega}{e^2} \int (\Delta t) \Delta^2 (\Delta^2 - 2\Delta + 1) \sin \nu d\nu \\ &= \frac{3e}{2} \sin^2 i \sin^2 \omega \left[\frac{\tau (1+e)^3}{30e^3} (-1 + 3e - 6e^2) \right. \\ &\quad \left. + \frac{\pi}{30e C_1} (2 + 3e^2) \right] \quad (\text{A.1.24}) \end{aligned}$$

$$\begin{aligned}
& \frac{3e}{2} \sin^2 i \cos^2 \omega \int (\Delta t) \Delta^2 \sin^3 v \, dv \\
&= \frac{3e}{2} \sin^2 i \cos^2 \omega \int (\Delta t) \Delta^2 \sin v (1 - \cos^2 v) dv \\
&= \frac{3e}{2} \sin^2 i \cos^2 \omega \left[\frac{\tau(1+e)^3}{30e} (1 - 3e - 4e^2) + \frac{\pi}{30e^3 C_1} (-2 + 17e^2) \right] \quad (\text{A.1.25})
\end{aligned}$$

$$\frac{3e}{2} \sin^2 i \sin 2\omega \int (\Delta t) \Delta^2 \sin^2 v \cos v \, dv$$

$$= 0 \text{ as } (\Delta t) \text{ is odd about } v = \pi$$

$$- \frac{\sin^2 i}{2} \sin 2\omega \int (\Delta t) \Delta^3 (\cos^2 v - \sin^2 v) dv$$

$$= 0$$

$$- \sin^2 i \cos 2\omega \int (\Delta t) \Delta^3 \sin v \cos v \, dv$$

$$= - \sin^2 i \cos 2\omega \left[\frac{\tau(1+e)^4}{20e^2} (1 - 4e) + \frac{\pi}{20e^2 C_1} (7e^2 - 2) \right] \quad (\text{A.1.26})$$

Putting Eqs. (A. .23) to (A. .26) together, and simplifying,

$$\text{Term (2)} = \frac{9nK}{\epsilon} \left[\frac{\pi}{6C_1} (3 \sin^2 i - 2) + \frac{\tau}{6} (1+e)^3 (1 - 3 \sin^2 i \sin^2 \omega) \right] \quad (\text{A.1.27})$$

Finally,

$$\begin{aligned}
\text{Term (3)} &= -\epsilon^{1/2} (\cos i (\Delta\Omega) + (\Delta\omega)) \\
&= \frac{9}{2} K \pi \epsilon^{1/2} \left(\sin^2 i - \frac{2}{3} \right) \quad (\text{A.1.28})
\end{aligned}$$

Then

$$\begin{aligned} (\Delta M_*)_{ob} &= \text{secular variation in } M_* \text{ due to } J_{20} \\ &= \text{Term (1)} + \text{Term (2)} + \text{Term (3)} \end{aligned}$$

Summing Eqs. (A.1.18), (A.1.27) and (A.1.28)

$$\begin{aligned} (\Delta M_*)_{ob} &= -3K\epsilon^{1/2} \pi (3 \sin^2 i - 2) \\ &\quad + \frac{3}{2} K \pi \frac{n}{\epsilon C_1} (3 \sin^2 i - 2) \\ &\quad + \frac{3}{2} K \pi \epsilon^{1/2} (3 \sin^2 i - 2) \\ &\quad + \frac{3}{2} n \pi \frac{K}{\epsilon} (1+e)^3 (1 - 3 \sin^2 i \sin^2 \omega) \end{aligned}$$

Substituting $\frac{n}{\epsilon C_1} = \epsilon^{1/2}$ and $n\pi = 2\pi$,

$$(\Delta M_*)_{ob} = \frac{3K\pi}{\epsilon} (1+e)^3 (1 - 3 \sin^2 i \sin^2 \omega) \quad (\text{A.1.29})$$

Features of ΔM_*

There are several interesting features in the final expression for the secular variation in M_* over an orbital period of the satellite, as given by Eq. (A.8.29). Firstly,

$$\frac{K}{\epsilon} = J_2 \frac{R_e^2}{p \epsilon} = \frac{J_2 R_e}{a^2 \epsilon^3} \quad (\text{A.1.30})$$

Since a is relatively invariant in high eccentricity orbits, Eq. (A.1.30) shows that ϵ (being of magnitude $0.1 \sim 0.2$) acts as a small divisor in $(\Delta M_*)_{ob}$ (as also in $(\Delta \Omega)_{ob}$ and $(\Delta \omega)_{ob}$).

The effect is rather pronounced in $(\Delta M_*)_{ob}$ because ϵ^3 is present while, in $(\Delta \Omega)_{ob}$ and $(\Delta \omega)_{ob}$, ϵ^2 is present. Thus small inaccuracies in e , the eccentricity, are magnified.

Secondly, because of the presence of ϵ^3 in the denominator, the magnitude of $(\Delta M_*)_{ob}$ is rather large. This is confirmed by experimental results as shown in Chapter 2.

Thirdly, the final expression for ΔM_* arises exclusively from Term (2) in the integration process (Eq. (A.1.27)). The contributions of Term (1) (Eq. (A.1.18)) and Term (3) (Eq. (A.1.28)) cancel with part of Eq. (A.1.27). Thus, the "short-period" variations in the semi-major axis contribute to the secular variation of M_* .

Fourthly, the secular variation in M_* is zero only when

$$1 - 3 \sin^2 i \sin^2 \omega = 0$$

Secular Variation of Roth's Sixth Element

From Eq. (2.21) of Chapter 2,

$$\frac{dT}{dv} = \frac{r^4}{\mu e \sqrt{\mu p}} [-F_1 \cos v + (1 + \frac{r}{p})F_2 \sin v] \quad (A.1.31)$$

Substituting from Eq. (A.1.11) and after some manipulation

$$\frac{dT}{dv} = \frac{Ke^{3/2}}{ne} [-3P_2 \cos v - P_2' \sin i \sin v \cos(\omega+v)(1 + \frac{1}{\Delta})] \quad (A.1.32)$$

Instead of transforming to E , the eccentric anomaly, as the independent variable, this expression will be integrated with

respect to the true anomaly. The result in either case will be the same so far as the secular variation over an orbit is concerned. Detailing the integration term-by-term, the limits being assumed,

$$\begin{aligned} \text{Term (1)} &= - \int \left[\frac{9}{2} \sin^2 i \sin^2(\omega+v) \cos v - \frac{3}{2} \cos v \right] dv & (\text{A.1.33}) \\ &= 0 & (\text{A.1.33}) \end{aligned}$$

$$\begin{aligned} \text{Term (2)} &= - \int \frac{3}{2} \sin^2 i \sin v \sin 2(\omega+v) dv \\ &= 0 & (\text{A.1.34}) \end{aligned}$$

$$\text{Term (3)} = - \frac{3}{2} \sin^2 i \int \frac{dv}{\Delta} [\sin v \sin 2(\omega+v)]$$

Splitting Term (3) further,

$$\text{Term (3.1)} = \sin 2\omega \int \frac{\sin v}{\Delta} \cos^2 v dv = 0$$

$$\text{Term (3.2)} = -\sin 2\omega \int \frac{\sin^3 v}{\Delta} dv = 0$$

$$\begin{aligned} \text{Term (3.3)} &= 2 \cos 2\omega \int \frac{\sin^2 v}{\Delta} \cos v dv \\ &= 2 \cos 2\omega \left[\int \frac{\cos v}{\Delta} dv - \int \frac{\cos^3 v}{\Delta} dv \right] \\ &= 2 \cos 2\omega \left[\frac{1}{e} \int \frac{(\Delta-1)}{\Delta} dv \right. \\ &\quad \left. - \frac{1}{3} \int (\Delta^3 - 3\Delta^2 + 3\Delta - 1) \frac{dv}{\Delta} \right] \end{aligned}$$

Substituting

$$\int \frac{dv}{\Delta} = \frac{2\pi}{\epsilon^{1/2}} \quad \text{between the limits}$$

and carrying out some simplifications,

$$\text{Term (3.3)} = -2\pi \frac{\cos 2\omega}{e^3} (1 - \epsilon^{1/2})^2$$

Summing Terms (3.1), (3.2) and (3.3),

$$\text{Term (3)} = \frac{3\pi}{e^3} \sin^2 i \cos 2\omega (1 - \epsilon^{1/2})^2 \quad (\text{A.1.35})$$

Summing Eq. (A.1.33) to Eq. (A.1.35) and substituting in the integration of Eq. (A.8.32),

$$(\Delta T)_{\text{ob}} = 3\pi K \frac{\epsilon^{3/2}}{ne^4} (1 - \epsilon^{1/2})^2 \sin^2 i \cos 2\omega \quad (\text{A.1.36})$$

This is the final expression for the secular variation of the time at epoch, due to J_{20} , as obtained from Roth's sixth element. Notice that ϵ does not appear as a small divisor unlike in Eq. (A.1.31). Thus, the magnitude of $(\Delta T)_{\text{ob}}$ would not be large.

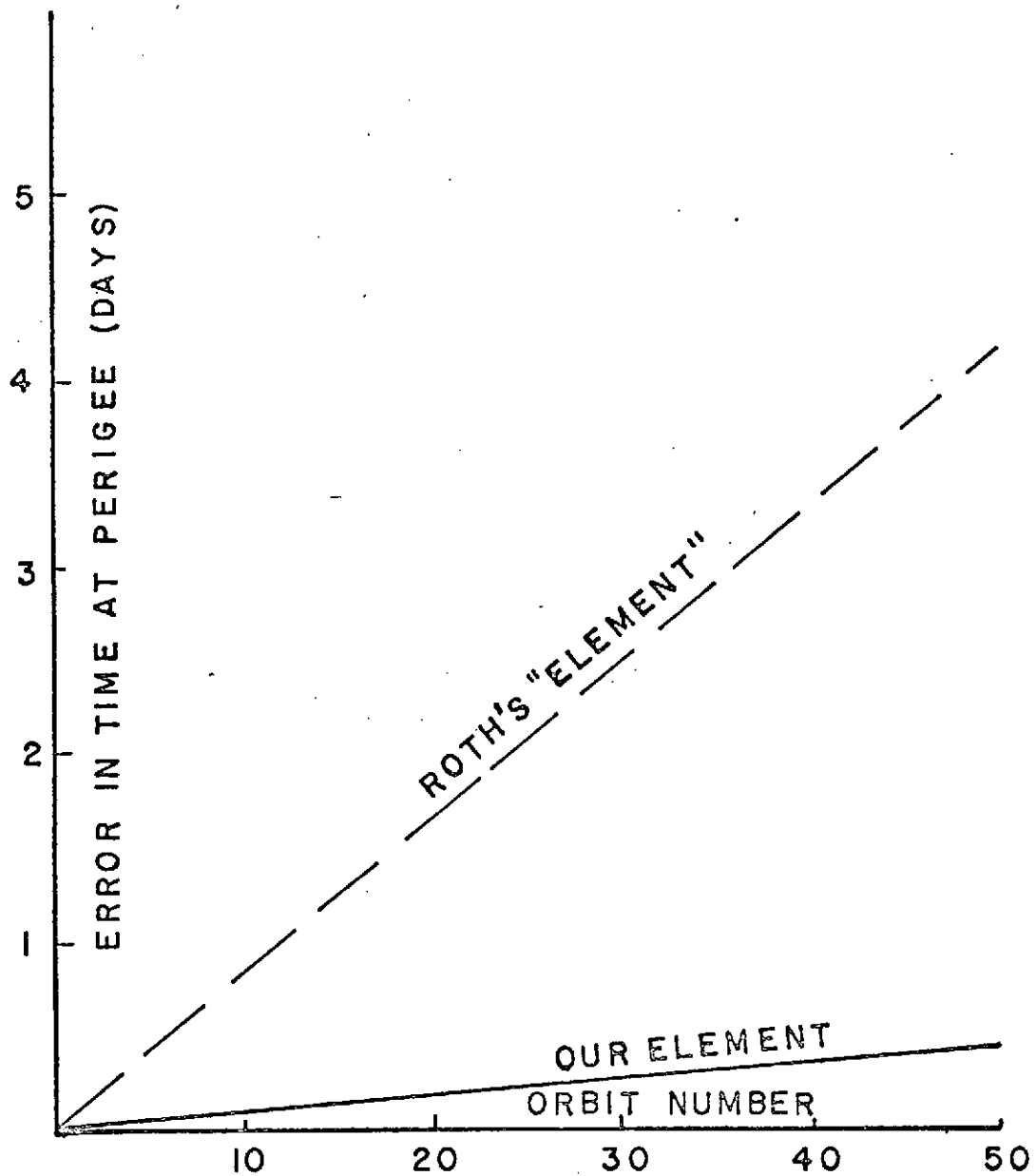


FIG. A.1. COMPARISON OF ROTH'S SIXTH "ELEMENT"
WITH OUR SIXTH ELEMENT.
(OBLATENESS ONLY)

(NOTE: QUANTITY PLOTTED ON THE
Y-AXIS IS THE MAGNITUDE
OF THE ERROR.)

CHAPTER 5

Singularity-free Methods, Using Regularization,
for Circular and Elliptic Orbits

5.1 Introduction and Motivation

Under this grant, singularity-free methods of orbit calculation, using regularization, and applicable to both the circular ($e=0$) and elliptical orbits, have been developed and comparatively studied, in a Ph.D. thesis by S.K. Bhate^[5-1], as the Principal Investigator's (M.L. Renard) advisee. For a much more detailed treatment, the reader should refer to Ref. [5-1]. Although the original grant, in April 1968, had the title "Launch Window Analysis of Highly Eccentric Orbits", it became readily apparent that for missions such as that of IMP-H, methods of orbital and mission analysis for large circular orbits were required, which should be insensitive to the following singularities introduced by the choice of the standard "osculating elements"

$$a, e, i, \omega, \Omega, T_0 \tag{5.1-1}$$

- a) $e = 0$. The orbit is exactly circular. Since perigee strictly does not exist, the "argument of perigee" or "time of passage at perigee" lose their meaning. Mathematically, in the equations expressing the time-rate of change of the osculating elements, (5.1-1), small or zero divisors "e" appear .
- b) $i = 0^\circ$ or 180° . The orbit is exactly equatorial, prograde or retrograde. Since the line of nodes strictly

does not exist, the "nodal line" is left undefined.

Mathematically, small or zero divisors "sin i" appear.

If the small, perturbing forces do not derive from a potential, or if such forces might have to be encompassed by the theory, it appears normal to write the equations expressing the time-variations of the elements in Gaussian form. The problem of developing a variation of parameters scheme in which derivatives are expressed in terms of perturbing forces was attempted by A.M. Garafalo^[5-2], R.R. Newton^[5-3], C.J. Cohen and E.C. Hubbard^[5-4]. In all of these studies, however, absence of any perturbations, which defeats the very purpose of the method of variation of parameters. S. Pines^[5-5] presented the first "authentic" variation of parameters scheme, which used as osculating elements the position and velocity vector at some instant, time being and as the independent variable. Basically, the same method was used later by P. Wong^[5-6], S. Herrick^[5-7], E. Pitkin^[5-8, 5-9]. Program NICE-T developed under this grant at C-MU, and described in Chapter 6 of this work, has been written based on Pitkin's version of the variation of parameters, and will be compared to other methods presented in this chapter.

In the following, non-singular elements such as the radius and velocity vector at some epoch are combined with the use of differential transformation of the independent to result in the extremely simple form for the unperturbed equations of motion; those of the harmonic oscillator. Based on this unperturbed solution, a singular free method of variation of parameters can be developed. This is the

object of Section 5.2. In Section 5.3, a modification of Brouwer's method of "perturbations in rectangular coordinates"^[5-10] which is applicable to circular orbits is developed, again starting from the unperturbed solution mentioned before. In Section 5.4, the perturbing forces due to a third gravitational body (such as the sun or the moon) are expressed in terms of mixed Fourier-Chebyshev series, for which series computational algorithms are derived which maintain a good accuracy by avoiding the problem of taking the differences of large, close numbers. This leads to the development of a theory which is semi-analytic, namely closed form integration is performed on series of the type indicated, the coefficients of which are numbers "valid" over one orbit of the perturbed body (the satellite). In Section 5.5, a numerical comparison is made between the results of the integration, in their various forms, of the system of differential equations. Two "benchmark" examples are considered: an orbit of large eccentricity ($e = 0.936227$) with a period of 4.45 days, and an essentially circular orbit ($e = 0.8018212 \times 10^{-5}$) having a period of 12.05 days (orbital radius = 35 mean Earth radii).

For such "large circular" or "high eccentricity" orbits, it should be stressed that:

- as compared to close-to-earth orbits, the oblateness effect and atmospheric drag, as perturbing forces, are most of the time, or even always, much smaller than those due to the gravitational perturbations of the sun and the moon.

- as compared to classical problems of Celestial Mechanics dealing with natural satellites: the perturbing forces considered in

these problems are small either because of the large distances involved, compared to the orbital semi-major axis (in the case of the moon) or on account of the small ratio of the masses (the largest for Jupiter but still $< 10^{-3}$). Typically, the ratio of the magnitude of the perturbing force to that of the central force is largest in the case of Mars perturbed by Jupiter, and is $.763 \times 10^{-5}$ at most.

To fix the ideas, the relative order of magnitudes of the perturbing forces, with the central force as a norm, are, along large circular orbits:

Atmospheric pressure	$< 10^{-27}$
Radiation pressure	$< 10^{-16}$
Oblateness	$< 10^{-5}$
Perturbation due to the sun	$\approx 10^{-3}$
Perturbation due to the moon	$\approx 10^{-2}$

Now, in studying orbits, the main motivation might be:

- 1) High accuracy computation of ephemerides: for this, numerical integration is well suited and can be carried out to a very high degree of precision.
- 2) Determination of the evolution of the orbital elements, for mission analysis purposes: Here, since the requirement on accuracy is relaxed, it might be allowed to linearly superpose perturbations, at least over one orbit of the satellite, in spite of the significant magnitude of some of the forces listed above. One might then consider to use close-earth satellite theories^[5-10 to 5-15]. Lunar

and planetary theories would have to be excluded if the perturbing function is expanded in powers of the inclination as a small parameter, and if the theory is therefore unsuitable for the large inclination commonly encountered for artificial satellites. A notable exception is Tisserand's^[5-16] theory for the computation of Pallas perturbed by Jupiter, in which the perturbing function is expanded in powers of both $\sin^2 \frac{i}{2}$ and $\cos^2 \frac{i}{2}$.

- 3) Orbit classification: Here the emphasis is on qualitatively classifying orbits, such as being able to say if they are of circulatory (line of apsides rotates monotonously) or oscillatory (line of apsides oscillates between limits) nature^[5-17]. To this effect, some sort of development in series (Legendre Polynomials and Taylor series^[5-17], Fourier series in M and M' ^[5-18,5-19]) is considered and some "main" contribution is analyzed to define a qualitative behavior of classes of orbits.

The present chapter strive for the development of methods of relatively moderate accuracy and concentrates on this objective along the lines described in item 2).

As a last remark in this introduction, we should mention that we initially proposed, in 1969, that the study of large circular geocentric orbits be a part of the material studied under this grant^[5-20], for orbits having a ratio of the orbital semi-major axis to the semi-major axis of the moon up to about $\frac{1}{2}$, along the following lines of effort:

- Regularization (for instance, Kustaanheimo-Stiefel's transformation)
- Closed form theories.

These are indeed, the directing lines taken in this chapter. However, in view of the magnitude of the dynamical perturbations, the "analytical" integration of the equations of motion was carried out with numerical coefficients (as opposed to literal coefficients) inside the computer program and its result evaluated to give the desired output. Hence the name "semi-analytic integration" was thought to be more appropriate.

5.2 Unperturbed and perturbed two-body motion

5.2.1 Development of the linear equations for the unperturbed problem

In its classical form, the unperturbed two-body problem, referred to the center of the Earth, say, is described by the non-linear differential equations

$$\ddot{\vec{r}} + \mu \frac{\vec{r}}{r^3} = 0 \quad (5.2-1)$$

in which \vec{r} is the geocentric vector to the perturbed body, and $\mu = k^2 (M_{\text{earth}} + m_{\text{satellite}})$ or $\mu \approx k^2 M_{\text{earth}}$ if $m_{\text{satellite}} \ll M_{\text{earth}}$. If a perturbing force \vec{F} , assumed to be always of "small" magnitude compared to the magnitude of the central force, is present, (5.2-1) has r.h. side \vec{F} .

Using the well-known Sundman's transformation

$$\frac{d}{d\hat{x}} \equiv \frac{r}{\sqrt{\mu}} \frac{d}{dt} \quad (5.2-2)$$

leading to

$$\frac{d}{dt} = \frac{\sqrt{\mu}}{r} \frac{d}{d\hat{x}}; \quad \frac{d^2}{dt^2} = \frac{\sqrt{\mu}}{r} \frac{d}{d\hat{x}} \left(\frac{\sqrt{\mu}}{r} \frac{d}{d\hat{x}} \right) = \frac{\mu}{r^2} \frac{d^2}{d\hat{x}^2} - \frac{\mu}{r^3} \frac{dr}{d\hat{x}} \frac{d}{d\hat{x}}$$

Equation (5.2-1) from which the consideration of collision orbits is excluded (thus $r \neq 0$), will read after multiplication by $r^2 \mu^{-1}$,

$$\frac{d^2 \vec{r}}{d\hat{x}^2} - \frac{1}{r} \left(\frac{dr}{d\hat{x}} \right) \left(\frac{d\vec{r}}{d\hat{x}} \right) + \frac{\vec{r}}{r} = 0 \quad (5.2-3)$$

which is still non-linear. Now, in two-body motion with an inverse-square attractive law of forces, and with $\vec{c} = \vec{r} \wedge \vec{r}' = \text{constant vector}$ (' are derivatives with respect to time)

$$\begin{aligned} \vec{r}'' \wedge \vec{c} &= \frac{d}{dt} (\vec{r}' \wedge \vec{c}) \\ &= -\mu \left(\vec{r} \frac{\vec{r} \cdot \vec{r}'}{r^3} - \vec{r}' \frac{1}{r} \right) \\ &= \mu \left(\frac{\vec{r}'}{r} - \vec{r} \frac{\vec{r}'}{r} \right) = \mu \frac{d}{dt} \left(\frac{\vec{r}}{r} \right) \end{aligned}$$

Therefore, upon integration,

$$e\vec{P} = \vec{r}' \wedge \left(\vec{r} \wedge \vec{r}' \right) - \mu \frac{\vec{r}}{r} \quad (5.2-4)$$

Let \vec{A} be the Laplace vector

$$\vec{A} \stackrel{\text{def}}{=} -\frac{e}{\mu} \vec{P} = \frac{\vec{r}}{r} - \frac{1}{\mu} \vec{r}' \wedge \left(\vec{r} \wedge \vec{r}' \right) \quad (5.2-5)$$

It is a constant in the unperturbed motion. So is the energy integral ($a > 0$ for elliptic orbits)

$$E = -\frac{\mu}{2a} = \frac{\vec{r}^2}{2} - \frac{\mu}{r} \quad (5.2-6)$$

or equivalently the quantity

$$\alpha = \frac{2}{\mu} E = \frac{1}{\mu} \frac{d\vec{r}}{dt} \cdot \frac{d\vec{r}}{dt} - \frac{2}{r} = -\frac{1}{a} \quad (5.2-7)$$

Now \vec{A} and α are rewritten in \hat{x} variables as

$$\vec{A} = \frac{\vec{r}}{r} - \frac{1}{r^2} \frac{d\vec{r}}{d\hat{x}} \wedge (\vec{r} \wedge \frac{d\vec{r}}{d\hat{x}}) \quad (5.2-8)$$

$$\alpha = \frac{1}{r^2} \frac{d\vec{r}}{d\hat{x}} \cdot \frac{d\vec{r}}{d\hat{x}} - \frac{2}{r} \quad (5.2-9)$$

From these expressions, $\alpha \vec{r} + \vec{A}$ can be expressed as

$$\begin{aligned} \alpha \vec{r} + \vec{A} &= -\frac{2\vec{r}}{r} + \frac{1}{r^2} \left(\frac{d\vec{r}}{d\hat{x}} \cdot \frac{d\vec{r}}{d\hat{x}} \vec{r} - \frac{d\vec{r}}{d\hat{x}} \cdot \frac{d\vec{r}}{d\hat{x}} \vec{r} \right) + \frac{\vec{r}}{r} \\ &\quad + \frac{1}{r^2} \left(\frac{d\vec{r}}{d\hat{x}} \cdot \vec{r} \right) \frac{d\vec{r}}{d\hat{x}} \end{aligned} \quad (5.2-10)$$

$$= -\frac{\vec{r}}{r} + \frac{1}{r} \frac{d\vec{r}}{d\hat{x}} \frac{d\vec{r}}{d\hat{x}}$$

Equation (5.2-3) is rewritten

$$\frac{d^2\vec{r}}{d\hat{x}^2} - \alpha \vec{r} = \vec{A} \quad (5.2-11)$$

Defining a new, auxiliary vector which is constant in the unperturbed motion,

$$\vec{B} \stackrel{\text{def}}{=} a\vec{A} \quad (5.2-12)$$

we obtain

$$\frac{d^2\vec{r}}{d\hat{x}^2} - \alpha(\vec{r} - \vec{B}) = 0 \quad (5.2-13)$$

A variable \vec{z} is defined as

$$\vec{z} \stackrel{\text{def}}{=} \vec{r} - \vec{B} = \vec{r} - a\vec{A} \quad (5.2-14)$$

and the final system of uncoupled, constant coefficient system of linear differential equations reads

$$\frac{d^2\vec{z}}{d\hat{x}^2} + \frac{1}{a}\vec{z} = 0 \quad (5.2-15)$$

Its solution is, in terms of the z variable

$$\vec{z} = \vec{z}_0 \cos \sqrt{\frac{\hat{x}}{a}} + \sqrt{a} \left(\frac{d\vec{z}}{d\hat{x}} \right)_0 \sin \sqrt{\frac{\hat{x}}{a}} \quad (5.2-16)$$

$$\frac{d\vec{z}}{d\hat{x}} = -\frac{\vec{z}_0}{\sqrt{a}} \sin \sqrt{\frac{\hat{x}}{a}} + \left(\frac{d\vec{z}}{d\hat{x}} \right)_0 \cos \sqrt{\frac{\hat{x}}{a}}$$

in which \vec{z}_0 , $\left(\frac{d\vec{z}}{d\hat{x}} \right)_0$ are the initial conditions, given at $\hat{x} = 0$. In terms of \vec{r}

$$\vec{r} = \vec{B} + (\vec{r}_0 - \vec{B}) \cos \sqrt{\frac{\hat{x}}{a}} + \sqrt{a} \left(\frac{d\vec{r}}{d\hat{x}} \right)_0 \sin \sqrt{\frac{\hat{x}}{a}} \quad (5.2-17)$$

$$\frac{d\vec{r}}{d\hat{x}} = -\frac{\vec{r}_0 - \vec{B}}{\sqrt{a}} \sin \sqrt{\frac{\hat{x}}{a}} + \left(\frac{d\vec{r}}{d\hat{x}} \right)_0 \cos \sqrt{\frac{\hat{x}}{a}}$$

(5.2-17) is the solution of the unperturbed two-body problem in terms of independent variable \hat{x} . The time t corresponding to any \hat{x} , is if $t = t_0$ for $\hat{x} = \hat{x}_0 = 0$,

$$t = \int_0^{\hat{x}} \frac{|\vec{r}|}{\sqrt{\mu}} d\hat{x} + t_0 \quad (5.2-18)$$

Looking at Equation (5.2-17), it appears natural to introduce a new variable $\frac{\hat{x}}{\sqrt{a}}$. However, since a is not a constant in the perturbed motion, the introduction of the new variable "E" is done in differential form:

$$dE = \frac{d\hat{x}}{\sqrt{a}} \quad (5.2-19)$$

In the unperturbed problem, considering that a is a constant of motion, by integrating (5.2-19), we obtain

$$E = \frac{\hat{x}}{\sqrt{a}} \quad \text{with } E = 0 \text{ for } \hat{x} = 0 \quad (5.2-20)$$

whereas for the perturbed problem

$$\hat{x} = \int_0^E \sqrt{a} dE \quad \text{with } \hat{x} = 0 \text{ for } E = 0 \quad (5.2-21)$$

With this new variable,

$$\frac{d}{d\hat{x}} = \frac{dE}{d\hat{x}} \frac{d}{dE}$$

$$\frac{d^2}{d\hat{x}^2} = \frac{1}{\sqrt{a}} \frac{d}{dE} \left(\frac{1}{\sqrt{a}} \frac{d}{dE} \right) \quad (5.2-22)$$

$$= \frac{1}{a} \left(\frac{d^2}{dE^2} - \frac{1}{2a} \frac{da}{dE} \frac{d}{dE} \right)$$

In the unperturbed problem, $\frac{da}{dE}$ is zero. Thus Equations (5.2-3), (5.2-11) and (5.2-15) become

$$\frac{d^2\vec{r}}{dE^2} - \frac{1}{r} \frac{dr}{dE} \frac{d\vec{r}}{dE} + a \frac{\vec{r}}{r} = 0 \quad (5.2-23)$$

$$\frac{d^2\vec{r}}{dE^2} + \vec{r} = \vec{B} \quad (5.2-24)$$

$$\frac{d^2\vec{z}}{dE^2} + \vec{z} = 0 \quad (5.2-26)$$

Therefore, in variable "E" and for the unperturbed problem,

$$\vec{z} = \vec{z}_0 \cos E + \left(\frac{d\vec{z}}{dE}\right)_0 \sin E \quad (5.2-27)$$

$$\frac{d\vec{z}}{dE} = -\vec{z}_0 \sin E + \left(\frac{d\vec{z}}{dE}\right)_0 \cos E$$

$$\vec{r} = \vec{B} + (\vec{r}_0 - \vec{B}) \cos E + \left(\frac{d\vec{r}}{dE}\right)_0 \sin E$$

$$\frac{d\vec{r}}{dE} = -(\vec{r}_0 - \vec{B}) \sin E + \left(\frac{d\vec{r}}{dE}\right)_0 \cos E$$

To obtain the differential equation satisfied by the scalar r , the identity

$$r^2 = \vec{r} \cdot \vec{r}$$

is differentiated twice with respect to E

$$r \frac{dr}{dE} = \vec{r} \cdot \frac{d\vec{r}}{dE}$$

$$\vec{r} \cdot \frac{d^2\vec{r}}{dE^2} + \left(\frac{d\vec{r}}{dE}\right)^2 = r \frac{d^2r}{dE^2} + \left(\frac{dr}{dE}\right)^2$$

From Equation (5.2-23)

$$\vec{r} \cdot \frac{d^2\vec{r}}{dE^2} = \left(\frac{\vec{r}}{r} \cdot \frac{d\vec{r}}{dE}\right) \frac{dr}{dE} - ar = \left(\frac{dr}{dE}\right)^2 - ar$$

Substituting, and dividing by r ,

$$\frac{d^2r}{dE^2} = -a + \frac{1}{r} \left(\frac{dr}{dE}\right)^2 \quad (5.2-29)$$

From (5.2-9)

$$\alpha = \frac{1}{r^2} \frac{d\vec{r}}{d\hat{x}} \cdot \frac{d\vec{r}}{d\hat{x}} - \frac{2}{r} = \frac{1}{ar^2} \frac{dr}{dE} \cdot \frac{dr}{dE} - \frac{2}{r}$$

we obtain in Equation (5.2-29)

$$\frac{1}{r} \left(\frac{dr}{dE}\right)^2 = ar\alpha + 2a = -r + 2a$$

Hence

$$\frac{d^2r}{dE^2} + r - a = 0 \quad (5.2-30)$$

or with $z \stackrel{\text{def}}{=} r - a$,

$$\frac{d^2z}{dE^2} + z = 0 \quad (5.2-31)$$

the solutions of which are

$$z = c_1 \sin E + c_2 \cos E$$

(5.2-32)

$$\frac{dz}{dE} = c_1 \cos E - c_2 \sin E$$

and

$$r = a + c_1 \sin E + c_2 \cos E = a + (r_0 - a) \cos E + \left(\frac{dr}{dE}\right)_0 \sin E$$

$$\frac{dr}{dE} = c_1 \cos E - c_2 \sin E$$

(5.2-33)

with c_1, c_2 constants equal to

$$c_1 = \left(\frac{dr}{dE}\right)_0$$

$$c_2 = r_0 - a$$

Note that the above equations (5.2-32), (5.2-33) will still hold true for a perturbed problem, if a, r_0 and $\left(\frac{dr}{dE}\right)_0$ are osculating parameters of the orbit at any given time.

The equation relating time to E , in the unperturbed problem, is

$$t - t_0 = \int_0^E \sqrt{a} \frac{r}{\sqrt{\mu}} dE \quad \text{with } t = t_0 \text{ for } E = 0$$

or

$$t - t_0 = \frac{a^{3/2}}{\sqrt{\mu}} \left[E + \left(\frac{r_0}{a} - 1\right) \cos E + \frac{1}{a} \left(\frac{dr}{dE}\right)_0 (1 - \cos E) \right] \quad (5.2-34)$$

If the reference ($t = t_0; E = 0$) is the perigee of the unperturbed orbit, then,

$$r_0 = a(1 - eE)$$

$$\left(\frac{dr}{dE}\right)_0 = 0$$

Therefore, in (5.2-34),

$$t - t_0 = \frac{a^{3/2}}{\sqrt{\mu}} [E - e \sin E] \quad (5.2-35)$$

which is the classical form of Kepler's equation of time, E being the "eccentric anomaly". (5.2-34) this appears as a more general equation, or generalized equation of time, with E playing the role of a generalized eccentric anomaly.

5.2.2 Differential equations in the perturbed problem

If a perturbing force \vec{F} exists, Equation (5.2-3) written with \hat{x} as the independent variable will read

$$\frac{d^2 \vec{r}}{dx^2} - \frac{1}{r} \frac{d\vec{r}}{d\hat{x}} \left(\frac{d\vec{r}}{d\hat{x}} \right) + \frac{\vec{r}}{r} = \frac{\vec{F}}{\mu} r^2 \quad (5.2-36)$$

Similarly, with E as independent variable, and taking Equation (5.2-22) into account,

$$\frac{d^2 \vec{r}}{dE^2} - \frac{1}{r} \frac{d\vec{r}}{dE} \left(\frac{d\vec{r}}{dE} \right) + a \frac{\vec{r}}{r} = \frac{\vec{F}}{\mu} r^2 a + \frac{1}{2a} \frac{da}{dE} \frac{d\vec{r}}{dE} \quad (5.2-37)$$

or

$$\frac{d^2 \vec{r}}{dE^2} + \vec{r} - \vec{B} = \frac{\vec{F}}{\mu} r^2 a + \frac{1}{2a} \frac{da}{dE} \frac{d\vec{r}}{dE} \quad (5.2-38)$$

5.2.3 Formulation of the variation of parameters method, with E as independent variable

5.2.3.1 Variational equations

Following Lagrange's method of variation of constants, the solution to the perturbed problem is written as

$$\vec{r} = \vec{B} + (\vec{r}_o - \vec{B}) \cos E + \left(\frac{d\vec{r}}{dE}\right)_o \sin E \quad (5.2-39)$$

$$\frac{d\vec{r}}{dE} = -(\vec{r}_o - \vec{B}) \sin E + \left(\frac{d\vec{r}}{dE}\right)_o \cos E$$

If at the instant considered, i.e. for the value of E considered, the perturbations were removed, vectors \vec{B} , \vec{r}_o and $\left(\frac{d\vec{r}}{dE}\right)_o$ would be constants of the motion in the unperturbed motion that would ensue. However, due to the continuing action of \vec{F} , \vec{B} , \vec{r}_o and $\left(\frac{d\vec{r}}{dE}\right)_o$ will be functions of E , the variations of which are now determined.

Taking the derivative of r in Equation (5.2-39),

$$\begin{aligned} \frac{d\vec{r}}{dE} &= \frac{d\vec{B}}{dE}(1 - \cos E) + \frac{d\vec{r}_o}{dE} \cos E + \frac{d}{dE}\left(\left(\frac{d\vec{r}}{dE}\right)_o\right) \sin E - (\vec{r}_o - \vec{B}) \sin E \\ &\quad + \left(\frac{d\vec{r}}{dE}\right)_o \cos E \end{aligned} \quad (5.2-40)$$

Subtracting the second equation of (5.2-39) from (5.2-40), we obtain

$$\frac{d\vec{B}}{dE}(1 - \cos E) + \frac{d\vec{r}_o}{dE} \cos E + \frac{d}{dE}\left(\left(\frac{d\vec{r}}{dE}\right)_o\right) \sin E = 0 \quad (5.2-41)$$

The l.h. side of Equation (5.2-36) is equal to $\frac{d^2\vec{r}}{dE^2} + \vec{r} - \vec{B}$, thus in the perturbed problem

$$\begin{aligned} \frac{d^2\vec{r}}{dE^2} + \vec{r} - \vec{B} &= \frac{d\vec{B}}{dE} \sin E - \frac{d\vec{r}_o}{dE} \sin E + \frac{d}{dE}\left(\left(\frac{d\vec{r}}{dE}\right)_o\right) \cos E \\ &= \frac{\vec{F}}{\mu} r^2 a + \frac{1}{2a} \frac{da}{dE} \frac{d\vec{r}}{dE} \end{aligned}$$

In terms of $\frac{d\vec{r}}{dE}$ and $\frac{d}{dE}\left(\frac{d\vec{r}}{dE}\right)_o$, this is rewritten

$$-\sin E \frac{d\vec{r}_o}{dE} + \cos E \frac{d}{dE}\left(\frac{d\vec{r}}{dE}\right)_o = \frac{\vec{F}}{\mu} r^2 a - \frac{d\vec{B}}{dE} \sin E + \frac{1}{2a} \frac{da}{dE} \frac{d\vec{r}}{dE} \quad (5.2-42)$$

Solving (5.2-41) and (5.2-42) for the six-vector $\frac{d}{dE} \begin{pmatrix} \vec{r}_o \\ \left(\frac{d\vec{r}}{dE}\right)_o \end{pmatrix}$, yields

$$\frac{d}{dE} \begin{pmatrix} \vec{r}_o \\ \left(\frac{d\vec{r}}{dE}\right)_o \end{pmatrix} = \begin{pmatrix} \cos E & -\sin E \\ \sin E & \cos E \end{pmatrix} \times \begin{pmatrix} -\frac{d\vec{B}}{dE} (1 - \cos E) \\ -\frac{d\vec{B}}{dE} \sin E + \left(\frac{\vec{F}}{\mu}\right) r^2 a + \frac{1}{2a} \frac{da}{dE} \frac{d\vec{r}}{dE} \end{pmatrix} \quad (5.2-43)$$

or explicitly

$$\frac{d\vec{r}_o}{dE} = -\frac{\vec{F}}{\mu} r^2 a \sin E - \frac{1}{2a} \frac{da}{dE} \frac{d\vec{r}}{dE} \sin E + \frac{d\vec{B}}{dE} (1 - \cos E) \quad (5.2-44)$$

$$\frac{d}{dE}\left(\frac{d\vec{r}}{dE}\right)_o = \frac{\vec{F}}{\mu} r^2 a \cos E + \frac{1}{2a} \frac{da}{dE} \frac{d\vec{r}}{dE} \cos E - \frac{d\vec{B}}{dE} \sin E$$

This system of differential equations of sixth order defines the variation of parameters scheme, describing the variation with E of the osculating elements $\vec{r}_o, \left(\frac{d\vec{r}}{dE}\right)_o$, integrals of the unperturbed motion.

To be complete, there remains to compute $\frac{da}{dE}, \frac{d\vec{B}}{dE}$,

$$\frac{da}{dE} = \frac{da}{dt} \frac{dt}{dE}$$

Now, by definition

$$-\frac{1}{a} = \frac{1}{\mu} \frac{d\vec{r}}{dt} \cdot \frac{d\vec{r}}{dt} - \frac{2}{r}$$

$$\begin{aligned} \frac{1}{a^2} \frac{da}{dt} &= \frac{2}{\mu} \frac{d\vec{r}}{dt} \cdot \frac{d^2\vec{r}}{dt^2} + \frac{2}{r^2} \frac{dr}{dt} \\ &= \frac{2}{\mu} \frac{d\vec{r}}{dt} \cdot \left(\vec{F} - \mu \frac{\vec{r}}{r^3} \right) + \frac{2}{r^2} \frac{dr}{dt} \\ &= \frac{2}{\mu} \vec{F} \cdot \frac{d\vec{r}}{dt} - \frac{2}{r^2} \frac{dr}{dt} + \frac{2}{r^2} \frac{dr}{dt} \end{aligned}$$

$$\frac{da}{dt} = \frac{2a^2}{\mu} \left(\vec{F} \cdot \frac{d\vec{r}}{dt} \right) \quad (5.2-45)$$

Thus

$$\frac{da}{dE} = \frac{2a^2}{\mu} \left(\vec{F} \cdot \frac{d\vec{r}}{dE} \right) \quad (5.2-46)$$

To obtain $\frac{d\vec{B}}{dt}$, since by definition

$$\vec{A} = \frac{\vec{r}}{r} - \frac{1}{\mu} \frac{d\vec{r}}{dt} \wedge \left(\vec{r} \wedge \frac{d\vec{r}}{dt} \right)$$

$$\vec{B} = a \vec{A}$$

$$\frac{d\vec{B}}{dt} = \frac{da}{dt} \vec{A} + a \frac{d\vec{A}}{dt}$$

$$\frac{d\vec{A}}{dt} = \frac{1}{r} \frac{d\vec{r}}{dt} - \frac{\vec{r}}{r^2} \frac{dr}{dt} - \frac{1}{\mu} \frac{d^2\vec{r}}{dt^2} \wedge \left(\vec{r} \wedge \frac{d\vec{r}}{dt} \right) - \frac{1}{\mu} \frac{d\vec{r}}{dt} \wedge \left(\vec{r} \wedge \frac{d^2\vec{r}}{dt^2} \right)$$

$\frac{d^2\vec{r}}{dt^2}$ is substituted from (5.2-1) and triple products are expanded,

$$\begin{aligned} \frac{d\vec{A}}{dt} = & \frac{1}{r} \frac{d\vec{r}}{dt} - \frac{\vec{r}}{r^2} \frac{dr}{dt} + \frac{\vec{r}}{r^2} \frac{dr}{dt} - \frac{1}{r} \frac{d\vec{r}}{dt} + \frac{1}{\mu} (\vec{F} \cdot \vec{r}) \frac{d\vec{r}}{dt} \\ & - \frac{1}{\mu} (\vec{F} \cdot \frac{d\vec{r}}{dt}) \vec{r} - \frac{1}{\mu} \left(\frac{d\vec{r}}{dt} \cdot \vec{F} \right) \vec{r} + \frac{1}{\mu} \left(\vec{r} \cdot \frac{d\vec{r}}{dt} \right) \vec{F} \end{aligned}$$

Finally,

$$\frac{d\vec{A}}{dt} = \frac{1}{\mu} \left[(\vec{F} \cdot \vec{r}) \frac{d\vec{r}}{dt} + \left(\vec{r} \cdot \frac{d\vec{r}}{dt} \right) \vec{F} - 2 \left(\vec{F} \cdot \frac{d\vec{r}}{dt} \right) \vec{r} \right] \quad (5.2-47)$$

To compute $\frac{d\vec{B}}{dE}$,

$$\frac{d\vec{B}}{dE} = 2a \left(\frac{\vec{F}}{\mu} \cdot \frac{d\vec{r}}{dt} \right) (a\vec{A} - \vec{r}) + a \left(\frac{\vec{F}}{\mu} \cdot \vec{r} \right) \frac{d\vec{r}}{dt} + a \left(\vec{r} \cdot \frac{d\vec{r}}{dt} \right) \frac{\vec{F}}{\mu} \quad (5.2-48)$$

and

$$\frac{d\vec{B}}{dE} = 2a \left(\frac{\vec{F}}{\mu} \cdot \frac{d\vec{r}}{dE} \right) (a\vec{A} - \vec{r}) + a \left(\frac{\vec{F}}{\mu} \cdot \vec{r} \right) \frac{d\vec{r}}{dE} + a \left(\vec{r} \cdot \frac{d\vec{r}}{dE} \right) \frac{\vec{F}}{\mu} \quad (5.2-49)$$

Equation (5.2-43) together with Equations (5.2-46) and (5.2-49)

are a complete formulation of the method of variation of parameters in elements \vec{r}_0 , $\left(\frac{d\vec{r}}{dE} \right)_0$, with E as independent variable

5.2.3.2 Equation of time

Using equation

$$t - t_0 = \int_0^E \sqrt{a} \frac{r}{\sqrt{\mu}} dE \quad (t = t_0 \text{ for } E = 0) \quad (5.2-50)$$

in which necessarily r is given by

$$r = a + (r_0 - a)\cos E + \left(\frac{dr}{dE}\right)_0 \sin E$$

as in (5.2-33), but this time with the elements a , r_0 , $\left(\frac{dr}{dE}\right)_0$

functions of E . Substituting in (5.2-50),

$$\begin{aligned} t - t_0 &= \int_0^E \frac{\sqrt{a}}{\sqrt{\mu}} [a + r_0 - a)\cos E + \left(\frac{dr}{dE}\right)_0 \sin E] dE \\ \sqrt{\mu} (t - t_0) &= a^{3/2} E - \int_0^E E \frac{d}{dE}(a^{3/2}) dE + \sqrt{a}(r_0 - a) \sin E \\ &\quad - \int_0^E \sin E \frac{d}{dE}(\sqrt{a}(r_0 - a)) dE - \left[\sqrt{a} \left(\frac{dr}{dE}\right)_0 \cos E \right]_0^E \\ &\quad + \int_0^E \frac{d}{dE} \left\{ \left(\frac{dr}{dE}\right)_0 \sqrt{a} \right\} \cos E dE \end{aligned}$$

or

$$\begin{aligned} t - t_0 &= \frac{a^{3/2}}{\sqrt{\mu}} \left[E + \left(\frac{r_0}{a} - 1\right) \sin E + \frac{1}{a} \left(\frac{dr}{dE}\right)_0 (1 - \cos E) \right] + \int_0^E \frac{f(E)}{\sqrt{\mu}} dE \\ &\quad + \frac{\sqrt{a}_0 \left(\frac{dr}{dE}\right)_0 - \sqrt{a} \left(\frac{dr}{dE}\right)_0}{\sqrt{\mu}} \end{aligned} \quad (5.2-51)$$

with

$$f(E) = - E \frac{d}{dE}(a^{3/2}) - \sin E \frac{d}{dE}[\sqrt{a}(r_0 - a)] + \cos E \frac{d}{dE}[\sqrt{a} \left(\frac{dr}{dE}\right)_0] \quad (5.2-52)$$

Written in the form of (5.2-51), and by comparison with Equation (5.2-34)

for the unperturbed motion, it can be seen that the "change in time" is given by the last two terms

$$t_{\text{perturbed}} - t_{\text{unperturbed}} = \int_0^E \frac{f(E)}{\sqrt{\mu}} dE + \frac{\sqrt{a_0} \left(\left(\frac{dr}{dE} \right)_0 \right)_0 - \sqrt{a} \left(\frac{dr}{dE} \right)_0}{\sqrt{\mu}} \quad (5.2-53)$$

By observation of Equation (5.2-53), it can be seen that in order to know the perturbed time, one more integration in E is needed (the order of the system being seven). This feature is equivalent to that of a double integration, a step which cannot be avoided at some point as commented upon by J. Kovalevsky^[5-2]

5.2.3.3 An approximate variation of parameters scheme: a approximately constant

If the nature of forces is such that along the perturbed orbit

$$\frac{da}{dt} = 2 \frac{a^2}{\mu} \vec{F} \cdot \frac{d\vec{r}}{dt} \approx 0 \quad (5.2-54)$$

is approximately zero (i.e. always much smaller than the time-rate of the other elements), or if, in the absence of a priori knowledge of such smallness of $\left| \frac{da}{dt} \right|$, numerical experiments have shown that such was the case in the problem at hand, a simplified scheme can be developed along the lines described in what follows. Extreme caution has to be exercised, however, in making sure that (5.2-54) holds sufficiently well.

Let E be defined here as in the unperturbed problem:

$$E \stackrel{\text{def}}{=} \frac{\hat{x}}{\sqrt{a}}$$

Thus

$$\begin{aligned}\frac{d\hat{x}}{dE} &= \sqrt{a} + \frac{1}{2} \frac{E}{\sqrt{a}} \frac{da}{dE} \\ &= \sqrt{a} \left(1 + \frac{1}{2} \frac{E}{a} \frac{da}{dE} \right)\end{aligned}$$

$$\frac{d}{d\hat{x}} = \frac{1}{\left[\sqrt{a} \left(1 + \frac{1}{2} \frac{E}{a} \frac{da}{dE} \right) \right]} \frac{d}{dE}$$

The simplification made is that $\frac{da/2a}{dE/2E}$ is always very small compared to unity, thus

$$\frac{dE}{d\hat{x}} = \frac{1}{\sqrt{a}}$$

With this simplification, i.e. $\frac{da}{dE}$ neglected in the differential transformation, the equations for the perturbed motion as given in Section 5.2.3.1 simply reduces to

$$\frac{d^2 \vec{r}}{dt^2} + \vec{r} - \vec{B} = \frac{\vec{F}}{\mu} r^2 a$$

and the Equation (5.2-44) for the variation of the parameters become

$$\frac{d\vec{r}_e}{dE} = (1 - \cos E) \frac{d\vec{B}}{dE} - \left(\frac{\vec{F}}{\mu} r^2 a \right) \sin E \quad (5.2-55)$$

$$\frac{d}{dE} \left[\left(\frac{d\vec{r}_e}{dE} \right)_0 \right] = -\sin E \frac{d\vec{B}}{dE} + \frac{\vec{F}}{\mu} r^2 a \cos E$$

The relation between time and E is given by (5.2-34).

5.2.4 Formulation of the method of variation of parameters, with time as independent variable.

The solutions developed for the unperturbed or perturbed motion, with E as independent variable, are now transformed to the case where

t (time) is the independent variable.

5.2.4 Unperturbed motion

One wishes to obtain

$$\vec{r}(t) = f(t) \vec{r}_0 + g(t) \left(\frac{d\vec{r}}{dt}\right)_0$$

(5.2-56)

$$\frac{d\vec{r}}{dt} = \dot{f} \vec{r}_0 + \dot{g} \left(\frac{d\vec{r}}{dt}\right)_0$$

designating now derivatives with respect to t. Since, from

Equation (5.2-38),

$$\vec{r} = \vec{B} + (\vec{r}_0 - \vec{B}) \cos E + \left(\frac{d\vec{r}}{dE}\right)_0 \sin E$$

Now

\vec{B} = constant in unperturbed motion

$$= a \frac{\vec{r}}{r} - \frac{a\vec{r}}{\mu} \left(\frac{d\vec{r}}{dt}\right) + \frac{a}{\mu} \left(r \frac{dr}{dt}\right) \frac{d\vec{r}}{dt}$$

$$= a\vec{r} \left(\frac{1}{r} - \frac{2}{r} + \frac{1}{a}\right) + \frac{ar}{\mu} \left(\frac{dr}{dt}\right) \frac{d\vec{r}}{dt}$$

$$= \vec{r}_0 \left(1 - \frac{a}{r_0}\right) + \frac{ar_0}{\mu} \left(\frac{dr}{dt}\right)_0 \left(\frac{d\vec{r}}{dt}\right)_0$$

Using the relation $dt = dE \frac{r\sqrt{a}}{\sqrt{\mu}}$,

$$\vec{r} = \vec{r}_0 \left\{1 - \frac{a}{r_0} (1 - \cos E)\right\} + \frac{r_0\sqrt{a}}{\sqrt{\mu}} \left\{\sin E + \frac{\sqrt{a}}{\sqrt{\mu}} \left(\frac{dr}{dt}\right)_0 (1 - \cos E)\right\} \left(\frac{d\vec{r}}{dt}\right)_0$$

Therefore, in Equations (5.2-56),

$$f = 1 - \frac{a}{r_0} (1 - \cos E)$$

$$g = \frac{r_0\sqrt{a}}{\sqrt{\mu}} \left(\sin E + \frac{\sqrt{a}}{\sqrt{\mu}} \left(\frac{dr}{dt}\right)_0 (1 - \cos E)\right) \quad (5.2-57)$$

Computing the time-derivatives:

$$\frac{df}{dt} = -\frac{a}{r_0} \sin E \frac{1}{r} \frac{\sqrt{\mu}}{\sqrt{a}}$$

$$\dot{f} = -\frac{\sqrt{\mu} \sqrt{a}}{r r_0} \sin E$$

$$\dot{g} = \frac{r_0 \sqrt{a}}{\sqrt{\mu}} \left(\cos E + \frac{\sqrt{a}}{\sqrt{\mu}} \left(\frac{dr}{dt} \right)_0 \right) \sin E \frac{\sqrt{\mu}}{r \sqrt{a}}$$

$$= \frac{r_0}{r} \left(\cos E + \frac{\sqrt{a}}{\sqrt{\mu}} \left(\frac{dr}{dt} \right)_0 \right) \sin E$$

To summarize,

$$\dot{f} = -\frac{\sqrt{\mu} \sqrt{a}}{r r_0} \sin E$$

(5.2-58)

$$\dot{g} = \frac{r_0}{x} \left(\cos E + \frac{\sqrt{a}}{\sqrt{\mu}} \left(\frac{dr}{dt} \right)_0 \right) \sin E$$

From these expressions, an algorithm can be implemented, which for a given value of t , will require, to obtain the corresponding value of E , to solve the transcendental generalized Kepler equation (5.2-34) by some numerical method.

5.2.4.2 Perturbed motion

Again the perturbed solution is written in the form

$$\vec{r}(t) = f \vec{r}_0 + g \left(\frac{d\vec{r}}{dt} \right)_0$$

(5.2-59)

$$\frac{d\vec{r}}{dt} = \dot{f} \vec{r}_0 + \dot{g} \left(\frac{d\vec{r}}{dt} \right)_0$$

where \vec{r}_o , $(\frac{d\vec{r}}{dt})_o$ are now functions of time, and f , g , \dot{f} , \dot{g} are functions given in 5.4.2.

From Equations (5.2-44) and $dt = dE \frac{r\sqrt{a}}{\sqrt{\mu}}$, and Equation (5.2-49), (5.2-45) for $\frac{d\vec{B}}{dt}$, $\frac{da}{dt}$

$$\frac{d\vec{r}_o}{dt} = -\frac{\vec{F}}{\mu} r\sqrt{a} \sin E - \frac{1}{2\sqrt{\mu a}} \frac{da}{dt} r \frac{d\vec{r}}{dt} \sin E + \frac{d\vec{B}}{dt} (1 - \cos E) \quad (5.2-60)$$

$$\frac{d\vec{B}}{dt} = 2a \left(\frac{\vec{F}}{\mu} \cdot \frac{d\vec{r}}{dt} \right) (a\vec{A} - \vec{r}) + a \left(\frac{\vec{F}}{\mu} \cdot \vec{r} \right) \frac{d\vec{r}}{dt} + a \left(r \frac{dr}{dt} \right) \frac{\vec{F}}{\mu}$$

$$\frac{da}{dt} = 2 \frac{a^2}{\mu} \vec{F} \cdot \frac{d\vec{r}}{dt}$$

Finally, $(\frac{d\vec{r}}{dt})_o$ is needed. From Equation (5.2-44),

$$\begin{aligned} \frac{d}{dE} \left[\left(\frac{d\vec{r}}{dE} \right)_o \right] &= \frac{d}{dE} \left[\left(\frac{d\vec{r}}{dt} \right)_o \frac{r_o \sqrt{a}}{\sqrt{\mu}} \right] \\ &= \frac{d}{dt} \left[\left(\frac{d\vec{r}}{dt} \right)_o \right] \frac{r_o r_o a}{\mu} + \left(\frac{d\vec{r}}{dt} \right)_o \left[\frac{dr_o}{dE} \frac{\sqrt{a}}{\sqrt{\mu}} + \frac{r_o}{2\sqrt{a}} \frac{da}{dt} \right] \\ &= \frac{r_o r_o a}{\mu} \left[\frac{d}{dt} \left(\frac{d\vec{r}}{dt} \right)_o \right] + \left(\frac{d\vec{r}}{dt} \right)_o \left(\frac{1}{r_o} \frac{dr_o}{dt} + \frac{1}{2a} \frac{da}{dt} \right) \end{aligned}$$

and

$$\begin{aligned} \frac{d}{dt} \left[\left(\frac{d\vec{r}}{dt} \right)_o \right] &= -\frac{\sqrt{\mu}}{r_o \sqrt{a}} \frac{d\vec{B}}{dt} \sin E + \left(\vec{F} + \frac{1}{2a} \frac{da}{dt} \frac{d\vec{r}}{dt} \right) \frac{r}{r_o} \cos E \\ &\quad - \left(\frac{1}{2a} \frac{dr_o}{dt} + \frac{1}{2a} \frac{da}{dt} \right) \left(\frac{d\vec{r}}{dt} \right)_o \end{aligned} \quad (5.2-61)$$

Given the form (5.2-59) to the solution of the perturbed problem, Equations (5.2-60) and (5.2-61) define the equations for the variations

of parameters \vec{r}_0 , $(\frac{d\vec{r}}{dt})_0$, with time as the independent variable.

This form of the method of variation of parameters is implemented in program NICE-T, described in Chapter 6.

5.2.5 Brief Comments

To conclude this section, a few comments are made on other similar approaches taken by other workers. In his "Theory of Orbits", Szebehely gives a treatment of regularization, with an extensive bibliography. The attention is focused on the restricted three-body problem, two-body problem and the collision orbits (one-dimensional problem). In this, the Levi-Civita transformation, or the use of complex variables, is possible. A recent extension of the Levi-Civita transformation to 4-dimensional space (its extension to three-dimensional space not being possible), by Kustaanheimo and Stiefel (KS transformation) is used by Stiefel and Scheifele^[5-22], with the same independent variable as was used here. A disadvantage of using the KS transformation is that the degree of the differential equation increases to ten, whereas the present treatment uses only six differential equations, plus one additional one to go back to physical time, in a derivation which is thought to be simple and straightforward. The method of variation of parameters developed by Stiefel and Scheifele^[5-22] has ten parameters, with the equations of constraints used as numerical checks during integration. Furthermore, and this is of particular importance in view of our goal to develop methods suitable also for circular orbits, Stiefel and Scheifele's parameters^[5-22] make reference to perigee and as such are not suitable

for circular orbits. Finally, as compared to Pitkin's^[5-3] development of the method of variation of parameters with time as the independent variable using the perturbative operator technique, the method developed here is thought to be much more straightforward.

5.3 A Modification of Brouwer's Method of Perturbations in Rectangular Coordinates, Applicable to Circular Orbits.

5.3.1 Introduction

In 1944, D. Brouwer^[5-23] published a method of calculating perturbations in rectangular coordinates, which is described in Brouwer and Clemence "Methods of Celestial Mechanics"^[5-24] as being apart from Hansen's method, the only other one that "need to be considered seriously for application where the numerical values of the elements are used from the start, and where a precision compatible to that of observation is desired." The method was applied by M.S. Davis^[5-25] to compute the motion of Eunicke (first order). Recently, S.A. Hamid^[5-26] developed a second-order planetary theory using this method.

In Brouwer's method, two main parts exist: the first one is to set up the differential equations of motion, the second one to integrate a suitable representation of the perturbing potential or forces, in expressions which are easily integrable.

In order to assess Brouwer's method as regards to formulation of the differential equation, a comparison is made in Chapter 6 between Brouwer's approach and the classical variation of parameters method

method using the same package for computing the forces and identical algorithms for the integration. On this very limited sample, it appears that a slight advantage might exist for Brouwer's method.

5.3.2 Differential equations in a form valid also for circular orbits.

Since Brouwer's method was using a reference orbit given in Delaunay's variables, it cannot be used for circular orbits. A new method is developed on the basis of the equations of Section 5.2, namely the use of elements $\vec{r}_0, \dot{\vec{r}}_0$ with E as the independent variable.

In Section 5.2, the variable

$$\vec{z} = \vec{r} - \vec{B}$$

was introduced. In the unperturbed case, it satisfied the equation

$$\frac{d^2 \vec{z}_0}{dE^2} + \vec{z}_0 = 0 \quad (5.3-1)$$

with subscript "0" reminding us that it is the solution in the case where perturbations are removed. With the same notation, we can define

$$\vec{B}_0 \stackrel{\text{def}}{=} \vec{B} \text{ on the two-body reference orbit (a constant)}$$

$$\vec{r}_0 \stackrel{\text{def}}{=} \vec{r} \text{ on two-body reference orbit, at E}$$

$$\vec{z} \stackrel{\text{def}}{=} \vec{r} - \vec{B}_0, \vec{r} \text{ taken along the perturbed orbit}$$

This gives in Equation (5.2-38), from which (5.3-1) is subtracted, and in which $\frac{da}{dE} = \left(\frac{\vec{F}}{\mu} \cdot \frac{d\vec{r}}{dE}\right) 2a^2$ is substituted,

$$\frac{d^2(\vec{z} - \vec{z}_0)}{dE^2} + (\vec{z} - \vec{z}_0) = \vec{B} - \vec{B}_0 + \frac{\vec{F}}{\mu} r^2 a + \left(\frac{\vec{F}}{\mu} \cdot \frac{d\vec{r}}{dE}\right) a \frac{d\vec{r}}{dE}$$

Let

$\delta \vec{z} \stackrel{\text{def}}{=} \vec{z} - \vec{z}_0$, the vector difference between
actual and reference orbit

$$\delta \vec{B} \equiv \vec{B} - \vec{B}_0$$

Thus

$$\frac{d^2}{dE^2} (\delta \vec{z}) + \delta \vec{z} = \delta \vec{B} + \frac{\vec{F}}{\mu} r^2 a + \left(\frac{\vec{F}}{\mu} \cdot \frac{d\vec{r}}{dE} \right) a \frac{d\vec{r}}{dE} \quad (5.3-3)$$

The solution to (5.3-1) can be written as in (5.2-27), with \vec{C} , \vec{D}
introduced to avoid confusion in the notations,

$$\vec{z}_0 = \vec{C} \sin E + \vec{D} \cos E \quad (5.3-4)$$

$$\left(\frac{d\vec{z}}{dE} \right)_0 = \vec{C} \cos E - \vec{D} \sin E$$

The solution to Equation (5.3-3) in its homogeneous form (r.h. side = 0)
is of the same form as (5.3-4), thus

$$\delta \vec{z} = \sum_{i=1}^6 K_i \frac{\partial \vec{z}_0}{\partial C_i} \quad (5.3-5)$$

in which the K_i 's are constant coefficients, and C_i ($i = 1, 2, 3$) are
the projections of \vec{C} on axes X, Y, Z; C_i ($i = 4, 5, 6$) are the projections
of \vec{D} on the same axes.

In the perturbed case, one requires that (5.3-5) still be the solu-
tion to (5.3-3), but now with the K_i 's being 6 unknown functions of E,
which can be determined with the additional requirement that the actual
and osculating velocity be the same.

Thus,

$$\frac{d}{dE} (\delta \vec{z}) = \underbrace{\sum_{i=1}^6 K_i \frac{d}{dE} \left(\frac{\partial z_o}{\partial C_i} \right)}_{\uparrow} + \sum_{i=1}^6 \frac{dK_i}{dE} \frac{\partial z_o}{\partial C_i} \quad (5.3-6)$$

term appearing
in unperturbed pro-
blem

and it is required that

$$\sum_{i=1}^6 \frac{dK_i}{dE} \frac{\partial z_o}{\partial C_i} = 0$$

Further differentiation of (5.3-6) gives

$$\frac{d^2}{dE^2} (\delta \vec{z}) = \sum_{i=1}^6 \left(\frac{dK_i}{dE} \right) \frac{\partial}{\partial C_i} \left(\frac{d\vec{z}_o}{dE} \right) + \sum_{i=1}^6 K_i \frac{\partial}{\partial C_i} \left(\frac{d^2 \vec{z}_o}{dE^2} \right)$$

Replacing $\frac{d^2 \vec{z}_o}{dE^2}$ by $-\vec{z}_o$,

$$\frac{d^2}{dE^2} (\delta \vec{z}) = \sum_{i=1}^6 \left(\frac{dK_i}{dE} \right) \frac{\partial}{\partial C_i} \left(\frac{d\vec{z}_o}{dE} \right) + \sum_{i=1}^6 K_i \frac{\partial}{\partial C_i} (-\vec{z}_o)$$

or using (5.3-5)

$$\frac{d^2}{dE^2} (\delta \vec{z}) + \delta \vec{z} = \sum_{i=1}^6 \frac{dK_i}{dE} \frac{\partial}{\partial C_i} \left(\frac{d\vec{z}_o}{dE} \right)$$

Thus we have six equations for the $\frac{dK_i}{dE}$

$$\sum_{i=1}^6 \frac{dK_i}{dE} \frac{\partial}{\partial C_i} \left(\frac{d\vec{z}_o}{dE} \right) = [G_x \ G_y \ G_z]_T \quad (5.3-8)$$

in which

$$\vec{G} \stackrel{\text{def}}{=} \frac{\vec{F}}{\mu} r^2 \vec{a} + \left(\frac{\vec{F}}{\mu} \cdot \frac{d\vec{r}}{dE} \right) \vec{a} \frac{d\vec{r}}{dE} + \delta \vec{B} \quad (5.3-9)$$

From Equation (5.3-4), if \vec{C} has components (C_1, C_2, C_3) and \vec{D} components (C_4, C_5, C_6) , the following holds

$$\begin{aligned} \frac{\partial}{\partial C_i} (z_o, j) &= \delta_{i-3}^j \sin E \quad (i, j=1, 2, 3) \\ &= \delta_{i-3}^j \cos E \quad (i = 4, 5, 6; j = 1, 2, 3) \end{aligned}$$

$$\frac{\partial}{\partial C_i} \left(\frac{dz_o}{dE} \right)_j = \delta_{i-3}^j \cos E \quad (i, j = 1, 2, 3)$$

$$\frac{\partial}{\partial C_i} \left(\frac{dz_o}{dE} \right)_j = -\delta_{i-3}^j \sin E \quad (i = 4, 5, 6; j = 1, 2, 3)$$

In matrix form

$$\begin{pmatrix} \sin E & 0 & 0 & \cos E & 0 & 0 \\ 0 & \sin E & 0 & 0 & \cos E & 0 \\ 0 & 0 & \sin E & 0 & 0 & \cos E \\ \cos E & 0 & 0 & -\sin E & 0 & 0 \\ 0 & \cos E & 0 & 0 & -\sin E & 0 \\ 0 & 0 & \cos E & 0 & 0 & -\sin E \end{pmatrix} \begin{pmatrix} 0 \\ 0 \\ 0 \\ G_x \\ G_y \\ G_z \end{pmatrix} \quad (5.3-9)$$

After inversion

$$\frac{d}{dE} \begin{pmatrix} K_1 \\ K_2 \\ K_3 \\ K_4 \\ K_5 \\ K_6 \end{pmatrix} = \begin{pmatrix} \sin E & 0 & 0 & \cos E & 0 & 0 \\ 0 & \sin E & 0 & 0 & \cos E & 0 \\ 0 & 0 & \sin E & 0 & 0 & \cos E \\ \cos E & 0 & 0 & -\sin E & 0 & 0 \\ 0 & \cos E & 0 & 0 & -\sin E & 0 \\ 0 & 0 & \cos E & 0 & 0 & -\sin E \end{pmatrix} \begin{pmatrix} 0 \\ 0 \\ 0 \\ G_x \\ G_y \\ G_z \end{pmatrix}$$

or

$$\frac{dK_1}{dE} = \cos E G_x$$

$$\frac{dK_2}{dE} = \cos E G_y$$

$$\frac{dK_3}{dE} = \cos E G_z \quad (5.3-10)$$

$$\frac{dK_4}{dE} = -\sin E G_x$$

$$\frac{dK_5}{dE} = -\sin E G_y$$

$$\frac{dK_6}{dE} = -\sin E G_z$$

To go back to physical time, t , use can be made of Equation (5.2-48).

Alternatively, using

$$dt = \frac{n\sqrt{a}}{\sqrt{\mu}} dE$$

$$t - t_0 = \frac{1}{\sqrt{\mu}} \int_0^E (r\sqrt{a} - r_0\sqrt{a_0}) dE + \frac{1}{\sqrt{\mu}} \int_0^E r_0\sqrt{a_0} dE \quad (5.3-11)$$

r_0 having here the meaning of r , along the reference orbit, at E . But it is known that, if $()_0$ designates the value of the quantity between parenthesis at $E = 0$,

$$r_0 = a_0 + ((r_0)_0 - a_0) \cos E + \left(\left(\frac{dr}{dE}\right)_0\right) \sin E$$

Let, in (5.3-11)

$$\frac{dK_7}{dE} \stackrel{\text{def}}{=} r\sqrt{a} - r_0\sqrt{a_0} \quad (5.3-12)$$

Then the equation of time becomes

$$t - t_0 = \frac{1}{\sqrt{\mu}} \int_0^E \frac{dK_7}{dE} dE + \frac{\sqrt{a_0}}{\mu} \{a_0 E + ((r_0)_0 - a_0) \sin E + \left(\left(\frac{dr}{dE}\right)_0\right) (1 - \cos E)\} \quad (5.3-13)$$

An algorithm can be developed on the basis of the above formulae^[5-1] and is implemented in program BROUWER-E described in Chapter 6.

5.4 Semi-Analytic Integration Method: Mixed Fourier-Chebyshev Series

5.4.1 Introduction

Given a system of differential equations describing the rates of change of the parameters, the first step in Picard's iteration scheme will consist in substituting in the r.h. side of the equation the solution to the unperturbed problem, and proceeding to analytically integrate this r.h. side to obtain the changes in the parameters over a suitably selected interval.

For the large circular orbits considered here, it has been found that results of sufficient accuracy (in a sense to be precised later)

are obtained over a range $(0, 2\pi)$ for E . For larger intervals of E , one proceeds to the integration over $(0, 2\pi)$, "updates" the elements by adding their changes over the interval to the initial values, and so on.

The r.h. sides in the differential systems, in order to be able to integrate these numerically, are to be expressed in a series of suitable analytic functions, the coefficients of which are numerical, introduced from the start using the initial conditions. Such analytic functions are oftentimes double Fourier Series in the mean anomalies of perturbed and perturbing bodies. However, in the case of artificial satellites undergoing strong perturbations, it is no longer true that the elements will not "change" too much over a period of the perturbing body. From that viewpoint, the periodicity in M' , say (mean anomaly of the perturbing body), for constant a, e, \dots , has been destroyed, and it appears perfectly reasonable to use non-periodic approximation functions, valid over a suitable interval in E , to represent the motion of the perturbing body. Chebyshev's polynomials have been used in planetary theory by Carpenter^[5-27]

The analytic series chosen here to represent the terms in the r.h. side are mixed Fourier-Chebyshev series: the Fourier part accounts for the motion of the satellite, and the Chebyshev part, having an argument which has a linear relation with the variable in the Fourier Series, represents the motion of the perturbing body.

5.4.2 Development of mixed Fourier-Chebyshev Series for the derivatives

The point of departure is the system of equations for the variation of parameters $\vec{r}_0, \left(\frac{d\vec{r}}{dE}\right)_0$, with E as independent variable, written in

(5.2-44), which are repeated here

$$\frac{d\vec{r}_o}{dE} = -\frac{\vec{F}}{\mu} r^2 a \sin E - \frac{1}{2a} \frac{da}{dE} \frac{d\vec{r}}{dE} \sin E + (1 - \cos E) \frac{d\vec{B}}{dE}$$

$$\frac{d}{dE} \left(\left(\frac{d\vec{r}}{dE} \right)_o \right) = \frac{\vec{F}}{\mu} r^2 a \cos E + \frac{1}{2a} \frac{da}{dE} \frac{d\vec{r}}{dE} \cos E - \sin E \frac{d\vec{B}}{dE} \quad (5.4-1)$$

$$\frac{d\vec{B}}{dE} = 2a \left(\frac{\vec{F}}{\mu} \cdot \frac{d\vec{r}}{dE} \right) (a\vec{A} - \vec{r}) + \left(\frac{\vec{F}}{\mu} \cdot \vec{r} \right) a \frac{dr}{dE} + \frac{\vec{F}}{\mu} (r \frac{dr}{dE}) a$$

$$\frac{da}{dE} = 2a^2 \frac{\vec{F}}{\mu} \cdot \frac{d\vec{r}}{dE}$$

with \vec{A} (in this first order scheme) being a constant vector depending on the initial conditions.

In order to determine what calculations are involved here in the development in series of the r.h. sides of (5.4-1), we shall, as announced in the beginning of this chapter, consider the analysis is limited to gravitational perturbing forces due to other bodies (moon and sun):

$$\frac{\vec{F}}{\mu} = \sum_{\substack{p=\text{moon,} \\ \text{sun}}} \left(\frac{\mu_p}{\mu} \right) \left(\frac{\vec{r}_p \cdot \vec{r}}{r_{1p}^3} - \frac{\vec{r}}{r_p^3} \right) \quad (5.4-2)$$

Standard notations are used: \vec{r}_p , \vec{r} are the geocentric vectors to the perturbing body and satellite, respectively, and r_{1p} is the magnitude of vector $|\vec{r}_p - \vec{r}|$.

First of all, the r.h. sides of (5.4-1) involve scalar r and vectors \vec{r} , $\frac{d\vec{r}}{dE}$, \vec{B} , which are to be taken as those of the undisturbed motion, namely

$$\vec{r} = \vec{B} + (\vec{r}_o - \vec{B})\cos E + \left(\frac{d\vec{r}}{dE}\right)_o \sin E$$

$$\frac{d\vec{r}}{dE} = -(\vec{r}_o - \vec{B})\sin E + \left(\frac{d\vec{r}}{dE}\right)_o \cos E$$

$$\vec{r} = a + (\vec{r}_o - a)\cos E + \left(\frac{d\vec{r}}{dE}\right)_o \sin E \quad (5.4-3)$$

$$\frac{d\vec{r}}{dE} = -(\vec{r}_o - a)\sin E + \left(\frac{d\vec{r}}{dE}\right)_o \cos E$$

Substitution of (5.4-3) into (5.4-1) permits to express the r.h. sides as Fourier Series in E, multiplied by $\frac{\vec{F}}{\mu}$. In Equation (5.4-2) it can be seen that for given \vec{r}_p , $\frac{\vec{F}}{\mu}$ could be expressed as a Fourier series in E; \vec{r}_p could be developed as a Fourier series in the mean anomaly of the perturbing body. However, here, these series lose their validity rapidly, if the range of E, for which (5.4-3) is adopted with values of \vec{r}_o , $\left(\frac{d\vec{r}}{dE}\right)_o$, \vec{B} at E = 0, exceeds (0, 2 π). It was decided to adopt Chebychev series for representing \vec{r}_p , by the method of special values^[5-28]. With a judicious choice of the argument of the Chebychev series, the integration of the resulting mixed series could also be simplified.

Let x be an argument linearly related to E as follows

$$E = (x + 1)\pi \quad (5.4-4)$$

Thus, x has range (-1, +1) when E varies over (0, 2 π). The ephemeris time, t, corresponding to E, is obtained from Equation (5.2-34)

$$t - t_o = \frac{a^{3/2}}{\sqrt{\mu}} \left[E + \left(\frac{r_o}{a} - 1\right)\cos E + \frac{1}{a}\left(\frac{dr}{dE}\right)_o(1 - \cos E) \right] \quad (5.4-5)$$

\vec{r}_p corresponding to this t (or E) can be determined by any suitable means (ephemerides, tapes, tables) with a suitable interpolation routine (here: fourth order central differences). The numerical coefficients

of the expansion of \vec{r}_p in Chebychev's polynomials follows the method given by Fox and Parker [5-28].

Mixed Fourier-Chebychev Series will be expressions encountered in the r.h. side of (5.4-1) having the canonical form

$$f = \sum_{J=1}^{J_{\max}} \left\{ \sum_{K=1}^{K_{\max}} C_1(J,K) T_{K-1}(x) \right\} \cos(J-1)E$$

(5.4-6)

$$\sum_{J=1}^{J_{\max}} \left\{ \sum_{K=1}^{K_{\max}} S_1(J,K) T_{K-1}(x) \right\} \sin JE$$

The following properties and calculations are derived in S.K. Bhate's thesis [5-1], to whom the reader should refer for a more detailed proofs:

I) If f_1, f_2 are series such as in (5.4-6), so are

$$f_1 + f_2$$

$$cf_1 \text{ (c scalar)}$$

$$gf_1 \text{ (g Fourier Series in E)}$$

$$hf_1 \text{ (h Chebychev series in x)}$$

$$f_1 \times f_2$$

(From this results that when the proper substitutions and operations are carried out, all r.h. sides in system (5.4-3) will be mixed Fourier-Chebychev's Series, provided the components of $\frac{\vec{r}}{\mu}$ themselves can be expanded in such series.)

$$\text{II) } D_1 \stackrel{\equiv}{\text{def}} \left(\frac{r_p}{r_{1p}}\right)^3 \text{ and } D_p \stackrel{\equiv}{\text{def}} D_1^{-1} \quad (r < r_p)$$

are mixed Fourier-Chebychev series.

Indeed, let $\rho \stackrel{\text{def}}{=} \frac{r}{r_p} < 1$, $\theta =$ angle between \vec{r}_p and \vec{r} ,

$$\left(\frac{r}{r_{1p}}\right)^3 = \frac{r_p^3}{(r^2 + r_p^2 - 2rr_p \cos \theta)^{3/2}} = \frac{1}{(1 + \rho^2 - 2\rho \frac{\sigma + \sigma^{-1}}{2})^{3/2}}$$

if $\sigma \stackrel{\text{def}}{=} e^{j\theta}$. Thus, after Taylor's series expansion about $x_1 = \rho^\sigma = 0$, and $x_1 = \rho^{\sigma-1} = 0$,

$$\begin{aligned} \left(\frac{r}{r_{1p}}\right) &= \frac{1}{(1 - \rho\sigma)^{3/2}} \frac{1}{(1 - \rho\sigma^{-1})^{3/2}} \\ &= \left(\sum_{n=0}^{\infty} \frac{(2n+1)!}{2^{2n} n! n!} \rho^n \sigma^n \right) \left(\sum_{m=0}^{\infty} \frac{(2m+1)!}{2^{2m} m! m!} \rho^m \sigma^{-m} \right) \\ &= \sum_{n=0}^{\infty} \sum_{m=0}^{\infty} A_n A_m \rho^{n+m} \sigma^{n-m} \end{aligned} \quad (5.4-7)$$

with $A_k = \frac{(2k+1)!}{2^{2k} k! k!}$ ($k = n, m$)

Now, in Equation (5.4-7), the double summation is effected along lines, in an "n,m" plane, of constant $r_1 = n+m$ or $r_2 = n-m$. (5.4-7) simplifies

to

$$\begin{aligned} \left(\frac{r}{r_{1p}}\right)^3 &= \sum_{\substack{m=0 \\ (m=n)}}^{\infty} A_n^2 \rho^{2n} + \sum_{r_1=1}^{\infty} \left(\sum_{n=0}^{\infty} (A_n A_{m+r}) \rho^{m+r_1} \right) \sigma^{r_1} \\ &\quad + \sum_{r_2=1}^{\infty} \left(\sum_{n=0}^{\infty} (A_n A_{n+r_2}) \rho^{2n+r_2} \right) \sigma^{-r_2} \end{aligned}$$

$$= \sum_{n=0}^{\infty} A_n^2 \rho^{2n} + 2 \sum_{r=1}^{\infty} \left(\sum_{m=0}^{\infty} (A_m A_{m+r}) \rho^{2m} \right) \rho^r \cos r\theta$$

(m=n)

From the above expression for A_k , it is easy to see that

$$A_0 = 1$$

$$A_{k+1} = \left(1 + \frac{1/2}{k+1}\right) A_k$$

and one can calculate, for given m_{\max} ,

$$a_0 \stackrel{\text{def}}{=} \sum_{m=0}^{m_{\max}} A_m^2 \rho^{2m}$$

$$a_\ell \stackrel{\text{def}}{=} 2 \sum_{m=0}^{m_{\max}} A_m A_{m+\ell} \rho^{2m} \quad \ell \text{ integer} > 0 \quad (5.4-8)$$

Thus, $\left(\frac{r}{r_{1p}}\right)^3$ can be rewritten

$$\left(\frac{r}{r_{1p}}\right)^3 = a_0 + \sum_{r=1}^{\infty} a_r \rho^r \cos(r\theta) \quad (5.4-9)$$

It can be shown^[5-1] that the sum (5.4-9), truncated to N terms, can be computed without running into the problem of subtracting two almost equal numbers of large magnitude, in the following manner.

$$b_{N:2} = 0$$

$$b_{N:1} = 0$$

$$b_r = 2\rho \cos \theta b_{r+1} - \rho^2 b_{r+2} + a_r \quad (r = N, N-1, \dots, 0) \quad (5.4-10)$$

$$\text{SUM} = b_0 - b_1 \rho \cos \theta = \frac{1}{2} (b_0 - \rho^2 b_2 + a_0)$$

As is evident from (5.4-8) and (5.4-10), the mixed Fourier-Chebyshev series for ρ^{2m} and $\rho \cos \theta$ are needed. These are given in Appendix A-2.1 and A-2.2. Once these have been obtained, it has been proved that D and D_1 as defined above, are mixed Fourier-Chebyshev series.

III) The components of $\frac{\vec{F}}{\mu}$ can be expressed as mixed Fourier-Chebychev series. Indeed, with the above definitions, and assuming that $\frac{a}{r_p}$ has been developed in Chebychev series by the method of special values as in Reference [5-28],

$$\frac{\vec{F}}{\mu} = \frac{\mu_p}{\mu} \frac{1}{r_p^3} [D_p \vec{r}_p - D_1 \vec{r}] = \frac{\mu_p}{\mu} \frac{1}{a^2} \left(\frac{a}{r_p}\right) [D_p \vec{r}_p - D_1 \vec{r}]$$

From what precedes, the component terms between brackets should be Fourier-Chebychev series, and so is $\left(\frac{a}{r_p}\right)^3$. Thus, so are the components of $\frac{\vec{F}}{\mu}$.

The other terms in the r.h. side of (5.4-1), these not involving $\frac{\vec{F}}{\mu}$ alone, should also be shown to the series of some type. Indeed,

$$\frac{da}{dE} = 2a \left(\frac{\vec{F}}{\mu} \cdot \frac{d\vec{r}}{dE}\right) = \frac{\mu_p}{\mu} \frac{2}{a} \left(\frac{a}{r_p}\right)^3 [D_p \vec{r}_p \cdot \frac{d\vec{r}}{dE} - D_1 \vec{r} \cdot \frac{d\vec{r}}{dE}]$$

is such a series. Indeed, $\vec{r}_p \cdot \frac{d\vec{r}}{dE}$ and $\vec{r} \cdot \frac{d\vec{r}}{dE}$ are, from (5.4-3), the mixed Fourier-Chebychev series

$$\vec{r}_p \cdot \frac{d\vec{r}}{dE} = -(\vec{r}_p) (\vec{r}_o - \vec{B}) \sin E + (\vec{r}_p \cdot \left(\frac{d\vec{r}}{dE}\right)_o) \cos E$$

$$r \cdot \frac{d\vec{r}}{dE} = (\vec{B} \cdot \left(\frac{d\vec{r}}{dE}\right)_o) \cos E + (\vec{C} \cdot \left(\frac{d\vec{r}}{dE}\right)_o) \cos 2E$$

$$-\vec{B} \cdot \vec{C} \sin E + \frac{1}{2} \left[\left(\frac{d\vec{r}}{dE}\right)_o \cdot \left(\frac{d\vec{r}}{dE}\right)_o - \vec{C} \cdot \vec{C} \right] \sin 2E$$

Also, $\frac{d\vec{B}}{dE}$

$$\begin{aligned} \frac{d\vec{B}}{dE} = \frac{\mu_p}{\mu} \left(\frac{a}{r_p}\right)^3 \{ [D_p (\vec{r}_p \cdot \vec{r}) \frac{d\vec{r}}{dE} + (\vec{r}_p \cdot \frac{d\vec{r}}{dE}) (2\vec{B} - \vec{r}) + (\vec{r} \cdot \frac{d\vec{r}}{dE}) \vec{r}_p] \\ - D_1 (r^2 \frac{d\vec{r}}{dE} + (\vec{r} \cdot \frac{d\vec{r}}{dE}) (2\vec{B} - \vec{r})) \} \end{aligned}$$

will be a series of same kind provided

$$\vec{r}_p \cdot \vec{r} = (\vec{r}_p \cdot \vec{B}) + (\vec{r}_p \cdot \vec{C}) \cos E + (\vec{r}_p \cdot \left(\frac{d\vec{r}}{dE}\right)_0) \sin E$$

is of the same kind, which holds true.

In summary, the equations (5.4-1) for the variation of $\vec{r}_0, \left(\frac{d\vec{r}}{dE}\right)_0$ can be written with each r.h. side in the form of a mixed Chebychev-Fourier series. The latter can be integrated analytically to yield the changes of the elements over an interval $(0, 2\pi)$ for E .

5.4.3 Integration of mixed Fourier-Chebychev series

Ref. [5-1] develops in great detail the algorithms needed for the integration, with respect to E , of the mixed Fourier-Chebychev series present in the r.h. side of Equation (5.4-1). These algorithms are briefly listed in Appendix A- 23.

The following should be noted

- integration is to first order of Picard's iteration.
- the series $\left(\frac{r_p}{r_{1p}}\right)^3$ is suitably truncated
- the motion of the perturbing bodies are represented by finite Chebychev series.
- in series multiplication, truncation is effected without loss of accuracy

This being said, no other approximation is introduced, since the integration of the terms being kept is rigorous.

A computer program, based on the above technique, is developed and has been tested for close to zero as well as for large eccentricity orbits. It needs some more work, however, to incorporate time-saving shortcuts.

5.5 Conclusions

In this chapter, methods of deriving variational equations for the elements of elliptic or circular orbits which are totally singularity-free (in the absence of collisions) have been developed. They should be particularly useful for the study of nearly circular geocentric orbits strongly perturbed by the sun and the moon. Programs based on them furthermore have shown that significant savings in computer time could be realized for the same accuracy, compared to the more common versions of the method of variation of parameters, with time as the independent variable.

- [5-1] Bhate, S.K. "On some techniques of integration of perturbed orbits, with emphasis on circular orbits ($e=0$)," Ph.D. Thesis, Applied Space Sciences Program, Carnegie-Mellon University, August 1973.
- [5-2] Garafalo, A. M., "New Set of Variables for Astronomical Problems," *Astronomical Journal*, 1969, Vol. 65, pp. 117-121.
- [5-3] Newton, R. R., "Variables that are Determinate for any Orbit," *ARS Journal*, 1961, Vol. 31, pp. 364-366.
- [5-4] Cohen, C. J., Hubbard, E. C., "A Non-Singular Set of Orbit Elements," *Astronomical Journal*, 1962, Vol. 67, pp. 10-15.
- [5-5] Pines, S., "Variation of Parameters for Elliptic and Nearly Circular Orbits," *Astronomical Journal*, 1961, Vol. 66, pp. 5-7.
- [5-6] Wong, P., "Non-Singular Variation of Parameter Equations for Computation of Space Trajectories," *ARS Journal*, 1962, pp. 264-265.
- [5-7] Herrick, S., "Universal Variables," *Astronomical Journal*, 1965; Vol. 70, pp. 1-3.
- [5-8] Pitkin, E. T., "A Regularized Approach to Universal Variables," *AIAA Journal*, 1965, Vol. 3, pp. 1508-1510.
- [5-9] Pitkin, E. T., "Integration with Universal Variables," *AIAA Journal*, 1966, Vol. 4, pp. 531-534.
- [5-10] Brouwer, D., "Integration of the Equations of General Planetary Theory in Rectangular Coordinates," *Astronomical Journal*, 1944, Vol. 51, pp. 37-43.
- [5-11] Izsak, I. G., "On Satellite Orbits with Very Small Eccentricities," *Astronomical Journal*, April, 1961, Vol. 66, Number 3, pp. 129-131.
- [5-12] Kozai, Y., "Note on the Motion of a Close Earth Satellite with a Small Eccentricity," *Astronomical Journal*, April, 1961, Vol. 66, Number 3, pp. 132-134.

- [5-13] Lyddane, R. H., "Small Eccentricities or Inclinations in the Brouwer Theory of the Artificial Satellite," *Astronomical Journal*, 1963, Vol. 68, #8, pp. 555-557.
- [5-14] Felsentreger, T. L., "On the Perturbations of Small-Eccentricity Satellites," NASA TN D-4531, July 1968, National Aeronautics and Space Administration, Washington, D. C.
- [5-15] Deprit, A., Rom. A., "The Main Problem of Satellite Theory for Small Eccentricities," Boeing Scientific Research Laboratories Document D1-82-0888, August, 1969.
- [5-16] Tisserand, M. F., "Memoire sur le Développement de la Fonction Perturbatrice dans les cas ou l'inclination mutuelle des orbites est considerable. Application aux perturbations produites sur Pallas par Jupiter," *Annals Obs. Paris, Memoires*, Vol. XV, pp. C.1-C.52, 1880.
- [5-17] Lidov, M.L.: "The Evolution of Artificial Satellites of Planets under the Action of Gravitational Perturbations of External Bodies", *Planet. Space Science*, 9, pp. 719-759, 1962.
- [5-18] Musen, P.: "On the Long-Period Lunisolar Effect in the Motion of the Artificial Satellite", *Jl. of Geophys. Res.*, 66(6), June 1961, pp. 1659-1665.
- [5-19] Musen, P.: "A Discussion of Halphen's Method for the Secular Perturbations and its Application to the Determination of Long-Range Effects in the Motions of Celestial Bodies , Part 1", NASA Tech. Rept. R-176, 1963.
- [5-20] Renard, M.L., "Proposal for an extension of NASA Grant NGR-39-087-001 a" Applied Space Sciences Program, Carnegie-Mellon University, Dec. 1970.
- [5-21] Kovalevsky, J.: "Introduction to Celestial Mechanics", Springer-Verlag New York, Inc., 1967, p. 42.

- [5-22] Stiefel, E. L., Scheifele, G., "Linear and Regular Celestial Mechanics," 1971, Springer-Verlag, New York, Heidelberg, Berlin,
- [5-23] Brouwer, D., "Integration of the Equations of General Planetary Theory in Rectangular Coordinates," *Astronomical Journal*, 1944, Vol. 51, pp. 37-43.
- [5-24] Brouwer, D. and Clemence, G.M.: "Methods of Celestial Mechanics", Academic Press, 1961, p. 549.
- [5-25] M. S. Davis, "A Study of the Method of Rectangular Coordinates in General Planetary Theory," *Astronomical Journal*, Vol. 56, 1952, pp. 188-199.
- [5-26] S. E. Hamid, "Second Order Planetary Theory, Part I," Smithsonian Astrophysical Observatory, Special Report #302, July 1, 1969 (Smithsonian Astrophysical Observatory, Cambridge, Massachusetts 02138).
- [5-27] Carpenter, L. "Planetary Perturbations in Chebyshev Series", NASA TN D-3168, January 1966.
- [5-28] Fox, L., Parker, I. B., "Chebychev Polynomials in Numerical Analysis," 1968, Oxford University Press, New York, London, Toronto.

APPENDIX A-2

Auxiliary Developments in Singularity-Free Methods

A.1 Mixed Fourier-Chebyshev Series for ρ^{2m}

Since

$$\rho^{2m} = \left(\frac{r}{r_p}\right)^{2m}$$

we write, in the unperturbed motion

$$\frac{r}{a} = 1 + \left(\frac{r_0}{a} - 1\right) \cos E + \frac{1}{a} \left(\frac{dr}{dE}\right)_0 \sin E$$

Since $\left(\frac{r}{a}\right)^2$ is a Fourier series in E, so will $\left(\frac{r}{a}\right)^{2m}$ using the recurrence

$$\left(\frac{a}{r_p}\right)^{2m} = \left(\frac{a}{r_p}\right)^2 \left(\frac{a}{r_p}\right)^{2(m-1)}$$

Finally, ρ^{2m} is obtained as a Fourier-Chebyshev series by multiplication of the series for $\left(\frac{r}{a}\right)^{2m}$ and $\left(\frac{a}{r_p}\right)^{2m}$

A.2 Mixed Fourier-Chebyshev series for $\rho \cos \theta$

Since,

$$\rho \cos \theta = \frac{r}{r_p} \cdot \frac{\vec{r} \cdot \vec{r}_p}{a^2 r r_p} a = \left(\frac{r}{a}\right) \cdot \frac{\vec{r}}{a} \left(\frac{a}{r_p}\right)^2$$

$\frac{\vec{r}}{a}$ has components which can be developed in Chebyshev series

using the method of special values, with x as independent

variable. $\frac{\vec{r}}{a}$ has components which are Fourier series in E,

since

$$\frac{\vec{r}}{a} = \frac{\vec{B}}{a} + \left(\frac{r_0}{a} - \frac{B}{a}\right) \cos E + \frac{1}{a} \left(\frac{dr}{dE}\right)_0 \sin E$$

Therefore, $\rho \cos \theta$ will be a mixed Fourier-Chebyshev series,

because $\left(\frac{a}{r_p}\right)^2$ is in turn a Chebyshev series in x.

A.3 Integration Algorithms

Using the expressions given by Fox and Parker^[5-28] for the integrals with respect to x of Chebychev's polynomials $T_r(x)$, and by a judicious use of integration by parts, the following algorithms, proved in Ref. [5-1], were obtained:

(Note that $\frac{dE}{dx} = \text{constant} = \pi$)

a) Integration of $(\sum_{K=1}^{K_{\max}} S_0(J,K)T_{K-1}(x))\sin jE$

Let the integral of the above expressions be:

$$\left(\sum_{K=1}^{K_{\max}} S_1(J,K)T_{K-1}(x) \right) \sin jE + \left(\sum_{K=1}^{K_{\max}} C_1(J+1,K)T_{K-1}(x) \right) \cos jE$$

Then the algorithm follows, starting with the known S_0 's.

$$S_1(J, K_{\max}) = 0$$

$$C_1(J+1, K_{\max}) = -\frac{1}{J} S_0(J, K_{\max})$$

$$S_1(J, K_{\max}-1) = -\frac{2(K_{\max}-1)}{J \left(\frac{dE}{dx}\right)} C_1(J+1, K_{\max})$$

$$C_1(J+1, K_{\max}-1) = -\frac{1}{J} S_0(J, K_{\max}-1)$$

$$S_1(J, K_{\max}-2) = -2 \frac{K_{\max}-2}{J \frac{dE}{dx}} C_1(J+1, K_{\max}-1)$$

$$Z_2 = 2 \frac{K_{\max}-2}{\frac{dE}{dx}} S_1(J, K_{\max}-2)$$

$$Z_1 = \frac{2(K_{\max}-3)}{\frac{dE}{dx}} S_1(J, K_{\max}-2)$$

$$D\phi \quad 1 \quad K = K_{\max} - 3, 4, -1$$

$$C1(J+1, K) = \frac{1}{J} (SO(J, K) - Z2)$$

$$S1(J, K-1) = -2 \frac{K-1}{J} \frac{dE}{dx} C1(J+1, K) + S1(J, K+1)$$

$$Z22 = Z2$$

$$Z2 = Z1$$

$$1 \quad Z1 = 2 \frac{K-2}{J} \frac{dE}{dx} S1(J, K-1) + Z22$$

$$C1(J+1, 3) = -\frac{1}{J} (SO(J, 3) - Z2)$$

$$S1(J, 2) = -\frac{4}{J} \frac{dE}{dx} C1(J+1, 3) + S1(J, 4)$$

$$Z22 = Z2$$

$$Z2 = Z1$$

$$Z1 = \frac{1}{J} \frac{dE}{dx} S1(J, 2) + \frac{1}{2} Z22$$

$$C1(J+1, 2) = -\frac{1}{J} (SO(J, 2) - Z2)$$

$$S1(J, 1) = -\frac{1}{J} \frac{dE}{dx} C1(J+1, 2) + \frac{1}{2} S1(J, 3)$$

$$Z2 = Z1$$

$$C1(J+1, 1) = -\frac{1}{J} (SO(J, 1) - Z2)$$

END

b) Integration of $\left\{ \sum_{K=1}^{K_{\max}} CO(J+1, K) T_{K-1}(x) \right\} \cos jE$

Let the integral of the above expression be

$$\left(\sum_{K=1}^{K_{\max}} S1(J, K) T_{K-1}(x) \right) \sin jE + \left(\sum_{K=1}^{K_{\max}} C1(J+1, K) T_{K-1}(x) \right) \cos jE$$

Algorithm is as follows, starting with the known SO's

$$C1(J+1, K_{\max}) = 0$$

$$S1(J, K_{\max}) = \frac{1}{J} CO(J+1, K_{\max})$$

$$C1(J+1, K_{\max} - 1) = 2 \frac{K_{\max} - 1}{J \frac{dE}{dx}} S2(J, K_{\max})$$

$$S1(J, K_{\max} - 1) = \frac{1}{J} CO(J+1, K_{\max} - 1)$$

$$C1(J+1, K_{\max} - 2) = 2 \frac{K_{\max} - 2}{J \frac{dE}{dx}} S2(J, K_{\max} - 1)$$

$$Z2 = 2 \frac{K_{\max} - 2}{\frac{dE}{dx}} C1(J+1, K_{\max} - 1)$$

$$Z1 = 2 \frac{K_{\max} - 3}{\frac{dE}{dx}} C1(J+1, K_{\max} - 2)$$

$$D\emptyset \quad 1 \quad K = K_{\max} - 3, 4, -1$$

$$S1(J, K) = -\frac{1}{J} (CO(J+1, K) - Z2)$$

$$C1(J+1, K-1) = 2 \frac{K-1}{J \frac{dE}{dx}} S1(J, K) + C1(J+1, K+1)$$

$$Z22 = Z2$$

$$Z2 = Z1$$

$$1 \quad Z1 = 2 \frac{K-2}{\frac{dE}{dx}} C1(J+1, K-1) + Z22$$

$$S1(J,3) = \frac{1}{J} (CO(J+1, 3) - Z2)$$

$$C1(J+1, 2) = \frac{4}{J \frac{dE}{dx}} S1(J,3) + C1(J+1, 4)$$

$$Z22 = Z2$$

$$Z2 = Z1$$

$$Z1 = \frac{1}{\frac{dE}{dx}} C1(J+1, 2) + \frac{1}{2} Z22$$

$$S1(J,2) = -\frac{1}{J} (CO(J+1, 2) - Z2)$$

$$C1(J+1, 1) = \frac{1}{J \frac{dE}{dx}} S1(J,2) + \frac{1}{2} C1(J+1, 3)$$

$$Z2 = Z1$$

$$S1(J,1) = \frac{1}{J} (CO(J+1, 1) - Z2)$$

c) Constant of integration

The integrals being computed from $E = 0$ to E , we note that the perturbation should vanish at $E = 0$. Thus from the indefinite integral result, the value of the series at $E = 0$ (or $x = -1$) should be subtracted i.e., in the final series (containing the constant of integration,

$$C1(1,1) \text{ to be used} = C1(1,1) \text{ above} - \sum_{J=1}^{J_{\max}} \left\{ \sum_{K=1}^{K_{\max}} C1(J,K) T_{K-1}(-1) \right\}$$

the other coefficients remaining unchanged.

CHAPTER 6

Orbital Programs

6.1 Introduction

In this chapter we briefly list, analyze and compare various programs, developed under this grant for the integration of perturbed orbits^[6-1]. Other programs, such as SABAC, ECLIP, VOLER, etc. have been previously described. The program examined here differ from each other in the following aspects:

- a) the parameters, or osculating elements, being integrated
- b) the independent variable retained

In order to make comparisons valid, it was decided to integrate by all methods examples which would serve as numerical standards in the analysis. These two reference solutions were obtained by NASA's numerical integration program ITEM, based on a modified Encke's method and briefly described by B. Lowrey^[6-2].

In all methods

- identical integration techniques were used

The same integration routine was used, a fourth order prediction-corrector method, of the Hamming type, with fourth-order Runge-Kutta-Gill starter.

- identical perturbation forces models

These forces consist of

1. "Third" body gravitational perturbation (by sun and moon)
2. Gravitational perturbations due to the asphericity of the earth
3. Atmospheric drag
4. Solar radiation pressure

The two last forces were set to zero on the examples treated. The position of the sun is interpolated from the American Ephemeris data for the sun's position at 0 h. E.T. every day. The moon is given by formulae having an error of ± 0.75 min of arc at most, over 3 years from Jan 1, 1969.

- identical reference standards

6.2 Test

The conditions for these are listed below, for two examples, one for close to zero eccentricity ($e = 0.8 \times 10^{-5}$), $a = 0.58$ x Earth-moon distance, orbital period = 12.05 days; one for high eccentricity ($e = 0.936$), $a = 0.297$ x Earth-moon distance, orbital period = 4.45 days.

INITIAL CONDITIONS FOR THE NUMERICAL EXAMPLES

Example 1: Large Circular Orbit

$$\begin{aligned} \vec{r}_0 &= -0.2932796 \times 10^8 \vec{a}_x \\ &\quad - 2.0338597 \times 10^8 \vec{a}_y \\ &\quad + 0.87225166 \times 10^8 \vec{a}_z \quad \text{meters} \end{aligned}$$

$$\begin{aligned} \left(\frac{d\vec{r}}{dt}\right)_0 &= 1.2405 \times 10^3 \vec{a}_x \\ &\quad - 0.3358361 \times 10^3 \vec{a}_y \\ &\quad - 0.36598403 \times 10^3 \vec{a}_z \quad \text{meters/second} \end{aligned}$$

$$T_0 = \text{Feb. 18, 1971, 6.00 hours Ephemeris time}$$

From which

$$\begin{aligned} r_0 &= 223235.8 K_m = 35 \times \text{radius of earth mean} \\ &= 0.58 \times \text{mean earth moon distance} \end{aligned}$$

$$v_0 = 1.336252 K_m / \text{sec.}$$

$$a = 223234.0 K_m$$

$$e = 0.8018212 \times 10^{-5}$$

$$i = 28.50035^\circ$$

$$\Omega = 133.2179^\circ$$

$$\omega = -54.99945^\circ$$

$$v = 180.0285^\circ$$

$$\text{Period} = 12.05 \text{ days}$$

Example 2: Highly Eccentric Orbit

$$\begin{aligned} \vec{r}_o &= -0.39275819084844 \times 10^5 \vec{a}_x \\ &\quad -1.623139606007665 \times 10^5 \vec{a}_y \\ &\quad +0.8969904059411103 \times 10^5 \vec{a}_z \quad K_m \end{aligned}$$

$$\begin{aligned} \left(\frac{d\vec{r}}{dt}\right)_o &= 0.1954377352706032 \vec{a}_x \\ &\quad -0.7854274357862668 \vec{a}_y \\ &\quad +0.24190151060205798 \vec{a}_z \quad K_m/\text{sec} \end{aligned}$$

T_o = January 5, 1971, 18.5 hours Ephemeris time

From which

$$\begin{aligned} r_o &= 189563.5 K_m \approx 29.72 \times \text{radius of earth} \\ &\quad \approx 0.494 \times \text{mean earth-moon distance} \end{aligned}$$

$$v_o = 0.8447536 K_m/\text{sec}$$

$$\begin{aligned} a &= 114151.4 K_m \approx 17.9 \times \text{radius of earth} \\ &\quad \approx 0.297 \times \text{mean earth-moon distance} \end{aligned}$$

$$e = 0.936227$$

$$i = 33.40927^\circ$$

$$\Omega = 130.9163^\circ$$

$$\omega = -50.62353^\circ$$

$$v = 171.3767^\circ$$

$$\text{Period} = 4.45 \text{ days}$$

The programs were designed to be "modular" in structure. Some modules, concerned with the computation of the perturbing forces, are identical with all the programs. Those dealing with integration are almost identical, except for the number of differential equations required and some print-outs. Such a modular arrangement makes it much easier to bring changes in some part of the computational scheme.

A list of the programs to be discussed is given below

	INDEPENDENT VARIABLE	DEPENDENT VARIABLES
NICE-T (for <u>N</u> umerical <u>I</u> nte- gration of <u>C</u> ircular & <u>E</u> lliptic Orbits)	t	$\vec{r}_0, \dot{\vec{r}}_0$
NICE-E	E	$\vec{r}_0, \dot{\vec{r}}_0$
NICE-EA	E; elements kept constant over $(0, 2\pi)$ in E	$\vec{r}_0, \dot{\vec{r}}_0$
BROUWER-E (Brouwer's method modified for circu- lar orbits)	E	$K_i (i = 1, \dots, 6)$
EOLA-T	t	Conventional oscu- lating elements

6.2 Program NICE-T

Independent variable: time

Osculating parameters position vector \vec{r}_0 , and velocity vector $\dot{\vec{r}}_0$,
along the osculating orbit at time "T₀" (fixed)

Equations: six equations, in (5-2.60,61) of Chapter 5.

Tested: against NASA's ITEM, on the two examples quoted above.
Thereafter used as a standard of comparison.

Comparison with other programs: as most other programs had "E" as independent variables at intervals of 2π in E, data from these other programs consisting of time t; osculating parameters, elliptical osculating parameters, radius and velocity vectors at t were punched out. At these times, the output of NICE-T was computed. The differences in the instantaneous values of the osculating elements, \vec{r}_o and $(\frac{d\vec{r}}{dt})_o$, the elliptical parameters and the values of the instantaneous radius and velocity vectors were computed and compared. The differences were then normalized by the maximum values of the quantities, as shown below.

The integration spanned about 25 orbits, i.e. about 195 days in the high eccentricity case, and 300 days in the case of the large circular orbit.

Since their did not appear to exist any definite trend for these differences (except that the two first orbits had always much smaller differences than the remaining 23), it was decided to "represent" them in the tables by their arithmetic mean A_m and standard deviation S_D .

A comparison of computer times is given in each case (CMU 360/67 TSS) and will be commented upon for each program.

RELATIVE ACCURACIES AND SPEEDS OF VARIOUS COMPUTER PROGRAMS

Per unit errors in various quantities are defined as follows:

$$\epsilon_a = \frac{a - a_T}{a_T}$$

$$\epsilon_e = e - e_T$$

$$\epsilon_i = \frac{i - i_T}{180}$$

$$\epsilon_\Omega = \frac{\Omega - \Omega_T}{360}$$

$$\epsilon_\omega = \frac{\omega - \omega_T}{360}$$

$$\epsilon_v = \frac{v - v_T}{360}$$

$$\epsilon_r = \frac{|\vec{r} - \vec{r}_T|}{|\vec{r}_T|}$$

$$\epsilon_v = \frac{|\vec{r} - \overset{\circ}{r}_T|}{|\overset{\circ}{r}_T|}$$

where

a = semi-major axis (meters).

e = eccentricity.

i = inclination (degrees)

Ω = longitude of ascending nodes (degrees).

ω = argument of perigee (degrees).

v = true anomaly (degrees).

\vec{r} = instantaneous radius vector (meters).

\vec{v} = instantaneous velocity vector (meters/sec.).

Quantities with subscript 'T' refer to values computed by program

NICE T used as reference.

A_m = arithmetic mean of 25 values (one at the end of each orbit for 25 orbits).

S_D = standard deviation of the same 25 quantities.

Example 1 - Large circular orbits (data as per example 1)

Comparison of Computer Time/Orbit
(Average of 25 Orbits)

<u>Program</u>	<u>cpu Time/Orbit, Seconds</u>
NICE T	16.9
NICE E	4.08
NICE EA	2.8
NICE EP	3.88
BRØUWER E	4.84

Example 2: Highly eccentric orbit (data as per example 2)

Comparison of Computer Time/Orbit
(Average of 25 Orbits)

<u>Program</u>	<u>cpu Time/Orbit (Seconds)</u>
NICE T	26.1
NICE E	5.48
NICE EA	3.07
NICE EP	5.21
BROUWER E	5.15
EOLA - T	9.95

EXAMPLE 1

COMPARISON OF ACCURACIES

	NICE E		NICE EA		NICE EP		BROUWER E	
	A_m	S_D	A_m	S_D	A_m	S_D	A_m	S_D
ϵ_a	0.13×10^{-6}	0.94×10^{-12}	-0.18×10^{-2}	0.77×10^{-5}	0.81×10^{-3}	0.59×10^{-6}	0.11×10^{-5}	0.13×10^{-10}
ϵ_e	0.65×10^{-6}	0.20×10^{-8}	0.39×10^{-1}	0.19×10^{-2}	$-.15 \times 10^{-1}$	$.37 \times 10^{-2}$	0.19×10^{-4}	0.68×10^{-7}
ϵ_i	-0.27×10^{-6}	0.42×10^{-13}	-0.13×10^{-3}	0.11×10^{-6}	-0.40×10^{-3}	0.55×10^{-7}	-0.85×10^{-6}	0.62×10^{-12}
ϵ_Ω	-0.10×10^{-6}	0.12×10^{-13}	0.57×10^{-3}	0.11×10^{-6}	-0.17×10^{-3}	0.94×10^{-8}	-0.70×10^{-7}	0.17×10^{-12}
ϵ_ω	-0.75×10^{-5}	0.45×10^{-10}	-0.37×10^{-2}	0.26×10^{-2}	-0.10×10^{-1}	0.79×10^{-3}	0.91×10^{-5}	0.20×10^{-8}
e_v	0.94×10^{-5}	0.67×10^{-10}	-0.74×10^{-2}	0.28×10^{-2}	0.20×10^{-2}	0.74×10^{-3}	-0.42×10^{-4}	0.26×10^{-8}
e_r^+	-0.10×10^{-5}	0.39×10^{-11}	0.13×10^{-1}	0.34×10^{-4}	-0.44×10^{-2}	0.16×10^{-4}	0.11×10^{-4}	0.74×10^{-10}
e_r^o	0.11×10^{-5}	0.27×10^{-11}	-0.14×10^{-1}	0.53×10^{-4}	0.5×10^{-2}	0.18×10^{-4}	-0.11×10^{-4}	0.94×10^{-10}

EXAMPLE 2

COMPARISON OF ACCURACIES

	NICE E		NICE EA		NICE EP		BRØUWER E		T	
	A _m	S _D	A _m	S _D	A _m	S _D	A _m	S _D	A _m	S _D
ϵ_a	0.79×10^{-6}	0.32×10^{-10}	-0.46×10^{-2}	0.32×10^{-5}	0.12×10^{-3}	0.34×10^{-7}	0.56×10^{-5}	0.41×10^{-10}	-0.19×10^{-4}	0.47×10^{-9}
ϵ_e	-0.74×10^{-6}	0.18×10^{-12}	-0.19×10^{-3}	0.14×10^{-7}	0.28×10^{-4}	0.72×10^{-9}	-0.60×10^{-5}	0.17×10^{-10}	-0.18×10^{-4}	0.19×10^{-9}
ϵ_i	0.85×10^{-6}	0.36×10^{-12}	-0.13×10^{-3}	0.16×10^{-7}	-0.12×10^{-4}	0.18×10^{-9}	-0.13×10^{-5}	0.10×10^{-10}	0.29×10^{-4}	0.78×10^{-9}
ϵ_Ω	0.34×10^{-6}	0.18×10^{-12}	-0.90×10^{-4}	0.26×10^{-7}	-0.88×10^{-5}	0.51×10^{-9}	0.14×10^{-5}	0.10×10^{-10}	-0.20×10^{-4}	0.46×10^{-9}
ϵ_ω	-	-	-0.12×10^{-2}	0.48×10^{-6}	-0.66×10^{-4}	0.87×10^{-9}	0.17×10^{-5}	0.25×10^{-11}	0.71×10^{-5}	0.15×10^{-9}
ϵ_v	0.45×10^{-4}	0.11×10^{-10}	0.85×10^{-2}	0.44×10^{-4}	-0.79×10^{-3}	0.6×10^{-6}	0.76×10^{-5}	0.10×10^{-9}	0.11×10^{-3}	0.14×10^{-6}
ϵ_r^+	0.46×10^{-4}	0.10×10^{-8}	0.56×10^{-1}	0.14×10^{-2}	0.74×10^{-2}	0.53×10^{-4}	0.57×10^{-4}	0.67×10^{-8}	0.64×10^{-3}	0.16×10^{-4}
ϵ_r^o	-0.14×10^{-3}	0.11×10^{-7}	-0.36	0.96×10^{-1}	0.24×10^{-1}	0.56×10^{-3}	0.22×10^{-3}	0.98×10^{-7}	-	-

6.3 NICE-E

Independent variable: "E" of Chapter 5 (not eccentric anomaly)

Osculating parameters: $\vec{r}_0, \dot{\vec{r}}_0$ at $E = 0$

Number of differential equations: 7, given in
of Chapter 5.

Time required and accuracy: the method is about four times faster than that based on time as independent variable. At high eccentricities, a significant part of the gain could be that Kepler's equation of time does not have to be inverted. However, the small time needed to do this inversion at small eccentricities fails to explain that the same gain still exists. Maybe the reason is to be found in the regularizing effect of using variable E, rather than time, which could be equivalently be seen as using a variable epoch time T_0 along the unperturbed orbit, in a way which presumably reduces computer time for a prescribed relative accuracy by keeping the motion in space $(\vec{r}_0, \dot{\vec{r}}_0, T_0)$ small.

6.4 NICE-EA

Independent variable: E modified, defined as $\frac{\hat{x}}{\sqrt{a}}$ in

$$\hat{x} \text{ defined by } \frac{d}{d\hat{x}} = \frac{r}{\sqrt{u}} \frac{d}{dr}$$

Osculating parameters: $\vec{r}_0, \dot{\vec{r}}_0$ at $E = 0$

Approximation mode: $\left| \frac{E}{2a} \frac{da}{dE} \right| \ll 1$ used in the definition of the independent variable; see Section 5.

Time required and accuracy: least of all methods. If the above approximation can be justified, either by the nature of the perturbing forces or, a posteriori by numerical experiments, this method could give a 20% saving in analytical integration (6 equations instead of 7 are used). The (relatively low) accuracy is of the same order as that obtained by a first-order Picard scheme.

6.5 NICE-EP

If the differential equations of motion are integrated in the iterations of a Picard scheme, no adequate analysis seems to exist on how long an interval of integration and how high an order of iteration one should take to minimize the computer time required for computing over a given interval with a prescribed error bound.

Therefore, it was thought to be appropriate, to get an idea of what error is introduced only by retaining a first-order iteration scheme. To that effect, the equations of NICE-E were integrated over the typical $(0, 2\pi)$ interval for E while keeping the values of the elements constant over the interval.

6.8 EOLA-NU

This program integrates the classical elements a, e, i, ω, Ω with respect to v , and obtains time t by integrating equation (2.3-4).

No mean anomaly at epoch is used. The speed is comparable to that of EOLA-T.

REFERENCES - Chapter 6

- [6-1] Bhate, S.K.: "On Some Techniques of Integration of Perturbed Orbits with Emphasis on Circular Orbits ($e = 0$)", Ph.D. Thesis, Applied Space Sciences Program, Carnegie-Mellon University, August 1973.
- [6-2] Lowrey, B.: "Ephemeris of a Highly Eccentric Orbit: Explorer 28," Celestial Mechanics, 1972, Vol. 5, pp. 107-125.

CHAPTER 7

General Conclusions

At the conclusion of this work, we wish to briefly review the material developed under this grant and to make a few recommendations for future topics of study.

New methods have been developed for the mission analysis and orbital studies of satellites of the IMP-type, which describe trajectories strongly perturbed by the gravitational fields of the Sun and the Moon. These techniques cover a wide interval of the "accuracy vs. computer time" scale, ranging all the way from very fast methods of relatively low accuracy (as in SABAC) to high accuracy, more time-consuming schemes (as in the NICE programs) through a method based on non-numeric computation, giving results of intermediate accuracy and time-consumption (as in VOLER). All of these will be chosen at some point in the mission analysis: in the preliminary phase, in establishing large numbers of possible launch windows; later on, in more detailed studies of better accuracy, and finally, in a few calculations by means of high accuracy programs suitable for low or high eccentricities, and which appear to save computer time by a factor of 3 to 4, compared to conventional methods.

Without going in detail into possible ways of implementing these suggestions, we think that various topics of investigation deserve further study. One is the comparative analysis of existing methods, or the development of other techniques, which are most

suitable for multiple satellites, the dimensionality of the state vector $(\vec{r}_0, \dot{\vec{r}}_0)$, say, going from 6 to 12, 18 etc. Another topic would be the development of literal theories based on regularized variables, since much insight is gained in the qualitative behavior of orbits even by means of "low-order" theories. Another area where more study appears to be needed is in minimizing computer time for a given error bound, or conversely, on a small computer of limited memory, in determining which method, for a given calculation time, assures the best accuracy in orbit determination.